A Study of Functional Selectivity at the Cannabinoid Type 1 Receptor

Richard Priestley, BSc (Hons)

Thesis submitted to the University of Nottingham for the degree of Doctor of Philosophy

July 2015

Abstract

The cannabinoid CB_1 receptor is a G protein-coupled receptor (GPCR) which is important in the regulation of neuronal function, predominately via coupling to heterotrimeric $G_{i/o}$ proteins. The receptor has also been shown to interact with a variety of other intracellular signalling mediators, including other G proteins, several members of the mitogen activated kinase (MAP) superfamily and β-arrestins. The CB_1 receptor is recognised by an array of structurally distinct endogenous and exogenous ligands and a growing body of evidence indicates that ligands acting at GPCRs are able to differently activate specific signalling pathways, a phenomenon known as *functional selectivity* or *biased agonism*. This is important in future drug development as it may be possible to produce drugs which selectively activate signalling pathways linked to therapeutic benefits, while minimising activation of those associated with unwanted side effects. The main aim of this thesis, therefore, was to investigate ligand-selective functional selectivity at the cannabinoid CB_1 receptor both endogenously and exogenously expressed in a variety of cell lines.

Chinese hamster ovary (CHO) and human embryonic kidney (HEK 293) cells stably transfected with the human recombinant CB_1 receptor and untransfected murine Neuro 2a (N2a) cells, were exposed to a number of cannabinoid receptor agonists, including the endogenous agonist anandamide, the phytocannabinoid Δ^9-THC, and several synthetic ligands. Ligand affinity was determined using competition radioligand binding assays. Regulation of several CB_1 receptor-coupled intracellular signalling mediators was investigated; G protein activation was measured using the [^{35}S]-GTPγS binding assay; phosphorylation of extracellular signal-regulated kinases (ERK), c-Jun N-terminal kinases (JNK) and p38 MAP kinases was measured using the immunocytochemical In-cell Western technique. Modulation of cAMP accumulation and β-arrestin recruitment were measured using DiscoveRx detection assay kits. Using concentration-response data, agonist bias was analysed using equimolar comparison plots, and by comparison of intrinsic relative activities for all agonists, calculated relative to the high potency cannabinoid receptor agonist HU-210 for the transfected cells or WIN 55,212-2 for the Neuro 2a cells.

The PPARα agonist fenofibrate was identified as a previously unrecognized cannabinoid receptor agonist, exhibiting modest selectivity for the CB_2 receptor subtype (~25-fold). In addition to its functioning as an orthosteric agonist, fenofibrate, at high concentrations, appeared to act as a negative allosteric modulator at the CB_1 receptor expressed in CHO cells, identified by radioligand binding assays, and non-competitive inhibition of the orthosteric agonist CP 55,940 in the [^{35}S]-GTPγS binding assay.

All three cell lines showed CB_1- and $G_{i/o}$ protein-dependent activation of ERK and inhibition of forskolin-stimulated cAMP accumulation: however, the magnitude of these responses differed between the three cell lines, with the responses in the Neuro 2a cells being markedly smaller than in the recombinant cell lines. The synthetic agonists WIN 55,212-2 and ACEA both exhibited bias towards ERK activation, in comparison to inhibition of cAMP accumulation, in both the CHO and HEK cell lines. HU-210, Δ^9-THC, methanandamide and fenofibrate all exhibited bias towards ERK activation in the Neuro 2a cells, but only the HU-210 bias was quantified, as the other three agonists did not couple to cAMP formation or inhibition in this cell line. In addition, time-course experiments revealed further novel patterns of agonist bias in ERK signalling, with CP 55,940 alone producing a second phase sustained ERK response in CHO cells, while higher concentrations of WIN 55-212-2 produced a CB_1-receptor-dependent reversal of ERK phosphorylation in HEK cells at 20 min, but not 5 min, agonist stimulation. Additional cell-dependent responses were observed with HEK cells alone, exhibiting $G_{i/o}$ protein-independent ERK activation and increase in cAMP levels. Despite reports in the literature to the contrary, none of the cell lines tested showed receptor-mediated activation of JNK or p38 MAP kinase.

In conclusion, this thesis has demonstrated functional selectivity at the cannabinoid type 1 receptor in a number of cell lines, expressing both native and transfected recombinant receptors. These findings contribute to our increasing understand of the complexity of GPCR signalling, and potentially allow for the development of more targeted drugs able to selectively engage with beneficial signal transduction pathways.

Acknowledgements

I would like to express my deep thanks to my supervisors Professor Dave Kendall and Dr Steve Alexander. You have given me the opportunity to pursue my ambitions, and helped me with much needed advice and direction. I am undoubtedly a better person for having known you, and I count you both as dear friends. Thanks as well to the other staff and students at the University of Nottingham, without whom, this thesis would not have been possible.

I am sincerely grateful to Dr Sarah Nickolls who has given me great support from both near and afar. Your input and friendship has been vital to my success and I am happy to have worked with you, especially through my numerous moments of injury and illness. Thanks also to Pfizer-Neusentis for the financial support and the chance to learn from and befriend many talented and helpful people.

I wouldn't be anywhere without the support of my loved ones. My eternal thanks and love goes to my family and to Liz.

Finally, I wish to say thank you to my inspiration, Peter Parker. You have shown me that even the most science-obsessed nerdy person can have a big impact on the world. I will never forget that with great power there must also come, great responsibility.

The experiments described in chapter 4 were performed at Pfizer-Neusentis, under the supervisor of Dr Sarah Nickolls, and with the assistance of Linda Kitching, Gordon McMurray, David Winpenny and others. All other experiments were performed at the University of Nottingham under the supervisor of Professor Dave Kendall and Dr Stephen Alexander, and with the assistance of Michael Garle, Liaque Latif, Paul Millns, and others.

Contents

Abbreviations

2-AG	2-arachidonoyl glycerol
ACEA	arachidonyl-2'-chloroethylamide
AEA	anandamide (*N*-arachidonoyl ethanolamine)
AMP	adenosine monophosphate
ANOVA	analysis of variance
ATP	adenosine triphosphate
BAD	Bcl-2-associated death promoter
BSA	bovine serum albumin
cAMP	cyclic adenosine monophosphate
CB_1	cannabinoid type 1 receptor
CB_2	cannabinoid type 2 receptor
CHO	Chinese hamster ovary cells
CNS	central nervous system
COX	cyclooxygenase
CRIP	cannabinoid receptor-interacting protein
CV	coefficient of variance
BRET	bioluminescence resonance energy transfer
DAG	diacylglycerol
DMEM	Dulbecco's Modified Eagle Medium
DMEM/F12	Dulbecco's Modified Eagle Medium: Nutrient Mixture F12
EDTA	ethylenediaminetetraacetic acid
EFS	electrical field stimulation
EGR1	early growth response protein 1 (also known as Krox-24)

ERK	extracellular signal-regulated kinase
FAAH	fatty acid amide hydrolase
FBS	foetal bovine serum
FSK	forskolin
GASP	GPCR-associated sorting protein
GDP	guanosine diphosphate
GI	gastrointestinal
GPCR	G protein-coupled receptor
GPR18	G protein-coupled receptor 18
GPR55	G protein-coupled receptor 55
GPR119	G protein-coupled receptor 119
GRK	GPCR-regulating kinase
GTP	guanosine-5'-triphosphate
GTPγS	guanosine 5'-O-[gamma-thio]triphosphate
HEK	human embryonic kidney cells
HEPES	4-(2-hydroxyethyl)-1-piperazineethanesulfonic acid
IBMX	3-isobutyl-1-methylxanthine
IP_3	inositol 1,4,5-trisphosphate
JNK	c-Jun N-terminal kinase
MAGL	monoacylglycerol lipase
MAP(K)	mitogen-activated protein kinase
MEK	mitogen-activated protein kinase kinase
MEKK	mitogen-activated protein kinase kinase kinase
mRNA	messenger RNA
NADA	*N*-arachidonoyl dopamine

NAGly	*N*-arachidonoyl glycine
NArPE	*N*-arachidonoyl phosphatidylethanolamine
NSB	non-specific binding
PBS	phosphate buffered saline
PCR	polymerase chain reaction
PDE	phosphodiesterase
PFA	paraformaldehyde
PI3K	phosphoinositol 3-kinase
PIP_2	phosphoinositol 4,5-bisphosphate
PKA	protein kinase A / cAMP-dependent protein kinase
PKC	protein kinase C
PLC	phospholipase C
PMSF	phenylmethylsulfonylfluoride
PPAR(α, γ, β/δ)	peroxisome proliferator-activated receptors (alpha, gamma, beta/delta)
PTX	pertussis toxin
PWR	plasmon-wavelength resonance
RAi	intrinsic relative activity
ROS	reactive oxygen species
SAP(K)	stress-activated protein kinase
SB	specific binding
SD	standard deviation
SEM	standard error of the mean
siRNA	small interfering RNA
STAT3	signal transducer and activator of transcription 3

TB	total binding
THC	tetrahydrocannabinol
TRPV1	transient receptor potential cation channel subfamily V member 1

Chapter 1

General Introduction

1.1. Cannabinoid Receptors

The cannabinoid receptor family is a member of the 'rhodopsin-like' G protein-coupled receptor class; specifically it is a member of subgroup A13, which includes other lipid signalling receptors including the lysophosphatidic acid and sphingosine-1-phosphate receptors, and the melanocortin/ACTH receptor family (Joost & Methner, 2002). The general structure of cannabinoid receptors is similar to that of other GPCRs with an extracellular N-terminal domain followed by seven transmembrane α-helical domains connected sequentially by three intracellular and three extracellular loops, finally ending with an intracellular C-terminal domain (**Figure 1.1**) (Howlett *et al.*, 2002).

Currently, two distinct cannabinoid receptors have been identified – CB_1 and CB_2. The CB_1 receptor gene was initially identified in rat (Matsuda *et al.*, 1990), human (Gerard *et al.*, 1990) and mouse (Chakrabarti *et al.*, 1995a); however, orthologues of the gene encoding the receptor have now been identified in most mammalian, and several non-mammalian species (Murphy *et al.*, 2001). The human CB_1 receptor protein comprises 472 residues, and exhibits 97 – 99% sequence homology with the rat and mouse protein. The coding sequence for the CB_1 receptor comprises a single exon; however, at least one splice variant of the human type 1 receptor (CB_{1A}) has been reported, though it is yet unclear if this is normally expressed in any significant amount (Shire *et al.*, 1995). The CB_1 receptor is predominantly found in the CNS, being the most highly expressed GPCR in the brain (Tsou *et al.*, 1998). Its main CNS function appears to be the inhibition of neuronal activity, mediated by receptors present at pre-synaptic sites, and activated by endogenous cannabinoid ligands synthesised at the post synaptic

site. Peripheral receptor expression is present in a number of tissues including thyroid and adrenal glands, liver, gastrointestinal tract and reproductive organs (Pagotto *et al.*, 2006).

The CB_2 receptor was initially identified in the leukemic HL-60 cell line (Munro *et al.*, 1993). There is only 48% sequence homology between the two receptor types, which increases to 68% when comparing only the transmembrane regions (Cabral & Griffin-Thomas, 2009). The CB_2 receptor is not as evolutionarily conserved as the CB_1 receptor, with 81% sequence homology between the human and rat receptors (Cabral & Griffin-Thomas, 2009). The CB_2 receptor is also much shorter than the CB_1 receptor, comprising 360 residues, although, like the CB_1 receptor, the CB_2 receptor gene contains a single exon (Shire *et al.*, 1995). Despite this lack of homology, both receptor subtypes share a common pool of high affinity ligands with varying CB_1/CB_2 selectivity (see section **1.4**.). The CB_2 receptor is predominantly expressed in immune tissues with mRNA and protein present in spleen, tonsils, thymus and several haematopoietic cell types including lymphocytes and macrophages (Galiegue *et al.*, 1995). The role of the receptor in these tissues is probably largely immunosupressive, though this is still debated. CB_2 receptors are also present in the CNS, where they are primarily found in microglia (Carlisle *et al.*, 2002), and in the gastrointestinal tract where they may regulate motility (Izzo, 2004), and GI inflammation (Wright *et al.*, 2008). While there are some reports of neuronal CB_2 receptor expression, these findings remain controversial, with many groups unable to detect CB_2 receptor in neuronal tissue (Onaivi *et al.*, 2008).

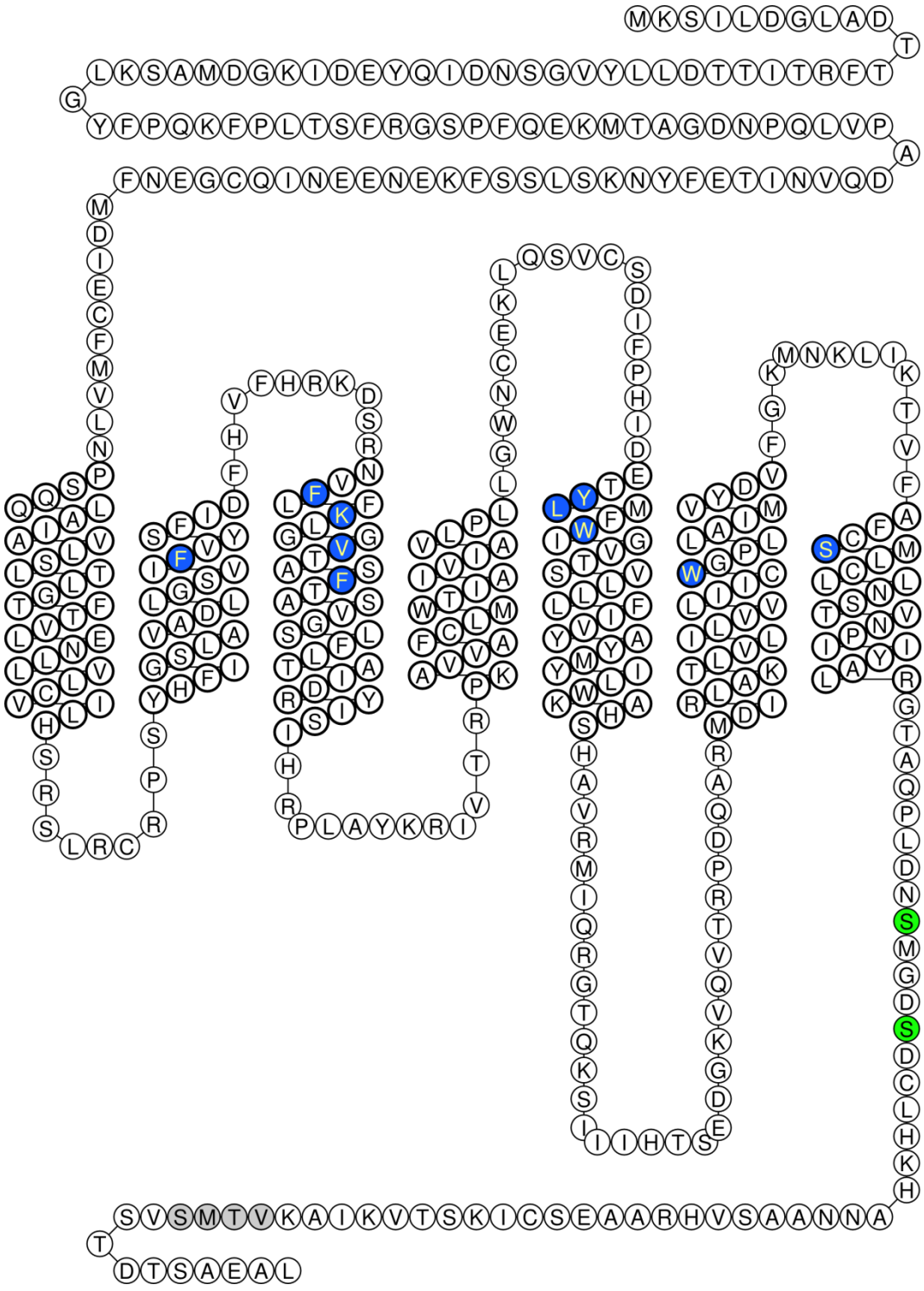

Figure 1.1 Two-dimensional snake plot diagram of the human cannabinoid type 1 receptor. Residues forming the ligand binding site are highlighted in blue, while GRK phosphorylation sites, important to receptor desensitisation and β-arrestin recruitment are highlighted in green.

There is mounting evidence for the existence of non CB_1/CB_2 cannabinoid GPCRs. GPR55 was initially isolated as an orphan receptor (Sawzdargo *et al.*, 1999) and subsequently characterised as a putative cannabinoid receptor by *in silico* comparison of the orthosteric ligand binding site with that of the established cannabinoid receptors (Baker *et al.*, 2006), though overall sequence homology with CB_1 (13.5 %) and CB_2 (14.4 %) is low (Pertwee *et al.*, 2010). GPR55 has been shown to couple to a range of cannabinoid ligands, although at present, lysophosphatidylinositol and its 2-arachidonoyl derivative are suspected to be the endogenous receptor ligands. The receptor is predominantly present in the brain, where it is widely expressed, with peripheral expression limited to the ileum. At present, the physiological function of GPR55 is unclear; however recent research has highlighted its importance in driving some cancer cell proliferation and migration, making it a potential oncological therapeutic target and biomarker. Other putative cannabinoid GPCRs include the *N*-arachidonoyl glycine (NAGly) receptor GPR18 (Gantz *et al.*, 1997) and GPR119 (Pertwee *et al.*, 2010).

The most prominent non-GPCR cannabinoid targets are the transient receptor potential cation channel subfamily V member 1 (TRPV1) and the peroxisome proliferator-activated receptors (PPARs). TRPV1 is a non-selective cation channel, predominantly expressed in peripheral sensory neurons which is activated by noxious stimulus, including heat (>43°C) and low pH. It is also activated by capsaicin, the phytocompound responsible for the 'heat' sensation from ingesting chilli peppers. The endogenous cannabinoid ligands anandamide (Ross, 2003) and N-arachidonoyl dopamine (Huang *et al.*, 2002a) have been thoroughly

characterised as TRPV1 agonists, with N-arachidonoyl dopamine, in particular, promoted as the putative endogenous TRPV1 ligand.

PPARs are members of the nuclear receptor superfamily and function as ligand-activated transcription factors, recognising a range of endogenous fatty acids and their derivatives, and are generally involved in metabolism and cellular differentiation (Michalik *et al.*, 2006). To date, three receptor isoforms have been identified, α, β/δ and γ, although, at present, only PPARα and PPARγ are therapeutic targets - PPARα is the target for the fibrate class of antihyperlipidaemic agents, while PPARγ is activated by the thiazolidinediones, used in the treatment of type 2 diabetes. All PPAR subtypes are expressed in the liver, with other major receptor populations present in adipose tissue and skeletal muscle. Their main function is as regulators of lipid metabolism; e.g. activation of PPARα leads to upregulation of genes involved in the uptake and utilisation of free fatty acids (Rakhshandehroo *et al.*, 2010). Many cannabinoid ligands, including anandamide, WIN 55,212-2 and Δ^9-THC have been reported as PPAR agonists *in vitro* (Pertwee *et al.*, 2010).

1.2. Cannabinoid Signalling Pathways

In keeping with the complex pattern of cell and tissue responses to cannabinoid receptor activation, cannabinoid receptors, particularly CB_1, have been shown to interact with a number of intracellular signalling pathways (**Figure 1.2**).

1.2.1. Heterotrimeric G proteins

A large body of research has shown both receptor subtypes to couple predominantly to $G_{i/o}$ (Howlett *et al.*, 2002), whose activation functionally inhibits the enzyme adenylyl cylcase (AC) and thus, production of the intracellular second messenger cAMP, which is involved in the activation of a number of intracellular effectors including cAMP-dependent kinase (PKA). Adding further complexity to the signalling pattern of cannabinoid receptors, CB_1 has been shown to couple to other G proteins. Coupling to G_s proteins has been shown in CB_1-transfected CHO cells (Felder *et al.*, 1998) and cultured rat striatal neurons (Glass & Felder, 1997), in which cAMP accumulation was observed upon stimulation with the CB_1 /CB_2 receptor agonist HU-210 and blocked by the selective CB_1 receptor antagonist rimonabant (SR141716A). However, these experiments were performed in the presence of pertussis toxin (PTX) and forskolin, which artificially increases cAMP levels by directly activating adenylyl cyclase. Other work has shown CB_1 receptor-mediated cAMP accumulation in transfected CHO cells without the inclusion of PTX and forskolin, though only at high agonist concentration (Maneuf & Brotchie, 1997). CB_1-mediated activation of the G_q signalling pathway has also been shown (Lauckner *et al.*, 2005). Stimulation of CB_1-transfected HEK-293 cells and cultured mouse hippocampal neurons with the CB_1/CB_2 receptor agonist WIN 55,212-2 increased intracellular calcium levels. This response was PTX-insensitive, but was blocked by transfected dominant negative $G_{q\alpha}$, which interferes with normal G_q activation.

1.2.2. Mitogen-activated protein kinases

Both receptor subtypes have also been shown to couple positively to members of the mitogen-activated protein (MAP) kinase family of serine/threonine protein kinases which regulate a variety of cellular responses, including gene expression, growth, cellular transformation and apoptosis (Pearson *et al.*, 2001). Extracellular signal-regulated (ERK) MAP kinases are important in the regulation of several cellular processes, including proliferation, division, differentiation and survival (for review see Shaul & Seger, 2007), while c-Jun N-terminal kinases (JNKs) and p38 kinases typically modulate cellular function in response to stressful stimuli, including UV radiation, reactive oxygen species (ROS), heat, osmotic shock and cytokines (Pearson *et al.*, 2001). CB_1 receptor-mediated activation of ERK has been shown in U373MG human astrocytoma (Bouaboula *et al.*, 1995), transfected CHO cells (Galve-Roperh *et al.*, 2002) and Neuro 2a and N1E-115, both murine neuroblastoma cell lines (Graham *et al.*, 2006; Bosier *et al.*, 2008), and via CB_2 receptor in HL-60 cells (Kobayashi *et al.*, 2001), with responses which were PTX-sensitive, suggesting the involvement of $G_{i/o}$ proteins. The mechanism by which cannabinoid receptors activate MAP kinases has not been fully elucidated, but a number of pathways have been suggested, including direct actions via activation of phosphoinositol 3-kinase (PI3K) (Galve-Roperh *et al.*, 2002) and release of the lipid second messenger ceramide, with subsequent activation of Raf, an upstream mediator of the ERK signalling cascade (Sanchez *et al.*, 1998), indirect actions through its effects on cAMP accumulation (Melck *et al.*, 1999), and at least one report of modulation via G_q proteins (Asimaki *et al.*, 2011). In addition, GPCR-dependent ERK activation can be mediated via β-arrestin (see **1.3.1**), which brings various components of the ERK signalling pathway into close proximity, by acting

as a protein scaffold (DeWire *et al.*, 2007). Sprague-Dawley rats treated with the non-selective cannabinoid agonist CP 55,940 showed enhanced levels of β-arrestin and ERK1/2 (Franklin *et al.*, 2013), while ERK activation in CB_1 receptor transfected HEK cells by the CB_1-selective allosteric modulator ORG27569 was nearly abolished by reduced expression of β-arrestin 1 using siRNA (Ahn *et al.*, 2013). Functionally, CB_1 receptor-mediated ERK activation is believed to play a role in synaptic plasticity and neuroprotection, as disruption of CB_1 signalling in hippocampal slices results in synaptic degradation.

Activation of both JNK and p38 kinases has been demonstrated in CB_1-transfected CHO cells (Rueda *et al.*, 2000) and in human primary coronary artery endothelial cells (Rajesh *et al.*, 2010). In addition JNK activation, has been observed in Neuro 2a (He *et al.*, 2005) and N1E-115 cells (Bosier *et al.*, 2008), in which p38 activation could not be detected. The activation of these two MAP kinases appears then, to some degree, to be cell/tissue type selective.

1.2.3. Modulation of ion channel function

Cannabinoid CB_1 receptors are able to regulate the activity of a number of calcium and potassium channels in a positive or negative manner, depending on the channel type. This functionality is thought to contribute significantly to the inhibition of neurotransmitter release from pre-synaptic sites. CB_1 receptors couple positively to voltage-gated rapidly inactivating A-type (Deadwyler *et al.*, 1995) and negatively to non-voltage-gated D-type K^+ channels (Mu *et al.*, 1999) in a PTX-dependent manner as observed in hippocampal neurons. These effects were shown to be mediated by a reduction in cAMP/PKA activity (Hampson *et*

al., 1995; Mu *et al.*, 1999). CB_1 receptors have been shown to couple positively to inwardly rectifying K_{ir} channels in a PTX-dependent manner in a number of systems, including transfected AtT20 (Mackie *et al.*, 1995) and HEK 293 cells (Vasquez *et al.*, 2003) and in mouse nucleus accumbens (Robbe *et al.*, 2001).

N-type Ca^{2+} channels are inhibited by CB_1 receptor activation in NG108-15 cells in a PTX-sensitive, cAMP pathway-independent manner (Mackie & Hille, 1992). This negative coupling to N-type channels has also been observed in rat superior cervical ganglion neurons (Pan *et al.*, 1996) and striatal neurons (Huang *et al.*, 2001). P/Q-type Ca^{2+} channels have also been shown to be negatively regulated via CB_1 receptors in a number of systems (Mackie *et al.*, 1995). In contrast to CB_1, CB_2 receptors have not been shown, as yet, to regulate ion channels.

1.2.4. Calcium ion flux

Activation of cannabinoid receptors can lead to increased free intracellular calcium concentration, $[Ca^{2+}]_i$, via release from internal stores. The classical pathway for the increase of cytoplasmic $[Ca^{2+}]$ is via phospholipase C (PLC), which cleaves phosphoinositol 4,5-bisphosphate, producing the second messengers diacylglycerol (DAG) and inositol 1,4,5-trisphosphate ($IP_{3)}$. DAG promotes activation of protein kinase C (PKC), while IP_3 causes release of Ca^{2+} from intracellular stores via activation of IP_3 receptors present on endoplasmic reticulum. Agonist stimulation of neuroblastoma/glioma hybrid NG108-15 cells produced an increase in $[Ca^{2+}]$i, which was blocked by PTX and rimonabant (Sugiura *et al.*, 1996). This response was subsequently shown to be blocked by the phospholipase C inhibitor U73122 (Sugiura *et al.*, 1997). CB_1 receptor promotion

of intracellular Ca^{2+} responses has also been reported in rat cerebellar granule neurons where it was also blocked by PTX, rimonabant, U73122 and the IP_3 receptor antagonist xestospongin C (Netzeband *et al.*, 1999). The data indicate that CB_1 receptors are able to couple to the PLC signalling pathway via $G_{i/o}$ proteins. CB_2 receptors have also been shown to couple to this pathway in calf pulmonary endothelial cells (Zoratti *et al.*, 2003). Other pathways coupling CB_1 receptors to the intracellular Ca^{2+} response have been described, including calcium release from internal stores via an IP_3-independent, arachidonic acid-dependent pathway (Begg *et al.*, 2001; Demuth *et al.*, 2005), and activation of G_q proteins (Lauckner *et al.*, 2005).

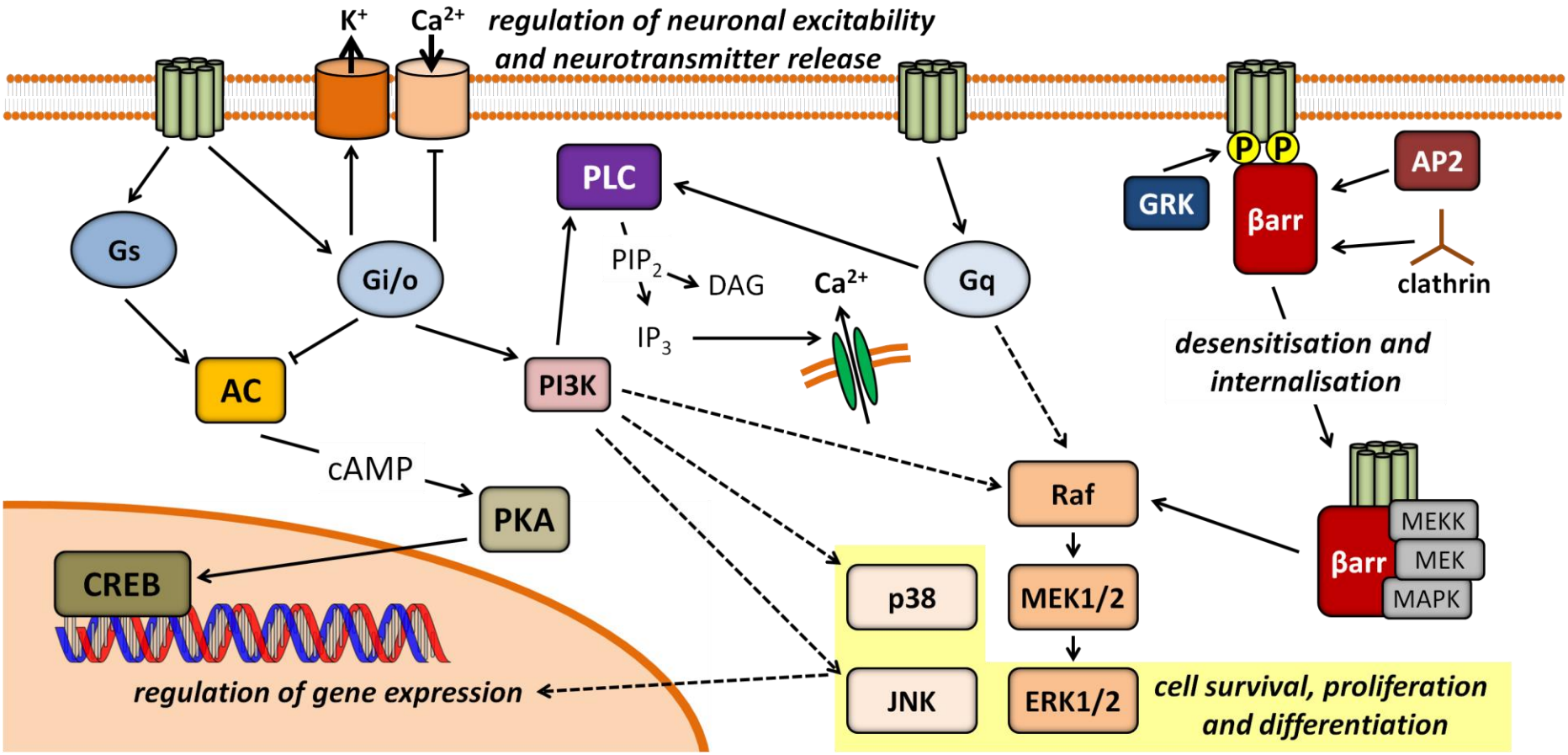
K+
Ca2+
regulation of neuronal excitability
and neurotransmitter release
Gs
Gi/o
PLC
PIP2
DAG
IP3
Ca2+
Gq
GRK
P
P
βarr
AP2
clathrin
desensitisation and
internalisation
AC
PI3K
cAMP
PKA
Raf
βarr
MEKK
MEK
MAPK
CREB
p38
MEK1/2
JNK
ERK1/2
cell survival, proliferation
and differentiation
regulation of gene expression

Figure 1.2 Cannabinoid post-receptor signalling. The CB_1 receptor couples predominantly to $G_{i/o}$ proteins, which inhibit the function of adenylyl cyclase, resulting in inhibition of the function of the cAMP-dependent kinase, PKA. $G_{i/o}$ protein-dependent modulation of various potassium and calcium ion channels allows the CB_1 receptor to regulate neuronal excitability and neurotransmitter release, in line with the endogenous cannabinoid ligands' role as retrograde neurotransmitters, inhibiting pre-synaptic neuronal activity. However, in certain cases, the CB_1 receptor has also been shown to couple to other G proteins, including G_s, which, in contrast to $G_{i/o,}$ activates AC, and G_q protein, which activates phospholipase C (PLC), resulting in release of calcium ions from intracellular stores and activation of protein kinase C . Cannabinoid receptors couple positively to several members of the mitogen-activated protein kinase superfamily, including ERK, JNK and p38. In particular, cannabinoid activation of ERK has been demonstrated via several distinct pathways, including via $G_{i/o}$ and G_q proteins and via β-arrestin, which is typically recruited to activated receptor as part of the processes of desensitisation and clathrin-dependent internalisation, but also promotes receptor signalling by acting as a scaffold protein for the recruitment of other signalling pathway mediators. Activated effector protein kinases including PKA and ERK modulate an array of transcription factors, thus altering gene expression.

Dashed lines represent incompletely defined signalling cascades.

1.3. Modulation of Cannabinoid Receptor Signalling

1.3.1. Receptor Regulation

Persistent ligand binding to GPCRs can produce a series of adaptations in receptor functionality and expression. GPCR *desensitisation* is characterised by attenuation of receptor-mediated effector activity, typically via phosphorylation of intracellular domains which prevent receptor interaction with signalling pathway effectors, such as G proteins, and promotes interaction with modulators of receptor desensitisation such as arrestin proteins (see below). Subsequently, GPCR *internalisation* may occur where receptors are sequestered to intracellular vesicles by endocytosis. Once internalised, receptors may be either recycled to the cell membrane or degraded in lysosomes via hydrolytic enzymes. *Downregulation* is a reduction in the receptor population as a result of receptor internalisation and degradation and/or a reduction in receptor gene expression.

Desensitisation and downregulation of CB_1 receptor has been reported in a number of endogenous and exogenous systems. Reduction in [^{35}S]GTPγS binding and/or B_{max} (receptor density) values, determined by measuring radioligand binding, have been observed upon chronic stimulation with Δ^9-THC (Sim *et al.*, 1996; Breivogel *et al.*, 1999), anandamide (Rubino *et al.*, 2000), CP 55,940 (Rubino *et al.*, 1997) and WIN 55,212-2 (Sim-Selley & Martin, 2002) in several distinct brain regions, and cultured cell lines. Furthermore, immunocytochemical staining demonstrates a reduction in the membrane receptor density upon stimulation with cannabinoid agonists (Hsieh *et al.*, 1999). Interestingly, the pattern of desensitisation and downregulation is tissue-dependent, which can be explained by the tissue-dependent expression of various effectors.

Receptor phosphorylation is promoted by a number of effectors, including the second messenger-dependent kinases PKA and PKC, and GPCR-regulating kinases or GRKs, which have higher affinity for active receptor conformations. Arrestins are proteins which bind to phosphorylated receptors, causing further reduction in receptor-signalling pathway coupling and promotion of receptor internalisation by facilitating binding with clathrin and the clathrin adaptor molecule AP2, which are important components of clathrin-mediated endocytosis. Interestingly, β-arrestins are also known to mediate GPCR signalling, particularly ERK activation, by acting as scaffolding proteins, as stated in section **1.2.2** (Lefkowitz & Whalen, 2004).

There is evidence to suggest that GRK and β-arrestin proteins play a role in CB_1 receptor regulation. Co-expression of GRK3 and β-arrestin 2 in *Xenopus* oocytes expressing rat CB_1 receptors significantly enhanced receptor desensitisation upon acute stimulation with WIN 55,212-2 (Jin *et al.*, 1999) and prolonged (18-24 hr) perfusion of rat hippocampal neurons with WIN 55,212-2 resulted in desensitisation of the agonist-mediated inhibition of $[Ca^{2+}]_i$ flux via voltage-gated calcium ion channels (Kouznetsova *et al.*, 2002). Receptor desensitisation was prevented by dominant negative mutants of GRK2 and β-arrestin 2, which block the function of their endogenous protein counterparts. Chronic treatment with the major phytocannabinoid tetrahydrocannabinol (Δ^9-THC) in mice increased levels of GRK 2 and 4 and β-arrestin 1 and 2, but not GRK 5 and 6 (Rubino *et al.*, 2006). This upregulation was present in hippocampus and prefrontal cortex, but absent in striatum and cerebellum of Ras-GRF1-null mice, providing further evidence of tissue-dependant receptor regulation.

The intracellular C-terminal tail of the CB_1 receptor appears to be important in GRK/arrestin-mediated CB_1 desensitisation. Mutation of putative phosphorylation sites at residues 460-463 prevented receptor internalisation in transfected AtT20 cells (Hsieh *et al.*, 1999). Subsequent research by the same group showed that mutation of phosphorylation sites at residues 426 and 430 attenuated desensitisation (Jin *et al.*, 1999), but had no effect on receptor internalisation. Together, the data indicate that pathways regulating desensitisation and internalisation involve distinct receptor domains, and that GRK/arrestin activity is not required for internalisation of CB_1 receptors.

Despite the evidence linking GRK/arrestin activity to CB_1 desensitisation, little evidence for direct interaction of these proteins currently exists, with no reports of CB_1 co-immunoprecipitation with GRK or arrrestins, and a recent study using bioluminescence resonance energy transfer (BRET) to measure protein proximity finding only weak interaction between the receptor and β-arrestin 2 (Vrecl *et al.*, 2009). The DiscoveRx PathHunter® β-arrestin receptor activation assays utilise β-arrestin recruitment to the receptor to give a measure of receptor activation with published examples of its use at the CB_2, GPR55 and GPR18 receptors present in the literature (McGuinness *et al.*, 2009; Yin *et al.*, 2009). Cells are transfected with modified receptor and β-arrestin, each tagged with complementary fragments of a β-galactosidase enzyme. Arrestin recruitment to the receptor forces the complementation of the two fragments to give a functioning enzyme which can be detected by the addition of substrate. Such assays have demonstrated that the cannabinoid receptors do interact with β-arrestin, albeit in an artificial system.

1.3.2. Receptor-Receptor Interaction

It is now well established that GPCRs are able to interact with each other to form multimeric complexes; indeed, it is generally believed that the majority of receptor activity involves such complexes. Receptor-receptor interactions may be either homomeric, involving receptors of the same type, or heteromeric, involving different receptor types. A CB_1 C-terminal polyclonal antibody exclusively labelled a high molecular weight form of the CB_1 receptor, consistent with homodimerized receptors in Sprague-Dawley rat brain (Wager-Miller *et al.*, 2002), which has been shown to be present in rat hippocampus (Hajos *et al.*, 2000; Wager-Miller *et al.*, 2002) and amygdala (Katona *et al.*, 2001) *in vivo*. The physiological role of CB_1 receptor homomers has yet to be identified.

CB_1 receptors have been shown to form heterodimers with a number of class A GPCRs. CB_1 and dopamine D_2 receptors have been co-immunoprecipitated from transfected HEK-293 cells (Kearn *et al.*, 2005) while BRET techniques have provided more direct evidence of receptor heterodimerisation (Navarro *et al.*, 2008). BRET analysis in live cells has also revealed direct CB_1 interactions with δ-, κ-, and μ-opioid receptors (Rios *et al.*, 2006). Other studies show CB receptor interactions with adenosine A_{2A} (Carriba *et al.*, 2007) and orexin OX_1 receptors (Ellis *et al.*, 2006).

One functional role of these receptor heterodimers appears to be modulation of receptor-coupled signalling responses. Dual activation of CB_1 receptors and dopamine D_2 receptors in cultured rat striatal neurons resulted in switching of CB_1 signalling from inhibition of adenylyl cyclase to PTX-insensitive AC stimulation

(Glass & Felder, 1997). Unstimulated D_2 receptor dimerization was also shown to have a similar effect on CB_1 receptor-mediated signalling in transfected HEK 293 cells (Jarrahian *et al.*, 2004). Stimulation of μ-opioid receptors resulted in a significant decrease in CB receptor-mediated G protein activation and ERK1/2 phosphorylation in endogenously and exogenously expressing cell lines respectively, indicating a functional role for opioid/cannabinoid dimers (Rios *et al.*, 2006).

Many questions have yet to be answered regarding CB_1 receptor-receptor interactions, including the elucidation of which other GPCRs can form heterodimers with CB_1, which CB_1 receptor domains are important for dimerisation and what is the full functional role of these heterodimers and CB_1 homomers (Mackie, 2005).

1.3.3. Other Receptor-Interacting Proteins

A number of other proteins are known to interact with GPCRs and cannabinoid receptors in particular. The GPCR-associated sorting protein GASP1 is a large protein shown to facilitate downregulation of certain GPCRs such as δ-opioid (Whistler *et al.*, 2002) and dopamine D_2 receptors (Bartlett *et al.*, 2005). GASP1 interacts with the intracellular tail domain of the receptor and promotes receptor trafficking to lysosomes for proteolytic degradation (Bartlett *et al.*, 2005). The dominant-negative C-terminal GASP1 fragment, cGASP reduced CB_1 receptor localisation to lysosomes, reduced receptor degradation and enhanced receptor recycling to the cell surface when co-expressed in HEK 293 cells. GASP1 interacted with a fusion protein containing the CB_1R C-terminal tail (Martini *et*

al., 2007), and endogenous GASP1 co-immunoprecipitated with CB_1R from transfected cells and rat brain tissue (Martini *et al.*, 2007; Tappe-Theodor *et al.*, 2007). Interestingly, mutations at the putative phosphorylation sites 460 and 464 did not interfere with co-immunoprecipitation of the receptor with GASP1, suggesting that these motifs do not play a role in CB_1/GASP1 interaction (Tappe-Theodor *et al.*, 2007). cGASP1 also decreased levels of receptor downregulation in cultured neurons (Tappe-Theodor *et al.*, 2007). cGASP1 had no effect on the rate or degree of receptor internalisation. *In vivo* administration of cGASP1 via a viral vector prevented analgesic tolerance to WIN 55,212-2 in rats (Tappe-Theodor *et al.*, 2007). Together, this research strongly indicates that GASP1 plays an important role in receptor downregulation by facilitating receptor localisation to lysosomes and subsequent receptor degradation.

A family of novel cannabinoid receptor-interacting proteins (CRIP) comprising two splice variants, $CRIP_{1a}$ and $CRIP_{1b}$ have been identified (Niehaus *et al.*, 2007). These proteins interact with the C-terminal domain of the CB_1 receptor at sites distinct from the phosphorylation sites involved in desensitisation and internalisation. $CRIP_{1a}$ orthologues are present in a number of vertebrates. $CRIP_{1a}$ was shown to decrease constitutive inhibition of voltage-gated calcium channels in superior cervical ganglion neurons transfected with CB_1, while having no effect on agonist-induced inhibition, suggesting a role in regulating constitutive receptor activity. $CRIP_{1b,}$ thus far, has only been identified in primates, with an, as yet, unknown function.

1.4. Cannabinoid Ligands

1.4.1. Endogenous Cannabinoids

The endogenous cannabinoid receptor ligands or endocannabinoids are eicosanoids, with the two most studied endocannabinoids to date being *N*-arachidonoyl ethanolamine (anandamide or AEA; **Figure 1.3**) and 2-arachidonoyl glycerol (2-AG). Other, putative endocannabinoids include 2-arachidonyl glyceryl ether (noladin ether) (Hanus *et al.*, 2001), *N*-arachidonoyl dopamine (NADA) (Huang *et al.*, 2002b) and *O*-arachidonoyl ethanolamine (virodhamine) (Porter *et al.*, 2002). Anandamide was the first endocannabinoid to be isolated and identified and its name derives from the Sanskrit word '*ananda*', meaning 'bliss' (Devane *et al.*, 1992). A number of pathways for the biosynthesis of AEA from the precursor *N*-arachidonoyl phosphatidylethanolamine (NArPE) have been proposed, with the enzyme NAPE-PLD being the most widely accepted (Sagar *et al.*, 2009). Others include the PLC-PTPN22 and αβh4 enzymatic pathways, which together with the NAPE-PLC pathway may combine to form an integrated system in which one pathway compensates if another is downregulated (Liu *et al.*, 2008). Biosynthesis of the acyl glycerol 2-AG from the immediate precursor diacylglycerol (DAG) is less well characterised but is believed to involve postsynaptically located DAG lipases and, potentially, a phospholipase A1 and phospholipase C complementary pathway (Sagar *et al.*, 2009). Endocannabinoid synthesis in the CNS occurs mainly at post-synaptic neuronal sites in a transient or 'on-demand' manner and they are believed to act as retrograde signalling molecules inhibiting pre-synaptic neuronal activity. Endocannabinoids are thus described as 'non-classical' neurotransmitters, in contrast to classical neurotransmitters which are pre-synthesised and stored in vesicles.

Endocannabinoids are hydrolysed post-synaptically by hydrolase pathways with fatty acid amide hydrolase (FAAH) and monoacylglycerol lipase (MAGL) being the most prominent metabolic routes for AEA and 2-AG respectively (Sagar *et al.*, 2009). The oxidative enzyme cyclooxygenase type-2 (COX-2) also metabolises these two endocannabinoids.

In terms of its pharmacology, anandamide is a CB_1/CB_2 ligand with moderate nanomolar affinity (**Table 1.1**). The inclusion of a non-specific amidase inhibitor, such as phenylmethylsulfonylfluoride (PMSF) is usually a pre-requisite when using anandamide, and indeed most endocannabinoids, in assays involving intact tissue preparations, to prevent degradation of the endocannabinoid by endogenous hydrolase activity. Interestingly, anandamide appears to act as a partial agonist in a number of *in vitro* functional assays and shows modest (~5-fold; **Table 1.1**) CB_1 receptor selectivity. Anandamide has also been conclusively shown to act as an agonist at TRPV1 (see **1.1**), a non-selective cation channel involved in neuronal detection of noxious physical and chemical stimuli.

2-AG, like anandamide, exhibits marginal CB_1 selectivity (~3-fold; **Table 1.1**) with a reported affinity in the low micromolar range; significantly lower than that reported for anandamide. However, unlike anandamide, 2-AG appears to be a full agonist at the CB_1 receptor, or at least has higher activity than anandamide, with a number of functional studies reporting quantitatively similar results to those found with other more prominent full agonists, including R-(+)-WIN 55,212-2 (Howlett *et al.*, 2002).

Noladin ether, an ether of 2-AG, has affinity for both receptor types, but the data available thus far indicate that it is significantly (140-fold; **Table 1.1**) CB_1 receptor-selective. Virodhamine is reported as an endogenous *in vivo* CB_1 antagonist, while acting as a full agonist at the CB_2 receptor (Porter *et al.*, 2002). *N*-arachidonoyl dopamine (NADA) was initially synthesised as part of a larger series of *N*-acyl dopamines (Bisogno *et al.*, 2000), but was later identified as an endogenous molecule in rat and bovine neuronal tissue (Huang *et al.*, 2002b). NADA appears to be CB_1 receptor-selective, but still has micromolar affinity for CB_2 receptors expressed in rat spleen tissue. NADA was reported as being 45-fold more potent than anandamide in eliciting intracellular Ca^{2+} increase in neuroblastoma cells, but still produced a sub-maximal response compared to HU-210. NADA appears to be a TRPV1 agonist, with potency significantly greater than that reported for anandamide. This has led some to the conclusion NADA is a putative endogenous TRPV1 ligand, or endovanilloid (Huang *et al.*, 2002b).

The endocannabinoids can be seen as part of a larger group of well established cannabinoid receptor agonists of which the 'classical', 'non-classical' and aminoalkylindole cannabinoids are the other prominent members. Each group is comprised of lipophillic compounds which bind to CB_1 and CB_2 receptors with high affinity but have distinct chemical structures (**Figure 1.3**).

Table 1.1
K_i values for cannabinoid ligands determined via *in vitro* displacement of radioligand, in nM (adapted from Howlett *et al*. 2002)

Ligand	**CB_1 K_i value**	**CB_2 K_i value**
Anandamide	61[a, b]	1930[a, c]
	89[a]	371[a]
	543	1940
	71.7[a, b]	279[a, b]
	252[b]	581
2-arachidonoyl glycerol	472[b]	1400
	53.8[d]	145[d]
Noladin Ether	21.2[b]	>3000
R-(+)-methanandamide	17.9[a, b]	868[a, c]
	20[a, b]	815[c]
ACEA	1.4[a, b]	>2000[a, b]
Δ^9-THC	53.3	75.3
	39.[5b]	40
	40.7	36.4
	80.3[b]	32.2
	35.3[b]	3.9[b]
HU-210	0.0608	0.524
	0.1[b]	0.17
	0.73	0.22
CP 55,940	5	1.8
	3.72	2.55
	1.37[b]	1.37[b]
	0.58	0.69
	0.50[a, b]	2.80[a, b]
R-(+)-WIN 55,212-2	9.94[b]	16.2[b]
	4.4[a, b]	1.2[a, b]
	1.89	0.28
	62.3	3.3
	123	4.1
Rimonabant	11.8	13,200
(SR 141716A)	11.8	973
	12.3	702
	5.6	>1000
	1.98[b]	>1000[b]

[a] with phenylmethylsulfonyl fluoride
[b] binding to rat receptor
[c] binding to mouse receptor
[d] species unspecified. All other data from experiments using human receptor

1.4.2. Classical Cannabinoids

Classical cannabinoid agonists contain ABC-tricyclic dibenzopyran rings and are either naturally occurring phytocannabinoids in the *Cannabis sativa* plant or are synthetic derivatives of natural compounds. The most prominent phytocannabinoid is the archetypal cannabinoid Δ^9-tetrahydrocannabinol (Δ^9-THC; **Figure 1.3**), which was the first cannabinoid agonist identified and is the main psychoactive constituent of cannabis. Δ^9-THC exhibits nanomolar affinity for cannabinoid receptors, with similar affinity for both CB_1 and CB_2 receptors (**Table 1.1)**. Like anandamide, Δ^9-THC acts as a partial agonist at the CB_1 receptor, with an apparent intrinsic efficacy significantly lower than that of reported full agonists such as CP 55,940 and R-(+)-WIN55,212-2 (Howlett *et al.*, 2002). The intrinsic activity of Δ^9-THC at CB_2 receptors is even lower than at the CB_1 receptor, with a number of functional activity experiments showing Δ^9-THC to act as an antagonist. Other prominent phytocannabinoid agonists include Δ^8-THC, which exhibits similar potency and efficacy for the two CB receptor types as Δ^9-THC, and the weak agonist cannabinol, a Δ^9-THC metabolite (Howlett *et al.*, 2002).

One of the most widely employed synthetic phytocannabinoid analogues is 11-hydroy-Δ^9-THC-dimethylheptyl (HU-210) (**Figure 1.3**). Like Δ^9-THC, HU-210 has similar affinity for both CB_1 and CB_2 receptors, but has a significantly (~100 - 700 fold) higher affinity for the receptors than Δ^9-THC. Also, unlike Δ^9-THC, HU-210 is a full CB receptor agonist, with intrinsic activity comparable to other full agonists. Most phytocannabinoids and first-generation synthetic analogues, such as HU-210 are non-selective for the two CB receptor types; however, more

recently developed compounds such as HU-308, JWN-051 and L-759633, exhibit CB_2 receptor selectivity.

1.4.3. Non-Classical Cannabinoids

Non-classical cannabinoids lack the dihydropyran ring structure, instead being bi- or tri-cyclic analogues. The best known compound from this group is the bicyclic CP 55,940 (2-[(1R,2R,5R)-5-hydroxy-2-(3-hydroxypropyl) cyclohexyl]-5-(2-methyloctan-2-yl)phenol; **Figure 1.3**), which is routinely used as a reference agonist or radiolabelled tracer in CB receptor binding assays. It is not selective for either CB receptor type with affinity within the nanomolar range, but it is reported as having lower affinity than HU-210 (**Table 1.1**). CP 55,940 has a similar potency and intrinsic activity at CB receptors as HU-210 as reported in a number of various functional assays (Howlett *et al.*, 2002). Another prominent bicyclic cannabinoid agonist is CP 47,497, the first non-classical analogue produced, which has high affinity and potency at both receptor types and acts as a full agonist. The tricyclic analogue CP 55,244 is reported to have a higher potency for CB receptors than HU-210, and several studies show it to have a higher intrinsic activity than most other current cannabinoid agonists.

1.4.4. Aminoalkylindoles

Aminoalkylindoles are cannabinoid agonists structurally unrelated to Δ^9-THC and the other classical and non-classical agonists and are derived from the non-steroidal anti-inflammatory drug-like compound pravadoline. The most prominent compound within this group is R-(+)-WIN 55,212-2, which exhibits high affinity for both receptor types and modest (~8-fold; **Table 1.1)** CB_2 receptor selectivity

(**Figure 1.3**). Like HU-210 and CP 55,940, WIN 55,212-2 is commonly used in functional receptor assays as a reference agonist. More recently synthesised aminoalkylindole compounds include JWH-015 and L-768242, exhibit greater CB_2 receptor selectivity (Howlett *et al.*, 2002).

1.4.5. Diarylpyrazoles

The main family of cannabinoid receptor inverse agonists and antagonists are the diarylpyrazole series. SR 141716A, now known officially as rimonabant, is a high affinity CB_1 receptor-selective ligand (**Table 1.1; Figure 1.3**). It was one of the first compounds from this group identified and is commonly used in *in vitro* and *in vivo* experiments to antagonise responses mediated by cannabinoid agonists. Next-generation analogues of SR141718A have been developed which have increased CB_1 receptor selectivity, with AM 251 being a good example. Unlike the other groups of cannabinoid ligands, a number of diarylpyrazoles exhibit high CB_2 receptor selectivity, including SR144528.

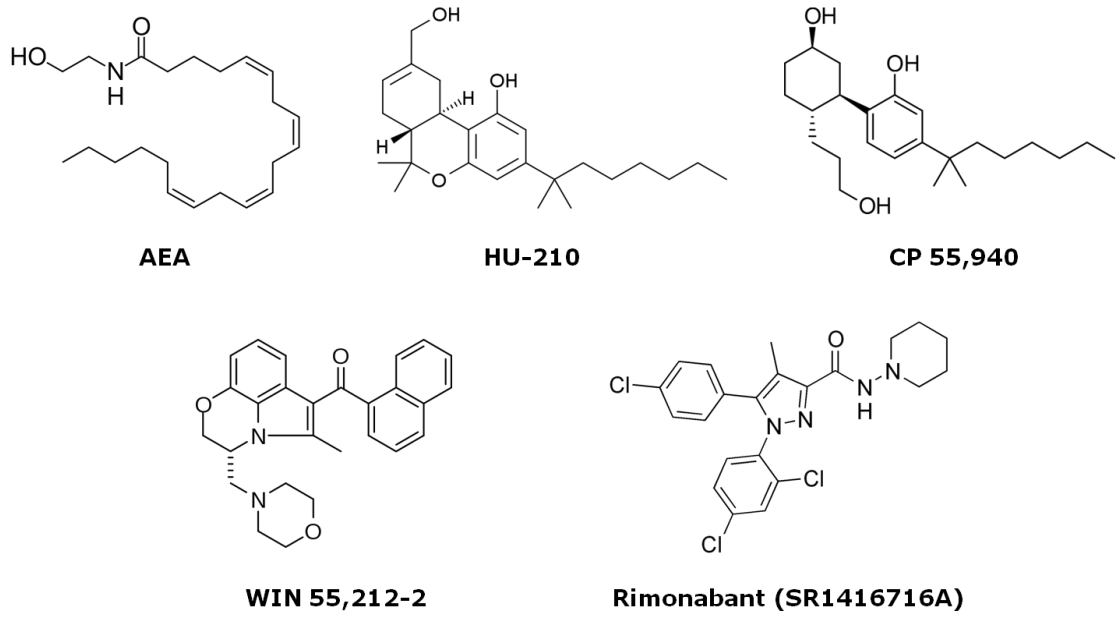

Figure 1.3 Structures of cannabinoid receptor ligands. An example from each of the main groups of ligands is present.

1.4.6. *In vivo* effects of cannabinoid ligands

Due to the abundance of CB_1 receptors in the CNS, and the important role the cannabinoid system plays in the modulation of neuronal excitability and modulation of neurotransmitter release, cannabinoid agonists exert well characterised psychotropic effects when administered *in vivo*. Some therapeutically beneficial effects include analgesia, antiemetic effects, appetite stimulation, and decreased GI motility, while potentially unwanted side effects include sedation, euphoria, dysphoria and effects of cognition and memory (for review see Howlett *et al.*, 2002). The standard animal model for characterising the effects of cannabinoid ligands at the CB_1 receptor *in vivo* is the tetrad test, which measures effects on antinociception, catalepsy, hypoactivity and hypothermia in

rodents, with a general correlation between ligand binding affinity at the CB_1 receptors, and the potencies in the four behavioural assays.

CB_1 receptor antagonists/inverse agonists, both block the psychotropic effect of pre-administered cannabinoid agonist, and exert opposing effects to those of the agonists, including suppression of appetite and improvements to short term memory, when administered alone. Rimonabant was developed as an anorectic, anti-obesity drug and was approved for sale in the European Union in 2006; however it was shortly after removed from the market, due to increased incidents of depression and suicidal thoughts in patients.

1.4.7. Other cannabinoid ligands

More recently, a family of novel, endogenous peptide cannabinoid receptor ligands has been reported (Gomes *et al.*, 2010). Enzyme-substrate capture analysis of proteosome-generated peptide fragments led to the identification of a nine-residue peptide (PVNFKFLSH) derived from the haemoglobin-α chain which caused hypotension in anesthetised rats, leading to the name hemopressin (Rioli *et al.*, 2003) (**Figure 1.4**). Hemopressin and the C-terminally truncated fragments PVNFKF and PVNFKFL were subsequently shown to exhibit orally active antihyperalgesic activity in a rat model of experimental pain induced by carrageenan and bradykinin (Dale *et al.*, 2005). Furthermore, this effect was not mediated via opioid receptors as the response was insensitive to the opioid receptor antagonist naloxone. A number of *in vitro* assays have shown hemopressin to be a highly CB_1-selective inverse agonist, effectively blocking HU-210-induced functional responses (Heimann *et al.*, 2007). A subsequent study

using an affinity purification approach in mouse brain identified two N-terminally extended peptide fragments - RVD-hemopressin-α and VD-hemopressin-α derived from the haemoglobin α-chain and VD-hemopressin-β derived from the β-chain (Gomes *et al.*, 2009). All three peptide fragments exhibit nanomolar affinity for CB receptors present in mouse cerebellum and were shown to be potent CB receptor agonists with RVD-Hpα and VD-Hpα being CB_1 receptor-selective, while VD-Hpβ exhibited similar activity at both receptor subtypes. Several attempts to replicate these initial finding were unsuccessful, and it was postulated that the ligands form peptide aggregates in aqueous solution, precluding them from the receptor binding site. Most recently it was shown that RVD-Hpα, and a range of further N-terminally extended peptides (termed Pepcans) acted as negative allosteric modulators of the CB_1 receptor, which may explain the atypical pharmacology previously reported (Bauer *et al.*, 2012).

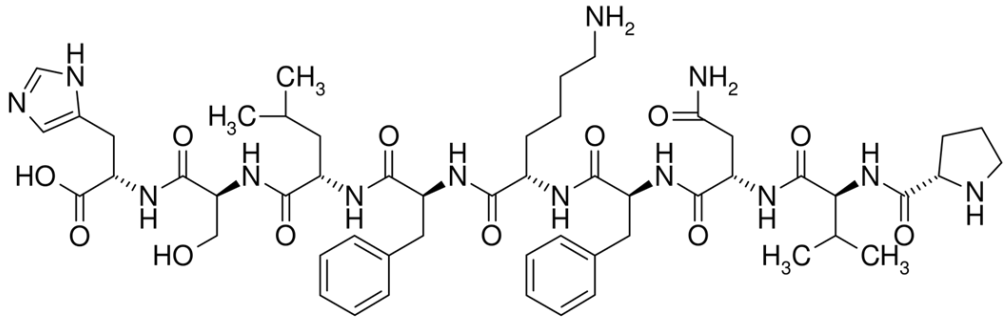

Figure 1.4 Structure and amino acid sequence of hemopressin peptide.

Yangonin, one of six major kavalactones present in the kava plant (*Piper methysticum*) was shown to possess significant affinity for the CB_1 receptor in

[^{3}H]-CP 55,940 competition binding assays, which may account for some of the intoxicating effects of kava ingestion (Ligresti *et al.*, 2012).

1.4.8. Cannabinoid Allosteric Modulators

GPCRs are able to interact with compounds termed 'allosteric modulators', which are proposed to interact with binding sites on the receptor which are topographically distinct from the binding site of the endogenous ligand, termed the orthosteric binding site, allowing them to alter the binding and functional properties of orthosteric agonists (Christopoulos & Kenakin, 2002). The first allosteric modulators at cannabinoid receptors to be reported were a series of novel compounds developed by Organon - Org 27569 (5-chloro-3-ethyl-1*H*-indole-2-carboxylic acid [2-(4-piperidin-1-yl-phenyl)-ethyl]-amide), Org 27759 (3-ethyl-5-fluoro-1*H*-indole-2-carboxylic acid [2-94-dimethylamino-phenyl)-ethyl]-amide) and Org 29647 (5-chloro-3-ethyl-1*H*-indole-2-carboxylic acid (1-benzyl-pyrrolidin-3-yl)-amide, 2-enedioicacid salt); **Figure 1.5**) (Price *et al.*, 2005). Using radioligand binding assays, the compounds were shown to interact non-competitively at CB_1 receptors, including partial displacement of [^{3}H]-rimonabant and facilitation of [^{3}H]-CP 55,940 binding in mouse brain membranes. The compounds appear to negatively modulate agonist-induced responses, which is in contrast to their positive facilitation of agonist binding, which goes against the standard notion of agonist efficacy being positively coupled to occupancy. Stimulation of mouse vans deferens with WIN 55,212-2 produced an inhibition of electrically-evoked tissue contraction and this inhibition was attenuated by all three compounds in a concentration-dependent manner, with no significant change in WIN 55,212-2 potency (Price *et al.*, 2005). The compounds were also shown to

reduce [^{35}S]GTPγS binding significantly in CP 55,940 and anandamide-stimulated mouse brain (Price *et al.*, 2005).

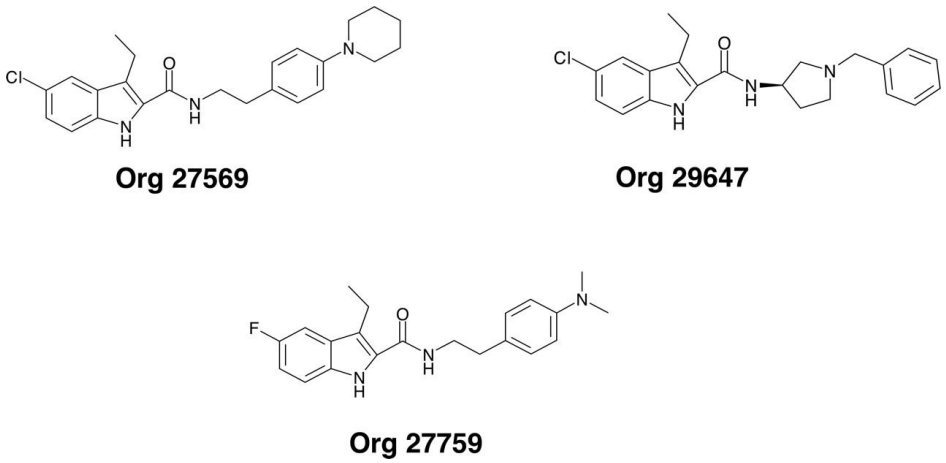

Figure 1.5 Structure of Organon compounds Org 27569, Org 29647 and Org 27759 (adapted from Price et al. 2005).

A second series of novel synthetic molecules, typified by the compound PSNCBAM-1 (4-chlorophenyl)-3-[3-(6-pyrrolidin-1-ylpyridin-2-yl)phenyl]urea); **Figure 1.6**) were also shown to be negative allosteric modulators (Horswill *et al.*, 2007). As with the Organon compounds, PSNCBAM-1 partially displaced [^{3}H]-rimonabant and facilitated [^{3}H]CP 55,940 binding, this time in HEK293-hCB$_1$ cell membranes. PSNCBAM-1 appears to act as a negative modulator, producing a robust concentration-dependent decrease in the intrinsic activity of CP 55,940-stimulated [^{35}S]GTPγS binding in HEK293-hCB$_1$ membranes, with no significant effect on potency. PSNCBAM-1 also reversed the CP 55,940- and anandamide-induced decrease in cAMP accumulation in HEK293-hCB$_1$ cells stimulated with forskolin. These results are consistent with PSNCBAM-1 acting as an allosteric

modulator, and are similar to the results seen for the Organon compounds. This is not surprising as they share common structural features, suggesting their pattern of receptor binding and alteration of receptor conformation may be similar. More recent studies of PSNCBAM-1 (Wang *et al.*, 2011), confirmed its activity as a non-competitive antagonist of CP 55,940- and WIN 55,212-2-stimulated [^{35}S]GTPγS binding in cerebellar membranes from C57BL/6 mice. Interestingly, however, PSNCBAM-1 exhibited agonist-selective potency, with a significantly higher potency for the CP 55,940-bound receptor than the WIN 55,212-2-bound receptor in cerebellar and HEK293-hCB_1 membranes. This suggests that CP 55,940 and WIN 55,212-2 induce distinct receptor conformations and highlights the potential of allosteric modulators as tools for analysing the molecular mechanisms behind ligand-induced differential signalling (see below).

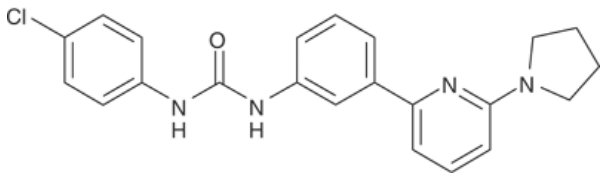

Figure 1.6 Structure of PSNCBAM-1 (adapted from Horswill et al, 2007).

A study by Navarro *et al.* (2009) suggested that a number of dopamine transporter inhibitors including the 3-phenyltropane RTI-371 (3b-(4-methylphenyl)-2b-[3-(4-chlorophenyl)isoxazol-5-yl]tropane) and the benzotropane JHW-007 (N-butyl-3a-[bis(4-fluorophenyl)methoxy]tropane) may exhibit allosteric modulation of CB_1 receptors (Navarro *et al.*, 2009). CP 55,940-stimulated calcium mobilisation in

RD-HGA16 cells (CHO cell line over-expressing the promiscuous G protein $G_{\alpha 16}$) transfected with hCB_1 was enhanced by a number of DAT inhibitors, suggesting a positive allosteric effect. However, some of the compounds were also shown to be non-competitive antagonists of μ-opioid receptors, which, along with their actions as DAT inhibitors, complicates their pharmacological profile.

1.5. Functional Selectivity

1.5.1. Concept and Background

Classical pharmacological theory holds that a GPCR exists in one of two distinct structural conformations - an active conformational state (R*) which couples to and activates downstream effectors, and an inactive state (R) which does not. Under basal conditions, a receptor population is comprised of receptors in both states, resulting in a constitutive level of effector activation. Agonists are ligands which preferentially bind to the active receptor conformation. This increases the ratio of the receptor population in the active state which in turn increases the level of receptor-mediated effector activation. Inverse agonists bind preferentially to the inactive receptor conformation causing a decrease in the ratio of active to inactive receptors and, therefore, a decrease in the constitutive activity. Antagonists exhibit no preference for either receptor conformation, do not change the active to inactive ratio and so have no appreciable effect on receptor-coupled effectors (Kenakin, 2001).

In this model, the GPCR can be seen as an ‘on/off’ switch, for which all agonists produce the same pattern of receptor activation in a concept known as *intrinsic efficacy*. The observation that some agonists produce sub-maximal functional

responses, described as partial agonism, is explained as lower (but still significant) increases in the ratio of receptor in the active conformation, relative to full agonists.

While this theory has been well established for decades, it is too simplistic to explain the complex pattern of pharmacology seen with a number of GPCRs. *Functional selectivity* (also known as agonist-directed trafficking or ligand–induced differential signalling) can be defined as the ability of a ligand to differently activate specific signalling pathways and can be expressed as differences in ligand potency and/or intrinsic activity in relation to a functional effect (e.g. activation of a particular second messenger) compared to one or more others (Urban *et al.*, 2007; Hudson *et al.*, 2010).

This extended theory posits that GPCRs, like other proteins, can adopt multiple distinct structural conformations, importantly, more than one active conformational state (i.e. R^{*1}, R^{*2}, R^{*3}, R^{*n} etc). Most GPCRs, including the cannabinoid receptors, orthosterically bind a number of structurally distinct endogenous and exogenous ligands. Each ligand may preferentially bind to a subset of active receptor conformations and each active receptor conformation may interact with a distinct set of downstream effectors resulting in ligand-dependent receptor signalling.

This phenomenon has been reported with increasing prevalence in the last decade for a number of GPCRs including adrenergic, muscarinic, dopamine and serotonin receptors (Urban *et al.*, 2007). For example, the 5-HT_2 receptor subgroup

independently couples, under the influence of different agonists, both to the PLC/Ca^{2+} signalling pathway via activation of $G_{q/11}$, and the PLA_2 signalling pathway which generates arachidonic acid (AA) from membrane lipids. Ligands acting at both the 5-HT_{2A} and 5-HT_{2C} receptors are able to differentially activate these two signalling pathways (Berg *et al.*, 1998).

Ligand-directed functional selectivity is not limited to receptor-coupled signal transduction pathways, but may include other consequences of receptor/ligand interactions including desensitisation and internalisation. For example, a number of 5-HT_{2C} receptor ligands exhibit ligand-selective desensitisation of the PLC/Ca^{2+} and PLA_2-AA signalling pathways (Stout *et al.*, 2002) while ligands for μ- , δ-opioid and β_2-adrenergic receptor show different patterns of relative efficacies between receptor internalisation and coupling to receptor-mediated effector pathways (Urban *et al.*, 2007).

1.5.2. Other Considerations

Care must be taken to consider the broader effector system when investigating ligands with distinct functional profiles, before concluding that true functional selectivity is present. Ligands may be acting at more than one pharmacological target. This is certainly true of the cannabinoid system, with ligands such as anandamide able to activate the vanilloid TRPV1 receptor and certain peroxisome proliferator-activated receptor (PPAR) subtypes, and non CB_1/CB_2 cannabinoid-like receptors such as GPR55 and GPR119 yet to be fully characterised.

Next, partial agonists may be able to maximally activate signalling pathways more strongly coupled to the receptor than other pathways. When compared to a full agonist, the ligands would appear to have functionally distinct profiles. This phenomenon is known as a *strength-of-signal* effect and differs from true functional selectivity, where any receptor-coupled signalling pathway may be selectivity activated, not just the most strongly coupled one.

Although functional selectivity is an inherent attribute of the receptor-ligand interaction, the receptor is part of a larger signalling complex which includes signalling effectors, mediators of desensitisation and internalisation, other receptors (both homo- and heteromers) and other proteins. All of these may have a direct and/or indirect effect on receptor function and pharmacology, including the functional selectivity of agonists (Kenakin, 2010). The presence of such modulators is highly tissue/cell type-dependent which means that ligand-selective differential signalling observed in one tissue type may be different or absent in another tissue type.

The extracellular environment, particularly the concentration of Na^+ and Mg^{2+} ions can alter the receptor conformational state which may directly affect the binding and functional profile of certain ligands.

1.5.3. Functional Selectivity at Cannabinoid Receptors

Cannabinoid receptors provide a particularly appealing model to investigate functional selectivity for a number of reasons: Firstly, members of the receptor family, particularly CB_1, are endogenously expressed in a wide array of

mammalian cell and tissue types, including being ubiquitously expressed in neuronal tissue.

Next, cannabinoid receptors couple to multiple intracellular signalling pathways, which increase their potential ligand-selective specific activation. The various structural groups of cannabinoid ligands discussed previously in this chapter may each bind to and activate different active receptor conformations. With at least five putative endogenous endocannabinoid ligands each with the potential to produce differential signalling via cannabinoid receptors, this system could provide a model for the role of functional selectivity in an endogenous system.

Finally, the cannabinoid signalling system has huge potential as a target for therapeutic treatment of a number of disorders including pain, inflammation and a variety of psychiatric disorders. It may be possible, in the future, to develop functionally selective compounds which maximise positive effects, while minimising activation of pathways associated with negative side-effects. This is particularly true of compounds targeting CB_1 receptors which often produce unwanted psychotropic side effects.

A growing body of research exists which is helping to elucidate the mechanisms of cannabinoid functional selectivity. This involves several aspects including characterising the distinct profile of signalling pathway activation, desensitisation and downregulation of cannabinoid signalling and the molecular mechanisms which may facilitate functional selectivity.

As previously described, cannabinoid receptors predominantly couple to $G_{i/o}$ proteins. However, there are several subtypes of $G_{i/o}$ protein, with certain cannabinoid ligands having distinct selectivity. Stimulation of CB_1 receptors exogenously expressed in Sf9 (*Spodoptera frugiperda*) cells with different cannabinoid ligands, led to different levels of $G_{i/o}$ protein activation (Glass & Northup, 1999). The classical cannabinoid HU-210 produced maximal activation of both G_i and G_o proteins. The endocannabinoid anandamide and aminoalkylindole WIN 55,212 both produced maximal activation of G_i proteins, but sub-maximal activation of G_o. The phytocannabinoid Δ^9-THC produced a sub-maximal activation of both G protein subtypes. The rank order of ligand potency was consistent for both G protein subtypes. Further study of ligand specificity for $G\alpha_i$ subtypes $G\alpha_{i1}$, $G\alpha_{i2}$ and $G\alpha_{i3}$ using a co-immunoprecipitation technique in N18TG2 neuroblastoma cells showed differential effects of chemically distinct ligands (Mukhopadhyay & Howlett, 2005). WIN 55,212-2 exhibited potency for all three subtypes investigated, while the tricyclic cannabinoid desacetyllevonantradol had potency for $G\alpha_{i1}$ and $G\alpha_{i2}$, but not $G\alpha_{i3}$, and the synthetic eicosanoid methanandamide only had an effect on $G\alpha_{i3}$. This ligand specificity appears to extend to G proteins of other families. In CHO cells exogenously expressing human CB_1 receptors, WIN 55,212-2 was a full agonist for G_i and G_s signalling pathways, measured by the inhibition and accumulation of cAMP respectively in forskolin-stimulated cells (Bonhaus *et al.*, 1998), whereas Δ^9-THC was a partial agonist for both signalling pathways. Interestingly, from a functional selectivity perspective, both the non-classical cannabinoid CP 55,940 and anandamide exhibited significantly higher intrinsic activity at the G_i signalling pathway, acting as full agonists when measuring inhibition of cAMP formation,

but acting as partial agonists when measuring cAMP accumulation. CB_1 receptor-mediated activation of $G_{q/11}$ protein also appears to be ligand-selective. WIN 55,212-2 was able to stimulate G_q-dependent intracellular Ca^{2+} release in HEK cells via transfected CB_1 receptor activation (Lauckner *et al.*, 2005). A series of other cannabinoid receptor ligands, including Δ^9-THC, HU-210, CP 55,940 and 2-AG, were unable to produce any response in the same assay.

A number of structural studies point to the potential mechanisms by which cannabinoid functional selectivity might be mediated. CP 55,940 and WIN 55,212-2 have been shown to induce distinct conformational changes in CB_1 receptors upon binding (Georgieva *et al.*, 2008). Use of the highly sensitive plasmon-wavelength resonance (PWR) spectroscopic technique showed that the two ligands produced changes in the PWR spectra of *myc*-His_6-tagged receptors which were of similar magnitude, but in opposite directions. This study also showed that the ability of these distinct receptor conformations to activate the G_{i1} protein subtype was significantly different, with the WIN 55,212-2-induced receptor conformation being much more potent. Mutant CB_1 receptors with single residue substitutions at position L7.60 in the intracellular C-terminal helix 8 produced ligand-selective receptor activation profiles (Anavi-Goffer *et al.*, 2007). Wild type receptors containing a leucine residue at position L7.60 gave a maximal response upon stimulation with HU-210, CP 55,940 and WIN 55,212-2. L7.60I mutations caused a significant decrease in the maximal response produced by all three ligands, while a L7.60F mutation only caused a significant decrease in the maximal response produced by CP 55,940 and WIN 55,212-2. Further investigation showed that the H8 domain of the receptor is important in CB_1-$G\alpha_{i3}$

and $G\alpha_o$ coupling but not $G\alpha_{i1}$ and $G\alpha_{i2}$ (Anavi-Goffer *et al.*, 2007). This research suggests that different ligands may preferentially activate signalling pathways through distinct receptor domains.

The novel cannabinoid peptide ligands RVD-Hp and VD-Hp appear to exhibit functional selectivity at the CB_1 receptor. The peptides produced quantitatively similar responses compared with HU-210 in a series of assays measuring functional consequences of receptor activation including neuronal outgrowth in neuro 2A cells and internalisation of *myc*-tagged receptor expressed in CHO cells (Gomes *et al.*, 2009). The profile of ERK phosphorylation differed between HU-210 and RVD-Hp, with the level and rate of increase in pERK being lower for RVD-Hp. The study also showed CB_1 receptor-mediated ligand-selective release of Ca^{2+} from intracellular stores in neuro-2A cells. Treatment with RVD-Hp, HU-210 and the endocannabinoid 2-AG leads to a sustained release in Ca^{2+} levels; however, the RVD-Hp mediated release is much quicker and significantly larger. Interestingly, the effects of RVD-Hp on both pERK levels and intracellular Ca^{2+} release are only partially blocked by PTX, whereas the response due to HU-210 is almost completely abolished. Further study showed that both RVD-Hp and VD-Hp are unable to promote G protein activation as measured by accumulation of [^{35}S]GTPγS in mice striatal and cerebellar membranes (Gomes *et al.*, 2010). These results suggest that the peptide ligands activate a G_i-independent signalling pathway distinct from HU-210.

While the majority of the reports on CB_1 receptor functional selectivity are from *in vitro* studies, there are some reports of ligand-specific responses *in vivo* (Bosier *et*

al., 2010). A SAR study of aminoalkylindole derivatives using the tetrad test demonstrated that while WIN 55,212-2 is more potent in inducing hypolocomotion that hypothermia and catalepsy, several WIN 55,212-2 derivatives were more potent in inducing catalepsy and hypothermia (Wiley *et al.*, 1998). However, differences in the metabolism of ligands *in vivo*, the presence of multiple pharmacological targets and the complex patterns of receptor distribution in various tissue all act to complicate the mechanisms by which ligand-specific responses occur *in vivo*. A more recent study has provided a clearer example of a true functionally selective response *in vivo* (Bosier *et al.*, 2012). Both HU-210 and CP 55,940 induced hypolocomotion and catalepsy in male Wistar rats. However, only HU-210 was able to upregulate tyrosine hydroylase expression in the striatum, in a rimonabant-sensitive manner, despite both agonists exhibiting equivalent levels of brain penetration and receptor occupancy, as determined by *ex vivo* binding assays.

1.6. Project Aim

The aim of the project described in this thesis was to clearly demonstrate ligand-selective functional selectivity at the cannabinoid receptor both endogenously and exogenously expressed in a variety of cell lines and tissues. Receptor stimulation by members of all the main groups of cannabinoid ligands was fully characterised using a number of functional assays, including [^{35}S] GTPγS binding to measure G-protein activation, measuring changes in cAMP levels induced by $G_{i/o}$ and G_s proteins, immunocytochemical techniques to characterise the pattern of MAP kinase activation and measurement of receptor-mediated β-arrestin recruitment, as well as the pharmacological profiling of novel cannabinoid allosteric modulators.

Chapter 2

Characterisation of fenofibrate as a novel cannabinoid receptor agonist and negative allosteric modulator

2.1. Introduction

The cannabinoid receptors are ligated by a variety of structurally unrelated compounds, with a range of potencies, efficacies and selectivities. Anandamide (N-arachidonoylethanolamine or AEA) and 2-arachidonoylglycerol (2-AG) are endogenous cannabinoid receptor lipid mediators derived from the fatty acid arachidonic acid. Other groups of receptor ligands include phytocannabinoids such as Δ^9-tetrahydrocannabinol (Δ^9-THC), derived from *Cannabis sativa,* and their synthetic analogues both classical, such as HU-210, and non-classical such as CP 55,940; the aminoalkyindoles such as WIN 55,212-2, which are structurally related to non-steroidal anti-inflammatory drugs, and diarylpyrazoles such as the CB_1-selective antagonist rimonabant, otherwise known as SR 141716A (for review see **Chapter 1**).

As well as these orthosteric ligands, a small number of allosteric modulators for the CB_1 receptor have been described. These are compounds that are proposed to interact with binding sites on the receptor which are topographically distinct from the orthosteric binding site, allowing them to alter the binding and functional properties of orthosteric agonists (Christopoulos & Kenakin, 2002). A series of compounds synthesised by Organon, typified by Org 27569 (Price *et al.*, 2005; Baillie *et al.*, 2013), and the compound PSNCBAM-1 (Horswill *et al.*, 2007; Wang *et al.*, 2011) have been reported to positively enhance agonist binding, while negatively modulating agonist function, leading to the recent characterization of the Org 27569 binding site (Shore *et al.*, 2013). Most recently, a series of peptide endocannabinoids, termed 'pepcans' have been identified,

which exhibit negative allosteric modulation of agonist binding and efficacy (Bauer *et al.*, 2012).

In addition to acting at cannabinoid receptors, many of the orthosteric ligands bind to and/or activate a number of other pharmacological targets, with examples including the orphan receptor GPR55, the transient receptor potential cation channel subfamily V member 1 (TRPV1) and the peroxisome proliferator-activated receptors (PPARs), (Pertwee *et al.*, 2010). PPARs are members of the nuclear receptor superfamily and function as ligand-activated transcription factors, recognising a range of endogenous fatty acids and their derivatives, and are generally involved in metabolism and cellular differentiation (Michalik *et al.*, 2006). To date, three receptor isoforms have been identified, α, β/δ and γ, although, at present, only PPARα and PPARγ are therapeutic targets. PPARα is expressed in the liver and adipose tissue, as well as heart, kidney and skeletal muscle, where its main function is as a regulator of lipid metabolism. Activation of PPARα leads to upregulation of genes involved in the uptake and utilisation of free fatty acids making it a target in the treatment of hyperlipidemia (Rakhshandehroo *et al.*, 2010).

Anandamide, Δ^9-THC and WIN 55,212-2 are reported to function as PPARα agonists *in vitro* (Fu *et al.*, 2003; Sun *et al.*, 2007), albeit at concentrations higher than those required to activate cannabinoid receptors.

While there has been some exploration of the pharmacology of cannabinoid ligands at PPARs, only very limited investigation into the potential

pharmacological effects of PPAR ligands at the cannabinoid receptors has been reported. Previously, McGuinness *et al.* (2009) reported that fenofibrate was a near-full agonist compared to CP 55,940 in a HEK293-CB_2 cell line using the PathHunter™ β-arrestin recruitment assay, with an EC_{50} value of 55nM. In addition, Pérez-Fernández *et al.* (2011) described a series of compounds combining pharmacophores of fenofibrate and SR 141716A with nanomolar affinity for both CB_1 and PPARα, although as these compounds were selective antagonists at the CB_1 receptor in the mouse vas deferens bioassay, it is likely that their CB_1 effects were mediated via the SR 141716A pharmacophore.

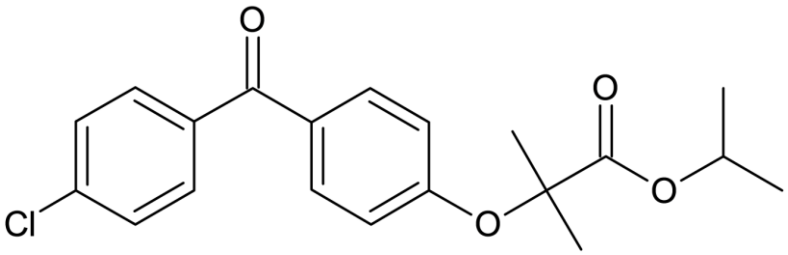

Figure 2.1 Chemical structure of fenofibrate.

2.2. Aims and objectives

One of the tools necessary to identify patterns of functional selectivity is having as wide a variety of structurally distinct receptor ligands as possible. This increases the probability of ligands promoting distinct active receptor conformations and thereby activating distinct patterns of signalling cascades. To this end then, the aims of this chapter were to identify and characterise any new cannabinoid receptor ligands. This was achieved by testing a series of PPAR agonists for cannabinoid receptor affinity. These compounds were then subsequently used to

investigate functional selectivity at the cannabinoid CB_1 receptor in a number of different expression systems.

2.3. Methods

2.3.1. Cell culture

Chinese Hamster Ovary cells stably transfected with the human CB receptor were kindly provided by Dr Sarah Nickolls from Pfizer-Neusentis. All cell culture was performed under sterile conditions in a class II laminar flow cabinet. All culture reagents were warmed to 37°C before use. Chinese Hamster Ovary (CHO) cells stably transfected with human cannabinoid type 1 (CB_1) or human cannabinoid type 2 (CB_2) receptor were cultured in 175 cm^2 culture flasks containing Dulbecco's Modified Eagle Medium: Nutrient Mixture F12 (DMEM/F12) supplemented with 10% foetal bovine serum, 2 mM L-glutamine and 400 µg/ml G 418, in a humidified incubator at 37°C and 5 % CO_2. Cells were cultured for 2 – 3 days until ~90% confluent, and then passaged. Cells were washed once with phosphate buffered saline (PBS), and then incubated with trypsin/EDTA solution for ~3 min until the majority of cells were detached from the culture flask. The cell suspension was diluted in culture medium to prevent further action of the trypsin, and then cells were collected by centrifugation at 200 x *g* for 3 min. The cell pellet was resuspended in fresh culture medium; the cell number determined using the Bio-Rad TC10™ Automated Cell Counter, and cells reseeded into new culture flasks containing fresh culture medium (3 million cells per flask).

2.3.2. Membrane preparation

Cells were cultured as described previously (see **2.3.1**). At confluence, cells were trypsinised for no more than 1 min, allowing for cell detachment from the culture flask but minimising proteolytic degradation of the surface proteins. Cells were collected by centrifugation at 200 x *g* for 3 min. All subsequent steps were performed at 0 - 4°C. Cell pellets were resuspended in ice-cold homogenisation buffer and pooled together (50 mM Tris base, pH 7.4), homogenised using a Polytron homogeniser for 30 sec and then washed 3 times by centrifugation (30,000 x *g* for 10 min at 4°C). The membrane pellet was resuspended in homogenisation buffer and the protein concentration was determined by Lowry protein assay (Lowry *et al.*, 1951). Serial dilution of a BSA standard (1 mg/ml) was prepared along with dilutions of membrane (1:10, 1:20 and 1:40). Lowry reagent (100 nM NaOH, 7 mM SDS, 200 mM Na_2CO_3, 0.005 % w/v $CuSO_4$ and NaK tartrate) was added to each sample/standard dilution and incubated at room temperature for 10 min, followed by addition of Folin phenol reagent and incubation at room temperature for 45 min. The samples were then loaded onto a clear 96-well assay plate and the absorbance was measured using a spectrophotometric plate reader (Molecular Devices, CA). The membrane sample protein concentrations were interpolated from the BSA standard curve. The membrane concentration was adjusted to 2.5 mg/ml protein and was stored in aliquots at -80°C.

2.3.3. Radioligand binding assays

2.3.3.1. Equilibrium binding assays

Competition binding assays were performed in the presence of either [^{3}H]-CP 55,940 (1 nM) or [^{3}H]-SR141716A (5 nM). CHO-hCB membrane (50 µg protein) was incubated in plastic vials at 30°C for 90 min in 1 ml (final volume) of assay buffer (50 mM Tris, 2 mM EDTA, 5 mM $MgCl_2$, 0.2 mg/ml BSA, pH 7.0), with radioligand and various serially diluted concentrations of unlabelled ligand or buffer. Non-specific binding was determined in the presence of unlabelled CP 55,940 (1 µM). The assay was terminated by rapid filtration through Whatman GF/B filters soaked in cold assay buffer containing 5 mg/ml BSA, using a 24-well Brandell harvester and washed three times with ice-cold assay buffer containing 0.1 mg/ml BSA. Radioactivity on dissected filters was measured by liquid scintillation spectrometry.

2.3.3.2. Dissociation Kinetics

Competition binding assays were performed in the presence of [^{3}H]-CP 55,940 (1 nM). Rat whole brain membranes (male Wistar rats; 50 µg protein) were incubated with radioligand for 90 min at 21°C in 1 ml (final volume) of assay buffer (50 mM Tris, 2 mM EDTA, 5 mM $MgCl_2$, 0.2 mg/ml BSA, pH 7.0). Dissociation was initiated by the addition of excess unlabelled CP 55,940 (1 µM) in the presence or absence of fenofibrate (30 µM), with a subsequent incubation time course ranging from 1 – 120 min at 21°C. Non-specific binding was determined by performing the experiment in the presence of unlabelled CP 55,940 (1 µM). The assay was terminated by rapid filtration through Whatman GF/B filters soaked in cold assay buffer containing 5 mg/ml BSA, using a 24-well

Brandell harvester and washed three times with ice-cold assay buffer containing 0.1 mg/ml BSA. Radioactivity on dissected filters was measured by liquid scintillation spectrometry.

2.3.4. [^{35}S]-GTPγS binding assays

CHO membranes were pre-incubated at 30°C for 20 min with GDP (final assay concentration 50 µM) in assay buffer (50 mM Tris, 10 mM $MgCl_2$, 100 mM NaCl and 0.2 mg/ml BSA, pH 7.4). Membrane (25 µg) was then incubated in plastic vials at 30°C for 90 min in 1 ml (final volume) of assay buffer with 0.02 nM [^{35}S]-GTPγS and various concentrations of unlabelled ligand or buffer. Non-specific binding was determined in the presence of 10 µM unlabelled GTPγS. The assay was terminated by rapid filtration through Whatman GF/C filters using a 24-well Brandell harvester and washed three times with ice-cold distilled water. Radioactivity on dissected filters was measured by liquid scintillation spectrometry.

2.3.5. Guinea-pig ileum contraction experiments

Briefly, sections of ileum were removed from Dunkin-Hartley guinea-pigs and immersed in Krebs-Henseleit solution [composition (in mM): NaCl - 118, KCl - 4.8, $MgSO_4.7H_20$ - 1.1, $NaHCO_3$ - 25, KH_2PO_4 - 1.2, D-glucose - 12 and $CaCl_2$ – 2.5, gassed with 95% O_2 and 5% CO_2 at room temperature]. For experimentation, the contents of the gut sections were flushed with buffer, and 3 cm segments of tissue were removed from the caecal end of the ileum. The tissue segments were mounted with cotton sutures onto platinum electrodes positioned transmurally and suspended in a 50 ml organ bath containing Krebs-Henseleit solution gassed with

95% O_2 and 5% CO_2 at 37°C at a tension of 0.5g. Tissue contractions were evoked by electrical field stimulation, (single pulses of 10 volts, 0.5 ms duration and 0.1 Hz frequency) from SR1 stimulators. Changes in tension (as g) were recorded via force transducers connected to a PowerLab 26T / LabChart data-acquisition system (AD Instruments, Charlgrove, Oxford, UK).

No compounds were added until the amplitude of the EFS-evoked responses were consistent for at least 30 min. Cumulative concentration-response curves were constructed to agonists with a minimum 15 min dosing interval.

2.3.6. Materials

[^{3}H]-CP 55,940, [^{3}H]-SR141716A, [^{35}S]-Guanosine 5'-O-[gamma-thio]triphosphate ([^{35}S]-GTPγS) and Ultima Gold liquid scintillation counter (LSC) cocktail were obtained from PerkinElmer (Boston, MA). Grade GF/B filter mats obtained from Brandel Inc. (Gaithersburg, MD). Test compounds, Bovine serum albumin, GDP, GTPγS and all other cell culture and assay reagents were obtained from Sigma-Aldrich (Poole, UK).

2.3.7. Data analysis

Data analysis was performed using GraphPad Prism v6.0 software (GraphPad software, Inc, San Diego, CA, USA). In radioligand binding experiments, the mean non-specific binding value was subtracted from all values to give the specific binding. The values were then expressed as a percentage of the basal binding/response, respectively. The inhibition of EFS-evoked responses by

cannabinoid agonists was expressed as a percentage inhibition of the response in the absence of compound.

Data for the competition binding assays were analysed using the following equation;

$$Y = \frac{(top - bottom)[L]}{[L] + IC_{50}}$$

where Y is the percentage of specific binding, [L] is the concentration of unlabelled ligand and IC_{50} is the concentration of L required to inhibit 50 % of radioligand specific binding.

The ligand affinities, as denoted by the equilibrium dissociation constants (K_i), were then determined using the Cheng-Prusoff equation;

$$K_i = \frac{IC_{50}}{1 + [RL]/K_D}$$

where [RL] is the radioligand concentration and K_d is the radioligand equilibrium dissociation constant.

The cooperativity factor (α) and equilibrium dissociation constant (K_B) for fenofibrate acting as an allosteric modulator at the CB_1 receptor were determined by non-linear regression using the allosteric ternary complex model (TCM) equation;

$$Y = \frac{[A]}{[A] + \frac{K_A + (1 + [B]/K_B)}{1 + \alpha[B]/K_B}}$$

where [A] and [B] represent concentration of orthosteric and allosteric ligands respectively, and K_A is the equilibrium dissociation constant for the orthosteric ligand.

The data for the dissociation kinetic experiments were analysis using the following two-phase exponential decay model;

$$Y = span1.e^{-k_1.x} + span2.e^{-k_2.x} + plateau$$

where span 1 and span 2 are the percentage of each phase, the plateau is the minimum asymptotic value and k_1 and k_2 are the respective dissociation rate constants. An extra-sum-of-squares (*F* test) was used to determine whether the data were significantly better fitted to this model rather than a simpler one-phase exponential decay model.

Concentration-response data were fitted to curves using the following four-parameter logistical equation;

$$Y = bottom - \frac{(top - bottom)}{1 + 10^{(logEC_{50} - x)n_H}}$$

where Y is the magnitude of the response, pEC_{50} is the negative logarithm of the curve midpoint, x is the log molar concentration of agonist and n_H is the curve slope.

2.3.8. Statistics

All data represents mean ± SEM of at least three independent experiments. Normality of data sets was determined using the D'Agostino-Pearson omnibus normality test. Statistical differences between mean values were determined using Student's paired and unpaired, two-tailed *t* tests or one-way ANOVA followed by Dunnett's multiple comparisons *post hoc* tests, where appropriate. A *p* value of <0.05 was considered significant.

2.4. Results

2.4.1. Competitive binding characterisation of fenofibrate

Initially, a range of PPAR ligands (all at 10 µM) were assessed for CB_2 receptor affinity using CHO membranes expressing hCB_2 receptors by Dave Kendall *et al.* at the University of Nottingham. The compounds tested include the fibrates fenofibrate, and its active metabolite fenofibric acid, bezafibrate, ciprofibrate, clofibrate, gemfibrozil and methyl clofenapate as PPARα ligands, the structurally unrelated selective PPARα agonist WY-14643 (also known as pirinixic acid) and the highly selective PPARγ antagonist T0070907 (data not shown). Only fenofibrate exhibited affinity for the CB_2 receptor, fully displacing receptor-bound [^{3}H]-CP 55,940 - all other compounds tested failed to show any significant competition for radioligand binding.

Further radioligand binding experiments were performed to characterise the binding of fenofibrate to cannabinoid receptors. In CHO cell membranes expressing hCB_1 receptors, unlabelled CP 55,940 displaced [^{3}H]-CP 55,940 in a concentration-dependent manner, with a pIC_{50} value of 8.8 ± 0.1 (**Figure 2.2A** and **Table 2.1**). Fenofibrate also displaced [^{3}H]-CP 55,940 binding in an apparently incomplete manner (% specific binding- CP 55,940 = 104 ± 3 %, fenofibrate = 80 ± 9 %). The pIC_{50} value for fenofibrate was 6.1 ± 0.1. In CHO cell membranes expressing hCB_2 receptors, unlabelled CP 55,940 and fenofibrate both fully displaced [^{3}H]-CP 55,940 binding, with pIC_{50} values of 9.3 ± 0.1 and 7.2 ± 0.1, respectively (**Figure 2.2B** and **Table 2.1**). These values were then used to calculate K_i values for CP 55,940 and fenofibrate at the two receptor subtypes (**Table 2.1**).

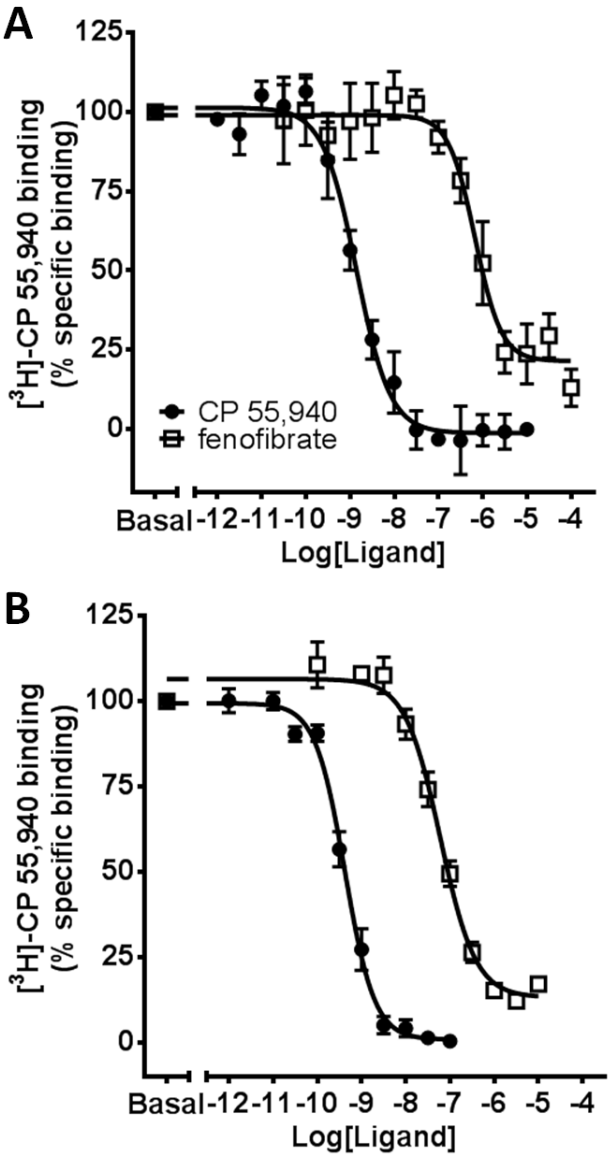

Figure 2.2 Characterisation of fenofibrate binding at (A) CB_1 and (B) CB_2 cannabinoid receptors. Membranes derived from CHO cells stably transfected with cannabinoid receptors were incubated with increasing concentrations of CP 55,940 (1 ρM – 10 μM) or fenofibrate (30 ρM – 100 μM) in the presence of [^{3}H]-CP 55,940 (1 nM) at 30°C for 90 min followed by filtration. Results were expressed as a % of the specific binding of radioligand in the absence of ligand. Data shown are the mean ± SEM from three independent experiments performed in triplicate. Curves were fitted by non-linear regression to a four parameter logistical equation using GraphPad Prism.

Table 2.1

Determination of the affinity (pK_i values) of CP 55,940 and fenofibrate at human CB_1 and CB_2 cannabinoid receptors expressed in CHO cells using [^{3}H]-CP 55,940.

Ligand	CHO-hCB_1	CHO-hCB_2
CP 55,940	9.0 ± 0.2	10.0 ± 0.4
fenofibrate	6.3 ± 0.9	7.7 ± 0.1

Data shown are mean ± SEM from three independent experiments performed in duplicate.

2.4.2. Functional characterisation of fenofibrate at human cannabinoid receptors

The functional pharmacological properties of fenofibrate were investigated using the GTPγS binding assay, which measures receptor-mediated enhancement of binding of radiolabelled [^{35}S]-GTPγS to G proteins present in the cell membranes. In CHO-hCB_1 membranes, CP 55,940 produced a concentration-dependent increase in GTPγS binding, with a pEC_{50} value of 9.0 ± 0.2 (**Figure 2.3A** and **Table 2.2**). Fenofibrate produced a smaller increase in GTPγS binding, relative to CP 55,940, with a maximally effective concentration of 3.1 μM. However at higher concentrations, there was a reduction in [^{35}S]-GTPγS binding, producing an atypical bell-shaped concentration-response curve (**Figure 2.3A**). In CHO-hCB_2 membranes, CP 55,940 again produced a concentration-dependent increase in GTPγS binding, with a pEC_{50} value of 9.7 ± 0.1 (**Figure 2.3B** and **Table 2.2**). In contrast to the CB_1 response, fenofibrate produced a typical concentration-

dependent response in CHO-hCB_2 membranes, with a pEC_{50} value of 7.7 ± 0.1. The fenofibrate R_{max} value was only slightly lower than that for CP 55,940, suggesting it may be a higher efficacy agonist at the hCB_2 receptor (% CP response = 90 ± 2%; paired, two-tailed *t*-test, $p<0.05$).

Table 2.2

Determination of potency (pEC_{50} values) and intrinsic activity (R_{max}) for CP 55,940- and fenofibrate-enhanced binding of [^{35}S]-GTPγS using human CB_1 and CB_2 cannabinoid receptors expressed in CHO cells.

Ligand	**CHO-hCB_1**			**CHO-hCB_2**		
	pEC_{50}	R_{max} (%)	R_{max} (% CP response)	pEC_{50}	R_{max} (%)	R_{max} (% CP response)
CP 55,940	9.0 ± 0.2	289 ± 20	100 ± 1	9.7 ± 0.1	400 ± 6	100 ± 1
fenofibrate	N.D.	N.D.	N.D.	7.7 ± 0.1	359 ± 14	90 ± 2*[a]

Data shown are mean ± SEM from three independent experiments performed in duplicate. N.D.: not determined due to lack of fit to non-linear regression curve.

* $p<0.05$, paired two-tailed *t*-test.

[a] compared to the corresponding CP 55,940 response.

2.4.3. Further characterisation of fenofibrate activity at the CB_1 receptor

In order to investigate the biphasic [^{35}S]-GTPγS response to fenofibrate in CHO-hCB_1 membranes, the sensitivity of the response to the CB_1 selective antagonist

AM 251 was investigated (**Figure 2.3C**). Increasing concentrations of AM 251 produced rightward shifts in the positive high potency GTPγS response, demonstrated by the increase in the fenofibrate concentration required to produce an *equiefficacious* response. Increasing concentrations of AM 251 also caused a reduction in the fenofibrate maximum response with 0.1, 1 and 10 nM AM 251 producing an absolute reduction of 5, 59 and 167 % basal response respectively. A concentration of 10 μM AM 251 completely abolished the biphasic fenofibrate response **(Figure 2.3C**).

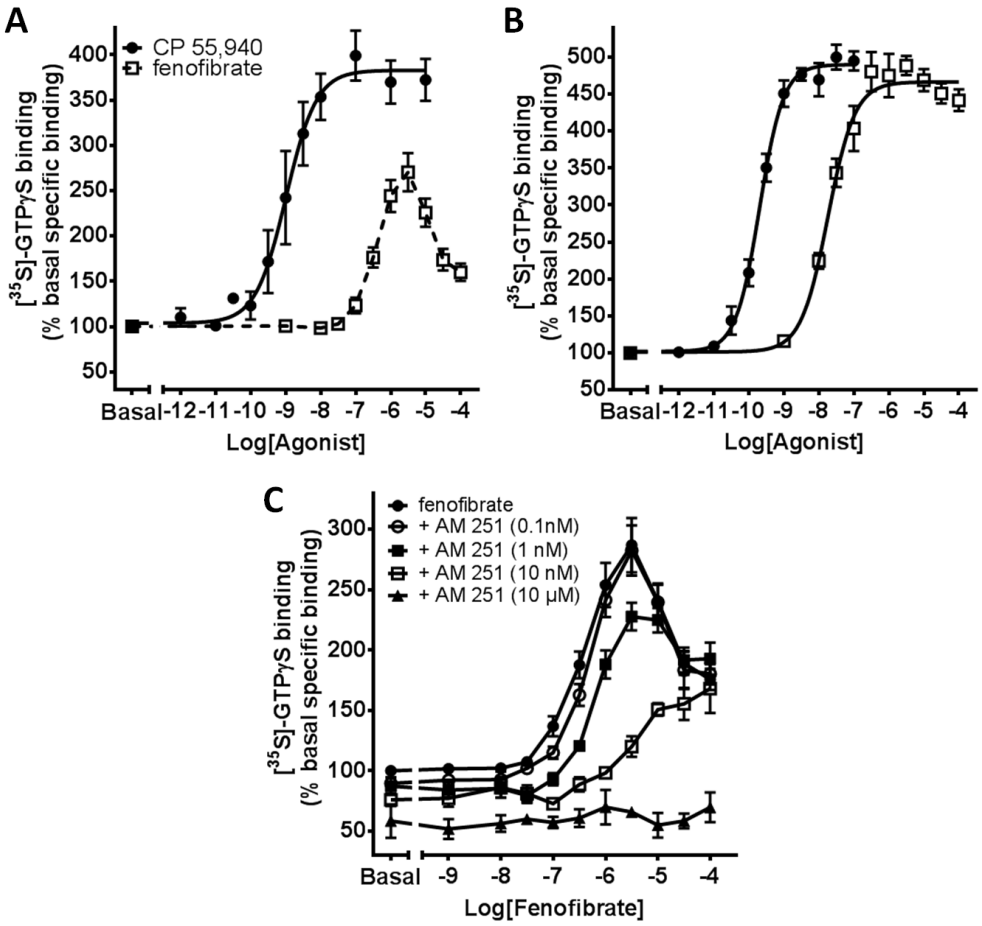

Figure 2.3 Characterisation of fenofibrate functional properties at (A) CB_1 and (B) CB_2 cannabinoid receptors. Membranes, derived from CHO cells stably transfected with cannabinoid receptors, and pre-incubated with GDP (50 μM) were incubated with increasing concentrations of CP 55,940 (1 ρM – 10 μM) or fenofibrate (1 nM – 100 μM) in the presence of [^{35}S]-GTPγS (0.02 nM) at 30°C for 90 min followed by filtration. Antagonist studies at the CB_1 receptor (C) were performed in the presence of increasing concentrations of AM 251. Results were expressed as a % of the specific binding of [^{35}S]-GTPγS in the absence of ligand. Data shown are the mean ± SEM from three independent experiments performed in duplicate. Full line curves were fitted by non-linear regression to a four parameter logistical equation and dashed lines using straight lines connecting neighbouring data points to illustrate overall response trend.

2.4.4. Fenofibrate as a negative allosteric modulator

One interpretation of these data is that, at higher concentrations, fenofibrate functions as a negative allosteric modulator. To test this hypothesis, the ability of fenofibrate to modulate CP 55,940-evoked responses was investigated. The competition radioligand binding data for fenofibrate (**Figure 2.2A**) were fitted to the allosteric TCM equation (see **2.3.7**), yielding estimated pK_B and α values of 6.2 ± 0.1 and 0.12 ± 0.1 respectively, indicating a strongly negative mode of modulation. The effect of fenofibrate on the dissociation of [^{3}H]-CP 55,940 binding to CB_1 receptor was determined. High variance in the specific radioligand binding in the CHO-hCB_1 membranes in provisional experiments meant that curves could not be fitted with any confidence; therefore, experiments were performed in rat whole brain homogenates, which have a greater level of CB_1 specific binding. Addition of unlabelled CP 55,940 (1 μM) promoted a significantly biphasic dissociation of the radioligand (**Figure 2.4A** and **Table 2.3**; $p<0.0001$; *F* test). Inclusion of fenofibrate (30 μM) produced a significant increase in both the slow and fast radioligand dissociation rate constants, with no significant change of the ratio between the two phases (**Table 2.3**; *$p<0.05$, **$p<0.01$; paired two-tailed *t*-test).

Table 2.3

Determination of the dissociation rate constants for [^{3}H]-CP 55,940 at cannabinoid receptor expressed in rat whole brain in the absence and presence of fenofibrate.

Ligand	**k_1 (slow)**	**Half-life slow**	**k_2 (fast)**	**Half-life fast**
	x 10^{-2} min^{-1}	*min*	*min^{-1}*	*min*
CP 55,940 (1 µM)	1.19 ± 0.20	61.3 ± 10.4	0.79 ± 0.14	0.93 ± 0.15
CP 55,940 & fenofibrate (30 µM)	3.84 ± 0.08**[a]	18.1 ± 0.40	1.50 ± 0.16*[a]	0.47 ± 0.06

Data shown are mean ± SEM from three independent experiments performed in duplicate. * $p<0.05$, ** $p<0.01$; paired, two tailed *t*-test.

[a] Relative to the corresponding *k* value in the absence of fenofibrate.

Next, the modulatory effect of fenofibrate on an orthosteric functional response was investigated by examining the effect of fenofibrate on the CP 55,940-enhanced GTPγS response (**Figure 2.4B**). Two equiefficacious concentrations of fenofibrate were chosen, one representative of the rising half and the other of the falling half of the bell-shaped curve. Both concentrations of fenofibrate produced an increase in the apparent basal level of GTPγS binding. Co-stimulation with a low concentration of fenofibrate (0.3 µM) did not significantly alter the maximal response to CP 55,940, as described by the upper asymptote of the concentration-response curve. However, a high concentration (30 µM) produced a significant reduction in both the maximal CP 55,940 response (86 ± 2 % control response; $p<0.01$; one-way ANOVA), as well as a significant rightward shift of the

concentration- response curve (pEC_{50} value, without fenofibrate = 8.9 ± 0.1, fenofibrate = 6.9 ± 0.1; $p<0.0001$; one-way ANOVA).

Finally, the effect of fenofibrate on binding to CHO-hCB_1 membranes of the antagonist radioligand [^{3}H]-SR 141716A was investigated. The CB_1–selective antagonist AM 251 produced a concentration-dependent displacement of [^{3}H]-SR 141716A binding, with a pIC_{50} value of 9.4 ± 0.1. In marked contrast, fenofibrate failed to compete for [^{3}H]-SR 141716A binding, but rather significantly enhanced binding at higher concentrations, although the magnitude of the enhancement was somewhat variable between individual experiments (**Figure 2.4C**).

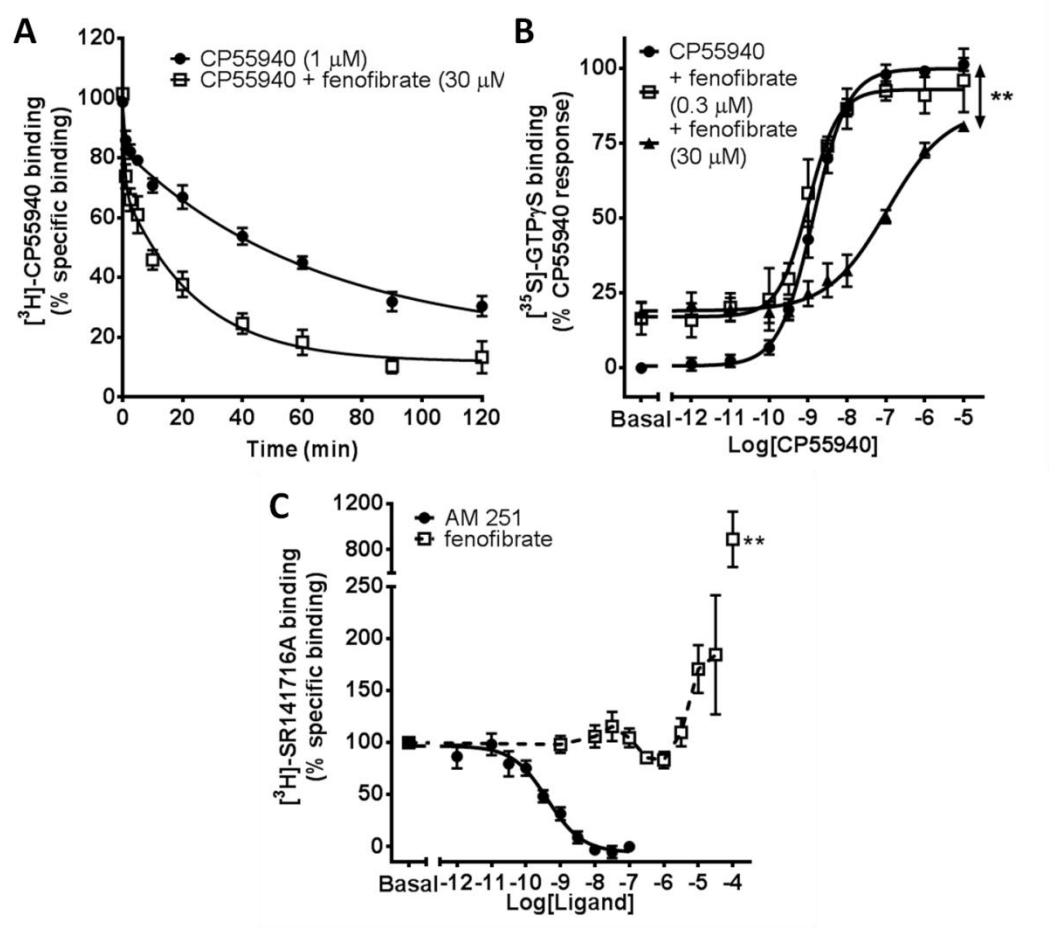

Figure 2.4 Characterisation of fenofibrate as a negative allosteric modulator.

A – Rat whole brain membranes pre-incubated with [^{3}H]-CP 55,940 (1 nM) were incubated with CP 55,940 (1 μM) in the absence or presence of fenofibrate (30 μM) at 21°C over a 120 min time course, followed by filtration. Results were expressed as a % of the specific binding of the radioligand in the absence of unlabelled ligand.

B - Membranes derived from CHO cells stably transfected with CB_1 receptors were incubated with increasing concentrations of AM 251 (1 ρM – 100 nM) or fenofibrate (30 ρM – 100 μM) in the presence of [^{3}H]-SR 141716A (5 nM) at 30°C for 90 min followed by filtration. Results were expressed as a % of the specific binding of radioligand in the absence of ligand.

C - Membranes derived from CHO cells stably transfected with CB_1 receptors and pre-incubated with GDP (50 µM) were incubated with increasing concentrations of CP 55,940 (1 ρM – 10 µM) in the presence of [^{35}S]-GTPγS (0.02 nM) and in the absence and presence of fenofibrate (0.3 and 30 µM) at 30°C for 90 min followed by filtration. Results were expressed as a % of the specific CP 55,940 response. Data shown are the mean ± SEM from 3 to 5 independent experiments performed in duplicate. Full line curves were fitted by non-linear regression to a four parameter logistical equation and dashed lines using straight lines connecting neighbouring data points to illustrate overall response trend. Statistical significance was determined by one-way ANOVA with Dunnett's multiple comparisons tests; * $p<0.05$, ** $p<0.01$.

2.4.5. The effects of fenofibrate in an *in vitro* isolated tissue preparation

To determine whether fenofibrate activity at the cannabinoid receptors is likely to be of relevance in 'real' tissues, the effects of fenofibrate on electrically-evoked contractions in guinea-pig ileum were investigated (**Figure 2.5**). CP 55,940 and fenofibrate both produced concentration-dependant inhibitions of electrically-evoked contractions with pEC_{50} values of 7.4 ± 0.7 and 6.0 ± 0.4, respectively. The inhibition evoked by fenofibrate was incomplete relative to the response to CP55940, with an R_{max} value of 78 ± 10 %, compared to 103 ± 10 % for CP55940. AM 251 (30 nM) produced a significant rightward shift in the fenofibrate concentration-response curve (pEC_{50} value = 4.9 ± 0.1; $p<0.05$; unpaired, two-tailed *t*-test), indicating that the effect was mediated via CB_1 receptors present in the tissue. The major PPARα-active metabolite fenofibric acid was unable to inhibit electrically-evoked tissue contractions in this tissue at concentrations up to 10 μM.

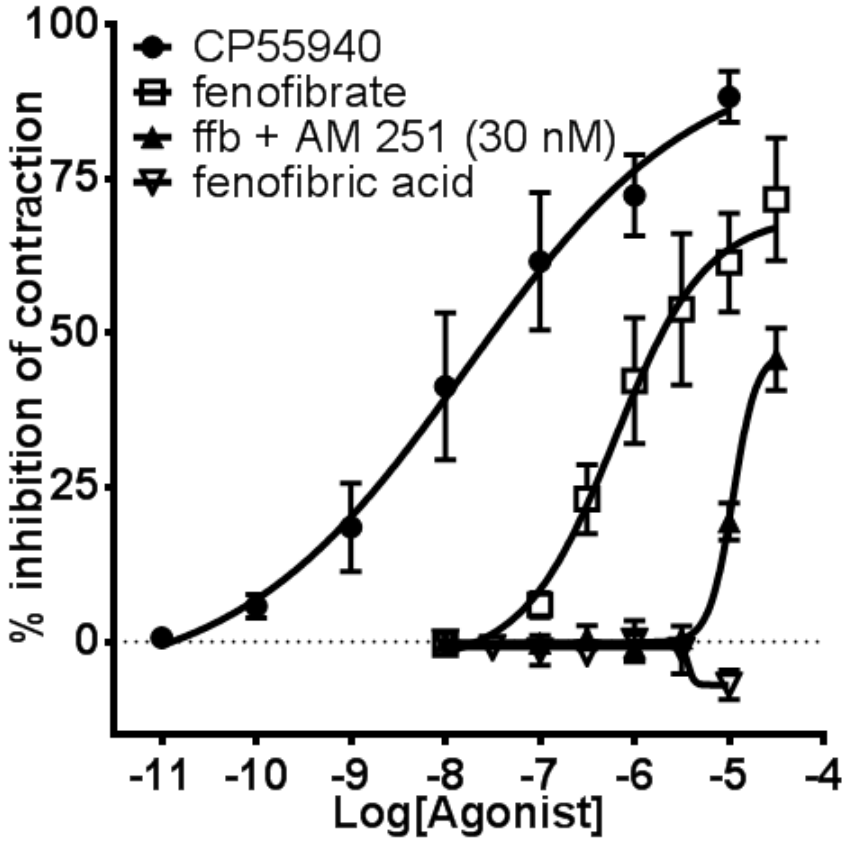

Figure 2.5 Cannabinoid effects on electrically-evoked contraction in guinea-pig ileum**.** Sections of ileum (~ 3 cm) were mounted transmurally onto electrodes and suspended in 50 ml organ baths in oxygenated Krebs Buffer. Tissue contractions were evoked by electrical field stimulation (single pulses of 10 volts, 0.5 ms duration and 0.1 Hz frequency). Tissue was incubated with increasing concentrations of compound in a cumulative fashion with a minimum 15 min dosing interval. Results were expressed as % inhibition of the electrically-evoked tissue contraction immediately prior to the first compound addition. Data shown are the mean ± SEM from at least three independent experiments, each using tissue from different animals. Curves were fitted by non-linear regression to a four parameter logistical equation using GraphPad Prism.

2.5. Discussion

The results presented in this chapter identify the PPARα agonist fenofibrate as a novel agonist at cannabinoid receptors, defining a chemically distinct structural group of cannabinoid ligands. In addition, fenofibrate at higher concentrations appears to act as a negative allosteric modulator at the CB_1 cannabinoid receptor.

Steady state binding experiments using a radiolabelled agonist revealed fenofibrate to be a ligand at both receptor subtypes, exhibiting ~25 fold selectivity for the CB_2 receptor versus CB_1 receptors. In addition, fenofibrate also exhibited efficacy at both receptor subtypes, as shown in the [^{35}S]-GTPγS binding assay, acting as a near full agonist at the CB_2 receptor and a partial agonist at the CB_1 receptor at lower concentrations. Fenofibrate, therefore, is ~60 and 1400 times more potent at the CB_1 and CB_2 receptors respectively than at PPARα (EC50 – 30 μM; Willson *et al.*, 2000). This is a significant finding given that fenofibrate is a common therapy for hypercholesterolemia and hypertriglyceridemia both alone and as a combined treatment with statins (Michalik *et al.*, 2006).

Once absorbed, fenofibrate is rapidly metabolised to the active compound fenofibric acid by tissue and plasma esterases (Caldwell, 1989), making it unfeasible to measure cannabinoid receptor-mediated effects of fenofibrate *in vivo*. Instead, we investigated its effect on isolated guinea-pig ileum tissue, with which we showed that fenofibrate, but not fenofibric acid, inhibited electrically-evoked contractions in guinea pig ileum in an AM 251-sensitive manner, confirming fenofibrate as a cannabinoid CB_1 receptor agonist and identifying a clinically relevant cannabinoid target for orally administered fenofibrate.

A link has been established between the endocannabinoid system and hyperlipidemia *in vivo*, in which low dose cannabinoid therapy (Steffens *et al.*, 2005), and systemic CB_2 gene deletion (Netherland *et al.*, 2010) have been shown to reduce the progression of atherosclerosis in apolipoprotein E and low-density lipoprotein receptor-deficient murine models of hyperlipidemia, respectively. Therefore, the possibility exists that fenofibrate may be mediating some of its hypolipidaemic effects and/or side effects via cannabinoid receptor targets. As stated above, fenofibrate is rapidly metabolised to the PPARα-active metabolite fenofibric acid by tissue and plasma esterases (Caldwell, 1989). As we have shown that fenofibric acid exhibits minimal activity at cannabinoid receptors, any effects of fenofibrate on cannabinoid receptors post-absorption appear unlikely. However, Murakami *et al.* (2010) reported that fenofibrate, but not fenofibric acid, increased AMP kinase phosphorylation in hepatoma cells, and oral administration of fenofibrate to C3H mice also increased the phosphorylation of AMP kinase in the liver, but not in skeletal muscle, indicating that unmetabolised fenofibrate accumulates in the liver. These results suggest that it is unlikely that the AMP kinase phosphorylation effect of fenofibrate was PPARα-mediated and it would be interesting to determine whether it might be due to CB receptor activation. CB_2 receptor modulation of AMP kinase has previously been reported to be involved in neuroprotection against ischaemic damage (Choi *et al.*, 2013) and hepatic encephalopathy (Dagon *et al.*, 2007).

Higher concentrations of fenofibrate (10 – 100 μM) produced a reversal in GTPγS binding mediated via the CB_1 receptor, producing a bell-shaped concentration-

response curve. This response appears to be limited to the CB_1 receptor as it was not seen with CB_2 receptors expressed in the same cell line, also indicating it was not a non-specific effect. These results raised the question of whether fenofibrate was acting as an allosteric modulator of CB_1 receptors at higher concentrations. Alteration of an orthosteric ligand's dissociation kinetics by a second compound is a clear demonstration of allosteric interaction, as dissociation is independent of orthosteric modulation (Christopoulos & Kenakin, 2002; May *et al.*, 2007). Both Org 27569 and the pepcan endogenous peptide ligands have been described as CB_1 allosteric modulators on the basis of this criterion (Price *et al.*, 2005; Bauer *et al.*, 2012). Dissociation kinetic experiments showed that fenofibrate significantly increased the dissociation rate constants of [^{3}H]-CP 55,940 from the CB_1 receptor, clearly indicating it to be a negative allosteric modulator of agonist binding at higher concentrations. It is noteworthy that radiolabelled agonist dissociation was significantly biphasic, which is in keeping with previous reports for this receptor (Price *et al.*, 2005). Fenofibrate caused an enhancement of antagonist radioligand binding at higher concentrations, though it is important to note there was variation between experiments in the magnitude of this response. This may be explained as an example of 'probe dependency' (May *et al.*, 2007), in which the modulator effects are dependent on the ligand bound to the receptor. This phenomenon has been previously observed for the CB_1 receptor with the compounds Org 27569 and PSNCBAM-1 which both exhibit opposing effects on [^{3}H]-CP 55,940 and [^{3}H]-SR 141716A binding. Functionally, fenofibrate appears to act as both an agonist, and a negative allosteric modulator, of CB_1 receptors. Co-incubation with a high, but not a low concentration of fenofibrate promoted a significant reduction in the

maximum CP 55,940 response, which is indicative of a negative allosteric interaction.

Our data suggest that fenofibrate acts at both orthosteric and allosteric binding sites; albeit with different potencies. There are several reports of compounds which appear to exhibit both orthosteric and allosteric effect on GPCRs, termed 'bitopic ligands' (Valant *et al.*, 2012). A clear example is the muscarinic M_2 partial agonist McN-A-343, which was initially characterised as both an allosteric modulator (Waelbroeck, 1994) and orthosteric agonist (Christopoulos & Mitchelson, 1997) in different assay systems. Recently, the compound has been identified as containing two distinct pharmacophores, one acting as an orthosteric agonist and the other as an allosteric modulator at the receptor (Valant *et al.*, 2008).

2.6. Conclusions

In conclusion, we have shown that fenofibrate is a potent agonist at the seven transmembrane cannabinoid receptors (CB_2 and CB_1), which are important regulators of neuronal and immune cell activity, in *in vitro* cell-based and isolated tissue systems. Subsequent chapters will aim to more fully characterise the signalling pattern of fenofibrate at the CB_1 cannabinoid receptor in a number of different expression systems, and to compare it to that of other cannabinoid ligands. Additionally, fenofibrate also exhibits complex pharmacology at the CB_1 receptor, with the results indicating it acts as a negative allosteric modulator at higher concentrations.

Overall, these results raise the possibility that some of the clinical effects of fenofibrate may involve cannabinoid receptor interactions and also provide the basis for the future development of novel compounds acting as cannabinoid receptor agonists and allosteric modulators.

Chapter 3

Investigation of Functional Selectivity at the Cannabinoid Receptor in Human CB_1 Receptor-Transfected Chinese Hamster Ovary Cells

3.1. Introduction

Chinese hamster ovary or CHO cells are an immortalised cell line developed by Theodore T. Puck in the early 1960s. They are the most commonly used cell line for expression of recombinant protein owing to their relatively low chromosomal number (n =22), ability to express high amounts of protein and their relative paucity of endogenously expressed protein. Typically, the cells are cultured as an adherent monolayer in media containing the amino acid proline. A large amount of the research on cannabinoid receptors has been conducted using CHO cells expressing recombinant CB_1 receptor; indeed the initial description of the CB_1 receptor by Matsuda *et al*. (1990) involved transfection into CHO-K1 cells. Other important examples of cannabinoid receptor research carried out with transfected CHO cells include the initial identification of CB_1 coupling to G_s proteins (Glass & Felder, 1997), and as well as papers demonstrating functionally selective cannabinoid signalling (Bonhaus *et al.*, 1998).

3.2. Aims and objectives

The aim of this chapter was to investigate functionally selective responses at the CB_1 receptor expressed in transfected CHO cells. This was achieved by stimulating cells with a range of cannabinoid agonists and measuring the modulation of a number of signal transduction mediators including the MAP kinases ERK, JNK and p38, the enzyme adenylyl cyclase via changes in cAMP levels, and β-arrestin recruitment to the receptor. This cell line provides an attractive model for investigating agonist bias as it has been thoroughly validated by previous studies, and the relatively high receptor population should provide clear responses, bringing confidence to the data generated.

3.3. Methods

3.3.1. Cell Culture and membrane preparation

The culture of CHO-hCB_1 cells and production of membranes were performed as described in Chapter 2 – Methods (see **2.3.1** and **2.3.2**)

3.3.2. Radioligand Binding

Equilibrium competition radioligand binding assays using [^{3}H]-CP 55,940 were performed as described in Chapter 2 – Methods (see **2.3.3.1**).

3.3.3. cAMP accumulation assay

Levels of cAMP accumulation were determined using the DiscoveRx HitHunter® cAMP XS+ assay kit. Cells were seeded into white 96-well assay plates at 20,000 cells/well (unless otherwise stated) in culture medium, in either the absence of presence of pertussis toxin (100 ng/ml), incubated for 1 hour at room temperature and then incubated overnight at 37°C. On the day of the assay, the culture medium was aspirated and replaced with assay medium, comprising serum-free culture medium containing rolipram (10 µM), forskolin (10 µM) and 1 mg/ml BSA. Addition of the CB_1-selective antagonist AM 251 (final concentration 10 nM) or buffer was made and the cells pre-incubated for 30 min at 37°C. Each subsequent step was followed by an incubation period of 1 hour at room temperature in a final assay volume of 30 µl. Cells were treated with serial dilutions of cannabinoid ligands, performed in assay medium. Once ligand treatment was complete, the assay was terminated by cell lysis via the addition of ED/Lysis CL working solution (40 µl/well) followed by the addition of EA reagent. The chemiluminescent signal, corresponding to the cAMP concentration, was detected

using a PerkinElmer TopCount NXT™. The data were expressed as a percentage of the forskolin response (10 µM).

3.3.4. Beta-arrestin recruitment assay

Levels of β-arrestin recruitment were determined using the DiscoveRx PathHunter® assay. This assay utilises a second CHO cell line, different from that used in the other assays, stably transfected with a recombinant version of the human CB_1 receptor. Cells seeded into white 96-well assay plates at 20,000 cells/well (unless otherwise stated) in culture medium, incubated for 1 hour at room temperature and then incubated overnight at 37°C. On the day of the assay, cells were pre-treated with buffer or AM 251 (final concentration 10 nM) for 30 min, followed by treatment with serial dilutions of cannabinoid ligands, performed in medium, and incubated at 37°C for 90 min in a final assay volume of 100 µl. After incubation, Detection Reagent Solution was added (50 µl/well) and the plates incubated for 60 min at room temperature. Chemiluminescent signal was detected using a PerkinElmer TopCount NXT™. The data were expressed as a percentage of the span of the HU-210 response curve.

3.3.5. Determination of MAP kinase phosphorylation

3.3.5.1. Protocol

Levels of MAP kinase phosphorylation were determined using the In-Cell Western™ assay, which is a quantitative fluorescent immunoassay where proteins are immunocytochemically labelled *in situ* in fixed cultured cells. Cells were seeded into 96-well clear bottom plates, at 40,000 cells/well (unless otherwise stated) in culture medium at room temperature for 1 hour and then incubated

overnight at 37°C, in the presence of pertussis toxin (100 ng/ml), where appropriate. 30 min prior to experimentation, the culture medium was removed from the assay plates by aspiration, the cells were washed once with PBS, and the medium replaced with serum-free medium containing 1 mg/ml BSA and 2 units/ml apyrase, unless otherwise stated. Cells were pre-treated with buffer or AM 251 for 30 min. Serial dilution of test ligands was performed in serum-free medium and added to test wells to a final volume of 200 µl per well. Assay plates were incubated for the stated period at 37°C during experimentation. After incubation, the assay medium was rapidly aspirated and the cells were fixed with 4% paraformaldehyde in PBS for 20 min at room temperature (150 µl/well). Each reagent was aspirated before the addition of the next reagent. Cells were then permeabilised with 0.1% (v/v) Triton™ X-100 in PBS for 20 min at room temperature (150 µl/well). Non-specific antibody binding sites were blocked with 5% (w/v) milk powder in PBS for 20 min at room temperature with gentle rocking.

Primary antibodies for anti-total and anti-phosphorylated MAP kinases (ERK1/2, p38 or JNK1/2/3; see **3.3.6.3**) were diluted together in blocking agent to form primary antibody solution. The assay of each MAP kinase was performed separately. Cells were incubated with primary antibody solution (50 µl/well) overnight at 4°C with gentle rocking. The next day, the primary antibody solution was aspirated and the cells were washed three times with PBS containing 1 mg/ml BSA (150 µl/well) for 5 min at room temperature with gentle rocking. The appropriate LI-COR IRDye® secondary antibodies were diluted 3:11000 in blocking agent, added to the cells (100 µl/well), and incubated in darkness for 60

min at 37°C with gentle shaking. The secondary antibody solution was aspirated and the cells washed three times with wash buffer as before.

3.3.5.2. Imaging

Plates were imaged by scanning simultaneously at 700 and 800 nm with the LI-COR Odyssey® NIR Imaging System at 82 µm resolution, medium quality and focus offset of 4.0123 mm. Quantification was performed using LI-COR Odyssey® Software v3.0. The secondary antibody non-specific response was subtracted from the data. The phospho- response was then normalised against the total protein response for each individual well and then the data was expressed as a percentage of the basal response.

3.3.5.3. Antibodies used

All primary antibodies used were obtained from Cell Signaling Technology (Boston, USA). All antibodies were used at the concentrations described below unless otherwise stated in **Results** (see **3.4**). Anti-ERK 1/2 rabbit, (1:400) # 9102; anti-phospho-ERK1/2 (Thr202/Tyr204) monoclonal mouse, (1:200) # 9106; anti-p38 rabbit, (1:200) # 9212; anti-phospho-p38 (Thr180/Tyr182) monoclonal mouse, (1:200) #9216; anti-JNK rabbit, (1:200) # 9252; anti-phospho-JNK (Thr183/Tyr185) monoclonal mouse, (1:200) # 9255.

3.3.6. Data analysis

All data were analysed using the GraphPad Prism software (v6). The data for the equilibrium competition binding assays, and the ligand affinities, as denoted by

the equilibrium dissociation constants (K_i), where determined using the equations previously described in Chapter 2 – Methods (see **2.3.7**).

Concentration-response data were fitted to curves using the four-parameter logistic equation, previously described in Chapter 2 – Methods (see **2.3.7**).

Estimates for the antagonist AM 251 equilibrium dissociation constant (pK_B) were calculated using the logarithmic form of the Schild equation;

$$pK_B = \log(CR - 1) - \log[B]$$

where CR is the concentration ratio of agonist EC_{50} value in the presence of antagonist divide by the agonist EC_{50} value in the absence of antagonist and [B] is the antagonist concentration.

Ehlert (2005) described a parameter termed 'intrinsic relative activity' (RA_i), which has subsequently been used to quantify agonist bias and ligand selectivity at GPCRs (Griffin *et al.*, 2007; Ehlert, 2008; Figueroa *et al.*, 2009). A value is calculated for each agonist *A*, relative to a constant standard agonist *B*, for each signalling pathway the agonist couples to, using the following equation;

$$RA_i = \frac{{R_{max}}^A \, {EC_{50}}^B}{{R_{max}}^B \, {EC_{50}}^A}$$

where the R_{max} is the maximum response of the agonist, defined by the span of the concentration-response curve. The bias of an agonist, or ΔRA_i, is then defined as the fold difference between two RA_i values.

3.3.7. Statistics

The quantitative data are expressed as mean ± SEM, obtained from at least three independent experiments performed in triplicate, unless otherwise stated. Normality of data sets was determined using the D'Agostino-Pearson omnibus normality test. Statistical significance of differences was determined by Student's paired or unpaired, two-tailed *t*-tests or one-way ANOVA followed by Dunnett's multiple comparison *post-hoc* tests, where appropriate. Statistical comparison of pK_B values was using two-way ANOVA. A p value of <0.05 was considered significant.

3.4. Results

3.4.1. Determination of the affinity on cannabinoid CB_1 receptors

The occupancy of a number of cannabinoid ligands from several distinct chemical groups at human cannabinoid CB_1 receptors expressed in transfected CHO cells was investigated to characterise the receptor population present in the cell line, and to provide comparison data for subsequent functional experiments. This was done by measuring the displacement of [^{3}H]-CP 55,940 specific binding at equilibrium in CHO-hCB_1 receptor membranes (**Figure 3.1**). The data were used to determine the affinity (expressed as pK_i), and the co-operativity (curve slope, or n_H) as summarised in **Table 3.1**. The rank order of affinity for the ligands was;

HU-210 > CP 55,940 > AM 251 > Δ^9-THC > WIN 55,212-2 ≥ methanandamide > fenofibrate > anandamide.

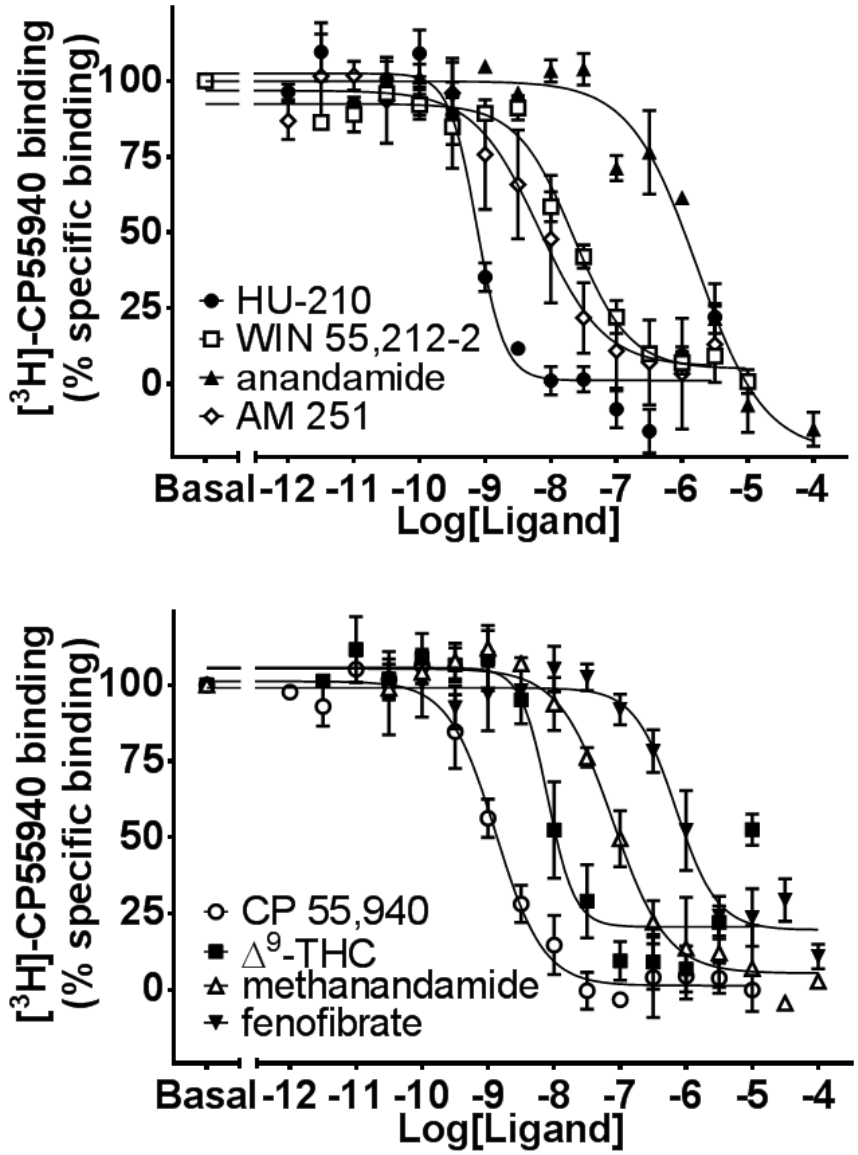

Figure 3.1 Effects of cannabinoid ligands on [^{3}H]-CP 55,940 binding on human CB_1 receptors expressed in CHO cells. Experiment was performed as stated in the methods (see **3.3.**2). The data shown represent mean ± SEM values from 3 independent experiments performed in triplicate. The curves were fitted using GraphPad Prism.

Table 3.1. Determination of the affinity (pK_i) and the co-operativity (n_H) of cannabinoid ligands on human cannabinoid CB_1 receptors expressed in transfected CHO cell membranes.

Ligand	**p*K*$_i$**	**n_H**
HU-210	9.4 ± 0.1	2.2 ± 0.4
CP 55,940	9.0 ± 0.1	1.1 ± 0.1
WIN 55,212-2	7.8 ± 0.1	1.1 ± 0.2
Δ^9-THC	8.2 ± 0.1	2.7 ± 0.7
Anandamide	5.9 ± 0.1	0.9 ± 0.3
Methanandamide	7.3 ± 0.5	0.9 ± 0.2
AM 251	8.3 ± 0.2	1.0 ± 0.2
Fenofibrate	6.3 ± 0.1	1.8 ± 0.7

Data shown are mean values ± SEM from three separate experiments.

3.4.2. Determination of ERK phosphorylation

3.4.2.1. Assay Optimisation

No prior comprehensive protocol had been established in-house for the use of the In-Cell Western assay, a fluorescence immunocytochemical-based technique, to quantify receptor-mediated changes in MAP kinase phosphorylation; therefore it was necessary to optimise the assay for use in this, and subsequent chapters.

Reduction of edge effect

Preliminary experiments revealed a clearly visible edge effect present on the assay plates when scanned (**Figure 3.2A**). Cells in the outer wells of the plate appeared

to be localised towards the outer peripheral well edge. Pre-incubation at room temperature for 1 hour immediately after seeding and prior to moving to the incubator markedly decreased the visible edge effect (**Figure 3.2B**).

The mean total-ERK signal intensity values for each column of plate A had a range of 39.1 to 48.4, with the lowest values at the outer rows A and H (41.9 and 39.1 respectively) and increasing towards the centre row (**Figure 3.2C**; ●), corresponding to the pattern of the visible edge effect. The mean total-ERK values for plate B had a markedly smaller range of 49.0 to 50.2 with little difference between each row (**Figure 3.2C**; □). Comparison of the coefficient of variance (%CV) for each column and row on both plates show the mean %CV was significantly lower after pre-incubation at room temperature for 1 hour (**Table 3.2**; paired, two-tailed *t*-test, column – $p<0.0001$; row – $p<0.002$,).

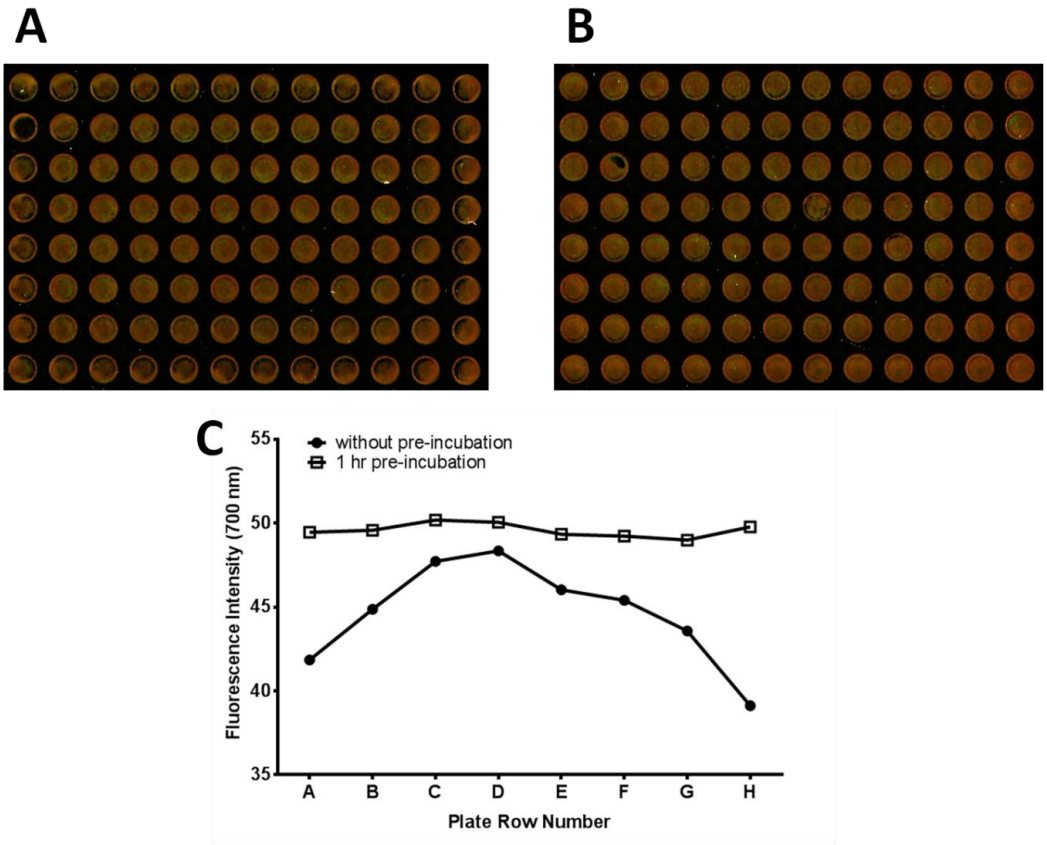

Figure 3.2 Pre-incubation at room temperature for 1hr decreases edge-effect. Composite (700 and 800nm) image of 96-well plate seeded with 40,000 cells/well were placed either (**A**) immediately into 37°C incubator, or (**B**) pre-incubated for 60 min at room temperature (21±1°C), prior to incubation at 37°C. Images show cells cultured for 48 hours, fixed and labelled with ERK polyclonal antibodies. **C** - Row mean signal intensity values for total-ERK signal (700nm) for plates either placed directed into incubator (●) or pre-incubated at room temperature for 1 hour (□). Data shown are mean replicate (n=12) values ± SEM from a single experiment.

Table 3.2

Coefficient of variance (% CV) values for plate columns and mean %CV values for plate rows and columns

	coefficient of variance (%CV)									
	A	**B**	**C**	**D**	**E**	**F**	**G**	**H**	**Column mean**	**Row mean**
No pre-incubation (Fig. 3.2A)	3.06	11.52	5.79	10.01	4.67	3.03	4.14	5.30	5.94	8.70
1 hr pre-incubation (Fig. 3.2B)	4.26	2.78	3.77	6.36	4.80	5.17	4.69	3.40	4.40 ****	2.87 **

Data shown are values from a single experiment

****p<0.0001; **p<0.002, paired, two-tailed t-test

Cell Seeding Density

The cannabinoid agonist HU-210 produced a phospho-ERK response at all cell seeding densities tested (**Figure 3.3A**) with no significant differences. However, the basal level of ERK phosphorylation for 40,000 cells/well was markedly lower than for the other seeding densities (**Figure 3.3A**). This cell number corresponded closest to 100% confluency. When the HU-210 response was expressed as % basal ERK phosphorylation 40,000 cell/well gave the largest response, which was significantly greater than the response at 60,000 cells/well (**Figure 3.**3B; one-way ANOVA, p<0.05).

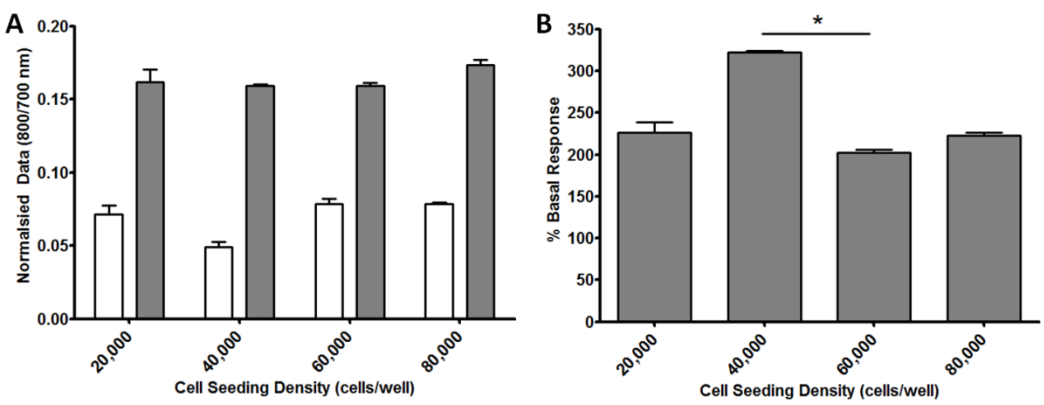

Figure 3.3 Effect of cell seeding density expressed as normalised data (**A**) showing values for basal (white) and HU-210-stimulated (grey) ERK phosphorylation, and as % basal phosphorylation (**B**). Data shown are mean triplicate values ± SEM. Statistical significance was determined using one-way ANOVA, *p<0.05.

Optimisation of primary antibody dilutions

All dilutions of total-ERK and phospho-ERK antibody tested produced a signal greater than that observed in the absence of the appropriate primary antibody i.e. non-specific binding (NSB) of the secondary antibody. For the total-ERK antibody, there was a significant increase in signal intensity at 1:200, 1:100 and 1:50 (**Figure 3.4A**; one-way ANOVA, *p<0.5, ***p<0.0001,). The signal intensity at all four antibody dilutions were significantly different from each other except for 1:100 and 1:50 where there was no significant difference (**Figure 3.4A**; one-way ANOVA, p>0.05).

For the phospho-ERK antibody, the signal intensity for both the basal phospho-ERK levels and the elevated HU-210 stimulated levels were measured, to allow the calculation of the % basal response. For the HU-210 response, there was a

significant increase in the signal intensity compared to the NSB value for all four antibody dilutions (and the signal intensity at 1:50 antibody dilution was significantly different from that for 1:400 and 1:200 (**Figure 3.4B**; one-way ANOVA, $p<0.0001$).

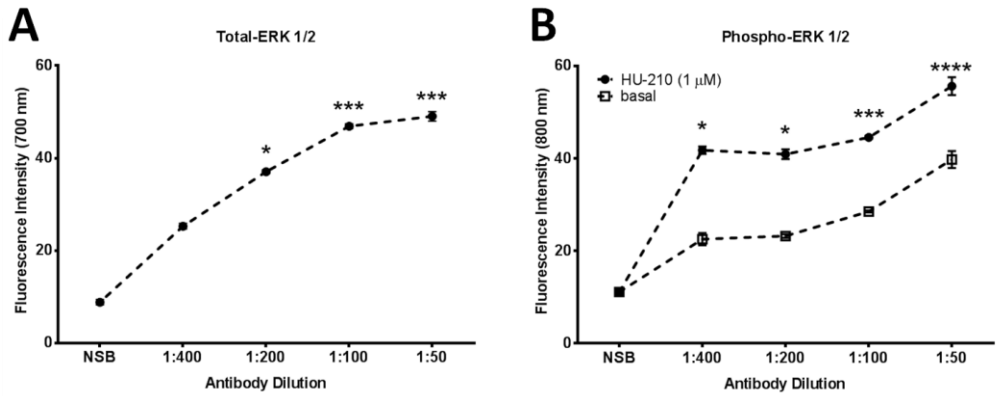

Figure 3.4 Optimisation of primary antibody concentration. Cells were incubated with various dilutions of (**A**) total ERK- and (**B**) phospho-ERK primary antibody. Blocking solution without primary antibody was included for both antibodies as a measure of the non-specific binding (NSB) of the secondary antibody. Data shown are mean values ± SEM. Statistical significance was determined using one-way ANOVA, $*p<0.05$. Values are significant relative to the corresponding NSB value.

To determine the potential effect of altering antibody dilution on the magnitude of the response when expressed as % basal phospho-ERK level, the mean signal intensity values for each phospho-ERK antibody dilution were normalised against the mean values for each total-ERK antibody dilution (**Table 3.3**). As the phospho-ERK antibody concentration decreased, the magnitude of the response increased, indicating increased assay sensitivity. In contrast, the dilution of the

total-ERK antibody had no impact on the magnitude of the response. However, as the antibody concentration decreased, the %CV of the signal intensities increased, for all three conditions (**Table 3.3**), indicating that the variation within the assay increased as the antibody dilution increased.

Table 3.3

Representative normalised data (phospho-/ total-ERK), expressed as % of the basal response, and associated coefficient of variance (% CV: italics) values, for various dilutions of the phospho- and total ERK primary antibodies

			Phospho-ERK (1:*x*)			
			400	**200**	**100**	**50**
		% CV	*18.3*	*11.4*	*11.0*	*5.2*
Total-ERK (1:*x*)	**400**	*15.6*	196	184	162	140
	200	*16.7*	196	184	162	140
	100	*4.8*	196	184	162	140
	50	*2.1*	196	184	162	140

Effects of apyrase

Preliminary experiments showed that the addition of vehicle (assay buffer containing 1 mg/ml BSA) without any agonist present was able to elicit a phospho-ERK response. It was suggested that this effect might be due to endogenous ATP release; therefore, the inclusion of apyrase, an ATPase, was investigated to test this hypothesis. Incubation with 2 units/ml apyrase for 30 min was able to significantly decrease the basal level of ERK phosphorylation (**Figure 3.5A**; paired, two-tailed *t*-test, $^{**}p<0.05$).

Cells were then stimulated over a 20 min time course with the addition of HU-210 (1 µM), vehicle (assay buffer) and exogenous ATP (10 µM), in the presence and absence of apyrase, and the area under the response curve plotted (**Figure 3.5B**). Apyrase significantly decreased the response to vehicle and ATP addition, while the response for HU-210 was not significantly affected (**Figure 3.5B**; paired, two-tailed *t*-test, *$p<0.05$, **$p<0.01$).

Finally the effect of apyrase on a HU-210 concentration-response curve, at 5 min agonist incubation, was investigated. Apyrase did not have any significant effect on the HU-210 concentration-response curve; however it did cause a reduction in basal and vehicle addition response and a related increase in the slope of the concentration response curve (**Figure 3.5C**; n_H without apyrase– 1.48, 2 units/ml - 2.09).

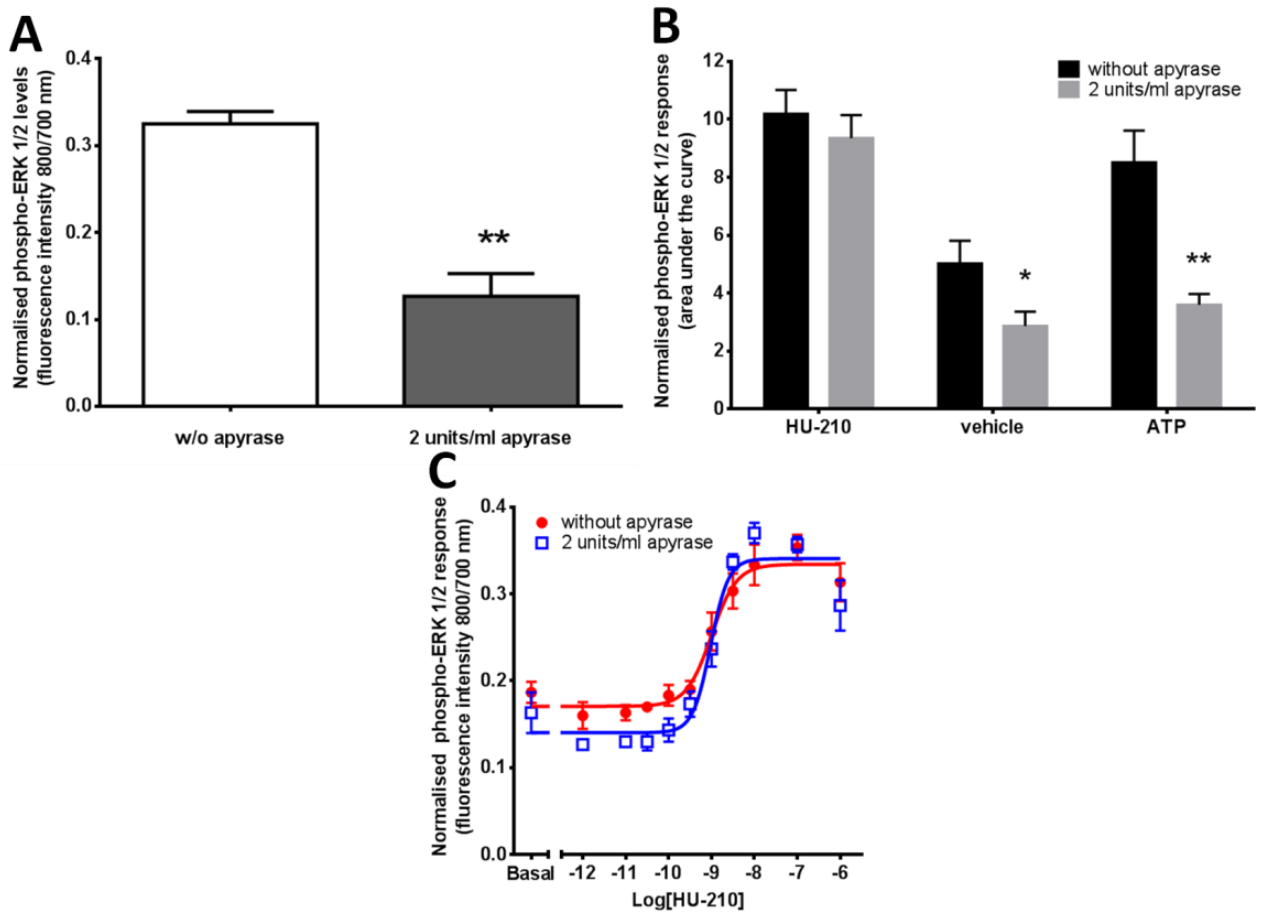
A
Normalised phospho-ERK 1/2 levels (fluorescence intensity 800/700 nm)
0.4
0.3
0.2
0.1
0.0
**
w/o apyrase
2 units/ml apyrase
B
Normalised phospho-ERK 1/2 response (area under the curve)
12
10
8
6
4
2
0
without apyrase
2 units/ml apyrase
*
**
HU-210
vehicle
ATP
C
Normalised phospho-ERK 1/2 response (fluorescence intensity 800/700 nm)
0.4
0.3
0.2
0.1
0.0
without apyrase
2 units/ml apyrase
Basal
-12
-11
-10
-9
-8
-7
-6
Log[HU-210]

Figure 3.5 Effect of apyrase on phospho-ERK response. **A** – Basal ERK phosphorylation in the absence (white bar), or presence (grey bar) of 2 units/ml apyrase incubation for 30 min. **B** – Phospho-ERK response upon stimulation by HU-210 (1 µM), vehicle and exogenous ATP (1 µM) over a 20 min time course, expressed as the area under the curve (AUC). C – HU-210 concentration response curve at 5 min in the absence and presence of 2 units/ml apyrase. Individual ERK phosphorylation values were normalised to the corresponding total-ERK values. Data shown are mean ± SEM values from three independent experiments performed in duplicate. *$p<0.05$, **$p<0.01$, paired, two-tailed *t*-test.

3.4.2.2. Effect of cannabinoid agonists on ERK phosphorylation – time course

CHO-hCB_1 cells were treated with high concentrations (10 μM) concentrations of the cannabinoid agonists HU-210, CP 55,940, WIN 55,212-2, Δ^9-THC, anandamide, methanandamide, arachidonyl-2'-chloroethylamide (ACEA) and fenofibrate at various time points (2 – 60 min), and the phospho-ERK responses measured. This temporal characterisation allowed for determination of the optimum agonist stimulation period for subsequent concentration-response experiments as well as providing the means to identify any multiphasic responses. All agonists produced a rapid increase in phospho-ERK levels, with a maximum response achieve between 4 – 6 min (**Figure 3.6**). After this time period, the phospho-ERK levels steadily decreased to reach near-basal levels by 20 min. From 20 min onwards, the HU-210 and CP 55,940 responses showed a gradual increase up to 60 min, while the response for the other agonists remained constant.

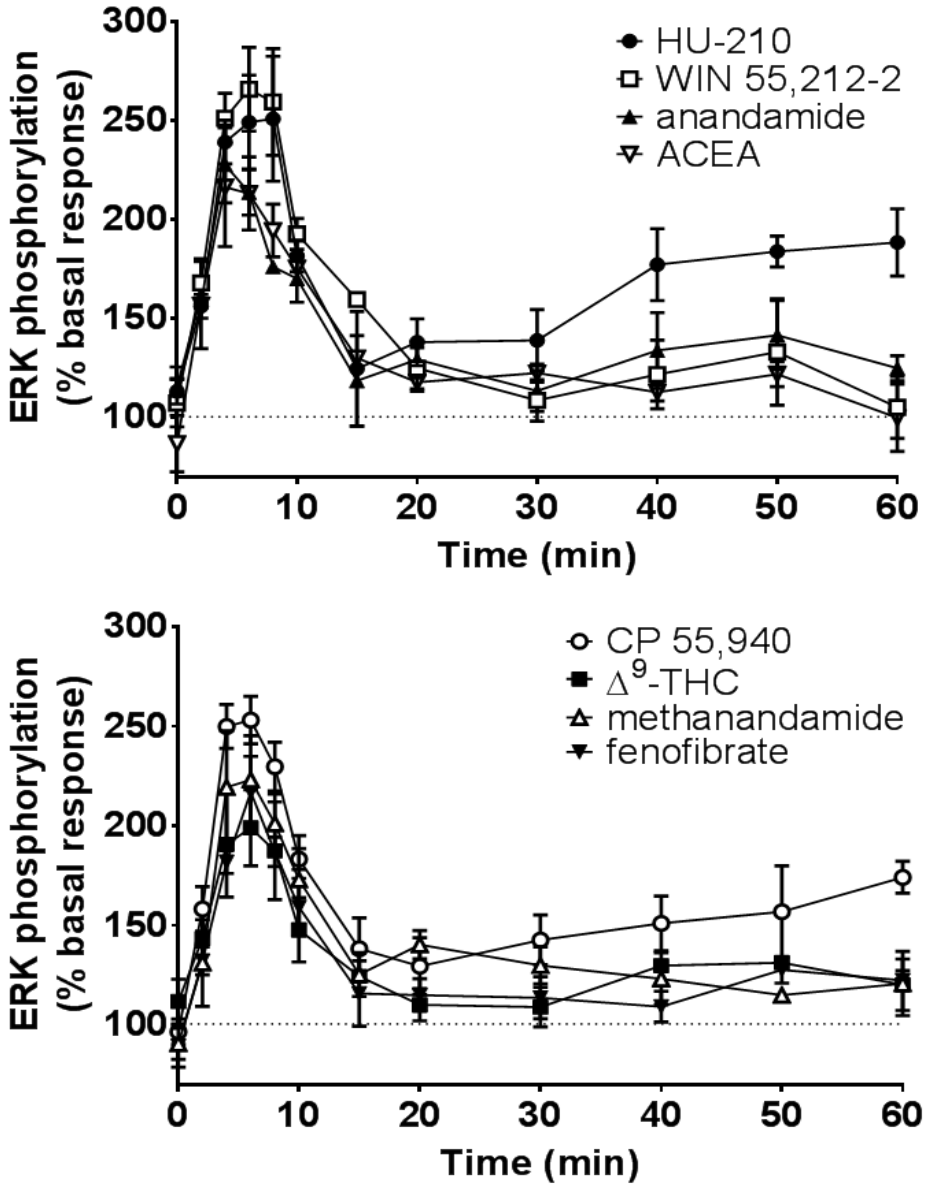

Figure 3.6 Effect of cannabinoid agonists on ERK phosphorylation in CHO-hCB_1 cells against time. Cells (40,000 cells/well) were cultured in medium for 24 hr, followed by serum starvation for 24 hr. Cells were stimulated with cannabinoid agonists (10 μM) at various time points (2 – 60 min), followed by rapid fixation with PFA solution. Detection of total and phospho-ERK levels was as stated in methods (see **3.3.5**). Individual ERK phosphorylation values were normalised to the corresponding total-ERK values. The data shown are mean ± SEM values from 3 independent experiments performed in duplicate.

Next, the experiments were repeated in cells pre-treated with pertussis toxin (100 ng/ml), to determine the role of $G_{i/o}$ protein in the cannabinoid-mediated phospho-ERK response, and whether any alternative $G_{i/o}$ protein-independent signalling could be identified. PTX was able to completely abolish all cannabinoid-mediated responses across the 60 min time course (**Figure 3.7**).

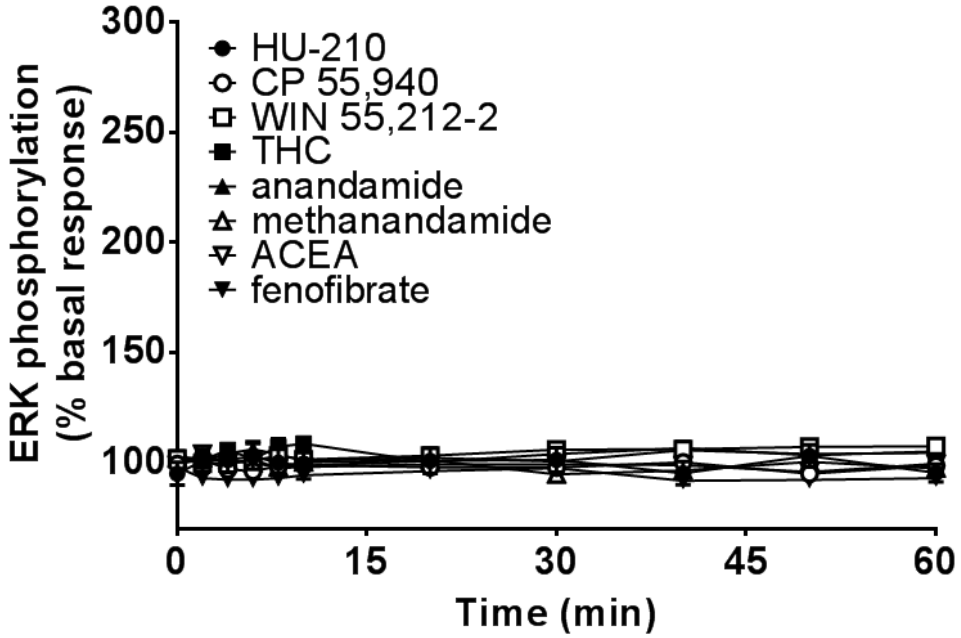

Figure 3.7 Effects of cannabinoid agonists on ERK phosphorylation in pertussis toxin-treated CHO-hCB_1 cells over time. Cells (40,000 cells/well) were cultured in medium for 24 hr, followed by serum starvation for 24 hr in medium containing 100 ng/ml PTX. Cells were stimulated with cannabinoid agonists (10 μM) at various time points (2 – 60 min), followed by rapid fixation with PFA solution. Detection of total and phospho-ERK levels was as stated in methods (see **3.3.5**). Individual ERK phosphorylation values were normalised to the corresponding total-ERK values. The data shown are mean ± SEM values from 3 independent experiments performed in duplicate.

A series of extended (5 – 360 min) time-course experiments were performed to further investigate the gradual second phase increases in phospho-ERK levels seen with CP 55,940. All four agonists tested (HU-210, CP 55,940, WIN 55,212-2 and methanandamide) produced a significant increase in phospho-ERK levels at 5 min, corresponding to the peak of the response seen previously (**Figure 3.8**). Both CP 55,940 and HU-210 produced a second, late phase with a peak at 90 min (CP - 184 ±1). The methanandamide-induced response returned to a near basal level 60 min after stimulation, while WIN 55,212-2 produced a sustained decrease in phospho-ERK levels with a profile distinct from those of CP 55,940 and HU-210 responses (~35 % basal response). At 180 min onwards, HU-210 caused cells to exhibit an atypical morphology, as well as causing a reduction in total-ERK levels, indicative of a cytotoxic effect (data not shown); therefore the data was not considered further. This effect was not observed with the other agonists tested. Overnight treatment of cells with PTX (100 ng/ml) was again used to determine the role of $G_{i/o}$ protein in the late-phase signal for CP 55,940. PTX was able to completely abolish both the initial and late phase phospho-ERK responses for CP 55,940 (**Figure 3.8**, ◊ symbol).

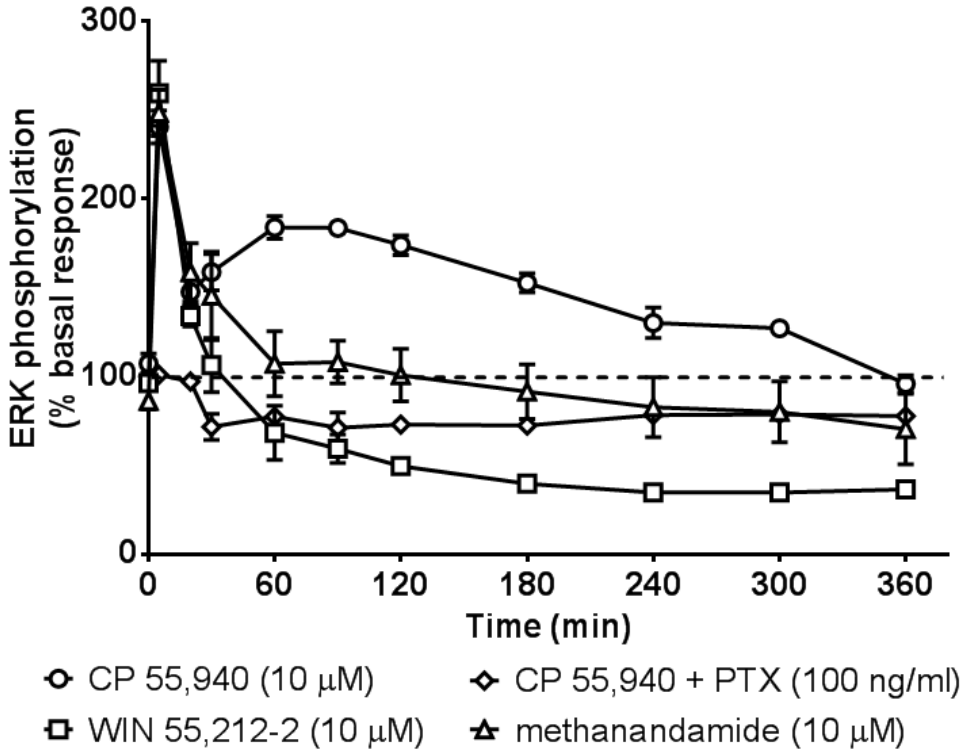

Figure 3.8 Effect of cannabinoid agonists on ERK phosphorylation in CHO-hCB_1 cells over time. Cells (40,000 cells/well) were cultured in medium for 24 hr, followed by serum starvation for 24 hr, with PTX where appropriate (100 ng/ml). Cells were stimulated with cannabinoid agonists (10 μM) at various time points (5 – 360 min), followed by rapid fixation with PFA solution. Detection of total and phospho-ERK levels was as stated in methods (see **3.3.5**). Individual ERK phosphorylation values were normalised to the corresponding total-ERK values. The data shown are mean ± SEM values from 3 independent experiments performed in duplicate.

3.4.2.3. Effects of cannabinoid agonists on ERK phosphorylation – concentration-response.

Initially, a stimulation period of 5 min was chosen for cannabinoid concentration-response experiments, representing the peak of the first phase response. All agonists produced a concentration-dependent increase in phospho-ERK levels (**Figure 3.9**). Higher concentrations of fenofibrate produced a clear decrease in the phospho-ERK response, generating an atypical bell-shaped concentration-response curve. It was, therefore, excluded from curve fitting. The rank order of potency (pEC_{50} values) of the agonists acting on CHO-hCB_1 cells from highest to lowest was HU-210 ≥ CP 55,940 > Δ^9-THC > ACEA ≥ WIN 55,212-2 > methanandamide ≥ anandamide (**Table 3.4**). There were some significant differences in the agonist R_{max} values. The R_{max} value for Δ^9-THC was significantly lower than that for HU-210 and ACEA, while the R_{max} value for methanandamide was significantly lower than that for HU-210 (**Table 3.4**; one-way ANOVA; $p<0.05$). To confirm the role of the CB_1 receptor in the cannabinoid agonist responses, the concentration-response experiments were repeated in the presence of the CB_1-selective competitive antagonist AM 251 (10 nM). AM 251 produced a significant rightwards shift of all the agonist concentration-response curves, resulting in significant decreases in all the pEC_{50} values (two-way ANOVA; $p<0.05$). These data were used to estimate the equilibrium dissociation constant for AM 251 (pK_B) in the presence of each individual agonist (**Table 3.4**). There was no significant difference between the pK_B values, except for the value determined using Δ^9-THC, which was significantly greater than that determined using anandamide (**Table 3.4**; one-way ANOVA; $p<0.01$).

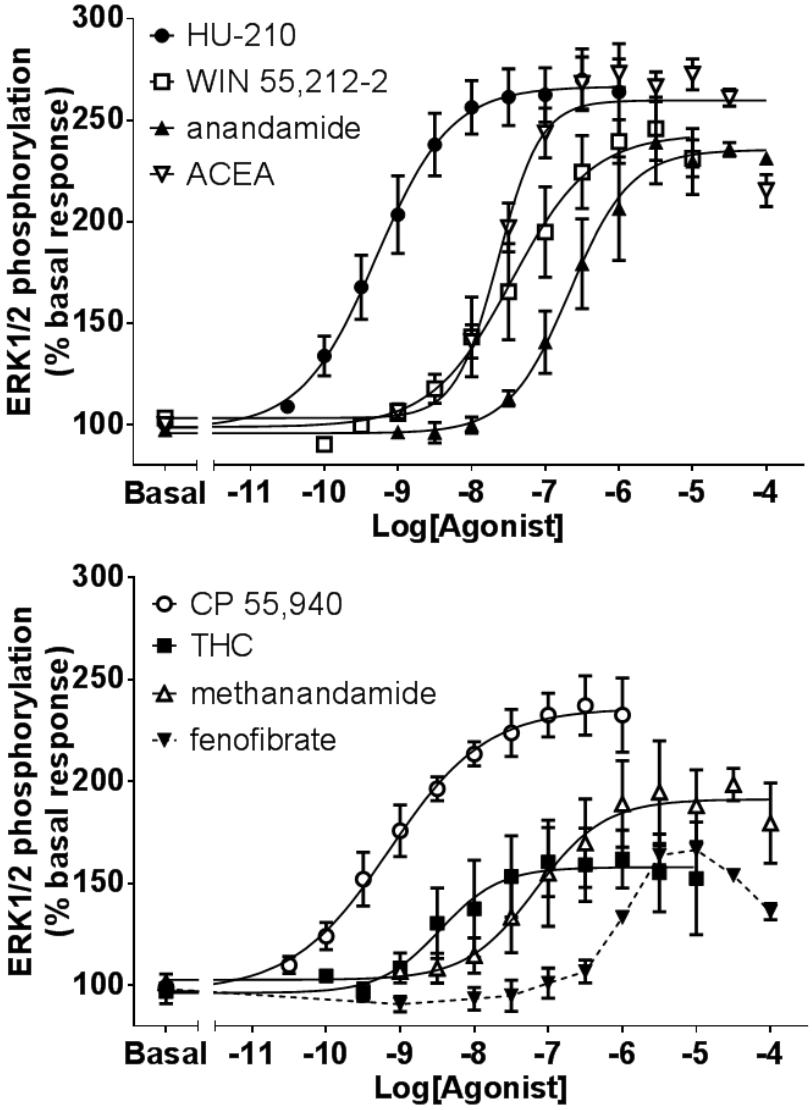

Figure 3.9 Effect of cannabinoid agonists on ERK phosphorylation in CHO-hCB_1 cells. Cells (40,000 cells/well) were cultured in medium for 24 hr, followed by serum starvation for 24 hr. Cells were stimulated with various concentrations of cannabinoid agonists for 5 min, followed by rapid fixation with cold PFA solution (4 % w/v). Detection of total and phospho-ERK levels was as stated in methods (see **see 3.3.5**). Individual ERK phosphorylation values were normalised to the corresponding total-ERK values. The data shown represent mean ± SEM values from 3-4 independent experiments performed in duplicate. The curves were fitted using GraphPad Prism. Dashed lines indicate that the data were not curve-fitted.

Table 3.4

Determination of potency (pEC_{50}), percentage of basal maximal response (R_{max}), curve slope (n_H) and estimated AM 251 dissociation constant (pK_B) of cannabinoid agonists on ERK phosphorylation in CHO-hCB_1 cells.

Agonists	**pEC_{50}**	**R_{max}**	**n_H**	**pK_B**
HU-210	9.3 ± 0.3	172 ± 18	1.0 ± 0.1	9.4 ± 0.2
CP 55,940	9.1 ± 0.3	143 ± 18	0.8 ± 0.1	9.5 ± 0.2
WIN 55,212-2	7.5 ± 0.4	142 ± 9	1.2 ± 0.1	9.4 ± 0.2
Δ^9-THC	8.6 ± 0.1	82 ± 7[bc]	1.3 ± 0.2	9.9 ± 0.1
Anandamide	6.6 ± 0.2	143 ± 1	0.9 ± 0.2	8.9 ± 0.1
Methanandamide	6.7 ± 0.8	108 ± 7[b]	1.0 ± 0.3	9.1 ± 0.2
ACEA	7.6 ± 0.1	157 ± 3	1.5 ± 0.1[a]	9.7 ± 0.1

Data shown are mean ± SEM values from 3-4 independent experiments performed in duplicate.

[a] n_H value significantly difference from unity (n_H = 1). Unpaired *t*-test; $p<0.05$

[b] value significantly less than that for HU-210. One-way ANOVA; $p<0.05$

[c] value significantly less than that for ACEA. One-way ANOVA; $p<0.05$

Concentration-response experiments using CP 55,940, with a stimulation period of 60 min were then performed to more fully characterise the nature of the second-phase response. CP 55,940 produced a concentration-dependent response best fitted by a biphasic concentration-response curve as determined by a *F* sum-of-squares test, with pEC_{50} values of 9.0 ± 0.2 and 4.5 ± 0.4 for the high and low potency responses respectively (**Figure 3.10**). Inhibition with a high concentration

of AM 251 (1 μM) appeared to abolish the high potency response, but had no observable impact on the low potency response (pEC_{50} – 5.3 ± 0.1).

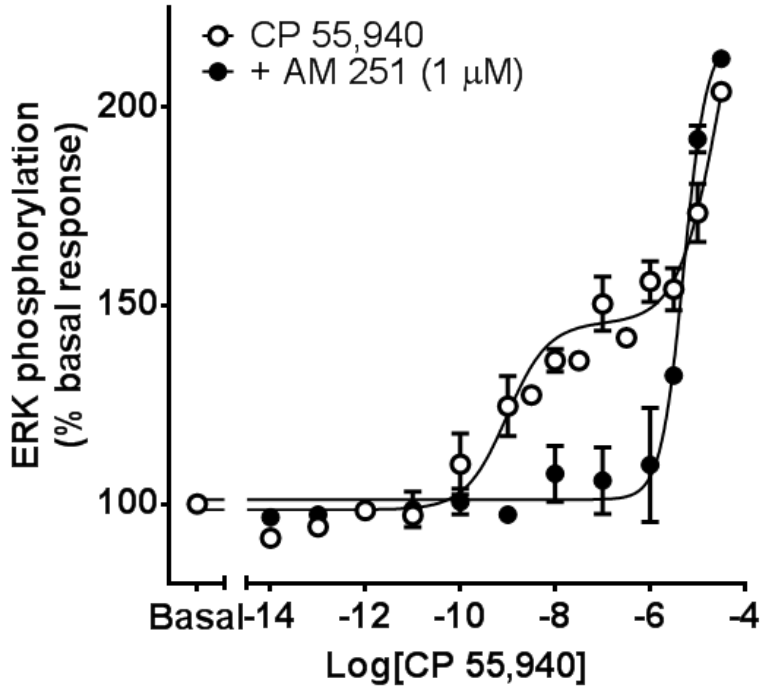

Figure 3.10 Effect of CP 55,940 on ERK phosphorylation in CHO-hCB_1 cells. Cells (40,000 cells/well) were cultured in medium for 24 hr, followed by serum starvation for 24 hr. Cells were stimulated with various concentrations of CP 55,940 for 1 hr, followed by rapid fixation with cold PFA solution (4 % w/v). Detection of total and phospho-ERK levels was as stated in methods (see **see 3.3.5**). Individual ERK phosphorylation values were normalised to the corresponding total-ERK values. The data shown represents mean ± SEM values from 3 independent experiments performed in duplicate. The most appropriate curve was determined by an extra sum-of-squares F test and fitted using GraphPad Prism.

3.4.3. Determination of JNK1/2/3 phosphorylation

The cannabinoid agonists were tested for their potential to promote JNK1/2/3 phosphorylation. The positive control, hydrogen peroxide (H_2O_2; 5 mM), produced a significant increase in phospho-ERK levels between 5 and 25 min (**Figure 3.11**; one-way ANOVA $p<0.0001$). None of the cannabinoid agonists tested significantly increased the phospho-JNK response above the basal level (**Figure 3.11**; one way ANOVA; $p>0.05$).

3.4.4. Determination of p38 phosphorylation

The cannabinoid agonists were tested for their potential to promote p38 MAP kinase phosphorylation. The positive control hydrogen peroxide (H_2O_2; 5 mM) produced a clear increase in phospho-p38, which was significantly greater than the basal from 50 min onwards (**Figure 3.12;** one-way ANOVA $p<0.0001$). None of the cannabinoid agonists tested were able to significantly increase the phospho-p38 response above the basal (**Figure 3.12**; one way ANOVA; $p>0.05$).

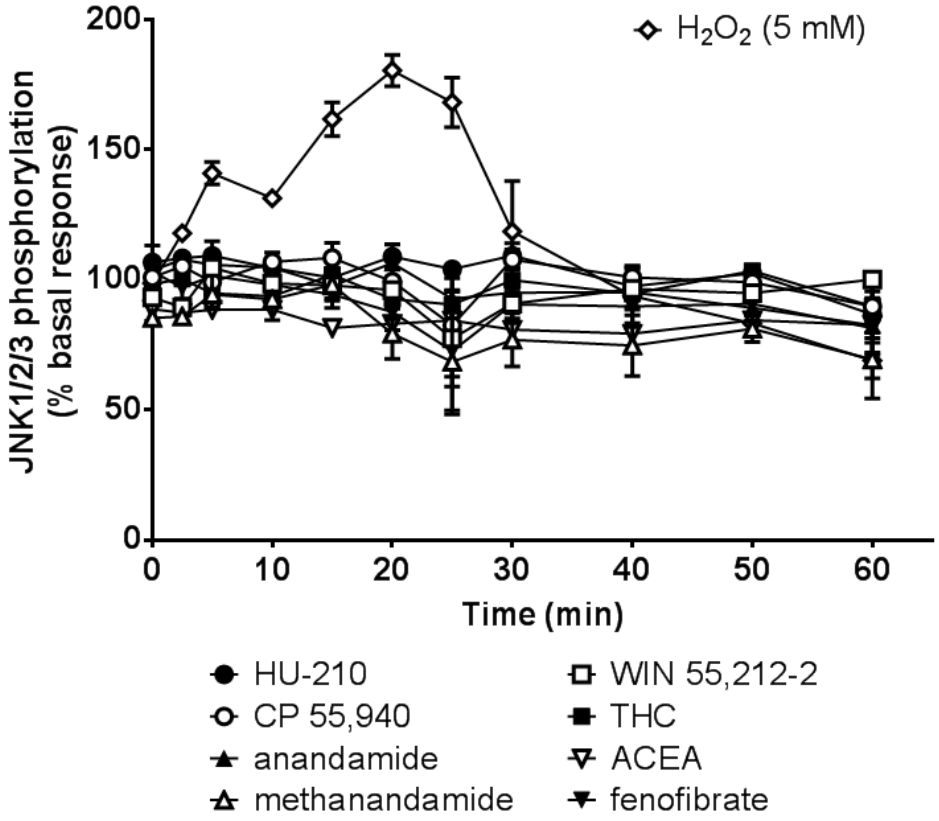

Figure 3.11 Effects of cannabinoid agonists on JNK phosphorylation in CHO-hCB_1 cells against time. Cells (40,000 cells/well) were cultured in medium for 24 hr, followed by serum starvation for 24 hr. Cells were stimulated with cannabinoid agonists (10 μM) or hydrogen peroxide (5 mM) at various time points (2.5 – 60 min), followed by rapid fixation with PFA solution. Detection of total and phospho-JNK1/2/3 levels was as stated in methods (see **3.3.5**). Individual JNK phosphorylation values were normalised to the corresponding total-JNK values. The data shown are mean ± SEM values from 3 independent experiments performed in duplicate.

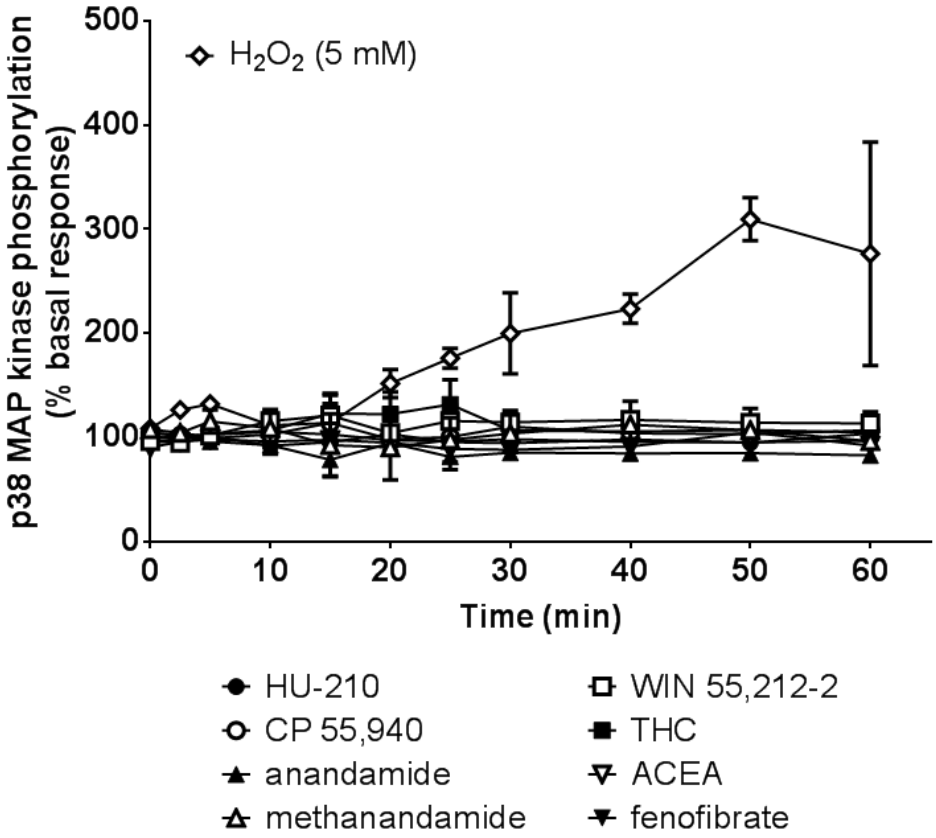

Figure 3.12 Effects of cannabinoid agonists on p38 MAP kinase phosphorylation in CHO-hCB_1 cells against time. Cells (40,000 cells/well) were cultured in medium for 24 hr, followed by serum starvation for 24 hr. Cells were stimulated with cannabinoid agonists (10 µM) or hydrogen peroxide (5 mM) at various time points (2.5 – 60 min), followed by rapid fixation with PFA solution. Detection of total and phospho-p38 levels was as stated in methods (see **3.3.5**). Individual p38 phosphorylation values were normalised to the corresponding total-p38 values. The data shown are mean ± SEM values from 3 independent experiments performed in duplicate.

3.4.5. cAMP accumulation

Assay Optimisation

A preliminary experiment was performed to determine the optimal cell seeding density and concentration of forskolin for use in subsequent cAMP assays (**Figure 3.13**). Forskolin produced a concentration-dependent increase in intracellular cAMP levels at all cell seeding densities tested. There was no apparent effect of the cell number on the span of the forskolin concentration-response. However, there was an apparent modest leftward shift in the concentration-response curve with increasing cell number, as well as a modest increase in the basal cAMP levels.

On the basis of these results, a cell seeding density of 20,000 cells/well and a forskolin concentration of 10 µM, as corresponding to the pEC_{80}, were chosen as optimised conditions for all subsequent experiments.

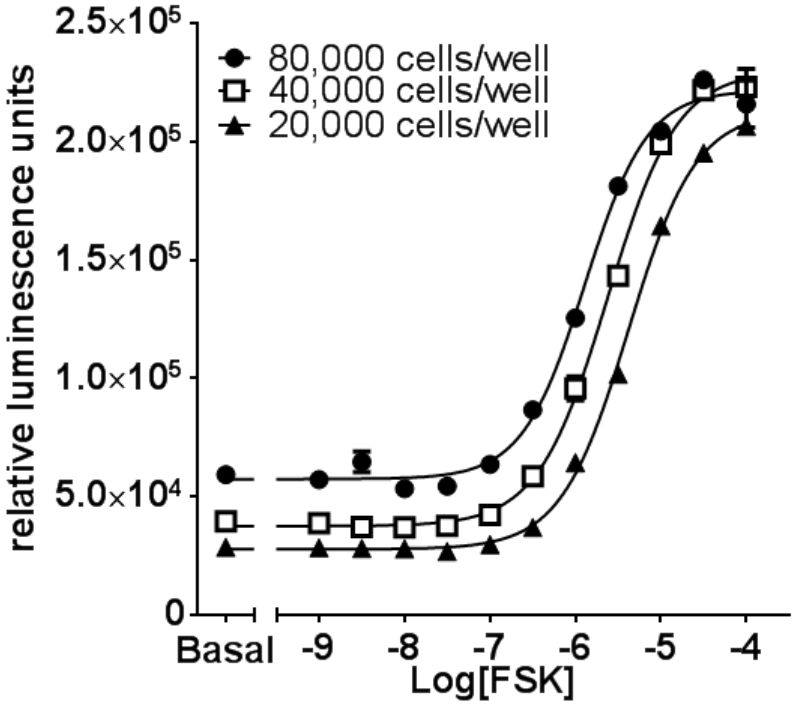

Figure 3.13 Optimisation of cAMP assay in CHO-hCB_1 cells. Cells (20, 40 and 80,000 cells/wells) in suspension in serum-free medium were pre-treated with rolipram for 10 min before incubation with increasing concentrations of forskolin (1 nM – 100 µM) for 30 min at room temperature. At the end of the incubation, the assay was terminated by the addition of lysis buffer, and the relative levels of cAMP determined using the HitHunter assay kit. The data shown represent a single experiment performed in duplicate and is given as the mean ± SEM value. The curves were fitted using GraphPad Prism.

Inhibition of forskolin-stimulated cAMP accumulation

CHO-hCB_1 cells treated with forskolin and the phosphodiesterase PDE4 inhibitor rolipram (both 10 µM), were stimulated with increasing concentrations of the cannabinoid agonists to determine the ability of these compounds to inhibit forskolin-stimulated cAMP accumulation (**Figure 3.14**). All agonists produced a

concentration-dependent inhibition of forskolin-stimulated cAMP accumulation. The rank order potency (pEC_{50} values) of the agonists acting on CHO-hCB_1 cells from highest to lowest was HU-210 ≥ CP 55,940 > Δ^9-THC > ACEA ≥ WIN 55,212-2 ≥ methanandamide > anandamide ≥ fenofibrate. The R_{max} of Δ^9-THC was significantly less than for HU-210 and CP 55,940 (one-way ANOVA; $p<0.05$). Treatment with 10 μM Δ^9-THC, produced an atypical enhancement of cAMP accumulation in all experiments (124 ± 15 %), which was not significantly affected by AM 251 (10 nM; 130 ± 19 %). As this was indicative of a distinct (non-CB_1) signalling mechanism, the data points derived from the highest concentrations were excluded from the concentration-response curve fitting.

To confirm the role of the CB_1 receptor in the cannabinoid agonist responses, the concentration-response experiments were repeated in the presence of the CB_1-selective competitive antagonist AM 251 (10 nM). AM 251 produced a rightward shift of all the agonist concentration-response curves, resulting in significant decreases in all the pEC_{50} values (two-way ANOVA; $p<0.05$). These data were used to estimate the equilibrium dissociation constant for AM 251 (pK_B) in the presence of each individual agonist (**Table 3.5**). There was no significant difference between the pK_B values, except for the value determined using ACEA, which was significantly less than that determined using HU-210 and CP 55,940 (one-way ANOVA; $p<0.01$).

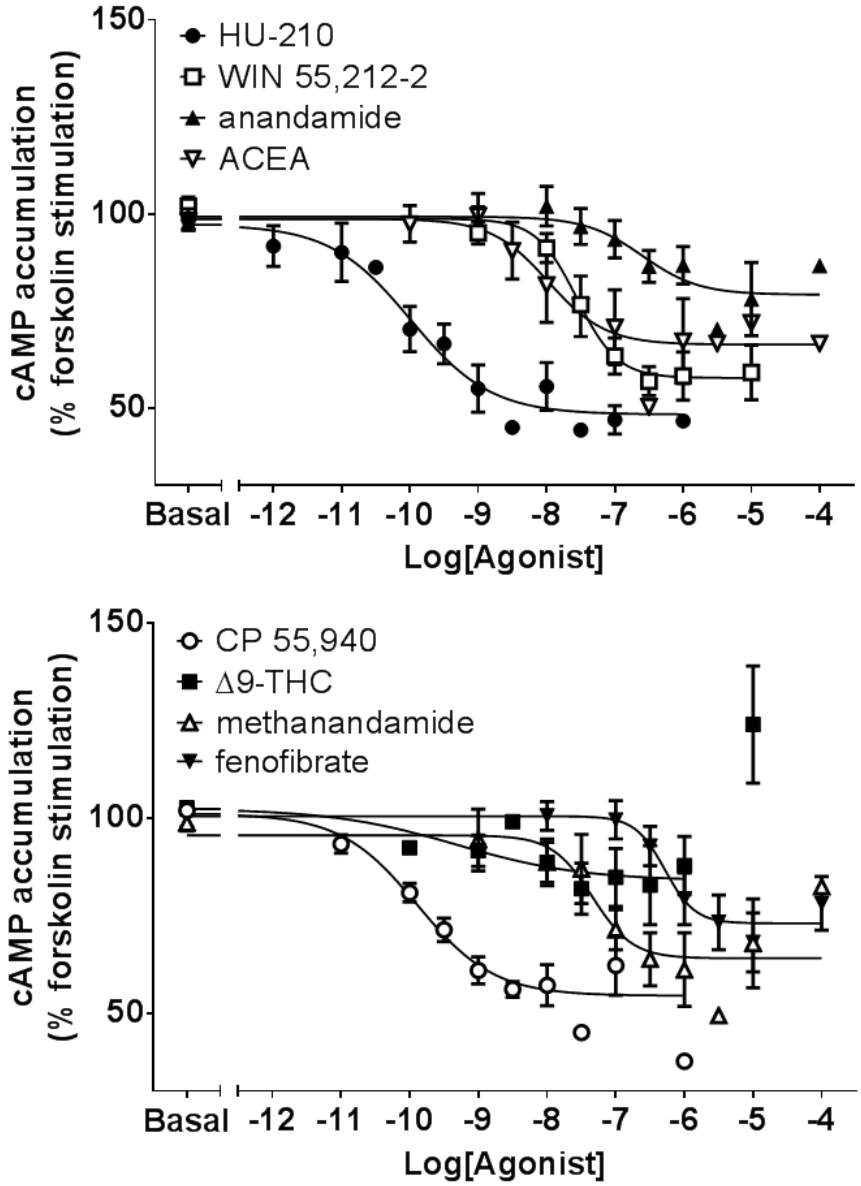

Figure 3.14 Effect of cannabinoid agonists on cAMP accumulation in CHO-hCB_1 cells. Cells in suspension in serum-free medium were pre-treated with forskolin and rolipram (both 10 μM) for 10 min before incubation with increasing concentrations of cannabinoid agonists for 30 min at room temperature. At the end of the incubation period, the assay was terminated by the addition of lysis buffer and the relative levels of cAMP determined using the HitHunter assay kit. The data shown represent mean ± SEM values from 4 individual experiments performed in triplicate. The curves were fitted using GraphPad Prism.

Table 3.5

Determination of potency (pEC_{50}), percentage of basal maximal response (R_{max}), curve slope (n_H) and estimated AM 251 dissociation constant (pK_B) of cannabinoid agonists on inhibition of forskolin-stimulated cAMP accumulation in CHO-hCB_1 cells.

Agonists	**pEC_{50}**	**R_{max}**	**n_H**	**pK_B**
HU-210	10.3 ± 0.2	47 ± 4	-1.6 ± 0.8	9.5 ± 0.3
CP 55,940	9.9 ± 0.1	48 ± 9	-1.0 ± 0.3	9.4 ± 0.1
WIN 55,212-2	7.6 ± 0.1	43 ± 8	-1.6 ± 0.3	9.3 ± 0.1
Δ^9-THC	8.8 ± 0.2	23 ± 11[b]	-1.4 ± 0.6	9.6 ± 0.3
Anandamide	6.7 ± 0.3	28 ± 7	-1.8 ± 0.7	8.9 ± 0.3
Methanandamide	7.4 ± 0.2	37 ± 9	-1.6 ± 1.0	9.2 ± 0.1
ACEA	8.1 ± 0.3	28 ± 10	-1.1 ± 0.3	8.5 ± 0.2
fenofibrate	6.4 ± 0.1	33 ± 5	-1.7 ± 0.1[a]	9.1 ± 0.1

Data shown are mean ± SEM values from 4 independent experiments performed in triplicate.

[a] n_H value significantly difference from unity (n_H = -1); unpaired *t*-test, $p<0.05$.

[b] significantly less than that for HU210 and CP 55,940; one-way ANOVA, $p<0.05$

The experiments were then repeated using cells which had been pre-treated with PTX (100ng/ml) and in the absence of forskolin, to determine the role of $G_{i/o}$ protein in the cannabinoid-mediated cAMP response, and whether any alternative $G_{i/o}$ protein-independent signalling could be identified. As before, forskolin produced a concentration-dependent increase in intracellular cAMP levels. None

of the cannabinoid agonists tested produced any significant effect on the cAMP levels (**Figure 3.15**).

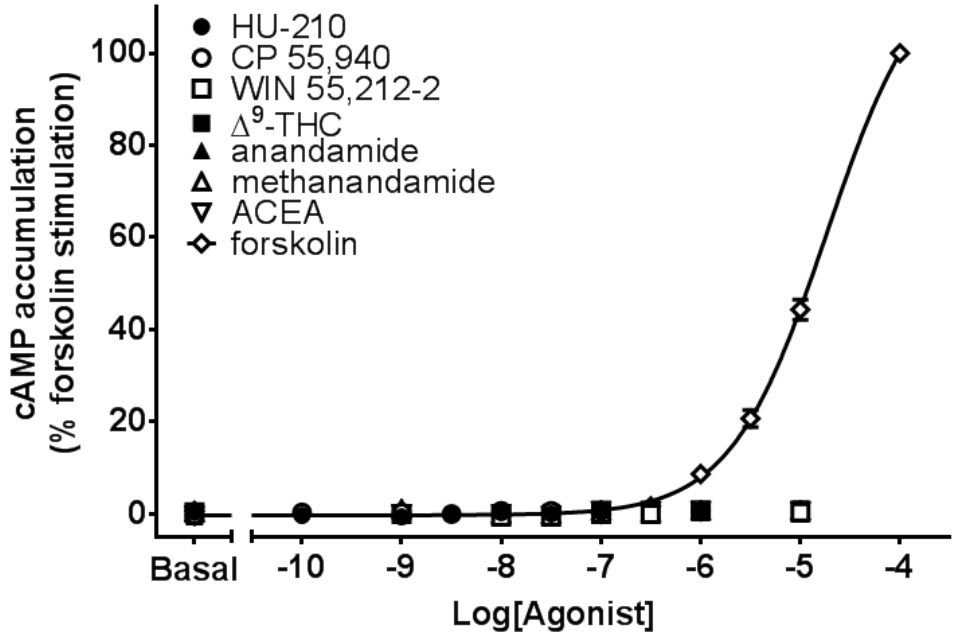

Figure 3.15 Effect of cannabinoid agonists on cAMP accumulation in pertussis toxin-treated CHO-hCB_1 cells. Cells in suspension in serum-free medium were pre-treated with PTX (100 ng/ml) overnight and rolipram (10 µM) for 10 min before incubation with increasing concentrations of cannabinoid agonists for 30 min at room temperature. At the end of the incubation period, the assay was terminated by the addition of lysis buffer and the relative levels of cAMP determined using the HitHunter assay kit. The data shown represents mean ± SEM values from 3 individual experiments performed in triplicate. The curves were fitted using GraphPad Prism.

3.4.6. β-arrestin recruitment

The cannabinoid agonists were tested for their ability to promote β-arrestin recruitment to the CB_1 receptor using the PathHunter™ β-arrestin assay. All agonists produced a concentration-dependent increase in β-arrestin recruitment as measured by an increase in chemiluminescent signal, which was then expressed as a % of the maximum HU-210 response (**Figure 3.16**). Higher concentrations of fenofibrate produced a clear decrease in the phospho-ERK response, producing an atypical bell-shaped concentration-response curve. It was, therefore, excluded from curve fitting. The rank order of potency (pEC_{50} values) of the agonists acting on CHO-hCB_1 cells from highest to lowest was HU-210 ≥ CP 55,940 > Δ^9-THC > WIN 55,212-2 ≥ ACEA ≥ methanandamide ≥ anandamide (**Table 3.6**). There was significant difference between the R_{max} values for the various agonists, in particular Δ^9-THC, anandamide and methanandamide were significantly less efficacious than HU-210, CP 55,940 and WIN 55,212-2, while ACEA was a partial agonist, relative to HU-210 only (**Table 3.6**; one-way ANOVA; $p<0.0001$).

To confirm the role of the CB_1 receptor in the cannabinoid agonist responses, the concentration-response experiments were repeated in the presence of the CB_1-selective competitive antagonist AM 251 (10 nM). AM 251 produced a rightward shift of all the agonist concentration-response curves, resulting in significant decreases in all the pEC_{50} values, except HU-210 (two-way ANOVA; $p<0.01$). These data were used to estimate the equilibrium dissociation constant for AM 251 (pK_B) in the presence of each individual agonist (**Table 3.6**). There was no significant difference between the pK_B values, except for the value determined

using HU-210, which was significantly less than that determined using all other agonists, except WIN 55,212-2 (one-way ANOVA; $p<0.01$).

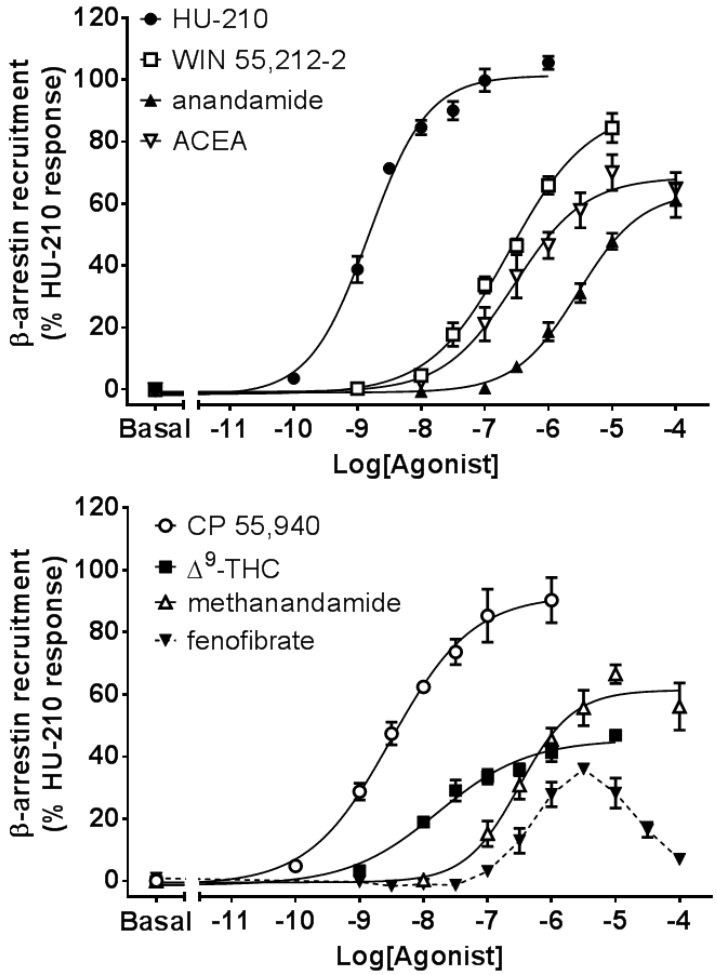

Figure 3.16 Effect of cannabinoid agonists on β-arrestin in CHO-hCB_1 cells. Cells (20,000 cells/well) were cultured in medium for 24 hr, before incubation with increasing concentrations of cannabinoid agonists for 90 min at 37°C. At the end of the incubation period, the assay was terminated by the addition of lysis/detection buffer and the relative levels of receptor β-arrestin recruitment measured using the PathHunter detection kit. The data shown represents mean ± SEM values from 3 individual experiments performed in triplicate. The curves were fitted using GraphPad Prism. Dashed lines indicate that the data were not curve-fitted.

Table 3.6

Determination of potency (pEC_{50}), percentage of basal maximal response (R_{max}), curve slope (n_H) and estimated AM 251 dissociation constant (pK_B) of cannabinoid agonists on β-arrestin recruitment in CHO-hCB_1 cells.

Agonists	**pEC_{50}**	**R_{max}**	**n_H**	**pK_B**
HU-210	8.8 ± 0.1	103 ± 4	1.0 ± 0.1	8.3 ± 0.1
CP 55,940	8.5 ± 0.1	93 ± 9	0.7 ± 0.1[a]	9.1 ± 0.2
WIN 55,212-2	6.6 ± 0.2	94 ± 8	0.7 ± 0.1[a]	8.8 ± 0.1
Δ^9-THC	7.6 ± 0.2	49 ± 5[b]	0.8 ± 0.3	9.2 ± 0.1
Anandamide	5.5 ± 0.1	62 ± 3[b]	0.9 ± 0.1	9.1 ± 0.1
Methanandamide	6.5 ± 0.1	64 ± 7[b]	1.1 ± 0.1	9.1 ± 0.1
ACEA	6.5 ± 0.2	72 ± 2[c]	0.8 ± 0.1	9.4 ± 0.1

Data shown are mean ± SEM values from 3 independent experiments performed in triplicate.

[a] n_H value significantly difference from unity (n_H = 1).); unpaired *t*-test, $p<0.05$.

[b] value significantly less than that for HU-210, CP 55,940 and WIN 55,212-2; one-way ANOVA, $p<0.0001$

[c] value significantly less than that for HU-210 only; one-way ANOVA, $p<0.05$.

3.4.7. Analysis of agonist bias

In an effort to graphically represent the agonist bias present at the CB_1 receptor, a series of bias plots were produced. The datasets for each pathway were first expressed as a % of the HU-210 response, to allow for direct comparison between pathways. Then, the response of an agonist in one pathway was expressed as a function of the response in another pathway for equimolar concentrations of

agonist, producing a correlation plot (**Figure 3.17**). When the curves deviate from unity, this indicates that an agonist produces a relatively higher response in one pathway over the other. Differences between the curves for two agonists provide a graphical representation of their bias for a particular pathway or pathways relative to each other. Due to the atypical nature of the ERK and β-arrestin responses to fenofibrate, it was not included in this analysis. Of particular note, anandamide and ACEA appear to exhibit a clear bias towards ERK phosphorylation, relative to the other agonists.

Next, to quantify the agonist bias present at the CB_1 receptor, intrinsic relative activity (RA_i) values were calculated for all agonists except fenofibrate. The RA_i values were calculated using HU-210 as the reference agonist, as opposed to the endogenous ligand anandamide, as anandamide did not produce a clear response from which to derive curve parameters in all experiments (**Table 3.7**). In particular, WIN 55,212-2, Δ^9-THC, anandamide and ACEA all exhibited at least a 10-fold bias for ERK phosphorylation versus inhibition of cAMP accumulation, compared to HU-210. These parameters were then plotted on a histogram, to allow for easier interpretation (**Figure 3.18**).

As previously highlighted, while all responses appeared to be sensitive to antagonism by AM 251, there was significant variation in the calculated pK_B values, dependent on the agonist and signalling pathway involved. In an effort to graphically represent this variation, the individual pK_B values from one signalling pathway were plotted against the respective values from another signalling pathway, akin to the bias plots previously described for the agonist responses

(**Figure 3.19**). The majority of the agonists exhibited no preference for one signalling pathway over the other, with the clear exceptions of HU-210 which was significantly less susceptible to AM251 antagonism (i.e. lower pK_B value) in the β-arrestin assay, compared to both ERK and cAMP (two-way ANOVA; $p<0.0001$), and ACEA which was significantly less antagonised in the cAMP assay compared to the other two effector systems (two-way ANOVA; $p<0.01$).

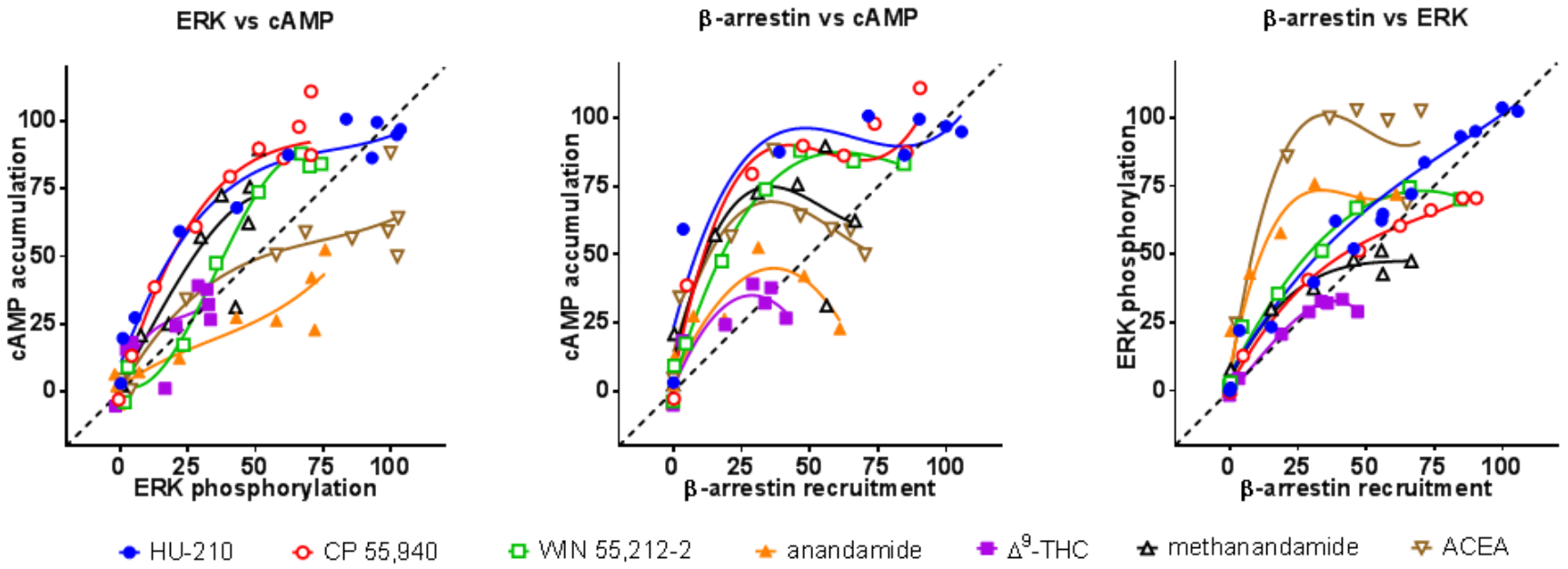

Figure 3.17 Bias plots for ERK phosphorylation, inhibition of forskolin-stimulated cAMP accumulation and β-arrestin recruitment in CHO-hCB_1 cells. Curves represent responses for the two respective pathways at equivalent concentrations of agonist. Divergence from unity represents agonist pathway selectivity, while divergence between curves in each plot represents agonist bias. Data is expressed as a % of HU-210 response, and represents mean values from 3-4 independent experiments. Curves of best fit were fitting using GraphPad Prism.

Table 3.7 Determination of intrinsic relative activities (RAi) and comparison of RAi values (ΔRAi) for cannabinoid agonists acting at human CB_1 receptors expressed in CHO cells.

agonist	RAi			ΔRAi		
	ERK	*cAMP*	*β-arrestin*	*ERK v cAMP*	*β-arrestin v cAMP*	*ERK v β-arrestin*
CP 55,940	7.36 ± 2.61 ($x10^{-1}$)	3.83 ± 1.91 ($x10^{-1}$)	4.69 ± 0.67 ($x10^{-1}$)	1.9	1.2	1.6
WIN 55,212-02	2.09 ± 0.55 ($x10^{-2}$)	2.01 ± 0.78 ($x10^{-3}$)	6.14 ± 1.19 ($x10^{-3}$)	10.4[a]	3.1	3.4
Δ^9-THC	8.04 ± 1.49 ($x10^{-2}$)	8.79 ± 6.42 ($x10^{-3}$)	3.23 ± 1.07 ($x10^{-2}$)	9.1[a]	3.7	2.5
Anandamide	1.44 ± 0.16 ($x10^{-3}$)	1.71 ± 0.95 ($x10^{-4}$)	3.29 ± 0.45 ($x10^{-4}$)	8.4[a]	1.9	4.4
Methanandamide	4.62 ± 2.30 ($x10^{-3}$)	1.49 ± 1.28 ($x10^{-3}$)	3.24 ± 0.84 ($x10^{-3}$)	3.1	2.2	1.4
ACEA	3.05 ± 1.57 ($x10^{-2}$)	3.12 ± 1.23 ($x10^{-3}$)	3.79 ± 1.69 ($x10^{-3}$)	9.8[a]	1.2	8.1[a]

RAi values shown are mean ± SEM values from 3-4 independent experiments performed in triplicate. ΔRAi values are comparison of mean RAi.

[a] difference between the two RAi values stated in the column header, as quantified by the ΔRAi value, are significantly different, indicating agonist bias (unpaired, *t*-test; $p<0.05$).

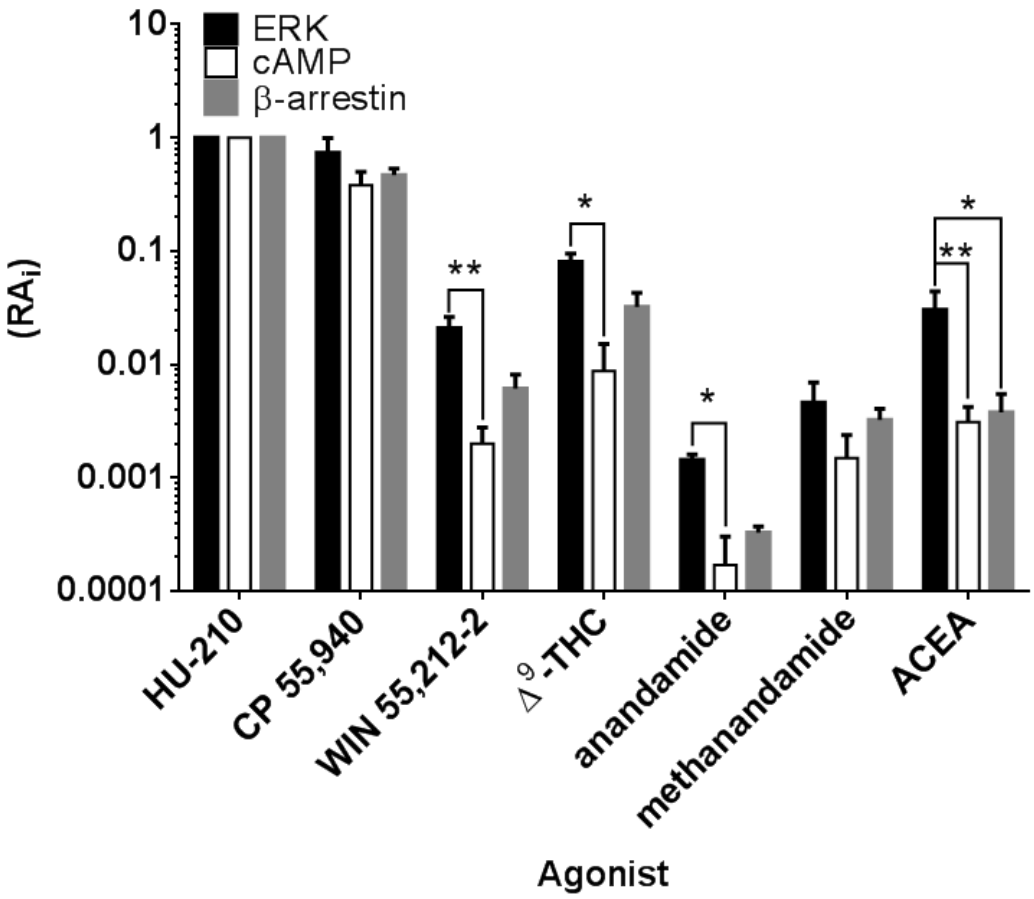

Figure 3.18 Comparison of the RAi values of cannabinoid agonists modulating ERK, cAMP and β-arrestin recruitment responses at human CB_1 receptors expressed in CHO cells. The data shown represents mean ± SEM values from 3-4 individual experiments performed in replicate. Statistical significance was determined using unpaired, two-tailed *t*-tests; *p<0.05, **p<0.01.

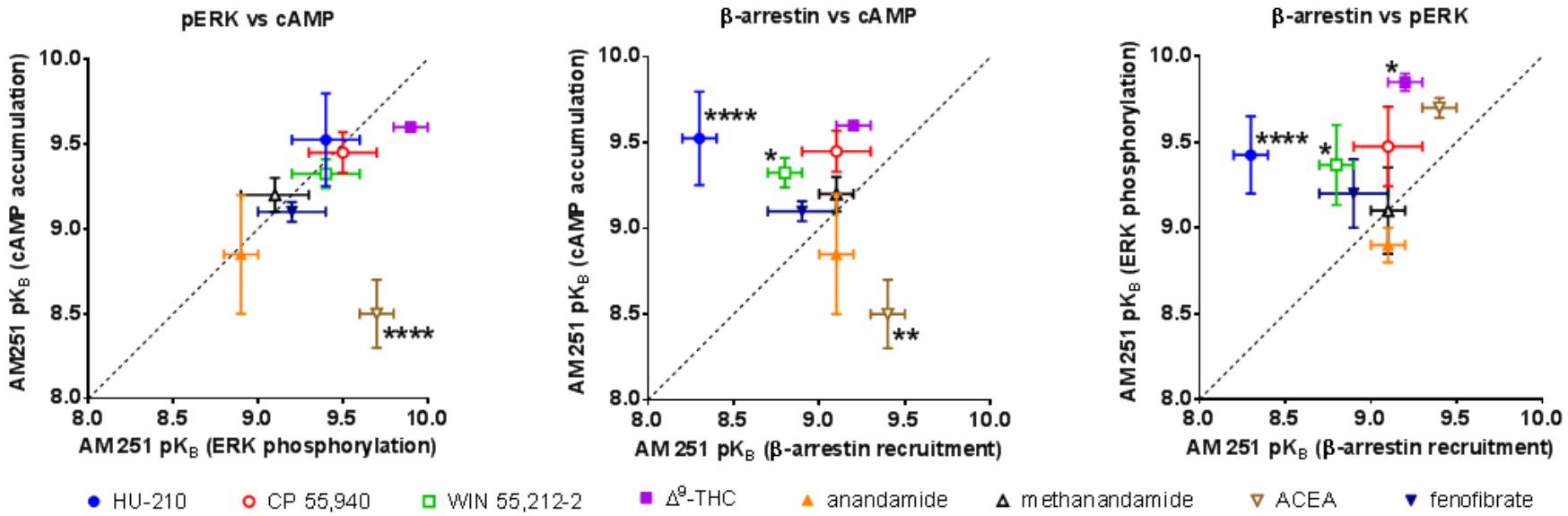

Figure 3.19 Correlation plots for calculated AM 251 (10 nM) pK_B values determined via measurement of ERK phosphorylation, inhibition of forskolin-stimulated cAMP accumulation and β-arrestin recruitment in CHO-hCB_1 cells. Divergence from unity (dashed line) represents pathway selectivity, while divergence between data points represents difference between agonists. Data points are mean ± SEM values from 3-4 independent experiments. Statistical significance was determined by two-way ANOVA. *p<0.05; **p<0.01; ****p<0.0001.

3.5. Discussion

The Chinese hamster ovary cell line, stably transfected with human CB_1 receptor is a well characterised model for investigating CB_1-mediated signalling, including some reports of agonist bias, and, therefore, was an appropriate model in which to study functional selectivity at the CB_1 receptor.

To begin with, competition radioligand binding assays were performed with membranes derived from CHO-hCB_1 cells, using [^{3}H]-CP 55,940. All ligands tested were able to inhibit competitively the specific binding of the radioligand in a concentration-dependent manner. Both the absolute equilibrium dissociation constant values (K_i) and the rank orders of affinity were consistent with previously reported values for the CHO-hCB_1 receptor (Govaerts *et al.*, 2004). In particular, the K_i value for the CB_1-selective antagonist AM 251 was consistent with its reported affinity for the CB_1 receptor, confirming the presence of CB_1 receptors in this cell line. These results validate the use of this cell line for functional studies of the CB_1 receptor, as well as providing reference data with which to compare subsequent results.

The first intracellular mediators to be investigated were the extracellular signal-regulated kinases or ERKs, a family of mitogen-activated protein kinases which regulate numerous cellular functions, including gene expression, growth, cellular transformation and apoptosis (Pearson *et al.*, 2001). This investigation was performed using the In-cell Western assay, a fluorescence immunocytochemical-based technique in which the target protein is probed with epitope-specific antibodies in fixed cultured cells in 96-well plates (Chen *et al.*, 2005; Daigle *et al.*,

2008). As this technique had not been used extensively in-house, it was necessary to determine its feasibility for measuring signalling in our cell line. Preliminary experiments revealed a clearly visible edge effect in the outer wells of the assay plate, due to an uneven distribution of cells. Edge effects are a well-recognised phenomenon in plate-based assays, and in this instance, they were most likely due to thermal gradients across the microplate affecting the cell adherence to the well bottom. Lundholt *et al*. (2003) reported that this effect could be minimised by incubating the plates at room temperature. Application of the same methodology to the CHO-hCB_1 In-Cell Western assay produced a clearly visible reduction in the edge effect which resulted in significantly less variation between wells. One major caveat of this approach is the potential impact on cell viability. While this technique is appropriate for CHO cells, the cell viability at room temperature over an hour is likely to vary significantly depending on the cell line used.

Initial testing showed that HU-210 was able to elicit a phospho-ERK response in CHO-hCB_1 cells after 5 min stimulation. These results are in keeping with previous reports of cannabinoid-mediated ERK signalling. Optimisation of the cell seeding number showed that 40,000 cells/well gave the lowest basal phospho-ERK level, and, therefore, the largest response to agonist when expressed as a % of the normalised basal response. Interestingly, this cell seeding number produced a cell monolayer closest to confluency at the point of experimentation (data not shown), while the other cell numbers were either under- or over-confluent.

Optimisation of primary antibody concentration is an important step in assay development, which can be seen as a balance between two considerations – on the

one hand determining the lowest effective antibody concentration to minimise the costs per assay plate, and on the other, choosing a high enough antibody concentration so as to minimise assay variance. Our results show that as the phospho-ERK antibody concentration was decreased, the assay sensitivity, i.e. the magnitude of the HU-210 response, relative to the basal response, increased. However, this was matched by an increase in the variance between assay replicates. The total-ERK primary antibody concentration did not have an impact on the magnitude of the normalised phospho-ERK response, but as with the phospho-ERK antibody, the variance did increase as antibody concentration decreased.

All cell lines, including CHOs, endogenously express an array of receptors, many of which couple to the ERK signalling pathway, which is why cells must be serum starved prior to stimulation with cannabinoid agonists. In addition, many of these cell lines produce endogenous ligands for these receptors, resulting in tonic ERK activation. In this instance, addition of vehicle to test wells without agonist (as a negative control) was able to elicit a phospho-ERK response. Addition of the ADP/ATP hydrolase enzyme apyrase was able to inhibit not only this effect, but also that due to addition of exogenous ATP, as well as reduce the basal level of phospho-ERK in unstimulated cells. These finding strongly indicate the vehicle response occurs via an endogenous-nucleotide (presumably ATP/P2Y receptor) signalling pathway and inhibition of this pathway is useful for increasing the signal to noise ratio of the cannabinoid-mediated response.

Time course experiments showed that all the cannabinoid agonists tested were able to promote ERK phosphorylation. The temporal profiles for all agonists tested were generally similar to each other, as well as being consistent with those reported previously in the literature (Daigle *et al.*, 2008; Dalton & Howlett, 2012); i.e. phospho-ERK levels increased rapidly upon stimulation with agonist, reaching a peak between 4 - 8 min, after which they steadily returned to near basal levels after 15 min. The exceptions to this pattern were HU-210 and CP 55,940, which both showed a modest second phase increase from 30 min onwards. Extension of the time course to 360 min confirmed that these two agonists did indeed promote a delayed-phase ERK response, reaching peak magnitude at 60 – 90 min. The other two agonists tested over the extended time course, WIN and mAEA did not produce any second-phase response, indeed WIN produced a clear reduction in phospho-ERK levels after 60 min, relative to the basal and the other agonists. At least one report exists which describes WIN-mediated inhibition of ERK, in rat C6 glioma cells; however no mechanism of action was suggested (Ellert-Miklaszewska *et al.*, 2005). Multiphasic ERK signalling via GPCRs is a well-recognised phenomenon, which can be mediated by G proteins, β-arrestins and other scaffolding proteins (Lefkowitz & Whalen, 2004; Kolch, 2005), as well as via transactivation of receptor tyrosine kinases (Wetzker & Bohmer, 2003). In the case of the CB_1 receptor, Asimaki *et* Mangoura (2011) reported biphasic ERK activation in cultured primary neurons derived from chick embryo telencephalon, involving sequential G_q and $G_{i/o}$ protein-mediated signalling, at 5 and 15 min respectively. In our study, treatment of CHO-hCB_1 cells with pertussis toxin completely abolished the ERK response of all agonists tested, including the CP 55,940-mediated late-phase response, clearly indicating the essential role of $G_{i/o}$

protein in ERK signalling in our cells. From 240 min onwards, cells treated with HU-210, but not the other test compounds, began to exhibit increased alterations in cell morphology and reduced cell number, indicative of a cytotoxic effect. This is in keeping with reports of some cannabinoids having toxic effects on certain cell types after prolonged exposure (Tomiyama & Funada, 2014).

All agonist-mediated phospho-ERK responses at 5 min were clearly shown to be concentration-dependent, with a rank order of potency consistent with their calculated pK_i values. Clear patterns of partial agonism were evident, with the R_{max} values for Δ^9-THC and methanandamide significantly less than that of HU-210. Fenofibrate, as described in the previous chapter, showed a clear decline in the phospho-ERK response at higher concentrations, resulting in an atypical concentration-response curve. This is not surprising given that the CB_1/ERK response is $G_{i/o}$ dependent, and the same pattern was seen when measuring G protein activation (see **Figure 2.3**). These results also demonstrate that the atypical fenofibrate response is not an artefact of using a membrane-based assay, as the profile was also evident when using whole cells. To the best of my knowledge, this is the first comprehensive characterisation of concentration-dependent CB_1-mediated ERK signalling in CHO-hCB_1 cells, using this or any other assay technique, though there are reports in the literature of ERK concentration-response experiments with individual cannabinoids (Bouaboula *et al.*, 1995; McIntosh *et al.*, 2007; Baillie *et al.*, 2013). The CB_1-selective antagonist AM 251 was able to produce a significant rightwards shift of all agonist concentration-response curves, clearly indicating that the responses were CB_1-receptor mediated. Interestingly, the calculated equilibrium dissociation constant (pK_B) values for

AM 251 in the ERK activation assay varied depending upon the agonist employed; this is discussed later in this chapter.

CP 55,940 produced a biphasic concentration-response curve at 60 min and the high potency component had an equivalent pEC_{50} to that seen at the 5 min stimulation time-point and was sensitive to AM 251, indicating a CB_1-mediated effect, while the low potency component had a very low pEC_{50} and was insensitive to AM 251. Both responses were $G_{i/o}$ protein-dependent as demonstrated by the abolition of the second phase response in the time course experiments. These responses provide a novel example of temporal functionally selective signalling in which CP 55,940 and HU-210 are able to promote two distinct ERK responses (albeit both apparently mediated by $G_{i/o}$), while the agonists WIN 55,212-2 and methanandamide are not, with at least part of both phases of the CP 55,940 response being CB_1-mediated.

The next signalling pathways investigated were the c-Jun N-terminal kinases or JNK, and p38 kinase, both of which are MAP kinase families which typically respond to stress stimuli including inflammatory cytokines, UV radiation, heat shock and reactive oxygen species (ROS) (Pearson *et al.*, 2001). Addition of hydrogen peroxide, a noxious stimulant and ROS at high concentrations produced clear phospho-JNK and phospho-p38 responses, demonstrating that these signalling pathways are functional in the CHO-hCB_1 cell line. None of the cannabinoid agonists tested elicited a phospho-JNK or p38 response up to 60 min stimulation. This is in contrast to a previous report in which CB_1 receptors were reported, using immunoblotting, to couple to JNK and p38 in transfected CHO

cells (Rueda *et al.*, 2000). Potentially, our particular subclone of CHO cells may be unsuited to CB_1/JNK/p38 coupling or alternatively the technique used is not sensitive enough to detect phospho-JNK or p38 levels present. A future step would be to repeat these experiments using conventional Western immunoblotting, to confirm that the results are independent of the assay technique used.

The CB_1 receptor is well known to couple to $G_{i/o}$ proteins in transfected CHO cells, which among other functions, inhibit the activity of the enzyme adenylyl cyclase (AC), an effect which can be observed by measuring changes in intracellular cAMP levels (Felder *et al.*, 1995; Bonhaus *et al.*, 1998). Stimulation of cells with forskolin (FSK), a receptor-independent activator of AC, produced a concentration-dependent increase in cAMP levels. All agonists tested produced clear concentration-dependent inhibitions of FSK-stimulated cAMP accumulation which were sensitive to AM 251, with a rank order of potency which was consistent with that seen in the radioligand binding and ERK activation assays. However, the absolute EC_{50} value for HU-210, but no other agonist, was significantly greater in the cAMP assay, compared to the ERK activation assay by approximately 10-fold, indicative of HU-210 positive agonist bias for cAMP vs. ERK signalling. Clear patterns of partial agonism could be identified, with the R_{max} value for Δ^9-THC being significantly less than that for HU and CP. These patterns of potency and intrinsic activity closely match literature reports for cAMP signalling in CHO-hCB_1 cells (Bonhaus *et al.*, 1998). One anomalous result of note was the consistent ability of a high concentration of Δ^9-THC (10 µM) to *enhance* cAMP accumulation in these cells. This would be expected to be a

receptor-mediated activation of G_s protein, which activates AC; however, in this instance, the response was insensitive to AM 251 antagonism, indicating that it is not CB_1-mediated. While interesting, the response falls beyond the remit of this thesis, and was excluded from analysis of the cAMP data.

Next, the effect of pertussis toxin on CB_1 receptor modulation of cAMP accumulation was investigated. Previous reports have clearly demonstrated that inhibition of $G_{i/o}$-mediated signalling can facilitate receptor coupling to other signalling mediators, such as G_s proteins (Glass & Felder, 1997; Maneuf & Brotchie, 1997; Bonhaus *et al.*, 1998). However, none of the cannabinoid agonists tested were able to produce a significant change in cAMP levels in PTX-treated cells, in stark contrast to the previous reports. As with the lack of JNK and p38 signalling, a probable explanation is that, in this particular subclone of CHO cells, coupling of the transfected CB_1 receptors to endogenous G_s proteins is weak and/or negligible.

The final signalling system to be investigated was receptor-mediated β-arrestin recruitment. These are proteins which bind to intracellular portions of GPCRs, and mediate receptor internalisation and coupling to signalling pathways. In this instance, the DiscoveRx PathHunter system was used to measure the β-arrestin response. In this assay, binding of arrestin protein to the receptor unifies two complimentary components of a β-galactosidase enzyme, which is then used to catalyse the formation of a chemiluminescent detection product. All agonists tested produced a concentration-dependent increase in β-arrestin recruitment which was sensitive to AM 251 antagonism. To the best of my knowledge, this is

the first reported concentration-dependent characterisation of cannabinoid agonist action at the CB_1 receptor using this reporter system. The rank order of potency was again consistent with that seen with the previously described signalling mediators, cAMP and ERK. Importantly however, the absolute pEC_{50} values of all agonists for the β-arrestin assay were significantly lower than those for the cAMP assay, while the anandamide and ACEA values were significantly lower than those for the ERK assay. These discrepancies are most likely due to the proximity of β-arrestin recruitment to the receptor activation event and the unitary ratio nature of this interaction (i.e. one activated receptor binds one β-arrestin protein only), resulting in a lack of signal amplification when compared to cAMP inhibition and ERK phosphorylation, which are events much further downstream in the signalling cascade with G protein and enzyme involvement. As with the ERK and cAMP assays, clear patterns of partial agonism were identified, with Δ^9-THC, anandamide and methanandamide partial, relative to HU-210. The β-arrestin response to fenofibrate, as with the G protein and ERK responses, produced an atypical bell-shaped concentration-response curve, demonstrating that this effect is mediated via multiple signalling pathways.

While comparison of response curve parameters between various signal mediators can give an indication of functional selectivity, this approach does not take into account other factors which may impact the results - differences in the sensitivity of an assay used to measure a particular pathway, termed *observational* bias, and the bias a receptor has for one pathway over another, as seen in the present results indicating differences between β-arrestin and the other two signalling mediators, termed *system* bias.

It is, therefore, necessary to analyse the data in a way that compensates for these other factors and focuses only on genuine agonist bias (Kenakin & Christopoulos, 2013b). Bias plots (also known as equimolar comparison) are a novel means of graphically illustrating the potential bias of several agonists with regard to two pathways (Gregory *et al.*, 2010; Kenakin & Miller, 2010; Rajagopal *et al.*, 2011), in which responses to the two pathways are normalised, in our case to HU-210-mediated responses, and then plotted against each other. In this instance, bias of individual agonists for particular pathways, in relation to other agonists can be easily identified; in particular anandamide and ACEA appeared to be clearly biased towards ERK activation compared with β-arrestin recruitment, and to a lesser extent cAMP accumulation. A limitation of using bias plots is that they do not allow for direct quantification of agonist bias. To overcome this limitation we have used a parameter termed *intrinsic relative activity* (RAi) which is calculated using both the potency and intrinsic activity of an agonist, in relation to a reference agonist, which in our case, was again HU-210. Our analysis confirmed the trends illustrated in the bias plots, as both anandamide and ACEA exhibited 8.4 and 9.8-fold bias towards ERK activation vs. cAMP signalling and 4.4 and 8.1-fold bias vs. β-arrestin recruitment. This signalling bias may have an impact on the downstream functional consequence of β-arrestin recruitment. While β-arrestin can mediate ERK activation, the bias we have demonstrated as well as the data showing the $G_{i/o}$ protein-dependent nature of the ERK responses indicates this is not likely in our cell line. Anandamide and ACEA may be less likely to promote receptor internalisation, another functional consequence of receptor/β-arrestin recruitment, which may have a major impact on agonist-selective responses.

Relative activity values are just one method available for quantifying agonist bias, with another being transduction coefficients, which are derived by fitting concentration-response data to the Black-Leff operational model. The advantage of using relative activities is that they are easy to understand and to calculate - however they become less accurate as measures of agonist bias when the concentration-response data differs significantly from unity. While this is not the case for the majority of the concentration response data in this chapter, the ERK response for ACEA, and the β-arrestin responses for CP 55,940 and WIN 55,212-2 are significantly different from $n_H = 1$. Future work should aim to quantify the agonist bias using the transduction coefficient model, which is independent of the curve slope.

The equilibrium dissociation constant (pK_B) for AM 251 calculated using the Schild equation, was determined using all agonists, at all signalling pathways. Typically, it is expected that all calculated pK_B values should be equal, regardless of the agonist or signalling mediator involved. Assay-dependent differences in incubation periods or temperatures may alter the antagonist binding kinetics and pK_B as measured between different signalling pathways, while differences between agonists in non-equilibrium assays may be due to differences in agonists' association rate constants. However, the complexity of divergence in our results, in which different agonists exhibit significantly different susceptibility to AM251 antagonism cannot be explained by these considerations and is most likely indicative of agonist-dependent bias in the activity of the antagonist. With this in mind, we posit that comparison of antagonist equilibrium dissociation constants, calculated using the Schild equation is a novel way of indicating agonist bias at a

GPCR. Our results show that HU-210 and ACEA are clearly biased against antagonism of the β-arrestin and cAMP pathways respectively, while WIN 55212-2 55,212-2 and Δ^9-THC are biased against the β-arrestin pathway to a lesser degree.

3.6. Conclusions

In conclusion, the results in this chapter clearly demonstrate that cannabinoid agonists are able to modulate ERK, AC and β-arrestin signalling in CHO cells via transfected human CB_1 receptors. Furthermore, activation of these signalling pathways appears to exhibit clear examples of agonist bias, with ligand-specific differences in temporal ERK signalling, as well as differential activation of the three signalling pathways investigated.

Chapter 4

Investigation of Functional Selectivity at the Cannabinoid Receptor in Human CB_1 Receptor-Transfected Human Embryonic Kidney 293 cells

4.1. Introduction

Expression of receptors in a cell line with a relatively uncomplicated spectrum of protein expression is an effective method for the study of signal transduction pathways. Common amongst these 'simple' host cell lines is the human embryonic kidney 293, HEK 293, or simply HEK cells, an immortalised cell line developed at Alex van der Eb's laboratory in Leiden, The Netherlands in the early 1970s (Graham *et al.*, 1977). Cultures of normal human embryonic kidney cells were transformed with sheared adenovirus 5 DNA which resulted in a ~4.5 kilobase insertion of viral genome into human chromosome 19 (Louis *et al.*, 1997). While the specific cell type of the HEK progenitor has been debated, the most recent consensus is that the cell line is neuronal in origin (Shaw *et al.*, 2002). HEK cells are extensively used in the study of transfected proteins, owing to the ease with which they can be cultured and transfected. A large amount of research on cannabinoid receptor has been conducted using HEK cells expressing transfected recombinant receptor, including studies on receptor-mediated modulation of ion channels (Vasquez *et al.*, 2003), coupling to G_q proteins (Lauckner *et al.*, 2005), formation of heteromeric receptor dimers (Kearn *et al.*, 2005) and characterisation of CB_1 receptor allosteric modulators (Horswill *et al.*, 2007).

4.2. Aims and objectives

The aim of this chapter was to investigate functionally selective responses mediated by the CB_1 receptor expressed in HEK cells. The objectives were to stimulate cells with a range of cannabinoid agonists and to measure the engagement of a number of signal transduction mediators including the MAP kinases ERK, JNK and p38 and the enzyme adenylyl cyclase (AC) via changes in

cAMP levels. The HEK cell line provides an attractive model for investigating agonist bias as it has been thoroughly validated by previous studies; the relatively high receptor population generated by transfection should provide clear responses, bringing confidence to the data generated, and it is a human cell line of potentially neuronal origin which is more physiologically relevant to CB_1 receptor function than some other cell lines of non-human, non-neuronal origin, such as the CHO cell line that have also been used for cannabinoid receptor studies.

4.3. Methods

4.3.1. Cell culture

HEK 293 cells stably transfected with the human cannabinoid CB_1 receptor, with a tetracycline inducer, and genes encoding antibiotic resistance, were cultured in Dulbecco's modified eagle's medium (DMEM) containing 10% tetracycline-negative foetal bovine serum, 2 mM L-glutamine and 200 µg/ml hygromycin at 37°C, 5% CO_2 in a humidified incubator. Cells were passaged every 2-3 days using TrypLE-E dissociation buffer. HEK-hCB_1 cells were treated with doxycycline (1 µg/ml) 24 hrs prior to experimentation to promote receptor expression.

4.3.2. Determination of MAP kinase phosphorylation

4.3.2.1. Time Course experiments - In-Cell Western

4.3.2.1.1. Protocol

Levels of MAP kinase phosphorylation were determined using the In-Cell Western™ assay, previously described. Cells were seeded into 384-well clear bottom plates, at 5,000 cells/well (unless otherwise stated) in culture medium at

room temperature for 1 hour and then incubated overnight at 37°C, in the presence of pertussis toxin (500 ng/ml) where appropriate. 30 min prior to experimentation, the culture medium was removed from the assay plates by aspiration, the cells were washed once with PBS, and the medium replaced with serum-free medium containing 1 mg/ml BSA. Dilution of test ligands was performed in serum-free medium and added to test wells to a final volume of 25 µl per well. Assay plates were incubated for the stated period at 37°C during experimentation. After incubation, the assay medium was rapidly aspirated and the cells were fixed with 4% paraformaldehyde in PBS for 20 min at room temperature (40 µl/well). Each reagent was aspirated before the addition of the next reagent. Cells were then permeabilised with 0.1% (v/v) Triton™ X-100 in PBS for 20 min at room temperature (40 µl/well). Non-specific antibody binding sites were blocked with 5% (w/v) milk powder in PBS for 60 min at room temperature with gentle rocking.

Primary antibodies for anti-total and anti-phosphorylated MAP kinases (ERK1/2, p38 and JNK1/2/3; see **4.3.2.1.3**) were diluted together in blocking agent. Cells were incubated with primary antibody solution (25 µl/well) overnight at 4°C with gentle rocking. The next day, the primary antibody solution was aspirated and the cells were washed three times with PBS containing 1 mg/ml BSA (40 µl/well) for 5 min at room temperature with gentle rocking. The appropriate LI-COR IRDye® secondary antibodies were diluted 1:4000 in blocking agent, added to the cells (25 µl/well), and incubated in darkness for 60 min at room temperature with gentle shaking. The secondary antibody solution was aspirated and the cells washed three times with wash buffer as before.

4.3.2.1.2. Imaging

Plates were imaged by scanning simultaneously at 700 and 800 nm with the LI-COR Odyssey® NIR Imaging System at 82 µm resolution, medium quality and focus offset of 4.0123 mm. Quantification was performed using LI-COR Odyssey® Software v3.0. The secondary antibody non-specific response was subtracted from the data. The phospho- response was then normalised against the total protein response for each individual well and then the data was expressed as a percentage of the basal response.

4.3.2.1.3. Antibodies used

All primary antibodies used were obtained from Cell Signaling Technology (Boston, USA). Antibodies were used at the concentrations described below unless otherwise stated in **Results** (see **4.4**). Anti-ERK 1/2 rabbit, (1:400) # 9102; anti-phospho-ERK1/2 (Thr202/Tyr204) monoclonal mouse, (1:200) # 9106; anti-p38 rabbit, (1:200) # 9212; anti-phospho-p38 (Thr180/Tyr182) monoclonal mouse, (1:200) #9216; anti-JNK rabbit, (1:200) # 9252; anti-phospho-JNK (Thr183/Tyr185) monoclonal mouse, (1:200) # 9255.

4.3.2.2. ERK phosphorylation concentration-response - AlphaScreen SureFire

4.3.2.2.1. Protocol

Levels of ERK phosphorylation in concentration-response experiments were determined using the AlphaScreen SureFire assay kit. Antibodies targeting the phospho-Thr202/Tyr204 epitope and a distal epitope capture AlphaScreen donor

and acceptor beads. Excitation of the donor beads promotes energy transfer to the acceptor beads resulting in emission of a detectable light signal, which corresponds to the relative level of ERK1/2 phosphorylation. Cells were plated into a 384-well plate at 5,000 cell/well unless otherwise stated, and incubated at 37°C for 24 hours, in the presence of pertussis toxin (500 ng/ml) where appropriate. 30 min prior to experimentation, the culture medium was removed from the assay plates by aspiration, the cells were washed once with PBS, and the medium replaced with serum-free medium containing 1 mg/ml BSA. Serial dilution of test ligands was performed in serum-free medium and added to test wells to a final volume of 25 µl per well, followed by 5 or 20 min incubation at 37°C. The assay was terminated by the addition of 5x lysis buffer (6.25 µl/well) and agitated for 10 min at ~350 rpm on a plate shaker

4 µl of the cell lysate was transferred to a white 384-well PerkinElmer proxiplate plus. The SureFire assay kit reaction mix was prepared by combining the Activation and Reaction buffers with AlphaScreen protein-conjugated acceptor and steptavidin-coated donor beads. 7 µl of reaction mix was added to the proxiplate; the plate was sealed with an opaque cover and incubated for 2 hours at room temperature. Preparation of the reaction mix and addition to the proxiplate was performed in low light conditions to minimise degradation of the reaction mix. The phospho-ERK1/2 levels were determined by exciting the proxiplate at 680 nm and detecting the emission of light at 520 – 620 nm using a PerkinElmer EnVision plate reader. The data were expressed as a percentage of the basal response .

4.3.3. cAMP accumulation assay

Intracellular cAMP levels were determined using the Cisbio HTRF femto cAMP kit, a TR-FRET-based immunoassay kit. Cells were passaged and pelleted by centrifugation and resuspended in assay buffer (Hank's buffered salt solution containing 20 mM HEPES (pre-prepared, Life Technologies), 0.5 mM $MgCl_2$, pH adjusted to 7.4 at room temperature), containing NKH 477 (3 µM) and IBMX (0.5 mM), unless otherwise stated. Cells (1,000 cells/well, unless otherwise stated) were incubated with increasing concentrations of cannabinoid agonist for 20 min at 37°C in a black 384-well micro volume plate in a final assay volume of 8 µl/well. A cAMP standard was included on each plate adding increasing concentrations of cAMP to cell-free assay buffer. The assay was terminated by the addition of detection mix and plates were then incubated for 24 hours at room temperature. Fluorescence emitted at 665 nm following stimulation at 320nm was measured using a PerkinElmer EnVision plate reader.

4.3.4. Materials

WIN 55,212-2, CP 55,940, arachidonoyl-2'-chloroethylamide, anandamide, (R)-+-methanandamide, AM 251, fenofibrate, bovine serum albumin and isobutylmethylxanthine (IBMX) were obtained from Sigma Aldrich (Poole, UK). HU-210 and Δ^9-tetrahydrocannabinol were purchased from Tocris Biosciences (Bristol, UK). Cell culture reagents DMEM, L-Glutamate, TrypLE™ Express dissociation buffer, hygromycin, phosphate-buffered saline, HEPES buffer and Hank's buffered salt solution (HBSS) were purchased from Life Technologies (Paisley, UK). Tetracycline negative foetal bovine serum was obtained from Lonza (Slough, UK). The cAMP femto 2 assay kit was purchased from Cisbio

Bioassays (Bedford, MA, USA). The AlphaScreen® SureFire® pERK1/2 (Thr202/Tyr204) Assay Kit was obtained from PerkinElmer (Bucks, UK). HEK 293 cells stably transfected with the human cannabinoid CB_1 receptor with a tetracycline promoter were kindly provided by Neusentis Ltd (Cambridge, UK).

4.3.5. Data Analysis

All data was analysed using the GraphPad Prism software (v6). Concentration-response data were fitted to curves using the four-parameter logistic equation, previously described in Chapter 2 – Methods (see **2.3.7**).

For the cAMP experiments, the raw counts were interpolated against an internal cAMP standard curve on a logarithmic *x* axis, and then transformed to actual cAMP concentration ([cAMP]) in nM.

Estimates for the antagonist AM 251 equilibrium dissociation constant (pK_B) and calculation of the intrinsic relative activities (RAi) for each individual agonist were as previously described in Chapter 3 – Methods (see **3.3.6**).

4.3.6. Statistics

The quantitative data are expressed as means ± SEM, obtained from at least three independent experiments performed in replicate, unless otherwise stated. Normality of data sets was determined using the D'Agostino-Pearson omnibus normality test. Statistical significance of differences was determined by Student's paired or unpaired, two-tailed *t*-tests or ANOVA followed by Dunnett's multiple comparisons *post-hoc* tests where appropriate. Statistical comparison of pK_B

values, and responses in non-toxin treated cells with the corresponding responses in PTX-treated cells was made using two-way ANOVA followed by Sidak's multiple comparisons test. A p value of <0.05 was considered significant.

4.4. Results

4.4.1. Determination of ERK phosphorylation

Assay Optimisation

A preliminary experiment was performed to determine the optimal cell seeding density and phospho-ERK1/2 antibody concentration for use in subsequent assays (**Figure 4.1**). Cell were stimulated with HU-210 (1 μM) for 7.5 min before fixation and immunocytochemical staining. A cell seeding density of 5,000 cells/well produced the largest magnitude response of all cell densities at all antibody dilutions tested, apart from 1:100. Within this, there was an increase in response magnitude as antibody dilution increased, with a 1:400 dilution giving the largest response.

On the basis of these results, a cell seeding density of 5,000 cells/well and a phospho-ERK primary antibody dilution of 1:400 were chosen as optimal conditions for all subsequent ERK time course experiments.

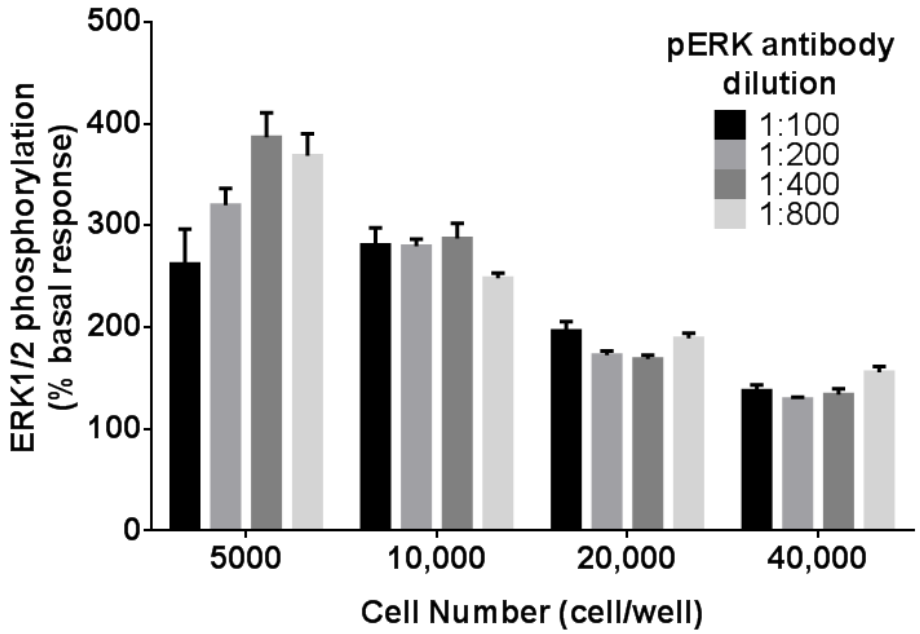

Figure 4.1 Optimisation of ERK phosphorylation assay in HEK-hCB$_1$ cells. Cells (5, 10, 20 and 40 000 cells/well) were cultured in medium for 24 hr, followed by serum starvation for 24 hr. Cells were stimulated with HU-210 (1 µM) for 7.5 min, followed by rapid fixation with cold PFA solution (4 % w/v). Detection of total and phospho-ERK levels was as stated in methods (see **4.3.2.1**). Individual ERK phosphorylation values were normalised to the corresponding total-ERK values. The data shown represent a single experiment, performed with six replicates and are presented as mean ± SEM.

Effect of cannabinoid agonists of ERK phosphorylation – time course

HEK-hCB$_1$ cells were treated with high (presumed to be maximally effective) concentrations of the cannabinoid agonists HU-210, CP 55,940 (both 1 µM), WIN 55,212-2 and methanandamide, (10 µM) at various time points (2 – 60 min) to identify any differences in the agonists' temporal response profile and to

determine which time point would provide the maximum phospho-ERK response for use in concentration-response experiments.

All agonists produced a rapid, significant increase in phospho-ERK levels with the maximum response occurring at 4 min (**Figure 4.2**, black symbols; one way ANOVA; $p<0.001$). After this time the phospho-ERK levels for all agonists steadily decreased, reaching a constant, but still elevated level from 10 min onwards. There were clear patterns of partial agonism present, with methanandamide producing a significantly smaller maximum response than those of the representative full agonists HU-210 and WIN 55-212-2 (one-way ANOVA; $p<0.05$). While the maximum WIN response appeared larger than that for HU and CP, there were no significant differences between the three. Some cells were pre-treated with pertussis toxin (PTX; 500 ng/ml) overnight to test for the involvement of $G_{i/o}$ proteins in the responses. PTX produced a significant decrease in the phospho-ERK responses to all agonists (**Figure 4.2**, white symbols; two-way ANOVA; $p<0.01$). In addition, the temporal profile of the response was slightly shifted, with the maximum response now typically achieved after 6 min of stimulation. As with the untreated cells, there were patterns of partial agonism observable in the presence of PTX, with the methanandamide maximum response being significantly lower than that for HU-210 (one-way ANOVA; $p<0.01$). PTX did not appear to have any effect on the post-10 min stimulation phospho-ERK response, as seen in the untreated cells.

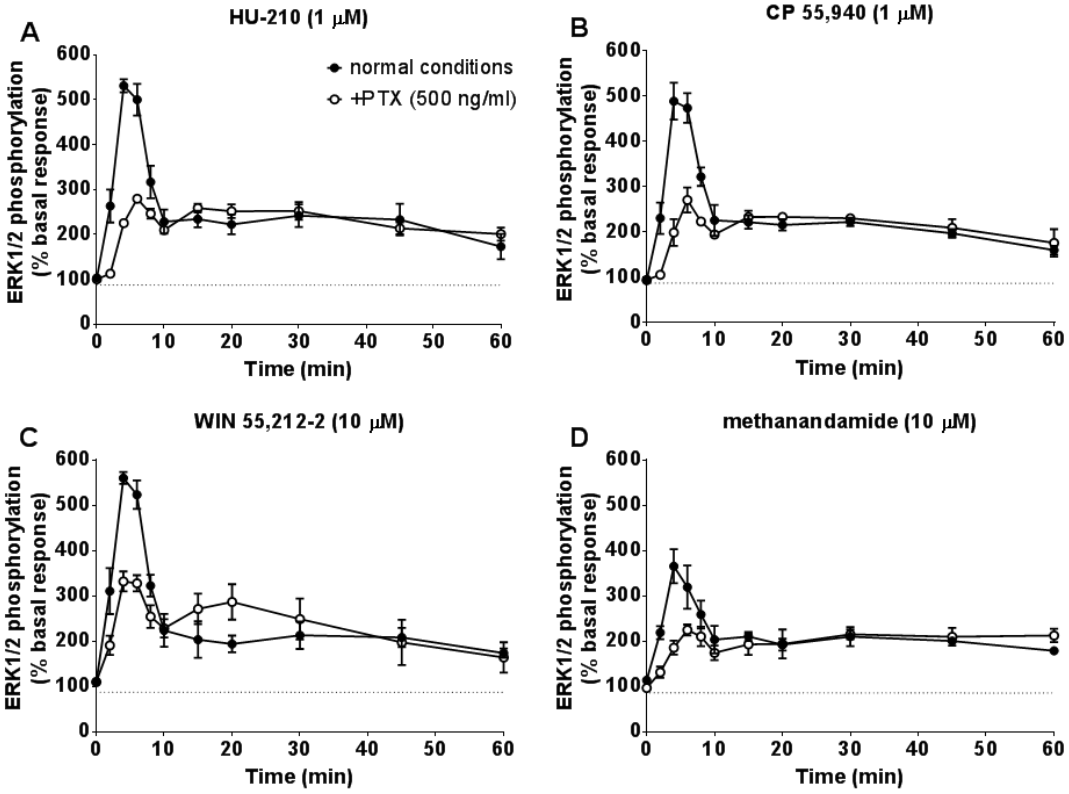

Figure 4.2 Time courses of the effects of cannabinoid agonists in the presence and absence of pertussis toxin on ERK phosphorylation in HEK-hCB_1 cells. Cells (5,000 cells/well) were cultured in medium for 24 hr, followed by serum starvation for 24 hr. Cells were stimulated with cannabinoid agonists at various time points (2 - 60 min), followed by rapid fixation with cold PFA solution (4 % w/v). Detection of total and phospho-ERK levels was as stated in methods (see **4.3.2.1**). The data shown represents mean ± SEM values from four independent experiments performed in triplicate.

Effect of cannabinoid agonists on ERK phosphorylation – concentration-response

The concentration-dependent effects of the cannabinoid agonists on ERK phosphorylation were assayed using the AlphaScreen SureFire kit; the cell seeding density was kept the same as that used in the time-course experiments to allow for more relevant comparison. The cannabinoid agonists HU-210, CP 55,940, WIN 55,212-2, Δ^9-THC, anandamide, methanandamide, arachidonyl-2'-chloroethylamide (ACEA) and fenofibrate all produced a concentration-dependent increase in phospho-ERK levels after 5 min stimulation (**Figure 4.3**). The rank order of potency (pEC_{50}) values of the agonists acting on HEK-hCB_1 cells from highest to lowest was CP 55,940 > HU-210 ≥ Δ^9-THC > WIN 55,212-2 > fenofibrate ≥ mAEA ≥ ACEA ≥ AEA (**Table 4.1**). The R_{max} value for Δ^9-THC was significantly less than that for HU-210, CP 55,940 and WIN 55,212-2 (one-way ANOVA; $p<0.05$). To confirm the role of the CB_1 receptor in the cannabinoid agonist responses, the concentration-response experiments were repeated in the presence of the CB_1-selective competitive antagonist AM 251 (10 nM). AM 251 produced a significant rightwards shift of all the agonist concentration-response curves, except for Δ^9-THC and fenofibrate whose responses were completely abolished, resulting in significant decreases in all the pEC_{50} values. These data were used to estimate the equilibrium dissociation constant (pK_B) for AM 251 in the presence of each individual agonist (**Table 4.1**). There were no significant differences between the pK_B values (one-way ANOVA; $p>0.05$).

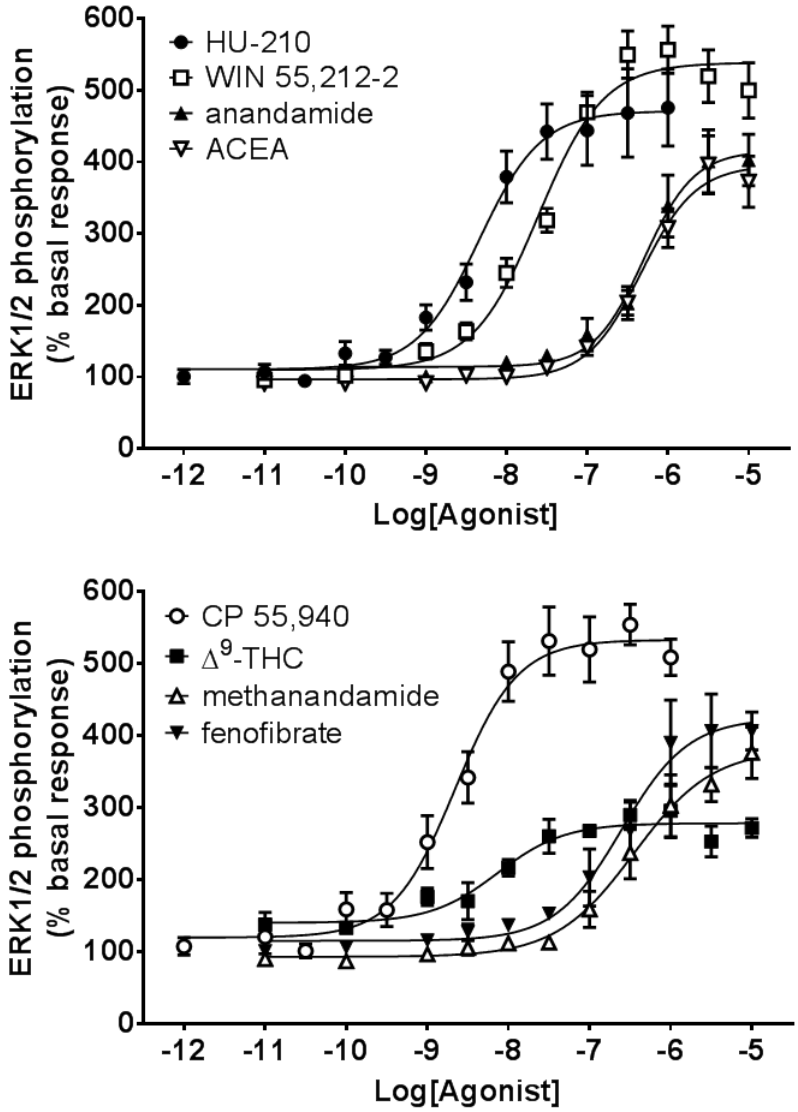

Figure 4.3 Effect of cannabinoid agonists on ERK phosphorylation in HEK-hCB_1 cells. Cells (5,000 cells/well) were cultured in medium for 24 hr, followed by serum starvation for 24 hr. Cells were stimulated with various concentrations of cannabinoid agonists for 5 min, followed by rapid addition of lysis buffer. Determination of the phospho-ERK response was as stated in methods (see **4.3.2.2**). The data shown represents mean ± SEM values from 3-6 independent experiments performed in duplicate. The curves were fitted using GraphPad Prism.

The concentration-response experiments were repeated with cells which had been pre-treated with PTX overnight (**Figure 4.4**). All agonists produced a concentration-dependent increase in phospho-ERK levels, except Δ^9-THC, which produced no response up to 10 μM. While fenofibrate was able to produce a clear concentration-dependent increase in phospho-ERK levels, it was impossible to fit a response curve to the data using GraphPad Prism. The rank order of pEC_{50} values of the agonists acting on HEK-hCB_1 cells, from highest to lowest potencies, was CP 55,940 > HU-210 > WIN 55,212-2 > anandamide ≥ methanandamide ≥ ACEA (**Table 4.1**). The R_{max} value for WIN 55,212-2 was significantly greater than that for HU-210, anandamide, methanandamide and ACEA, while the value for CP 55,940 was significantly greater than that for methanandamide (one-way ANOVA; $p<0.05$). Comparing the responses in the PTX-treated cells to those observed in untreated cells, the R_{max} for all agonists, and the pEC_{50} values for HU-210, CP 55,940 and WIN 55,212-2 were significantly smaller than the corresponding responses seen in untreated cells (two-way ANOVA; $p<0.05$).

To confirm the role of the CB_1 receptor in the cannabinoid agonist responses, the concentration-response experiments were repeated in the presence of the CB_1-selective competitive antagonist AM 251 (10 nM). AM 251 produced a significant rightward shift in the HU-210, CP 55,940 and WIN 55,212-2 concentration-response curves, resulting in significant decreases in all the pEC_{50} values. These data were used to estimate the equilibrium dissociation constant (pK_B) for AM 251 in the presence of each individual agonist (**Table 4.1**). There was no significant difference between the three pK_B values (one-way ANOVA; $p>0.05$). The

responses to the other agonists were either completely abolished, or could not be fitted to response curves by GraphPad Prism, in the presence of AM 251, therefore no pK_B values were estimated.

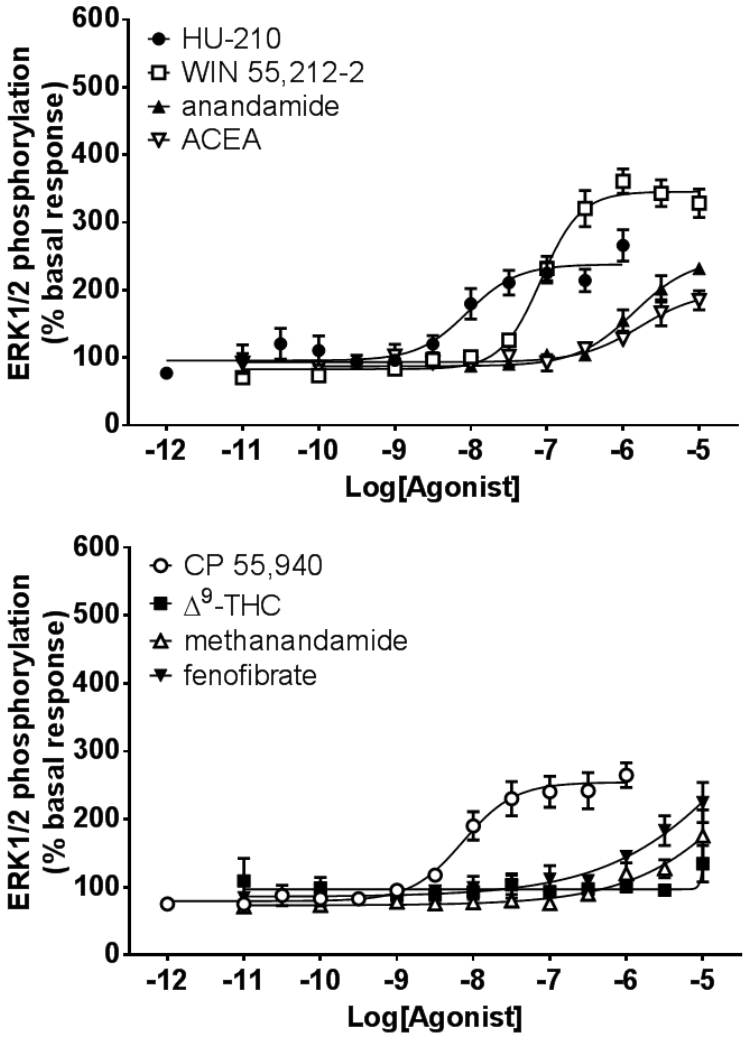

Figure 4.4 Effects of cannabinoid agonists on ERK phosphorylation in HEK-hCB_1 cells, pre-treated with pertussis toxin. Cells (5,000 cells/well) were cultured in medium for 24 hr, followed by serum starvation and treatment with PTX (500 ng/ml) for 24 hr. Cells were stimulated with various concentrations of cannabinoid agonists for 5 min, followed by rapid addition of lysis buffer. Determination of the phospho-ERK responses was as stated in methods (see **4.3.2.2**). The data shown represent mean ± SEM values from 3-6 independent experiments performed in duplicate. The curves were fitted using GraphPad Prism.

Table 4.1

Determination of potency (pEC_{50}), maximal response, expressed as % of the basal (R_{max}), and estimated AM 251 dissociation constant (pK_B) of cannabinoid agonists on ERK phosphorylation in HEK-hCB_1 cells at 5 min stimulation, in cells either untreated or pre-treated with PTX (500 ng/ml) overnight.

Agonist	**Non-treated cells**				**PTX-treated cells (500 ng/ml)**			
	pEC_{50}	R_{max}	n_H	pK_B	pEC_{50}	R_{max}	n_H	pK_B
HU-210	8.3 ± 0.1	372 ± 49	1.3 ± 0.2	9.2 ± 0.3	7.5 ± 0.2	168 ± 28[e]	0.9 ± 0.1	9.1 ±0.1
CP 55,940	8.7 ± 0.1	412 ± 33	1.1 ± 0.1	9.0 ± 0.4	7.9 ± 0.2	185 ± 15	1.4 ± 0.3	9.6 ± 0.1
WIN 55,212-2	7.6 ± 0.1	432 ± 36	1.1 ± 0.1	9.4 ± 0.2	7.1 ± 0.1	262 ± 16	1.9 ± 0.1[c]	9.6 ± 0.1
Δ^9-THC	8.2 ± 0.5	145 ± 28[d]	1.1 ± 0.1	[b]	[a]	[a]	[a]	[b]
anandamide	6.3 ± 0.1	306 ± 41	1.4 ± 0.1	8.9 ± 0.4	6.1 ± 0.1	146 ± 4[e]	1.9 ± 0.1	[b]
methanandamide	6.4 ± 0.3	295 ± 34	1.0 ± 0.1	9.4 ± 0.5	5.9 ± 0.4	66 ± 7[ef]	1.7 ± 0.4	[b]
ACEA	6.3 ± 0.1	299 ± 40	1.3 ± 0.1[c]	9.2 ± 0.1	5.7 ± 0.2	107 ± 11[e]	1.4 ± 0.5	[b]
fenofibrate	6.7 ± 0.1	337 ± 33	1.4 ± 0.4	[b]	[a]	[a]	[a]	[b]

The data shown represents mean ± SEM values from 4-5 independent experiments performed in triplicate.

[a] It was impossible to fit a response curve using GraphPad Prism. [b] It was not possible to calculate values for pK_B.

[c] n_H value significantly difference from unity ($n_H = 1$). [d] value significantly less than that for HU-210, CP 55,940 and WIN 55,212-2.

[e] value significantly less than that for WIN 55,212-2. [f] value significantly less than that for CP 55,940.

In an effort to determine the mechanistic differences between the PTX-sensitive and PTX-insensitive responses, the WIN 55,212-2 concentration-response experiments were repeated in the presence of a hypertonic concentration of sucrose (0.5 M), a known inhibitor of the formation of clathrin complexes, involved in β-arrestin-mediated endocytosis and signalling (Goggi *et al.*, 2007; Ivanov, 2008). WIN 55,212-2 was chosen as a representative agonist in these experiments as it produced the largest magnitude response, as typified by the R_{max} value (**Table 4.1**). The presence of sucrose caused a significant reduction in WIN 55,212-2 R_{max}, from 403 ± 28 to 191 ± 46 % basal response (**Figure 4.5**; one-way ANOVA; $p<0.05$). The addition of sucrose to cells pre-treated with PTX resulted in an almost complete abolishment of the WIN 55,212-2 response.

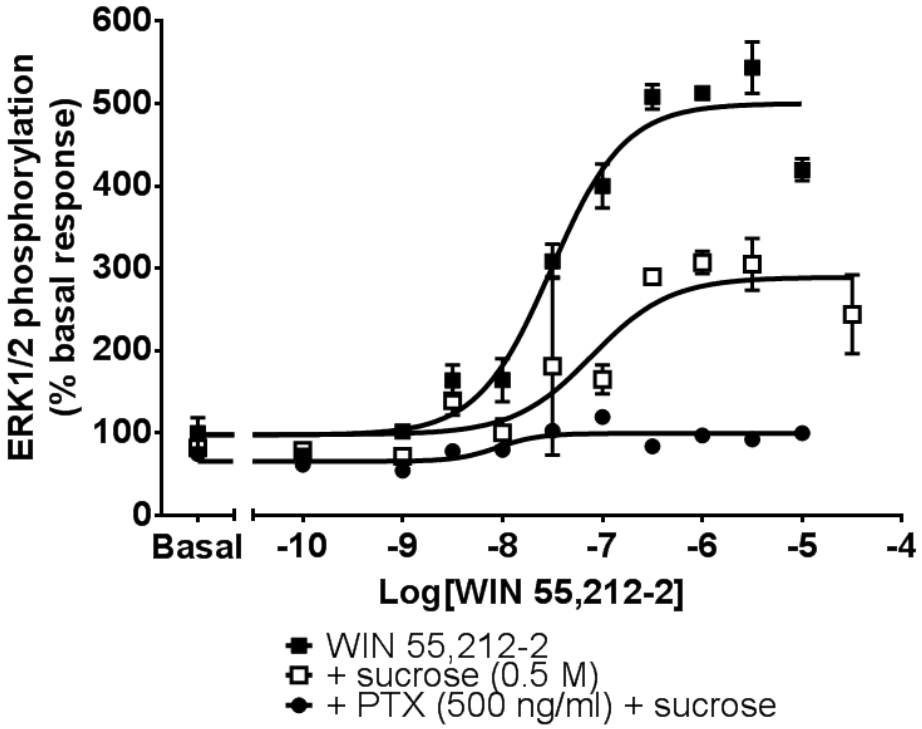

Figure 4.5 Effect of hypertonic sucrose on WIN 55,212-2-mediated ERK phosphorylation in HEK-hCB_1 cells. Cells (5,000 cells/well) were cultured in medium for 24 hr, followed by serum starvation and treatment with PTX (500 ng/ml) for 24 hr were appropriate. Cells were stimulated with various concentrations of cannabinoid agonists for 5 min, in the presence of sucrose (0.5 M), followed by rapid addition of assay lysis buffer. Detection of the phospho-ERK response was as stated in methods (see **4.3.2.2**). Individual ERK phosphorylation values were normalised to the corresponding total-ERK values. The data shown represents mean ± SEM values from 3 independent experiments performed in duplicate. The curves were fitted using GraphPad Prism

Next, concentration-response experiments were performed with HU-210, CP 55,940 and WIN 55,212-2 at 20 min stimulation to characterise the second-phase phospho-ERK response. All three agonists had concentration-dependent effects on

phospho-ERK levels, which were markedly less that those observed after 5 min stimulations (**Figure 4.6**). Both HU-210 and CP 55,940 produced a concentration-dependent increase in phospho-ERK levels, best fit with a sigmoidal concentration-response curve (**Figure 4.6A**). There were no significant differences in pEC_{50} and R_{max} values for the two agonists (**Table 4.2**). Both responses were antagonised by AM 251 (10 nM), allowing for the calculation of pK_B values (**Table 4.2**). In contrast to the results seen at 5 min stimulation, the pK_B value determined using HU-210 was significantly lower than that determined using CP 55,940.

WIN 55,212-2 produced an increase in phospho-ERK levels up to 100 nM (**Figure 4.6B**). At higher concentrations, the phospho-ERK responses to WIN were significantly sub-maximal (one-way ANOVA; $p<0.01$), resulting in a bell-shaped response curve which could not be fitted to a sigmoidal response curve (**Figure 4.6B**); however, the maximum response at 100 nM was not significantly different from the HU-210 and CP 55,940 R_{max} values (one-way ANOVA; $p>0.05$). Addition of a low concentration of AM 251 (10 nM) antagonised both components of the WIN 55,212-2 response, as characterised by a rightwards shift in the high potency positive response, and a reversal of the downturn in the phospho-ERK response at higher agonist concentrations (**Figure 4.6B**; black triangle). A high concentration of AM 251 (1 μM) was able to completely abolish the WIN 55,212-2 response (**Figure 4.6B**; white triangle).

As with 5 min stimulation, the experiments were repeated with cells pre-treated with PTX (500 ng/ml). All three agonists produced a concentration-dependent

increase in phospho-ERK levels. The reversal of elevated phospho-ERK levels by WIN 55,212-2 at higher concentrations was abolished by PTX, allowing the data for all three agonists to be fitted to sigmoidal response curves. The rank order of pEC_{50} values of the agonists from highest to lowest was HU-210 ≥ CP 55,940 > WIN 55,212-2 (**Table 4.2**). There were no significant differences in the R_{max} values for the three agonists (one-way ANOVA; $p>0.05$). When compared to the responses seen in untreated cells, the R_{max} and pEC_{50} values for HU and the pEC_{50} values for CP were significantly less in PTX-treated cells (two-way ANOVA; $p<0.05$), although the magnitude of the reduction in R_{max} with PTX was not as large as that seen after a 5 min stimulation. All three responses were antagonised by AM 251 allowing for the calculation of pK_B values (**Table 4.2**). As in the untreated cells, the pK_B value determined using HU-210 was significantly lower than that determined using the other agonists (one-way ANOVA; $p<0.05$).

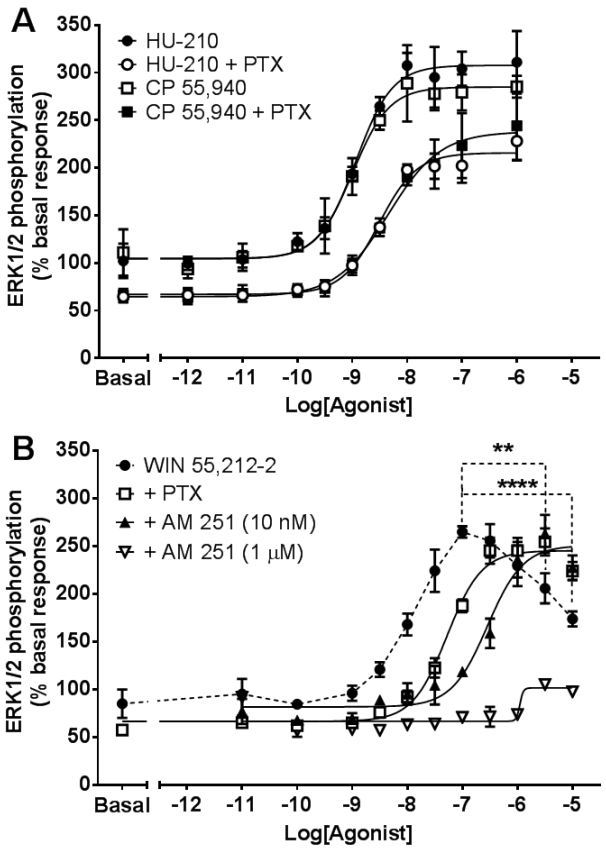

Figure 4.6 Effect of cannabinoid agonists on ERK phosphorylation in HEK-hCB_1 cells at 20 min stimulation. Cells (5,000 cells/well) were cultured in medium for 24 hr, followed by serum starvation and treatment with PTX (500 ng/ml) where appropriate, for 24 hr. Cells were stimulated with various concentrations of cannabinoid agonists for 20 min, followed by rapid addition of lysis buffer. Detection of the phospho-ERK response was as described in methods (see **4.3.2.2**). Individual ERK phosphorylation values were normalised to the corresponding total-ERK values. The data shown represent mean ± SEM values from 4-5 independent experiments performed in duplicate. Curves represented by unbroken lines were fitted by non-linear regression to a four parameter logistical equation and dashed lines simply join neighbouring data points to illustrate overall response trend. Statistical significance was determined by one-way ANOVA; ** $p<0.01$, **** $p<0.0001$.

Table 4.2

Determination of potency (pEC_{50}), maximal response, expressed as % of the basal (R_{max}), and estimated AM 251 dissociation constant (pK_B) of cannabinoid agonists with regard to ERK phosphorylation in HEK-hCB_1 cells after 20 min stimulations, either untreated or pre-treated with PTX (500 ng/ml) overnight.

Agonist	**Non-treated cells**				**PTX-treated cells (500 ng/ml)**			
	pEC_{50}	R_{max}	n_H	pK_B	pEC_{50}	R_{max}	n_H	pK_B
HU-210	8.9 ± 0.1	204 ± 188	1.4 ± 0.2	8.6 ± 0.1	8.5 ± 0.1	156 ± 16	1.3 ± 0.3	8.4 ± 0.2
CP 55,940	9.0 ± 0.1	177 ± 6	1.4 ± 0.1[c]	9.2 ± 0.1	8.3 ± 0.1	181 ± 19	0.9 ± 0.2	9.0 ± 0.1
WIN 55,212-2	[a]	[a]	[a]	[b]	7.3 ± 0.1	170 ± 17	1.4 ± 0.1[c]	9.2 ± 0.1

The data shown represents mean ± SEM values from 4-5 independent experiments performed in triplicate.

[a] It was impossible to fit a response curve using GraphPad Prism.

[b] It was not possible to calculate values for pK_B.

[c] n_H value significantly difference from unity ($n_H = 1$).

4.4.2. Determination of JNK1/2/3 phosphorylation

The cannabinoid agonists were tested for their ability to promote JNK1/2/3 phosphorylation. The antibiotic anisomycin (1 μM), a known activator of stress-activated protein kinases, produced a significant increase in phospho-JNK levels from 6 min onwards (**Figure 4.7**; one-way ANOVA $p<0.0001$). None of the cannabinoid agonists tested were able to significantly increase phospho-JNK levels above basal (**Figure 4.7**; one way ANOVA; $p>0.05$).

4.4.3. Determination of p38 MAP kinase phosphorylation

The cannabinoid agonists were tested for their ability to promote p38 MAP kinase phosphorylation. Anisomycin (1 μM) produced a clear increase in phospho-p38 levels, which was significantly greater than the basal from 6 min onwards (**Figure 4.8;** one-way ANOVA $p<0.0001$). None of the cannabinoid agonists tested were able to significantly increase the level of phospho-p38 above basal (**Figure 4.8**; one way ANOVA; $p>0.05$).

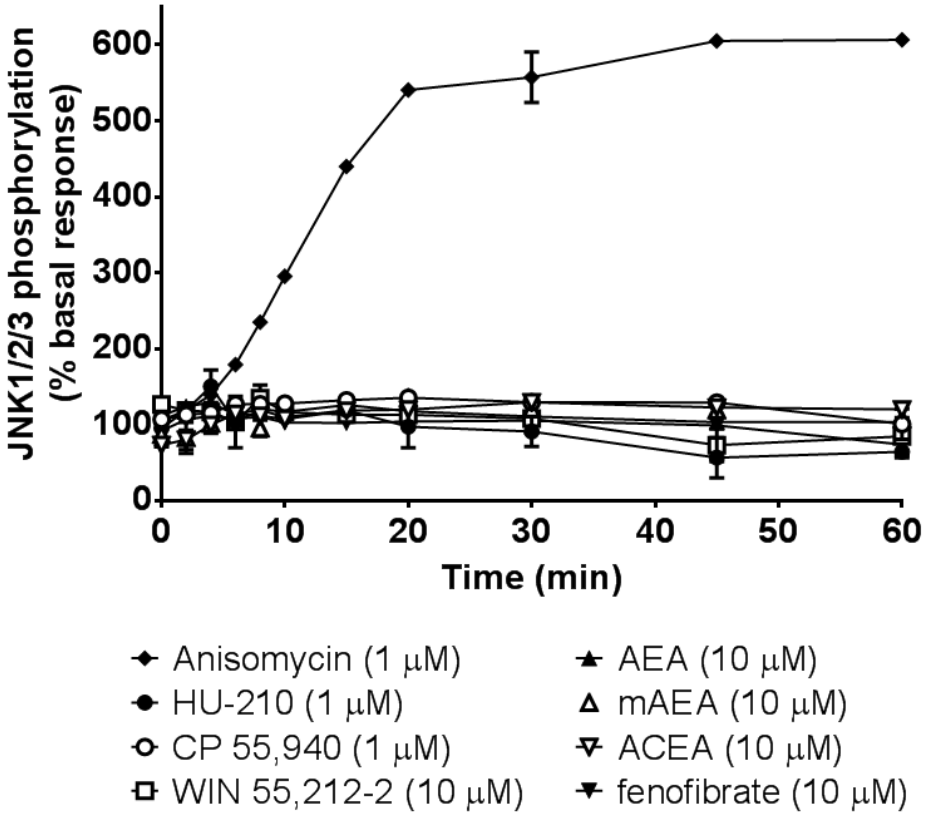

Figure 4.7 Lack of effect of cannabinoid agonists on JNK phosphorylation in HEK-hCB_1 cells over time. Cells (5,000 cells/well) were cultured in medium for 24 hr, followed by serum starvation for 24 hr. Cells were stimulated with cannabinoid agonists (1 or 10 μM) or anisomycin (1 μM) at various time points (2 – 60 min), followed by rapid fixation with PFA solution. Detection of total and phospho-JNK levels were as stated in methods (see **4.3.2.1**). Individual JNK phosphorylation values were normalised to the corresponding total-JNK values. The data shown are means ± SEM values from 3 independent experiments performed in duplicate.

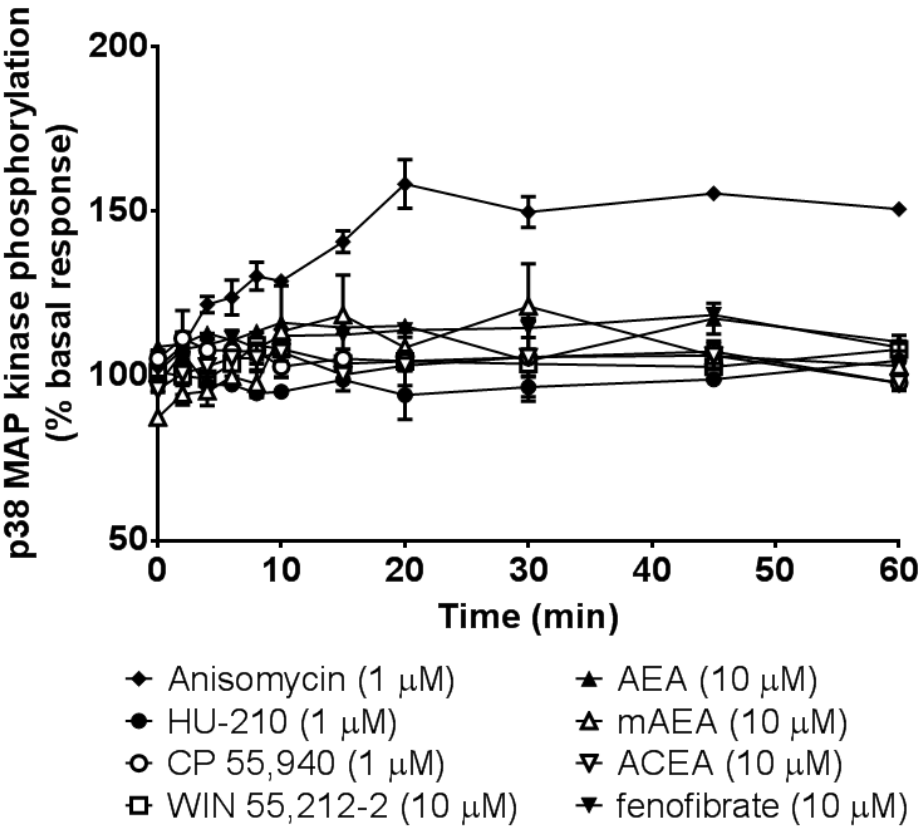

Figure 4.8 Lack of effect of cannabinoid agonists on p38 kinase phosphorylation in HEK-hCB$_1$ cells over time. Cells (5,000 cells/well) were cultured in medium for 24 hr, followed by serum starvation for 24 hr. Cells were stimulated with cannabinoid agonists (1 or 10 μM) or anisomycin (1 μM) at various time points (2 – 60 min), followed by rapid fixation with PFA solution. Detection of total and phospho-p38 levels were as stated in methods (see **4.3.2.1**). Individual p38 phosphorylation values were normalised to the corresponding total-p38 values. The data shown are mean ± SEM values from 3 independent experiments performed in duplicate.

4.4.4. cAMP accumulation

Assay Optimisation

A preliminary experiment was performed to determine the optimal conditions for cAMP assays using the transfected HEK cells. The raw signal was converted to [cAMP] (nM), by interpolating the data with the linear range of a cAMP standard curve (0.3 to 30 nM; **Figure 4.9**, black circle). Anything outside this range cannot be accurately expressed as [cAMP]. Cells were pre-treated with the non-selective phosphodiesterase inhibitor IBMX to prevent conversion of cAMP. Increasing concentrations of NKH 477, a water-soluble derivative of forskolin and direct activator of AC, produced a concentration-dependent decrease in fluorescent signal, corresponding to an increase in cAMP levels. A cell density of 1000 cells/well, and a NKH 477 concentration of 3 µM were chosen as optimised conditions as they provided the NKH 477 EC_{80} value most closely corresponding to the top of the linear range of the cAMP standard curve, which allows for the largest window for agonist-mediated inhibition of cAMP accumulation.

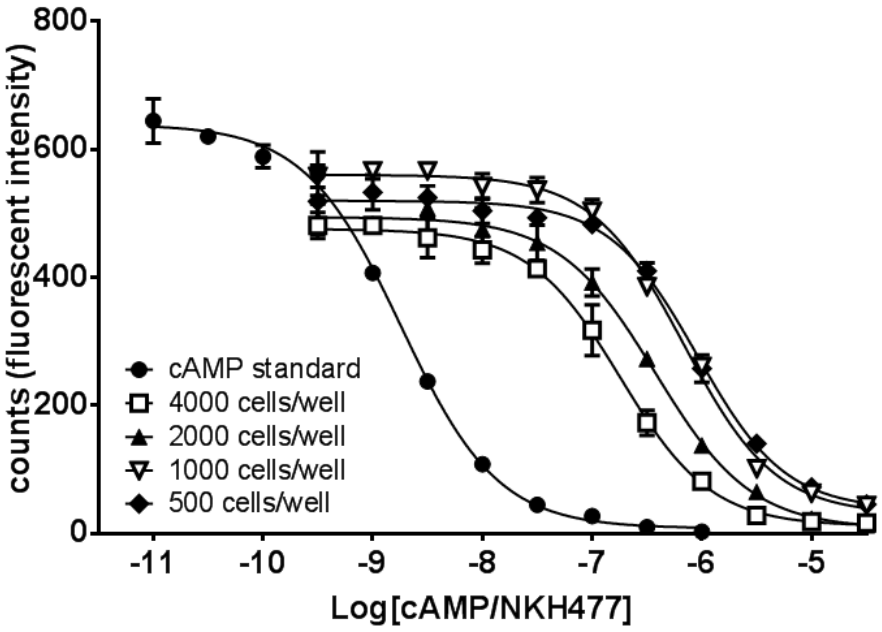

Figure 4.9 Optimisation of the cAMP assay in HEK-hCB$_1$ cells. Cells (0.5, 1, 2 and 4000 cells/well) in suspension in assay buffer were pre-treated with the phosphodiesterase inhibitor IBMX (0.5 mM) for 10 min before incubation with increasing concentrations of NKH 477 (0.3 – 30 µM) for 20 min at 37°C. A cAMP standard (1 nM – 1 µM) in cell-free media was included. At the end of the incubation period, the assay was terminated by the addition of detection mix and the actual levels of cAMP determined using the Cisbio femto cAMP assay kit (see **4.3.3**). The data shown represent a single experiment performed in triplicate, and are shown as means ± SEM. The curves were fitted using GraphPad Prism.

Inhibition of NKH 477-stimulated cAMP accumulation

HEK-hCB$_1$ cells pre-treated with NKH 477 (3 µM) and IBMX (0.5 mM), were stimulated with increasing concentrations of the cannabinoid agonists to determine the ability of these compounds to inhibit NKH 477-stimulated cAMP accumulation (**Figure 4.10**). All agonists produced a concentration-dependent inhibition of NKH 477-stimulated cAMP accumulation. The rank order of potency

of agonists acting on HEK-hCB$_1$ cells from highest to lowest was HU-210 ≥ CP 55,940 > Δ^9-THC ≥ WIN 55,212-2 ≥ anandamide > methanandamide ≥ fenofibrate ≥ ACEA (**Table 4.3**). All agonists, except Δ^9-THC, appeared to act as full agonists, with no significant differences between R_{max} values (**Table 4.3**; one-way ANOVA; p>0.05). Treatment with 100 µM anandamide, failed to inhibit NKH 477-stimulated cAMP accumulation. As this is indicative of a distinct signalling mechanism, the data point was excluded when fitting the concentration-response curves.

Next, the experiments were repeated in cells pre-treated with PTX (500 ng/ml) and in the absence of NKH 477, to determine the role of $G_{i/o}$ protein in the cannabinoid-mediated cAMP response, and whether any alternate $G_{i/o}$ protein-independent signalling could be identified. The agonists HU-210, C 55,940 and WIN 55,212-2 all produced clear, reproducible concentration-dependent increases in cAMP levels (**Figure 4.11**). Anandamide produced a clear increase in cAMP levels at 30 and 100 µM, but this response could not be fitted with a concentration-response curve. The other agonists tested, including the novel peptide cannabinoid agonist/allosteric modulator RVD-hemopressin, failed to produce a significant increase in cAMP levels. The rank order of potency from highest to lowest was HU-210 ≥ CP 55,940 > WIN 55,212-2 (**Table 4.3**). The R_{max} value for WIN 55,212-2 was significantly greater than that for HU-210 and CP 55,940 (**Table 4.3**; one-way ANOVA; p<0.05). Comparing the responses in the PTX-treated cells to those observed in untreated cells, the pEC_{50} values for the three agonists were all significantly smaller than the corresponding responses seen in untreated cells (two-way ANOVA; p<0.0001).

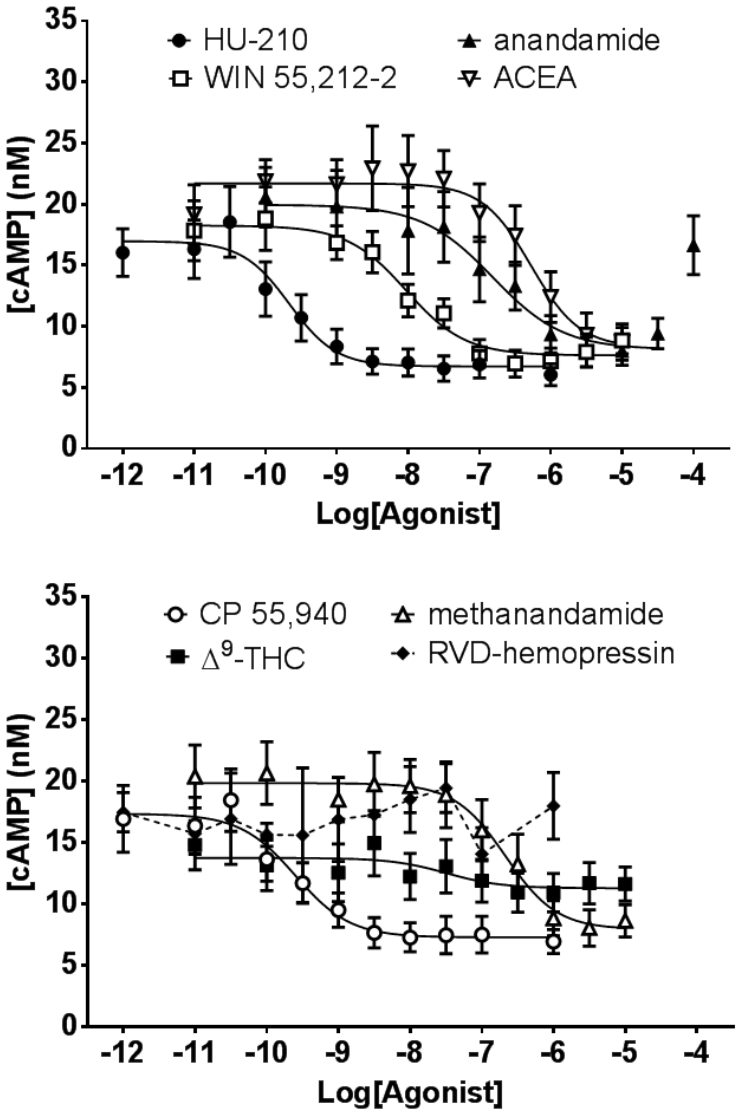

Figure 4.10 Effect of cannabinoid agonists on cAMP accumulation in HEK-hCB_1 cells. Cells in suspension in assay medium were pre-treated with NKH 477 (3 µM) and IBMX (0.5 mM) for 10 min before incubation with increasing concentrations of cannabinoid agonists for 20 min at 37°C. At the end of the incubation period, the assay was terminated by the addition of detection mix and the levels of cAMP (nM) determined using the Cisbio femto cAMP assay kit. The data shown represent mean ± SEM values from 6-7 individual experiments performed in triplicate. The curves were fitted using GraphPad Prism

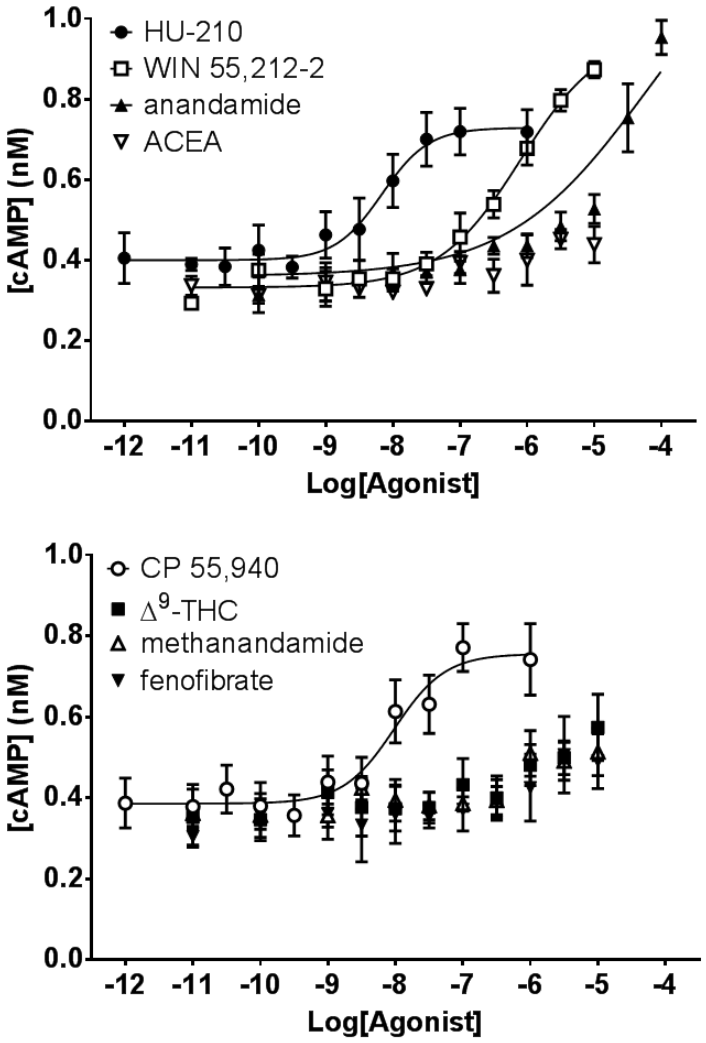

Figure 4.11 Effect of cannabinoid agonists on cAMP accumulation in HEK-hCB_1 cells, pre-treated with pertussis toxin. Cells, previously treated with PTX (500 ng/ml) for 24 hr, in suspension in assay medium were pre-treated with NKH 477 (3 μM) and IBMX (0.5 mM) for 10 min before incubation with increasing concentrations of cannabinoid agonists for 20 min at 37°C. At the end of the incubation period, the assay was terminated by the addition of detection mix and the actual levels of cAMP (nM) determined using the Cisbio femto cAMP assay kit. The data shown represent mean ± SEM values from 4 individual experiments performed in triplicate. The curves were fitted using GraphPad Prism.

Table 4.3 Determination of potency (pEC_{50}), concentration-response curve span (R_{max}), and curve slope (n_H) of cannabinoid agonists on cAMP accumulation in HEK-hCB_1 cells at 20 min stimulation, either untreated or pre-treated with PTX (500 ng/ml) overnight.

Agonist	**Inhibition of cAMP accumulation (untreated cells)**			**Stimulation of cAMP accumulation (PTX-treated cells)**		
	pEC_{50}	R_{max}	n_H	pEC_{50}	R_{max}	n_H
HU-210	9.7 ± 0.1	10.4 ± 1.9	-1.3 ± 0.1[b]	8.3 ± 0.2	0.4 ± 0.1[c]	1.3 ± 0.4
CP 55,940	9.6 ± 0.1	10.7 ± 2.3	-1.1 ± 0.1	8.0 ± 0.1	0.4 ± 0.1[c]	1.2 ± 0.1
WIN 55,212-2	8.0 ± 0.2	12.0 ± 2.7	-1.0 ± 0.1	6.1 ± 0.2	0.7 ± 0.1	0.8 ± 0.1
Δ^9-THC	8.2 ± 0.7	8.6 ± 2.0	-1.1 ± 0.3	[a]	[a]	[a]
anandamide	7.6 ± 0.4	8.8 ± 3.8	-0.9 ± 0.1	[a]	[a]	[a]
methanandamide	6.7 ± 0.1	11.6 ± 0.9	-1.4 ± 0.1[b]	[a]	[a]	[a]
ACEA	6.3 ± 0.1	13.2 ± 1.6	-1.6 ± 0.1[b]	[a]	[a]	[a]
fenofibrate	6.3 ± 0.3	14.9 ± 2.9	-2.2 ± 0.6[b]	[a]	[a]	[a]

The data shown represents mean ± SEM values from 4-7 independent experiments performed in triplicate.

[a] It was impossible to determine values for these parameters using GraphPad Prism.

[b] n_H value significantly difference from unity (n_H = +/-1).

[c] value significantly less than that for WIN 55-212-2.

4.4.5. Analysis of bias

In an effort to quantify bias at the CB_1 receptor between the different agonist responses, intrinsic relative activity (RAi) values were calculated for all agonists (see **4.3.5)**, using HU-210 as the reference agonist (**Table 4.4**). WIN 55,212-2, Δ^9-THC, ACEA and fenofibrate were all shown to be significantly positively biased towards ERK signalling versus inhibition of NKH 477-mediated cAMP accumulation (**Table 4.4**; unpaired, two-tailed *t*-test; $p<0.05$). In addition, WIN was also biased towards PTX-insensitive ERK activation versus PTX-sensitive ERK activation, after 5 min of agonist stimulation (**Table 4.4**; unpaired, two-tailed *t*-test; $p<0.05$). Some of these parameters were then plotted on a histogram, for easier interpretation, with comparison made between the ERK and cAMP responses in non-toxin treated cells (**Figure 4.12A**), and PTX treated cells (**Figure 4.12B**).

Table 4.4 Determination of intrinsic relative activities and comparison of RAi values (ΔRAi) for cannabinoid agonists acting at human CB_1 receptors expressed in HEK cells

Agonist	**RAi - Non-treated cells**			**RAi - PTX-treated cells (500 ng/ml)**			**ΔRAi (-fold difference)**			
	ERK (5 min)	*ERK (20 min)*	*cAMP*	*ERK (5 min)*	*ERK (20 min)*	*cAMP*	*ERK (5 min) vs. cAMP*	*ERK (5 min) PTX vs. NT*	*ERK (20 min) NT vs. PTX*	*cAMP NT vs. PTX*
CP 55,940	2.44 ± 0.38 ($x10^0$)	1.14 ± 0.19 ($x10^0$)	1.43 ± 0.62 ($x10^0$)	3.41 ± 0.94 ($x10^0$)	8.34 ± 1.80 ($x10^{-1}$)	5.65 ± 2.15 ($x10^{-1}$)	1.7	1.4	1.4	2.5
WIN 55,212-2	2.48 ± 0.33 ($x10^{-1}$)	N.D.	4.68 ± 2.82 ($x10^{-2}$)	6.53 ± 1.73 ($x10^{-1}$)	8.59 ± 2.41 ($x10^{-2}$)	1.61 ± 0.85 ($x10^{-2}$)	5.3[a]	2.6[a]	N.D.	2.9
Δ^9-THC	1.12 ± 1.06 ($x10^0$)	N.D.	3.68 ± 2.81 ($x10^{-2}$)	N.D.	N.D.	N.D.	30.3[a]	N.D.	N.D.	N.D.
anandamide	8.06 ± 1.12 ($x10^{-3}$)	N.D.	2.35 ± 1.50 ($x10^{-2}$)	2.28 ± 1.21 ($x10^{-2}$)	N.D.	N.D.	0.3	2.8	N.D.	N.D.
methanandamide	1.17 ± 0.30 ($x10^{-2}$)	N.D.	1.63 ± 0.63 ($x10^{-3}$)	1.49 ± 0.12 ($x10^{-2}$)	N.D.	N.D.	7.2[a]	1.3	N.D.	N.D.
ACEA	8.90 ± 2.10 ($x10^{-3}$)	N.D.	6.64 ± 1.96 ($x10^{-4}$)	1.60 ± 0.50 ($x10^{-2}$)	N.D.	N.D.	13.4[a]	1.8	N.D.	N.D.
fenofibrate	1.47 ± 0.33 ($x10^{-2}$)	N.D.	1.12 ± 0.55 ($x10^{-3}$)	N.D.	N.D.	N.D.	13.2[a]	N.D.	N.D.	N.D.

RAi values are mean ± SEM values from 3-7 independent experiments performed in replicate. ΔRAi values are the fold difference between the stated RAi values.

N.D. – not determined due to lack of curve parameters.

[a] – difference between the two RAi values stated in the column header, as quantified by the ΔRAi value, are significantly different, indicating agonist bias (unpaired, *t*-test; $p<0.05$).

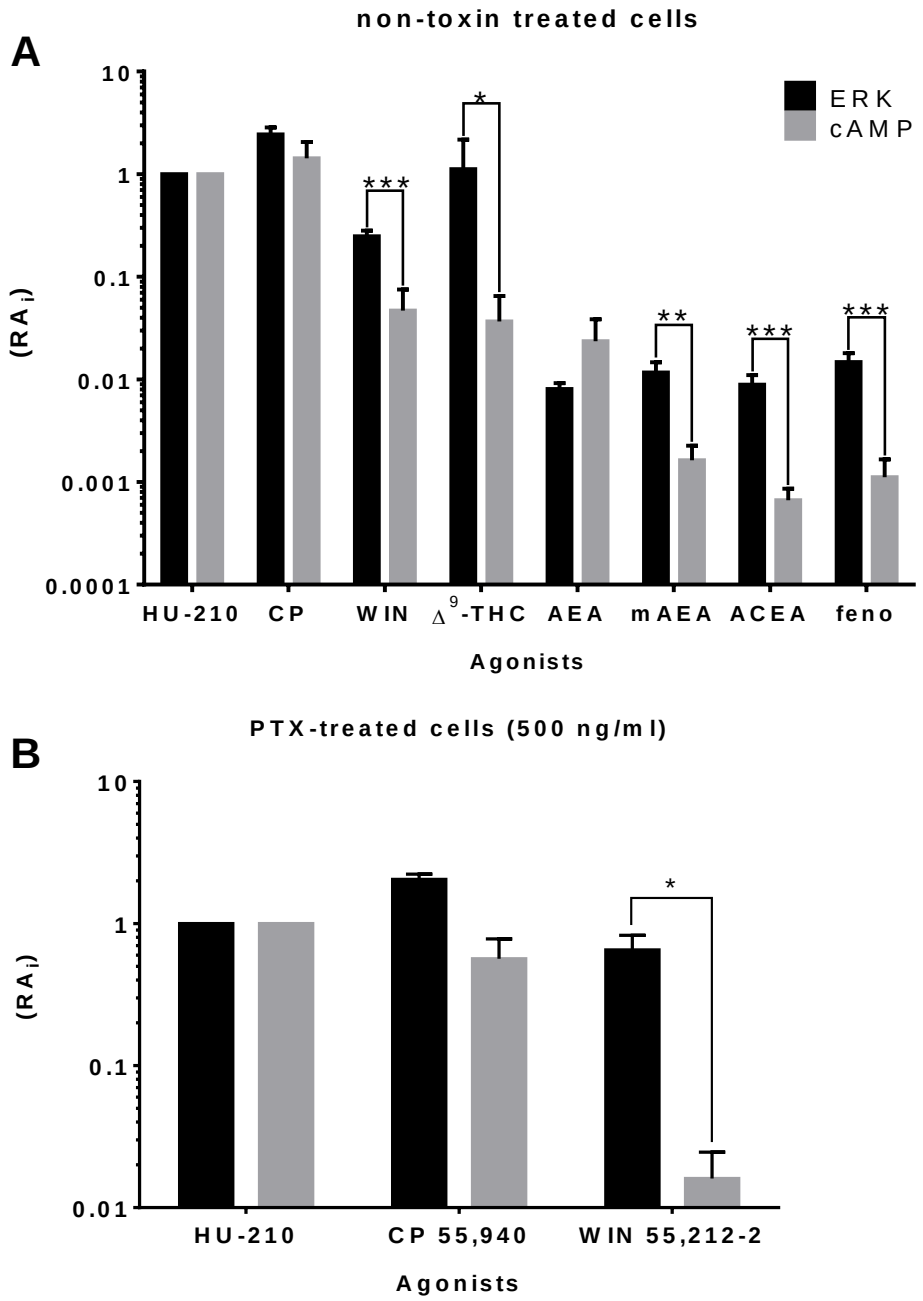

Figure 4.12 Comparison of the RAi values of cannabinoid agonists modulating ERK and cAMP responses at CB_1 receptors expressed in HEK cells either untreated (A), or pre-treated with pertussis toxin (B). The data shown represents mean ± SEM values from 3-7 individual experiments performed in replicate. Statistical significance was determined using unpaired, two-tailed *t*-test; **p*<0.05, ***p*<0.01, ****p*<0.001.

4.5. Discussion

The human embryonic kidney 293 (HEK) cell line, stably transfected with the human CB_1 receptor is a well characterised model for investigating CB_1-mediated signalling, including some reports of agonist bias (Lauckner *et al.*, 2005), and, therefore, is an attractive model for studying signalling at the CB_1 receptor.

Time-course experiments revealed a unique temporal profile for cannabinoid-mediated ERK activation in HEK-hCB_1 cells – while the initial phase was consistent with that observed previously with CHO-hCB_1 cells, as well as previous reports in the literature (Daigle *et al.*, 2008; Dalton & Howlett, 2012), the phospho-ERK response remained elevated from 10 min onwards, rather than returning to near basal levels. Furthermore, the initial phase response was only partially sensitive to inhibition with pertussis toxin, while the second phase appeared to be unaffected. Taken together, these results strongly indicate there are two distinct pathways for cannabinoid-mediated ERK signalling in HEK-hCB_1 cells – a large $G_{i/o}$ protein-dependent response with a rapid on-set and off-set, and a smaller $G_{i/o}$ protein-independent, PTX-insensitive, response, with a slightly delayed onset, which remains activated up to 60 min after agonist stimulation. It has been shown that, in addition to $G_{i/o}$ proteins, CB_1 receptor-dependent ERK activation can be mediated by activation of G_q proteins (Asimaki *et al.*, 2011), which is typically very rapid and transient and also via β-arrestin recruitment (Ahn *et al.*, 2013), which is typified by a delayed response of longer duration, making it the more likely mediator of the second phase responses. To test this, the effect of a hypertonic concentration of sucrose on both the $G_{i/o}$ protein-dependent and independent responses to WIN 55,212-2 was investigated. Sucrose is one of a

number of experimental tools used to inhibit the formation of clathrin lattices, which are important to β-arrestin function both in internalisation, and as a signalling mediator, with inhibition of this process having previously been shown to disrupt β-arrestin-mediated ERK activation (Luttrell *et al.*, 1997; Lin *et al.*, 1998). In the present study, the addition of sucrose completely inhibited the $G_{i/o}$ protein-independent response, and while it is not conclusive evidence, it is consistent with mediation of the response by β-arrestin.

Characterisation of the initial-phase ERK response using concentration-response experiments revealed a familiar pattern of agonist potency and intrinsic activity to that reported in the literature (Howlett *et al.*, 2002), as well as that observed in the previous chapters, with the notable exceptions of ACEA being less potent than expected, relative to the other agonists, while competitive inhibition of all agonist responses with AM 251 confirmed that ERK activation was mediated via CB_1 receptors. ACEA had a similar potency in the cAMP assays; these results contrasting sharply with those for CHO-hCB_1 cells, and with the description in the literature of ACEA as a high affinity agonist (K_i – 1.4 nM; Hillard *et al.*, 1999). It is uncertain whether this discrepancy is due to functionally selective signalling or whether the agonist undergoes enzymatic degradation in HEK cells.

The agonist-mediated $G_{i/o}$ protein-independent response at 5 min, in addition to being smaller than the $G_{i/o}$ protein-dependent responses, were also less potent for HU-210, CP 55,940 and WIN 55,212-2, further indicating the involvement of a distinct signalling pathway.

The $G_{i/o}$ protein-dependent WIN 55,212-2 response at 20 min, produced a bell-shaped concentration-response curve, characterised by a high potency increase in phospho-ERK levels, followed by a sub-maximal ERK activation at concentrations above 100 nM - in stark contrast to the responses seen with HU-210 and CP 55,940. Both the pattern of the response and the fact that both components were sensitive to antagonism by AM 251 strongly suggests that WIN 55,212-2 is functionally selective in regards to ERK signalling at the CB_1 receptor. Despite the WIN response being qualitatively different from responses to the other two agonists, all three responses appeared to be $G_{i/o}$ protein-dependent. One potential explanation for this is that the WIN-mediated inhibition of ERK activation may be dependent on a subtype of $G_{i/o}$ protein distinct from that which mediates ERK phosphorylation. The $G_{i/o}$ protein family includes three subtypes of $G\alpha_i$ protein, as well as the $G\alpha_o$ protein. WIN was previously been shown to activate a distinct pattern of $G\alpha_{i/o}$ protein subtypes from that of tricyclic cannabinoid agonists, such as HU-210 and synthetic endocannabinoid analogues (Glass & Northup, 1999; Mukhopadhyay & Howlett, 2005). The WIN response was also functionally selective when compared to $G_{i/o}$ protein-independent ERK responses at 20 min, which were sigmoidal for all three agonists. As stated in the previous chapter, there is a report of WIN-mediated inhibition of ERK activation in rat C6 glioma cells, which activates the Bcl-2-associated death promoter or BAD and leads to activation of pro-apoptotic changes in cell physiology (Ellert-Miklaszewska *et al.*, 2005). The possibility exists, therefore, that WIN may selectively activate pro-apoptotic responses in cells via a functionally selective CB_1 receptor mechanism. Future research should investigate the long term effect

of WIN exposure on HEK cell viability and whether WIN selectively activates BAD or associated signalling mediators compared to other agonists.

The antibiotic anisomycin, a known activator of stress-activated protein kinases produced a significant increase in phospho-JNK and phospho-p38 kinase levels, clearly demonstrating that these signalling pathways were active in the HEK cells. However, none of the cannabinoid agonists tested was able to activate JNK or p38 kinase signalling, despite CB_1–mediated signalling being previously reported in a number of other cell types (Rueda *et al.*, 2000; Bosier *et al.*, 2008; Rajesh *et al.*, 2010). This lack of JNK and p38 kinase signalling is in agreement with our previous observations in CHO-hCB_1 cells (see **3.4.4** and **3.4.5**), and is potentially due to an inability of the receptor to couple to the SAP kinase pathways in these cells.

In addition to ERK activation, the cannabinoid agonists were able to inhibit the function of AC, as demonstrated by the inhibition of NKH 477-mediated cAMP accumulation, which is consistent with the results for CHO-hCB_1 cells. However, in PTX-treated HEK cells HU-210, CP 55,940 and WIN 55,212-2 produced a clear concentration-dependent increase in cAMP levels, most likely due to a shift in receptor coupling from $G_{i/o}$ to G_s proteins, which activate AC. The receptor coupling to G_s proteins appeared to be much weaker that the coupling to $G_{i/o}$ proteins as illustrated by the significant decrease in the magnitude of the G_s protein responses relative to the $G_{i/o}$ protein-dependent responses. This is potentially due to difference in the expression levels of the various G protein subtypes, and the coupling efficiency of the G proteins to AC. While this

phenomenon was not observed in our study with CHO-hCB_1 cells, CB_1 receptor coupling to G_s protein in the presence of PTX in other transfected CHO cells and primary cultured rat neurons has been reported in the literature (Glass & Felder, 1997; Maneuf & Brotchie, 1997; Bonhaus *et al.*, 1998). As far as is known, this thesis provides the first characterisation of CB_1 receptor/G_s protein coupling in HEK cells. Furthermore, the responses exhibit a complex pattern of agonist bias – HU-210, CP 55,940, WIN 55,212-2 and anandamide activated both pathways, but the other agonists were only effective in the $G_{i/o}$ protein-dependent pathway. Also, while HU-210, CP 55,940, WIN 55,212-2 were equally efficacious in the reduction of cAMP levels, WIN 55,212-2 was more efficacious than the other two agonists in the $G_{i/o}$ protein-independent increase in cAMP levels, a pattern which is identical to that reported by Bonhaus *et al*. (1998) in CB_1-transfected CHO cells.

While separate investigation of the signalling pathways has revealed some clear examples of functionally selective signalling, comparison of the agonist responses across the signalling pathways by use of intrinsic relative activity (RAi) values is necessary to quantify less obvious agonist bias. In particular, Δ^9-THC was markedly positively biased towards ERK activation versus inhibition of cAMP accumulation, shown by the relatively greater intrinsic activity in ERK activation, compared to modulation of cAMP. In addition WIN 55,212-2 appeared uniquely biased towards $G_{i/o}$ protein-independent versus $G_{i/o}$ protein-dependent ERK signalling at the 5 min stimulation time-point, again demonstrated by the relatively greater intrinsic activity at the $G_{i/o}$ protein-independent signalling pathway. These

results illustrate the sometimes subtle pattern of agonist bias, as well as validating the use of RAi to quantify functional selectivity at the CB_1 receptor.

4.6. Conclusions

In conclusion, the results shown in this chapter clearly demonstrate that cannabinoid agonists are able to modulate ERK and AC signalling in HEK cells via transfected human CB_1 receptors coupled to $G_{i/o}$ protein-dependent and independent signalling pathways. Furthermore, activation of these signalling pathways exhibits clear examples of agonist bias, with ligand-selective differences in temporal ERK signalling, coupling to AC and differential activation between these two main signalling pathways.

Chapter 5

Investigation of Functional Selectivity at the Cannabinoid Receptor in an Endogenously Expressing Cell Line, Neuro 2a

5.1. Introduction

The Neuro-2a cell line is a neuroblastoma cell line derived from a spontaneous tumour from a strain A albino mouse (Klebe & Ruddle, 1969). Under normal culture conditions, the cells are spherical and undergo mitotic division. Removal of serum from the culture medium, or treatment with retinoic acid promotes cell differentiation, halting mitosis and causing cells to produce neurite outgrowths, needle-like projections several times the length of the cell body.

PCR analysis has detected CB_1 receptor mRNA in both native (Graham *et al.*, 2006; Jung *et al.*, 2011) and differentiated Neuro 2a cells, with treatment with retinoic acid resulting in a 3-fold increase in the observed mRNA levels (Jung *et al.*, 2011). Immunocytochemical studies have confirmed the presence of receptor protein, the majority of which appears to be within the cytoplasm with the remainder present in the cell membrane (Graham *et al.*, 2006; Rozenfeld *et al.*, 2012). Indeed, a recent study calculated the proportion of intracellular receptor expression to be 68% of the total receptor population (Grimsey *et al.*, 2010). No report has been made on the presence of CB_2 receptor in Neuro 2a cells, however due to their neuronal phenotype, they are unlikely to be present.

Treatment of undifferentiated Neuro 2a cells with cannabinoid agonists induces neurite outgrowth, akin to that seen in cell differentiation. Indeed, there is some evidence to suggest that Neuro 2a differentiation involves the cannabinoid system. Treatment of Neuro 2a cells with retinoic acid, causes an elevation of 2-AG levels, as well as upregulation of the DAG lipase α and β and the CB_1 receptor (Jung *et al.*, 2011), which is coupled to increased levels of neurite outgrowth. Addition of

the CB_1-selective antagonist rimonabant blocks retinoic acid-mediated neurite outgrowth.

Jordan *et al.* (2005) were the first to characterise CB_1 receptor-linked signalling in Neuro 2a cells, by demonstrating receptor-mediated regulation of Rap1, a member of the Ras superfamily of small GTPases, important to signal transduction. Treatment with the cannabinoid agonist HU-210 promoted the proteasomal degradation of the precursor Rap1GAPII, leading to Rap1 activation, in a rimonabant- and pertussis toxin-sensitive manner. In addition, treatment with rimonabant, PTX and expression of dominant negative Rap1 all blocked cannabinoid-induced neurite outgrowth. Further research more fully characterised this signalling pathway as illustrated in **Figure 5.1**, revealing sequential signal transduction, leading to STAT3 activation (He *et al.*, 2005). STAT3 is a transcription factor known to regulate numerous cell processes in response to cell stimuli, including growth and apoptosis (Qi & Yang, 2014). Treatment with HU-210 led to phosphorylation of Src and STAT3 in a rimonabant and PTX-sensitive manner, resulting in neurite outgrowth. A series of experiments determining the effects of dominant negative variant of the proteins Rap1, Ral, Src, STAT3 and Rac on protein activation and neurite outgrowth enabled the sequential profile of the transduction pathway to be elucidated (**Figure 5.1**). Src appeared to activate STAT3 both directly and indirectly via the phosphorylation of JNK. More recently, other studies have used STAT3 phosphorylation as a measure of CB_1 receptor activation in Neuro 2a cells, further validating this pathway (Rios *et al.*, 2006; Zorina *et al.*, 2010).

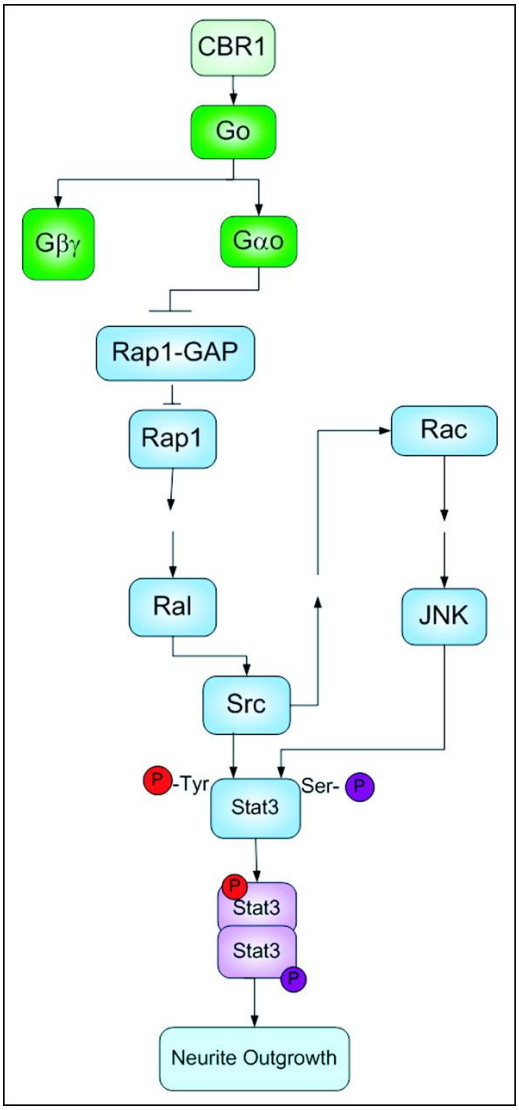

Figure 5.1 Schematic of CB_1 receptor Rap1/STAT3 signal transduction pathway in Neuro 2a cells. Activation of the cannabinoid CB_1 receptor results in the sequential activation of proteins leading to the phosphorylation of STAT3 and induction of neurite outgrowth. Adapted from He *et al.*, 2005.

Separately, Graham *et al.* (2006), identified a second CB_1 receptor signalling cascade in Neuro 2a cells involving the ERK-dependent activation of early growth response protein 1 or EGR1 (previously referred to as Krox-24), illustrated in **Figure 5.2**. Like STAT3, EGR1 is a transcription factor which upregulates target

genes involved in differentiation and mitogenesis. It appears to have a particular role in neuronal tissue, where EGR1 activation is associated with increased neuronal activity and neuronal plasticity (Knapska & Kaczmarek, 2004). Stimulation of Neuro 2a cells with HU-210 led to increased levels of ERK1/2 phosphorylation and induction of EGR1 mRNA and protein. Both responses were blocked by the addition of rimonabant and U0126, a MEK inhibitor. Interestingly, it was observed that blockade of the PI3K/Akt pathway or short term removal of serum (which contains factors which activate the PI3K/Akt pathway), resulted in a large increase in the proportion of cells exhibiting CB_1-dependent EGR1 induction, as well as an increase in the magnitude of both the pERK and EGR1 responses. Serum starvation or treatment with retinoic acid over 3 days (i.e. differentiating cells) all but abolished CB_1-mediated EGR1 responses, suggesting that this pathway is present only in mitotic cells.

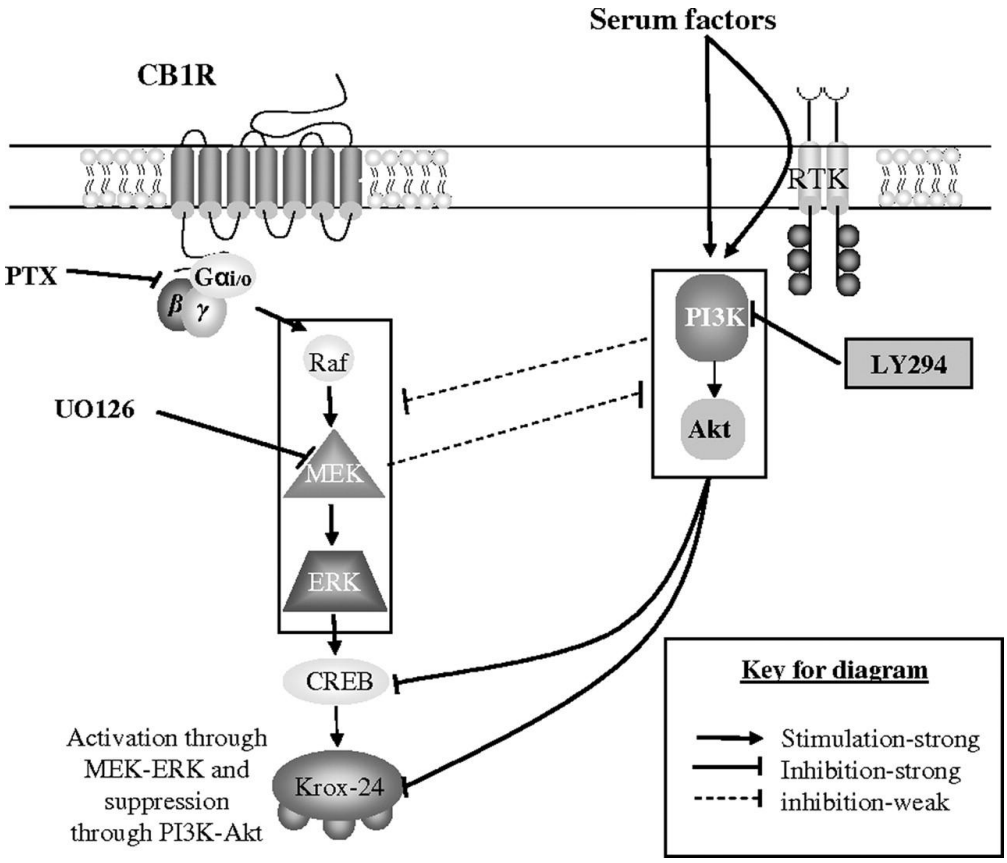

Figure 5.2 Schematic of CB_1 receptor ERK/CREB/EGR1 (Krox-24) signal transduction pathway in Neuro 2a cells. Activation of CB_1 receptor leads to activation of the ERK signalling pathway resulting in induction of EGR1 (Krox-24). Adapted from Graham *et al.*, 2006.

It is interesting to note that Graham *et al*. (2006) clearly state they were unable to detect any change in the level of phospho-JNK, as well as phospho-p38, upon stimulation with HU-210. These results are in contrast to the pattern of JNK activation observed by He *et al*. (2005). These conflicting results may potentially be explained by differences in the cell culture regimens used - He *et al.*, cultured cells in DMEM/F12 mixture with cells being serum starved for 24 hours prior to HU-210 treatment while Graham *et al*., cultured cells in DMEM alone, and treated cells in medium containing 10% FBS. Additionally, it is possible that the two

studies used two different sub clones of the Neuro 2a cell line, leading to putative differences in protein expression and phosphorylation.

5.2. Aims and objectives

As far as can be ascertained, only HU-210 and rimonabant have been used to investigate CB_1-mediated functional responses in Neuro 2a cells. The aim of this chapter was to investigate functionally selective responses at the CB_1 receptor in Neuro 2a cells by stimulating cells with a range of cannabinoid agonists. This will be achieved by measuring the modulation of a number of signal transduction mediators including the MAP kinases ERK, JNK, the transcription factor STAT3 and the enzyme adenylyl cyclase (AC) via changes in cAMP levels. This cell line provides an attractive model to investigate CB_1 receptor functional selectivity as it endogenously expresses the receptor, and has been shown to couple to at least two distinct signalling pathways.

5.3. Methods

5.3.1. Cell culture

Neuro 2a cells were kindly provided by Annabelle Chambers, (University of Nottingham). All cell culture was performed under sterile conditions in a class II laminar flow cabinet. All culture reagents were heated to 37°C before use. Cells were cultured in 175 cm^2 culture flasks containing Dulbecco's Modified Eagle Medium supplemented with 10% foetal bovine serum, 2 mM L-glutamine and 1% penicillin-streptomycin, in a humidified incubator at 37°C and 5 % CO_2. Cells were cultured for 3 days until ~90% confluent, and then passaged. Cells were washed once with phosphate-buffered saline (PBS), and then incubated with trypsin/EDTA solution for at least 5 min until the majority of cells were detached from the culture flask. The cell suspension was diluted in culture medium to prevent further action of the trypsin, and then cells were collected by centrifugation at 200 x *g* for 5 min. The cell pellet was resuspended in fresh culture medium and the cell number determined using the Bio-Rad TC10™ Automated Cell Counter; cells were then reseeded into new culture flasks containing fresh culture medium (4 million cells/flask).

5.3.2. cAMP accumulation assay

Levels of cAMP accumulation were determined using the DiscoveRx HitHunter® cAMP XS+ assay kit. Cells were seeded into white 96-well assay plates at 10,000 cells/well (unless otherwise stated) in assay medium, comprising serum-free culture medium containing rolipram (10 µM), forskolin (10 µM) and 1 mg/ml BSA. Each subsequent step was followed by an incubation period of 30 min at room temperature in a final assay volume of 30 µl. Cells were treated with serial

dilutions of cannabinoid ligands, performed in assay medium. Once ligand treatment was complete, the assay was terminated by cell lysis via the addition of ED/Lysis CL working solution (40 µl/well) followed by the addition of EA reagent (40 µl/well). The relative chemiluminescent signal, corresponding to the cAMP concentration, was detected using a PerkinElmer TopCount NXT™. The data were expressed as a % of the cAMP accumulation in the presence of forskolin (10 µM).

5.3.3. Determination of protein phosphorylation

5.3.3.1. Protocol

Levels of protein phosphorylation were determined using the In-Cell Western™ assay. Cells were seeded into 96-well clear bottom plates, at 20,000 cells/well (unless otherwise stated) in culture medium overnight at 37°C. All subsequent additions to assay plates, including compound addition were made against the well wall, to minimise perturbation of the cell monolayer. 24 hrs prior to experimentation, the culture medium was removed from the assay plates by gentle aspiration, and the medium replaced with serum-free medium. Cells were not washed with PBS, to minimise perturbation of the cell monolayer. Serial dilution of test ligands was performed in serum-free medium and added to test wells to a final volume of 200 µl per well. Assay plates were incubated for the stated period at 37°C during experimentation. After incubation, the assay medium was rapidly aspirated and the cells were fixed with 4% paraformaldehyde in PBS for 20 min at room temperature (150 µl/well). Each reagent was aspirated before the addition of the next reagent. Cells were then permeabilised with 0.1% (v/v) Triton™ X-100 in PBS for 20 min at room temperature (150 µl/well). Non-specific antibody binding

sites were blocked with 5% (w/v) milk powder in PBS for 20 min at room temperature with gentle rocking.

Primary antibodies for anti-total and anti-phosphorylated proteins (ERK1/2, JNK1/2/3 and STAT3; see **5.3.3.3**) were diluted together in blocking agent. Cells were incubated with primary antibody solution (50 µl/well) overnight at 4°C with gentle rocking. Control wells without primary antibody, to give a measure of the non-specific binding of the secondary antibody, were incubated with blocking solution only. The next day, the primary antibody solution was aspirated and the cells were washed three times with PBS containing 1 mg/ml BSA (150 µl/well) for 5 min at room temperature with gentle rocking. The appropriate LI-COR IRDye® secondary antibodies were diluted 1:4000 in blocking agent, added to the cells (50 µl/well), and incubated in darkness for 60 min at 37°C with gentle shaking. The secondary antibody solution was aspirated and the cells washed three times with wash buffer as before.

5.3.3.2. Imaging

Plates were imaged by scanning simultaneously at 700 and 800 nm with the LI-COR Odyssey® NIR Imaging System at 82 µm resolution, medium quality and focus offset of 4.0123 mm. Quantification was performed using LI-COR Odyssey® Software v3.0. Unless otherwise stated, the secondary antibody non-specific response was subtracted from the data. The phospho- response was then normalised against the total protein response for each individual well and then the data was expressed as a percentage of the basal response.

5.3.3.3. Antibodies used

All primary antibodies used were obtained from Cell Signaling Technology (Boston, USA). All antibodies were used at the concentrations described below unless otherwise stated in **Results** (**see 5.4**). Anti-ERK1/2 rabbit, (1:400) # 9102; anti-phospho-ERK1/2 (Thr202/Tyr204) monoclonal mouse, (1:800) # 9106; anti-JNK rabbit, (1:400) # 9252; anti-phospho-JNK (Thr183/Tyr185) monoclonal mouse, (1:400) # 9255.; anti-STAT3 monoclonal mouse (1:800) #9139; anti-phospho-STAT3 (Tyr705) XP monoclonal rabbit #9145. Secondary antibodies were obtained from LICOR, IRDye® labelled goat anti mouse (IRDye® 800CW conjugate) and goat anti-rabbit (IRDye® 680CW conjugate) secondary antibodies.

5.3.4. Data and statistical analysis

All data were analysed using the GraphPad Prism software (v6). Concentration-response data were fitted to curves using the four-parameter logistic equation, previously described in Chapter 2 – Methods (see **2.3.7**).

Estimates for the antagonist AM 251 equilibrium dissociation constant (pK_B) and calculation of the intrinsic relative activities (RAi) for each individual agonist were as previously described in Chapter 3 – Methods (see **3.3.6**).

5.3.5. Statistics

The quantitative data are expressed as means ± SEM, obtained from at least three independent experiments performed in replicate, unless otherwise stated. Normality of data sets was determined using the D'Agostino-Pearson omnibus normality test. Statistical significance of differences was determined by Student's

paired, two-tailed *t*-test or ANOVA followed by Dunnett's multiple comparisons *post-hoc* multiple comparison tests where appropriate. A p value of <0.05 was considered significant.

5.4. Results

5.4.1. Determination of ERK phosphorylation

Assay Optimisation

Initial testing of undifferentiated Neuro 2a cells revealed them to be only semi-adherent when cultured, with excessive perturbation of the cell monolayer causing significant cell detachment. An optimised protocol for the experiment was developed in which changing of culture medium and washing was minimised, additions to test wells, including addition of compound were made slowly and against the side of the well and the volume of the addition was minimised. This experimental technique resulted in suitable numbers of adherent Neuro 2a cells for use in immunocytochemical-based In-Cell Western assays, and was employed in all subsequent phosphorylation assays. Once fixed with paraformaldehyde, the cell monolayers were found to be highly adherent, with no additional measures necessary.

A preliminary experiment was performed to determine the optimal cell seeding number and phospho-ERK antibody concentration for all subsequent assays (**Figure 5.3**). Cells were stimulated with HU-210 (1 μM) for 5 min, before fixation and immunocytochemical staining. A cell seeding density of 20,000 cells/well produced the largest magnitude response of all cell densities at all three antibody dilutions tested. Within this there was an increase in response magnitude

as antibody concentration decreased with a 1:800 dilution giving the largest response.

On the basis of these results, a cell seeding density of 20,000 cells/well and a phospho-ERK primary antibody dilution of 1:800 were chosen as optimal conditions for all subsequent experiments.

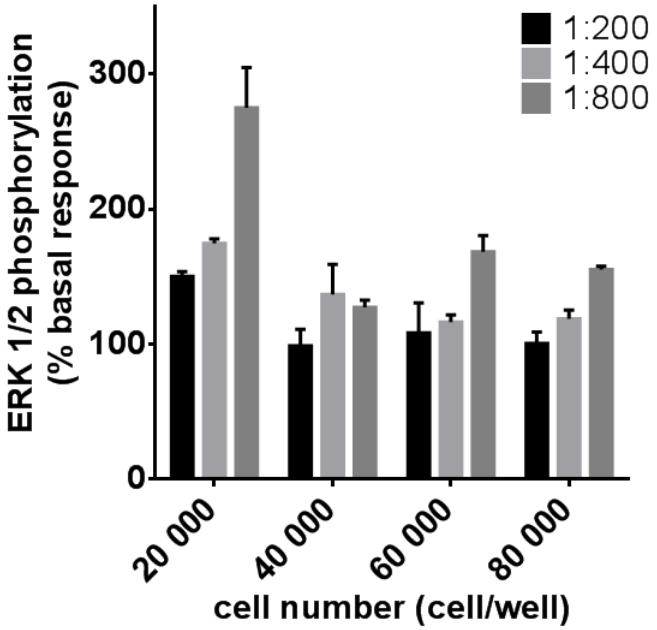

Figure 5.3 Optimisation of ERK phosphorylation assay in Neuro 2a cells. Cells (20, 40, 60 and 80 000 cells/well) were cultured in medium for 24 hr, followed by serum starvation for 24 hr. Cells were stimulated with HU-210 (1 µM) for 5 min, followed by rapid fixation with cold PFA solution (4 % w/v). Detection of total and phospho-ERK levels was as stated in methods (see **5.3.3**). Individual ERK phosphorylation values were normalised to the corresponding total-ERK values. The data shown represent a single experiment performed in quadruplicate and are given as mean ± SEM.

Effect of cannabinoid agonists on ERK phosphorylation – time course

Neuro 2a cells were treated with high concentrations of the cannabinoid agonists HU-210, CP 55,940 (both 1 μM), WIN 55,212-2, Δ^9-THC, anandamide, methanandamide, arachidonyl-2'-chloroethylamide (ACEA) and fenofibrate (all 10 μM) at various time point (2.5 – 90 min) to identify any differences in the agonists' temporal profile and to determine which time point would provide the maximum phospho-ERK response for use in concentration-response experiments. Addition of vehicle (assay buffer) was included as a negative control.

All agonists produced a rapid increase in phospho-ERK levels with the maximum response occurring between 5 and 10 min (**Figure 5.4**). After this time period the phospho-ERK levels for all agonists steadily decreased, reaching a constant, near-basal level at 45 min. There were clear patterns of partial agonism present with Δ^9-THC, anandamide and ACEA all producing smaller maximum responses than those of the representative full agonist HU-210. None of the agonists tested produced a noticeable second-phase response, up to 90 min.

On the basis of these results, an agonist stimulation period of 7.5 min was chosen for the subsequent concentration-response experiments.

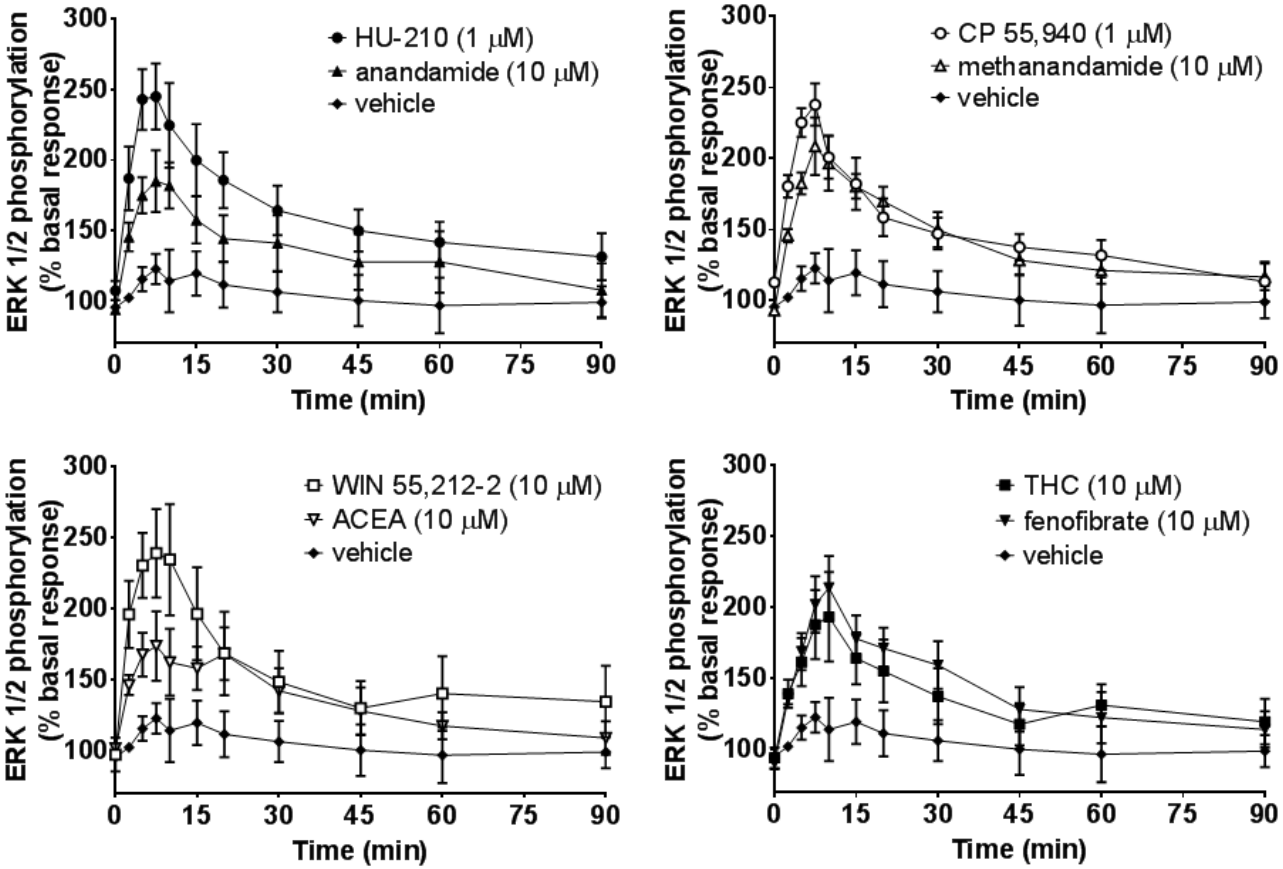

Figure 5.4 Effect of cannabinoid agonists on ERK phosphorylation in Neuro 2a cells over time. Cells (20,000 cells/well) were cultured in medium for 24 hr, followed by serum starvation for 24 hr. Cells were stimulated with cannabinoid agonists at various time points (2.5 - 90 min), followed by rapid fixation with cold PFA solution (4 % w/v). Detection of total and phospho-ERK levels was as stated in methods (see **5.3.3**). The data shown represents mean ± SEM values from five independent experiments performed in triplicate.

Effect of cannabinoid agonists on ERK phosphorylation – concentration response

All agonists produced a concentration-dependent increase in phospho-ERK levels (**Figure 5.5**). The rank order of pEC_{50} values of the agonists acting on Neuro 2a cells from highest to lowest was HU-210 ≥ CP 55,940 > WIN 55,212-2 ≥ Δ^9-THC > ACEA ≥ mAEA > AEA > fenofibrate (**Table 5.1**). There was no significant difference in the agonist R_{max} values (**Table 5.1**; one-way ANOVA; p>0.05).

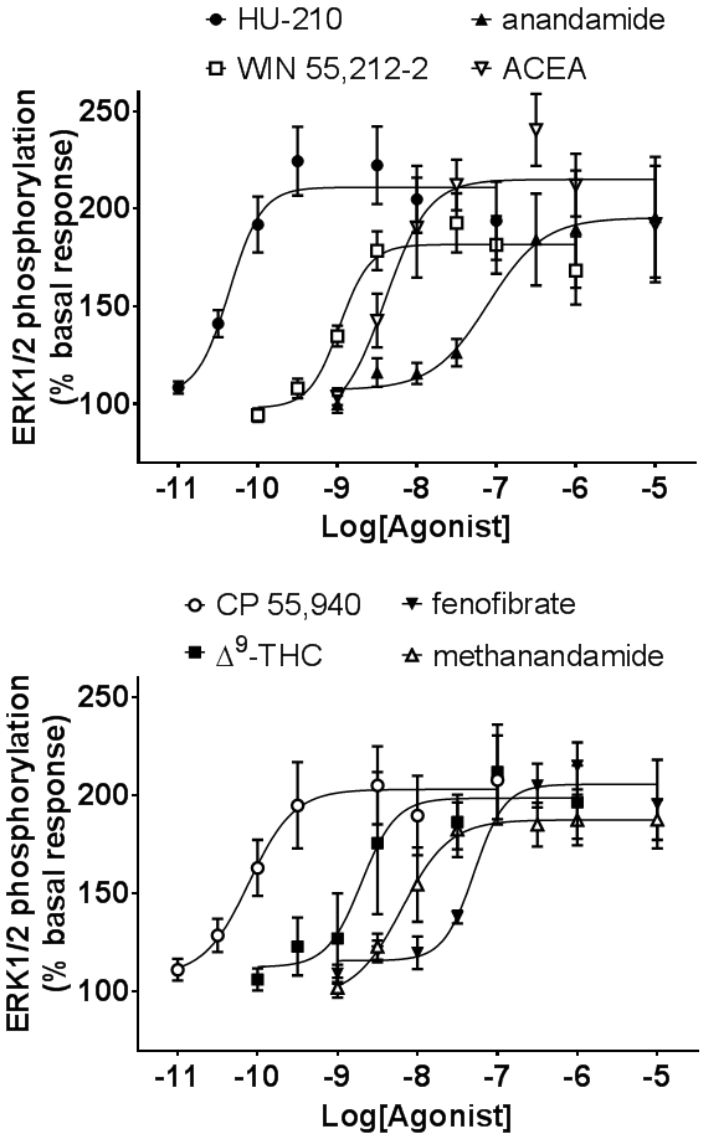

Figure 5.5 Effect of cannabinoid agonists on ERK phosphorylation in Neuro 2a cells. Cells (20,000 cells/well) were cultured in medium for 24 hr, followed by serum starvation for 24 hr. Cells were stimulated with various concentrations of cannabinoid agonists for 7.5 min, followed by rapid fixation with cold PFA solution (4 % w/v). Detection of total and phospho-ERK levels was as stated in methods (see **5.3.3**). Individual ERK phosphorylation values were normalised to the corresponding total-ERK values. The data shown represents mean ± SEM values from 4-5 independent experiments performed in triplicate. The curves were fitted using GraphPad Prism.

To confirm the role of the CB_1 receptor in the cannabinoid agonist responses, the concentration-response experiments were repeated in the presence of the CB_1-selective competitive antagonist AM 251 (10 nM). AM 251 produced a significant rightward shift of all the agonist concentration-response curves, resulting in significant decreases in all the pEC_{50} values (**Figure 5.6**). These data were used to estimate the equilibrium dissociation constant (pK_B) for AM 251 in the presence of each individual agonist (**Table 5.1**). There was no significant difference between the pK_B values, except for the value determined using Δ^9-THC, which was significantly greater than that determined using anandamide (one-way ANOVA; $p<0.01$).

Table 5.1

Determination of potency (pEC_{50}), maximal response, expressed as a % of the basal response (R_{max}), and estimated AM 251 dissociation constant (pK_B) of cannabinoid agonists on ERK phosphorylation in Neuro-2a cells.

Agonists	**pEC_{50}**	**R_{max} (% basal)**	**pK_B**
HU-210	10.3 ± 0.1	113 ± 17	9.4 ± 0.1
CP 55,940	10.0 ± 0.1	112 ± 23	9.6 ± 0.2
WIN 55,212-2	9.0 ± 0.1	86 ± 15	9.5 ± 0.4
Δ^9-THC	8.7 ± 0.2	96 ± 14	10.3 ± 0.1[a]
Anandamide	7.3 ± 0.4	107 ± 28	8.9 ± 0.2
Methanandamide	8.0 ± 0.2	85 ± 10	9.6 ± 0.1
arachidonyl-2'-chloroethylamide	8.2 ± 0.2	96 ± 8	9.5 ± 0.2
Fenofibrate	7.2 ± 0.1	98 ± 14	9.6 ± 0.1

Data shown are mean ± SEM values from 5 independent experiments performed in triplicate.

[a] Value significantly greater than that calculated using anandamide; one-way ANOVA with Dunnett's multiple comparisons test, $p<0.01$.

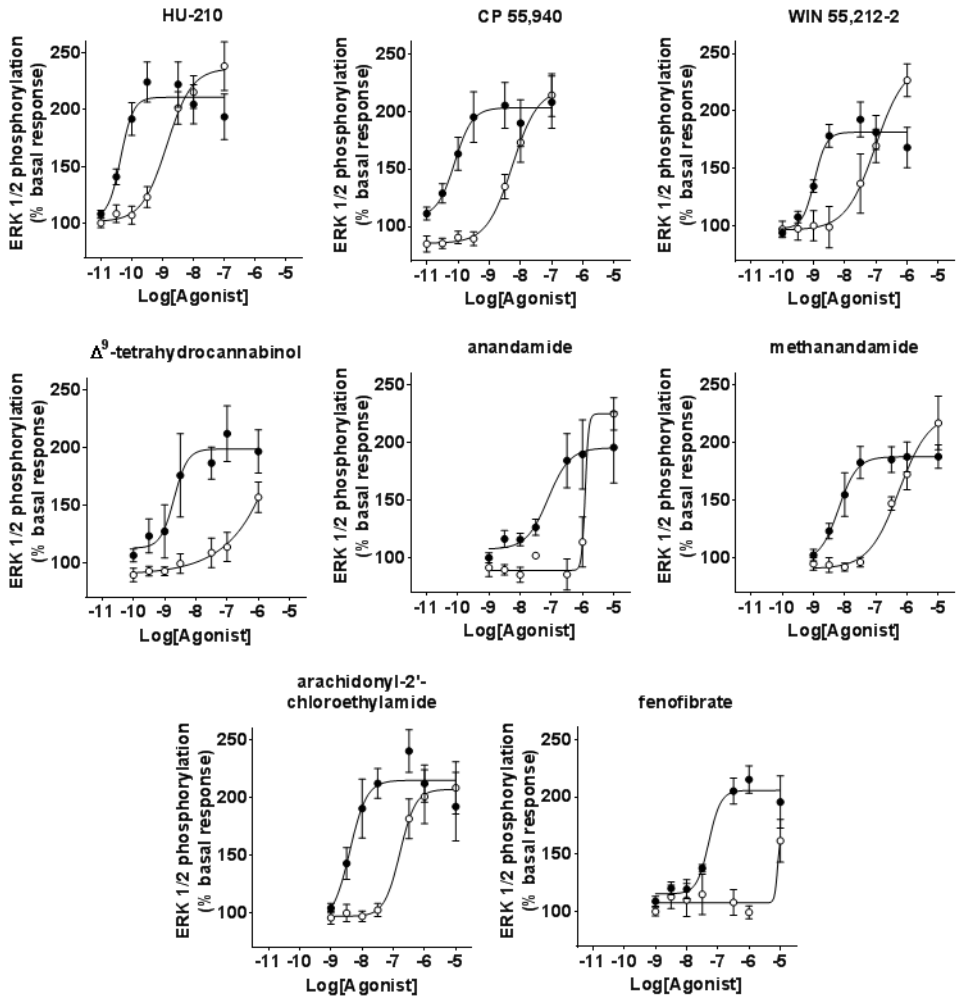

Figure 5.6 Effect of CB_1-selective antagonist AM 251 on cannabinoid agonists ERK phosphorylation concentration-response curves in Neuro 2a cells. Cells (20,000 cells/well) were cultured in medium for 24 hr, followed by serum starvation for 24 hr. Cells were pre-treated with AM 251 (○) or left untreated (●) for 10 min, followed by stimulation with various concentrations of cannabinoid agonists for 7.5 min, followed by rapid fixation with cold PFA solution (4 % w/v). Detection of total and phospho-ERK levels was as stated in methods (see **5.3.3**). Individual ERK phosphorylation values were normalised to the corresponding total-ERK values. The data shown represents mean ± SEM values from 4-5 independent experiments performed in triplicate. The curves were fitted using GraphPad Prism.

5.4.2. Determination of JNK1/2/3 phosphorylation

Assay Optimisation

A preliminary experiment was performed to determine the optimal phospho-JNK1/2/3 antibody concentration for all subsequent assays (**Figure 5.7**). Cells were stimulated with hydrogen peroxide (5 mM) at various time points (5 – 60 min), before fixation and immunocytochemical staining. Hydrogen peroxide produced an apparent continual increase in phospho-JNK levels. The magnitude of this response was greatest for 1:400 dilution of the primary phospho-JNK antibody, followed by 1:800 and then 1:200. On the basis of these results, a primary antibody dilution of 1:400 was chosen as optimal for all subsequent experiments.

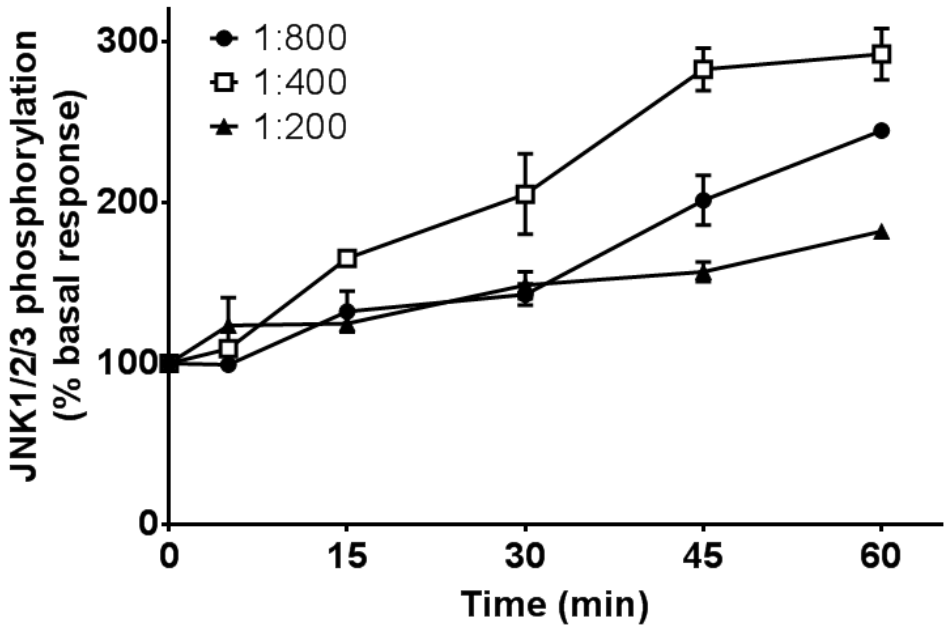

Figure 5.7 Optimisation of JNK1/2/3 phosphorylation assay in Neuro 2a cells. Cells (20,000 cells/well) were cultured in medium for 24 hr, followed by serum starvation for 24 hr. Cells were stimulated with hydrogen peroxide (5 mM) for various time points (5 - 60 min), followed by rapid fixation with cold PFA solution (4 % w/v). Detection of total and phospho-JNK levels was as stated in methods (**see 5.3.3**), with 1:200 (▲), 1:400 (□) and 1:800 (●) dilution of the primary phospho-JNK antibody tested. Individual JNK phosphorylation values were normalised to the corresponding total-JNK values. The data shown represent a single experiment performed in quadruplicate and are given as mean ± SEM.

Effect of cannabinoid agonists on JNK phosphorylation – time course

As in the optimisation experiment, the positive control hydrogen peroxide was able to significantly increase phospho-JNK levels in Neuro 2a cells from 5 min onwards (**Figure 5.8**; one way ANOVA; $p<0.05$). None of the cannabinoids tested was able to elicit a phospho-JNK response which was either significantly different from the basal phospho-JNK levels, or significantly different from the vehicle control (**Figure 5.8**; one-way ANOVA; $p>0.05$).

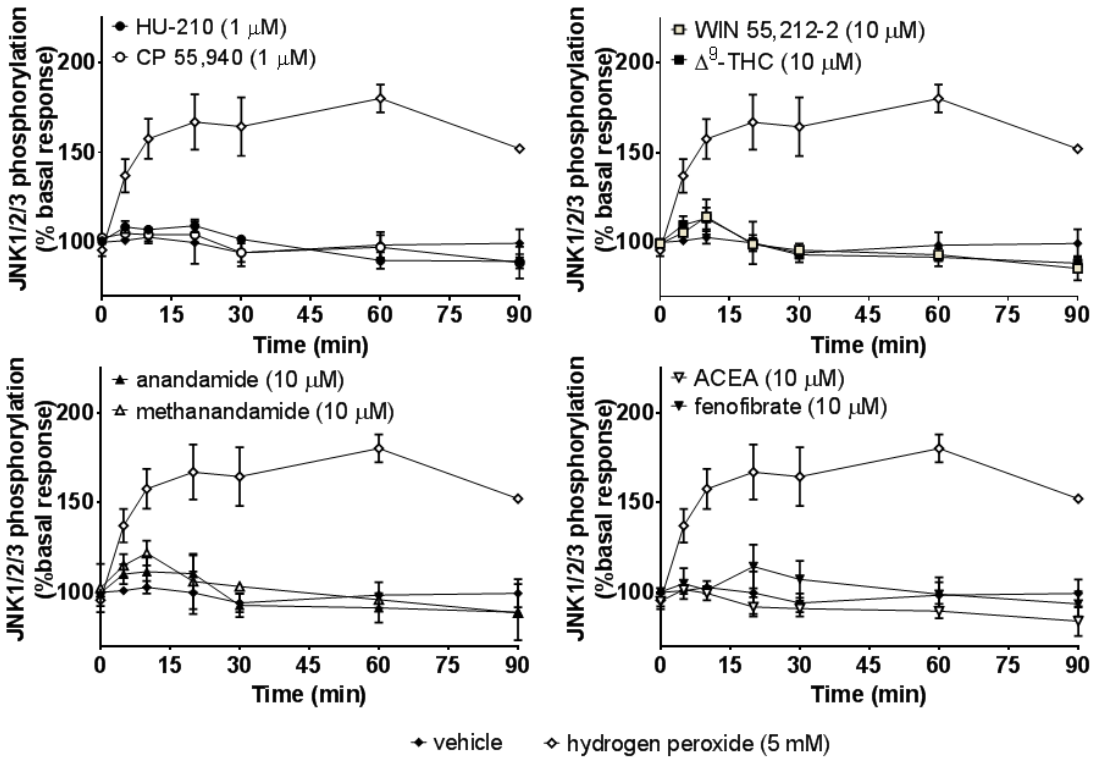

Figure 5.8 Effect of cannabinoid agonists on JNK phosphorylation in Neuro 2a cells against time. Cells (20,000 cells/well) were cultured in medium for 24 hr, followed by serum starvation for 24 hr. Cells were stimulated with cannabinoid agonists at various time points (5 - 60 min), followed by rapid fixation with cold PFA solution (4 % w/v). Detection of total and phospho-JNK levels was as stated in methods (see **5.3.3**). The data shown represents mean ± SEM values from four independent experiments performed in triplicate.

5.4.3. Determination of STAT3 phosphorylation

Assay Optimisation

A preliminary experiment was performed to optimise the phospho-STAT3 antibody concentration for all subsequent assays. Cells were stimulated with foetal bovine serum (FBS; 10 % v/v) for 5 min before fixation and immunocytochemical staining. FBS produced an apparent increase in phospho-STAT3 levels, relative to the basal. The magnitude of this response was greatest with the 1:50 dilution of the phospho-STAT3 antibody, and decreased as the antibody concentration decreased. On the basis of these results, a primary phospho-STAT3 antibody dilution of 1:50 was chosen as optimal for all subsequent experiments.

One technical issue with the assay was the lack of discernible difference between the basal phospho-STAT3 levels and the non-specific binding (NSB) of the secondary antibody (i.e. binding of secondary antibody in the absence of the phospho-STAT3 primary antibody), at even the highest primary antibody concentration, as shown in **Figure 5.9**. This indicates that the basal phospho-STAT3 levels are below the sensitivity range of the assay. In some instances, subtraction of the mean NSB values from the datasets, as stated in **Methods** (see **5.3.3.**), resulted in non-representative negative values. For this reason, the NSB for the phospho-STAT3 results was not subtracted from the other data as part of the data analysis.

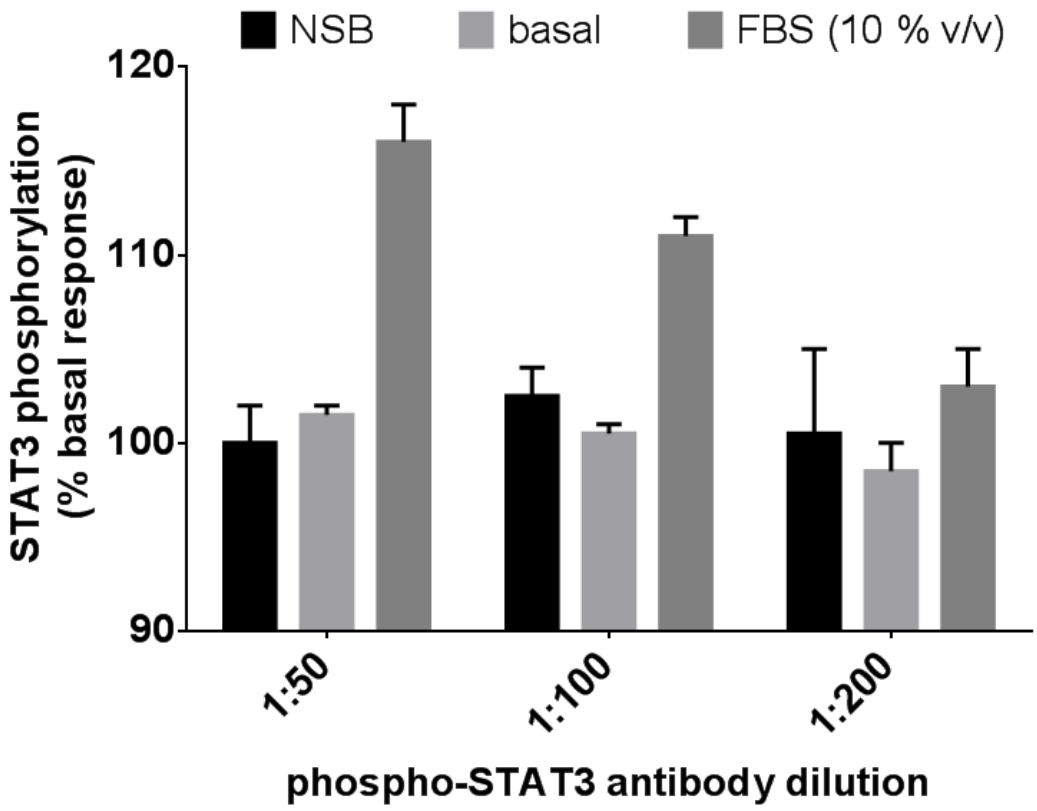

Figure 5.9 Effects of FBS on STAT3 phosphorylation in Neuro 2a. Cells (20,000 cells/well) were cultured in medium for 24 hr, followed by serum starvation for 24 hr. Cells were stimulated with foetal bovine serum (10 % v/v) for 5 min, followed by rapid fixation with cold PFA solution (4 % w/v). Detection of total and phospho-STAT3 levels was as stated in methods with various primary phospho-STAT3 antibody dilutions tested (**see 5.3.3**). The data shown represent a single experiment, performed in quadruplicate and are given as mean ± SEM.

Effect of cannabinoid agonist HU-210 on STAT3 phosphorylation – time course

The positive control FBS produced a rapid increase in the phospho-STAT3 levels, reaching a maximum response at 5 min, and steadily decreasing to return to a basal plateau from 60 min onwards (**Figure 5.10**). HU-210 was unable to produce a marked change in phospho-STAT3 levels over the same time course. Due to the

prohibitively high primary antibody concentration needed for a functional assay, and given that HU-210 appeared to have no effect on phospho-STAT3 levels, no additional cannabinoid agonist was tested for STAT3 activation.

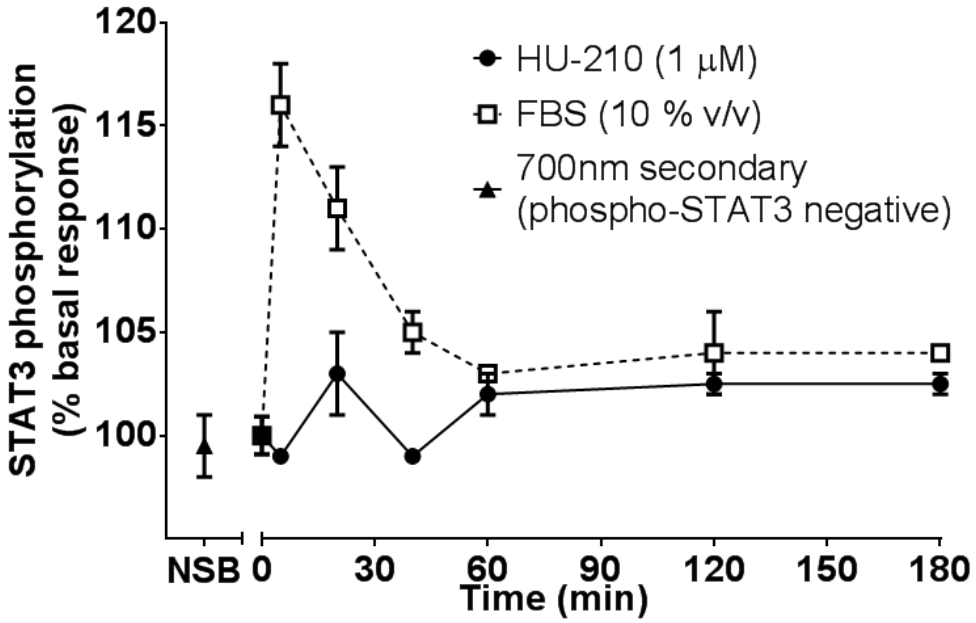

Figure 5.10 Effect of HU-210 on STAT3 phosphorylation in Neuro 2a cells against time. Neuro 2a cells (20,000 cells/well) were cultured in medium for 24 hr, followed by serum starvation for 24 hr. Cells were stimulated with foetal bovine serum (10 % v/v) or HU-210 (1 μM) at various time points (5 – 180 min), followed by rapid fixation with cold PFA solution (4 % w/v). Detection of total and phospho-STAT3 levels was as stated in methods (**see 5.3.3**). The data shown are given as mean ± SEM.

5.4.4. Determination of agonist effects on intracellular cAMP levels

Assay Optimisation

A preliminary experiment was performed to determine the optimal cell seeding density and concentration of forskolin for use in subsequent assays (**Figure 5.11**).

Forskolin produced a concentration-dependent increase in intracellular cAMP levels at all cell seeding densities tested. The span of the forskolin concentration-response markedly increased as the cell number was increased from 5,000 to 10,000 cells/well, while there appeared to be no apparent difference in the curve spans between 10, 20 and 40,000 cells/well. There was no apparent effect of the cell number on the concentration-response curve pEC_{50} values.

On the basis of these results, a cell seeding density of 10 000 cells/well and a forskolin concentration of 10 µM, as corresponding to the pEC_{80}, were chosen as optimised conditions for all subsequent experiments.

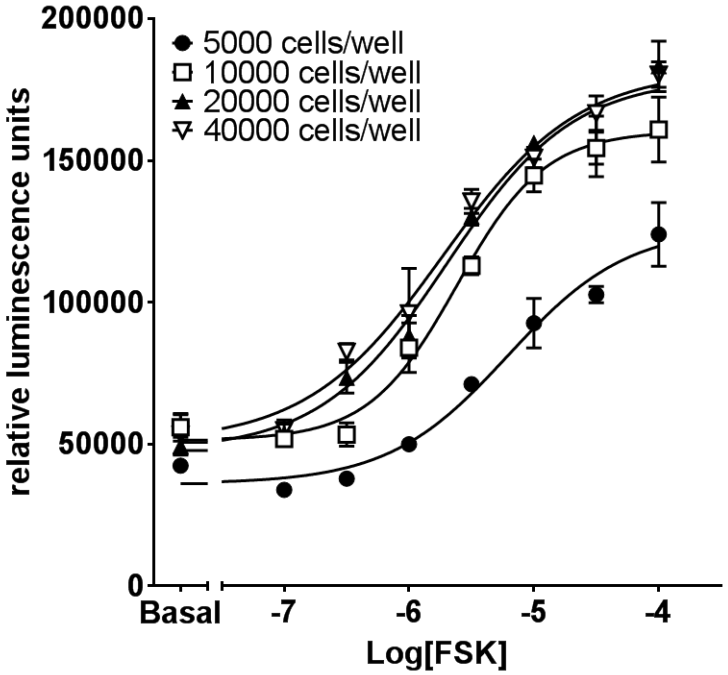

Figure 5.11 Optimisation of the cAMP assay in Neuro-2a cells. Cells (5, 10, 20 and 40 000 cells/well) in suspension in serum-free medium were pre-treated with the phosphodiesterase inhibitor rolipram for 10 min before incubation with increasing concentrations of forskolin (0.1 – 100 µM) for 30 min at room temperature. At the end of the incubation period, the assay was terminated by the addition of lysis buffer and the relative levels of cAMP determined using the HitHunter assay kit. The data shown represents a single experiment performed in triplicate, and are shown as mean ± SEM. The curves were fitted using GraphPad Prism.

Inhibition of forskolin-stimulated cAMP accumulation

Neuro 2a cells, treated with forskolin and the phosphodiesterase PDE4 inhibitor rolipram (both 10 µM), were stimulated with increasing concentrations of the cannabinoid agonists to determine the ability of these compounds to inhibit forskolin-stimulated cAMP accumulation (**Figure 5.12**). HU-210, CP 55,940,

WIN 55,212-2, anandamide and ACEA produced concentration-dependent decreases in cAMP accumulation, while Δ^9-THC, methanandamide and fenofibrate had no apparent effect with GraphPad Prism software unable to fit concentration-response curves to these data.

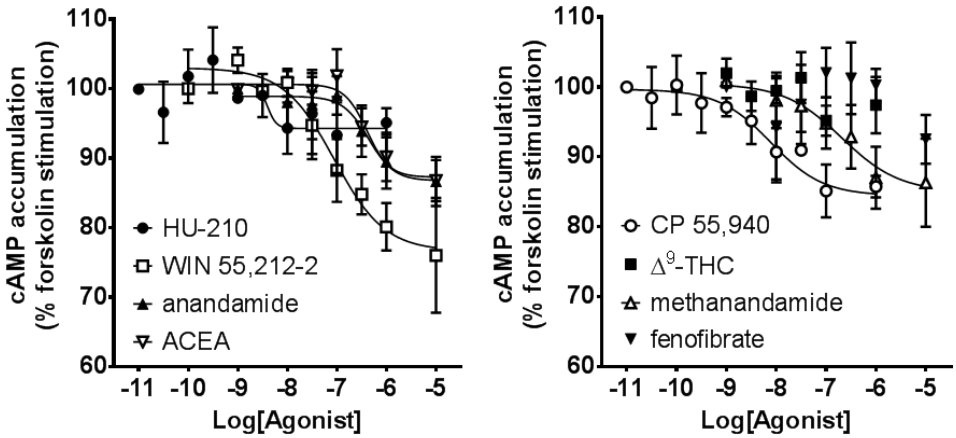

Figure 5.12 Effect of cannabinoid agonists on cAMP accumulation in Neuro 2a cells. Cells in suspension in serum-free medium were pre-treated with forskolin and rolipram (both 10 μM) for 10 min before incubation with increasing concentrations of cannabinoid agonists (see figure legend for list) for 30 min at room temperature. At the end of the incubation period, the assay was terminated by the addition of lysis buffer and the relative levels of cAMP determined using the HitHunter assay kit. The data shown represent mean ± SEM values from 4-6 individual experiments performed in triplicate. The curves were fitted using GraphPad Prism.

The rank order of potency (pEC_{50}) of the agonists which are able to inhibit cAMP accumulation from highest to lowest was CP 55,940 ≥ HU-210 > WIN 55,212-2 > ACEA ≥ anandamide (**Table 5.2**). The R_{max} of WIN 55,212-2 was significantly

greater than all the other agonists except CP 55,940, (**Table 5.2**; one-way ANOVA; $p<0.05$) while the R_{max} values for the other agonists were not significantly different from each other.

Table 5.2

Determination of potency (pEC_{50}) and percentage of basal maximal response (R_{max}) of cannabinoid agonists on Neuro-2a cells measuring inhibition of forskolin-stimulated cAMP accumulation

Agonists	**pEC_{50}**	**R_{max}**
HU-210	7.9 ± 0.1	10 ± 1
CP 55,940	8.1 ± 0.2	15 ± 2
WIN 55,212-2	7.1 ±0.2	20 ± 4[b]
Δ^9-THC	[a]	[a]
Anandamide	6.3 ± 0.1	13 ± 3
Methanandamide	[a]	[a]
arachidonyl-2'-chloroethylamide	6.5 ± 0.2	12 ± 1
Fenofibrate	[a]	[a]

Data shown are mean ± SEM values from 5 independent experiments performed in triplicate.

[a] It was impossible to determine values for these parameters using GraphPad Prism.

[b] Value significantly greater than that for all other agonists, except CP 55,940.

Effect on cAMP accumulation in pertussis toxin-treated cells

Neuro 2a cells, treated overnight (16-18 hr) with pertussis toxin, which inhibits $G_{i/o}$ protein function, were stimulated with increasing concentrations of the cannabinoid agonists to determine the potential ability of these compounds to increase, rather than inhibit cAMP accumulation (**Figure 5.13**). Forskolin produced a concentration-dependent increase in cAMP levels (**Figure 5.13A**).

Interestingly, the pEC_{50} for forskolin in the PTX-treated cells was markedly lower than compared to in the untreated cells (PTX – 4.9 ± 0.1; untreated – 5.6 ± 0.1). None of the cannabinoid agonists tested produced any significant effect on the cAMP levels (**Figure 5.13B**). High concentrations of some agonists, particularly anandamide and ACEA, were able to produce an increase in cAMP levels of around 5 % of the forskolin stimulated response, however as stated, these were not significantly greater than the basal.

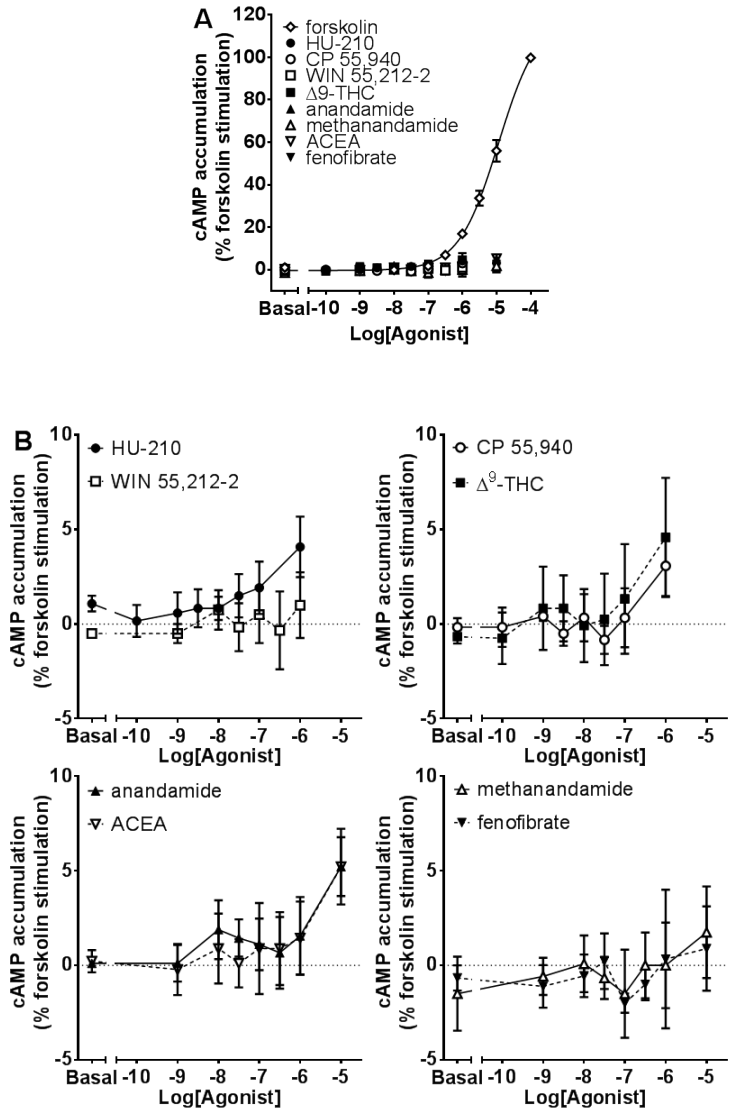

Figure 5.13 Effect of forskolin (A) and cannabinoid agonists (B) on cAMP accumulation in Neuro 2a cells cultured with PTX (100 ng/ml). Cells in suspension in serum-free medium were pre-treated with rolipram (both 10 µM) for 10 min before incubation with increasing concentrations of cannabinoid agonists for 30 min at room temperature. At the end of the incubation period, the assay was terminated by the addition of lysis buffer and the relative levels of cAMP determined using the HitHunter assay kit. The data shown represent mean ± SEM values from four individual experiments performed in triplicate. The curves were fitted using GraphPad Prism.

5.4.5. Analysis of agonist bias

To quantify the agonist bias present at the Neuro 2a CB_1 receptor, intrinsic relative activity (RA_i) values were calculated for the agonists HU-210, CP 55,940, WIN 55,212-2, AEA and ACEA for both the ERK and cAMP responses (**Figure 5.14**). The RA_i values were estimated using WIN 55,212-2 as the reference agonist, as opposed to the endogenous ligand anandamide, as it was the only agonist to produce a clear response from which to derive curve parameters in all individual experiments. The RA_i value for HU-210 ERK response was significantly greater than that for the HU-210 cAMP response with a ΔRA_i value of 12.8 (**Figure 5.14**; unpaired, two-tailed *t*-test; $p<0.05$), whereas there was no significant difference between the two values for the other agonists.

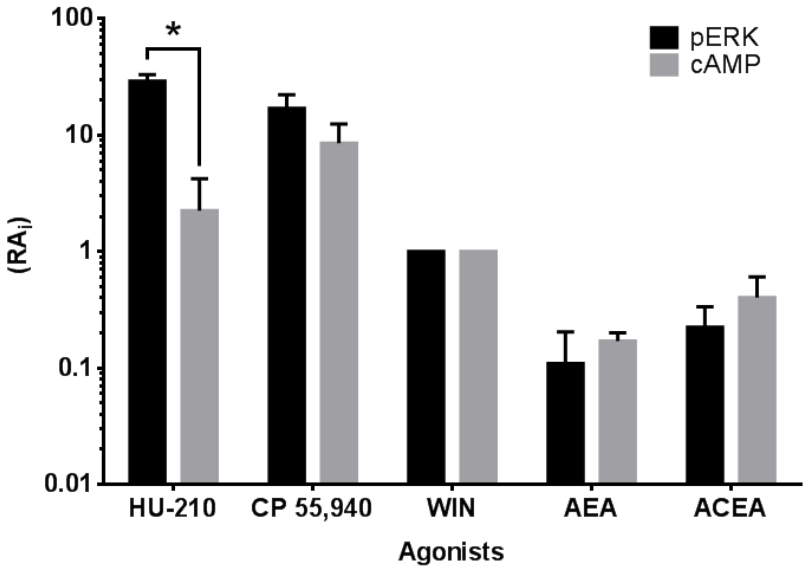

Figure 5.14 Comparison of the RAi values of cannabinoid agonists modulating ERK and cAMP responses in Neuro 2a cells via CB_1 receptors. The data shown represent mean ± SEM values from 5-6 individual experiments performed in triplicate. Statistical significance was determined using unpaired, two-tailed *t*-test; *$p<0.05$.

5.5. Discussion

Neuro 2a cells are a murine neuroblastoma cell line which has been previously shown to express the CB_1 cannabinoid receptor using both PCR analysis and immunocytochemistry, which in turn has been shown to couple to at least two distinct intracellular signalling pathways. This provides an attractive model to test the concept of functional selectivity at the CB_1 receptor, by measuring CB_1-mediated responses to a range of cannabinoid agonists.

The first intracellular mediators to be investigated were the extracellular signal-regulated kinases or ERK, a family of mitogen-activated protein kinases which regulate numerous cellular responses, including gene expression, growth, cellular transformation and apoptosis (Pearson *et al.*, 2001). Initial testing showed that HU-210 was clearly able to promote ERK phosphorylation after 5 minutes of stimulation with optimised conditions for cell number and primary phospho-ERK antibody dilution determined. These results are in keeping with previous reports which showed HU-210-mediated ERK phosphorylation in Neuro 2a cells (Graham *et al.*, 2006; Zorina *et al.*, 2010). It is of note that these results are the first published example of quantification of cannabinoid-mediated ERK signalling in Neuro 2a cells using the In-Cell Western technique, as most previously reported studies utilised Western blotting to measure phosphorylated protein levels. Subsequent time course experiments using HU-210 and the other cannabinoid agonists CP 55,940, WIN 55,212-2, Δ^9-THC, anandamide, methanandamide, ACEA and fenofibrate showed that all were able to promote ERK phosphorylation. The temporal profiles for all agonists tested were similar to each other, as well as generally consistent with those reported in other results chapters

for receptors expressed in CHO and HEK cell lines, i.e. phospho-ERK levels increased rapidly upon stimulation with agonist, reaching a peak between 5 – 10 mins, after which they steadily returned to near basal levels after 45 min. The results for HU-210 were also consistent with those reported by Graham *et al.* (2006), which showed a maximum response reached after 5 - 10 min and with subsequently decreased phospho-ERK levels at 20 and 40 min. However, in contrast to our findings, a report from Zorina *et* al. (2010) at Mount Sinai School of Medicine indicated an initial-phase maximum HU-210-mediated phospho-ERK response at 50 min. These differences may be due to different experimental technique, or use of different subclones of the Neuro 2a cell line.

All agonist-mediated phospho-ERK responses were clearly shown to be concentration-dependent, with a rank order of potency consistent with previously reported findings at the murine receptor (Govaerts *et al.*, 2004) and with that reported in previous results chapters in this thesis for human receptors expressed in other cell lines. It is noteworthy, however, that the absolute potency values were higher for the Neuro 2a receptor compared to the cannabinoid ERK responses at the transfected CHO human receptor. This is consistent with reports by Govaerts *et al.* (2004), which show the affinity of cannabinoid ligands HU-210, CP 55,940 and WIN 55,212-2 at the murine CB_1 receptors, as determined by [^{3}H]-CP 55,940 binding assay, to be around ten times greater than that reported for the human receptor determined using the same assay. Only one previous example of a HU-210 concentration response curve for ERK phosphorylation in Neuro 2a cells has been reported in the literature (Rozenfeld *et al.*, 2012), with a reported EC_{50} of 0.43 ± 0.01 nM, which corresponds very closely to our calculated value of 0.40 ±

0.01 nM. The response curves for the other agonists are, as far as can be ascertained, the first ones reported in the literature for this cell line. No pattern of partial agonism could be clearly identified, with no significant difference between the agonist R_{max} values, in contrast with the clear pattern of partial agonism present in the time course experiments, particularly for Δ^9-THC, anandamide and ACEA. This observation is most likely due to variance caused by using a relatively low concentration of phospho-ERK antibody (see In-cell western optimisation, **3.4.2.1**), something which is unavoidable as this concentration of antibody is needed to obtain results with a useable signal: basal ratio. The CB_1-selective antagonist AM 251, was able to produce a significant rightwards shift of all agonist concentration/ response curves, clearly indicating that the responses are CB_1-receptor mediated validating the cell line for use in our study of functional selectivity at an endogenously-expressed CB_1 receptor population.

The next signalling pathway to be investigated was the c-Jun N-terminal kinases or JNK, a second family of MAP kinases which typically responds to stress stimuli including inflammatory cytokines, UV radiation, heat shock and ROS. Addition of hydrogen peroxide, a noxious stimulant and ROS at high concentrations produced a clear phospho-JNK response, demonstrating that the activation of this signalling pathway is possible in the Neuro 2a cell line. All of the cannabinoid agonists tested failed to elicit a phospho-JNK response up to 90 min stimulation, which is in agreement with Graham *et al*. (2006) who also reported no change in phospho-JNK levels upon stimulation with HU-210 over 5 – 40 min, determined using both immunocytochemistry and Western blotting. However, this is in stark contrast to reports by He *et al.* (2005) at Mount Sinai

School of Medicine (NY, USA), which reported a clear increase in phospho-JNK1/2 levels after 30 min treatment with HU-210. As suggested in the introduction to this chapter, these differences in results may be due to the use of different subclones of the Neuro 2a cell line, leading to putative differences in protein expression and ability of the receptor to couple to the JNK signalling pathway.

The final protein phosphorylation pathway measured was for signal transducer and activator of transcription 3 or STAT3, a transcription factor which regulates cell processes including growth and apoptosis (Qi & Yang, 2014). Treatment with foetal bovine serum (FBS) produced a rapid increase in phospho-STAT3 levels with a maximum response at 5 min, returning steadily to near basal levels from 60 min onwards, demonstrating the activation of this signalling pathway in the Neuro 2a cell line. HU-210 was unable to produce a clear phospho-STAT3 response up to 180 min. This is in contrast to several reports, again from Mount Sinai School of Medicine, which provide clear examples of HU-210-CB_1-mediated STAT3 phosphorylation in Neuro 2a cells (He *et al.*, 2005; Rios *et al.*, 2006; Zorina *et al.*, 2010). The most likely reason for this difference is the use of phenotypically divergent subclones of the Neuro 2a cell line. It is important to note the technical issues encountered when performing these assays. First, the optimised phospho-STAT3 primary antibody dilution was 1:50, which is prohibitively high for use in multiple experiments. The antibody was chosen for use on the recommendation from colleagues at the University of Nottingham who are experienced in measuring STAT3 phosphorylation in other cell models (Palmer, personal communication, 2013). Also, as noted in **Results** (see **5.4**), there was no clear

difference in the basal level of phospho-STAT3 and the non-specific binding of the relevant secondary antibody, which indicates that basal levels of phospho-STAT3 are below the sensitivity range of the assay. So, while the FBS response clearly validates the use of the assay technique, any subsequent work would be better done using an alternative assay method, such as Western blotting or a STAT3 luciferase reporter.

The CB_1 receptor is well known to couple to $G_{i/o}$ proteins which, among other functions, inhibit the activity of the enzyme adenylyl cyclase (AC), an effect which can be observed by measuring changes in intracellular cAMP levels. Examples in the literature of $G_{i/o}$-coupled receptor modulation of cAMP accumulation in Neuro 2a cells include transfected μ- (Chakrabarti *et al.*, 1995b) and δ-opioid receptors (Zhang *et al.*, 2006). Stimulation of Neuro 2a cells with forskolin, which directly activates AC, produced a concentration-dependent increase in intracellular cAMP accumulation. Treatment with the cannabinoid agonists HU-210, CP 55,940, WIN 55,212-2, anandamide and ACEA, but not the other agonists produced a clear inhibition of FSK-stimulated cAMP accumulation. This contrasts strongly with the results for ERK phosphorylation where all agonists were able to activate the signalling pathway. The rank order of potency of these agonists is generally consistent with previous reports, though for all agonists the absolute pEC_{50} values were markedly lower than those for ERK phosphorylation ranging from anandamide which was 10-fold less potent, to CP 55,940 which was 80-fold les potent. In terms of efficacy, all of the agonists produced only modest effects, with WIN 55,212-2 being most efficacious with an R_{max} value of 20 ± 4 % inhibition of cAMP accumulation, which was significantly

greater than those of all other agonists, except CP 55,940. This contrasts with the results for ERK phosphorylation for which there was no significant difference in the agonist R_{max} values. These relatively modest responses also contrast with results from previous chapters looking at effects of the same agonists on transfected human CB receptors in different cell lines and with the examples of $G_{i/o}$-coupled receptor modulation of cAMP accumulation in Neuro 2a cells, mediated via transfected μ- and δ-opioid receptors which both produced inhibitions of about 60 % (Chakrabarti *et al.*, 1995b; Zhang *et al.*, 2006). This is probably due to weak coupling of this endogenous receptor to AC and the expected smaller receptor population compared to that of transfected over-expressed receptors.

Finally, the effect of pertussis toxin on CB_1 receptor modulation of cAMP accumulation was investigated. Several reports in the literature on both transfected (Felder *et al.*, 1998), and endogenously expressing neuronal cells (Glass & Felder, 1997), in addition to results in this thesis clearly demonstrate that CB_1 receptor coupling can be switched to G_s protein by inhibiting $G_{i/o}$ protein function with PTX. G_s protein activates AC, resulting in increases in intracellular cAMP levels. There is at least one example of endogenous receptor coupling to G_s protein in Neuro 2a cells, with treatment with prostaglandin E1 elevating cAMP levels, most likely via G_s-coupled EP2 or 4 receptors (Wu *et al.*, 1996). Forskolin produced a concentration-dependent increase in intracellular cAMP levels in PTX-treated Neuro 2a cells; however none of the agonists produced a significant change in basal cAMP levels, demonstrating negligible CB_1 receptor coupling to G_s protein.

Analysis of the data indicates that Δ^9-THC, methanandamide, and fenofibrate are biased towards ERK phosphorylation versus inhibition of cAMP accumulation as these compounds failed to elicit a response in the cAMP assay. It is difficult to ascertain whether this is due to a complete inability of the agonist-receptor complex to couple to the signalling pathway, or whether the agonists are partial to the point of being beyond the sensitivity of the detection assay, a phenomenon known as 'observational bias' (Kenakin & Christopoulos, 2013a). For those agonists which gave measurable responses for both pathways, the bias can be quantified and statistically analysed by comparing the estimated intrinsic relative activity (RA_i) for each agonist at each pathway. The significant differences between RA_i for a single agonist, termed ΔRA_i, demonstrate bias of that agonist for one pathway over another, while differences in ΔRA_i values between agonists demonstrate their functional selectivity relative to each other. HU-210, but not the other agonists, exhibited significant bias towards ERK versus cAMP signalling as indicated by its significantly greater ERK RA_i value.

5.6. Conclusions

The results in this chapter clearly demonstrate that cannabinoid agonists are able to modulate ERK and AC in Neuro 2a cells via endogenously expressed CB_1 receptors. Furthermore, activation of these signalling pathways appears to exhibit clear agonist bias.

Chapter 6

General Discussion

6.1. General discussion

The main aim of this project was to identify any patterns of functional selectivity at the cannabinoid type 1 (CB_1) receptor, expressed in a number of different cell types. While many examples of functionally selective signalling at the CB_1 receptor exist, prior to the initiation of this project no comprehensive studies existed looking at a variety of signal transduction pathways in a single cell type.

Prior to the start of full scale characterisation of cannabinoid receptor signalling in the cells, advantage was taken of recent in-house observation that fenofibrate represented a novel structural family of cannabinoid ligands. Fenofibrate was shown to be a cannabinoid receptor agonist, being moderately (~25-fold) CB_2 receptor-selective. Further testing demonstrated that fenofibrate was able to inhibit electrically-evoked smooth muscle contraction in isolated guinea-pig ileum in an AM 251-sensitive manner, confirming that fenofibrate is indeed a functional CB_1 receptor agonist, albeit within a restricted concentration range. The characterisation of fenofibrate as an example of a new class of cannabinoid receptor ligands is of great importance to our understanding of CB_1 receptor pharmacology as functional selectivity is most readily identified when comparing the responses to structurally distinct agonists. This is true of the CB_1 receptor, where the aminoalkylindole WIN 55,212-2 exhibited bias towards G_s and G_q protein coupling, when compared to structurally unrelated agonists (Bonhaus *et al.*, 1998; Lauckner *et al.*, 2005), while the classical ligand HU-210, and the non-classical ligand CP 55,940 exhibited reciprocal ERK and JNK activation in N1E-115 cells (Bosier *et al.*, 2008). Indeed, fenofibrate exhibited bias towards ERK signalling versus inhibition of cAMP accumulation in transfected HEK-hCB_1

cells. As a commonly prescribed drug for the treatment of hyperlipidemia, fenofibrate has an extensively characterised tolerability profile. This point, in combination with our results, means fenofibrate represents a very real basis for the generation of new, functionally selective drug-like compounds targeting cannabinoid receptors. To this end, current and future research within the University of Nottingham will aim to generate homologous compound series based on fenofibrate in an effort to produce compounds of greater receptor and pathway selectivity.

In addition to its action as an orthosteric agonist, as demonstrated by competitive inhibition with the orthosteric antagonist AM 251, fenofibrate appeared to act as a negative allosteric modulator of the CB_1 receptor at high concentrations (above 3 μM). These seemingly contradictory results can be explained by the theory of 'bitopic ligands'- molecules that exhibit concomitant interaction with the orthosteric and allosteric sites on a single GPCR (Lane *et al.*, 2013). Important future work would be to perform a SAR study on fenofibrate, in an effort determine whether or not distinct pharmacophores are responsible for these distinct effects.

Three cell lines were used in the investigation of functional selectivity at the CB_1 receptor - Chinese hamster ovary cells and human embryonic kidney cells, both transfected with the human CB_1 receptor, and the murine neuroblastomal Neuro 2a cell line, which endogenously expressed the mouse variant of the CB_1 receptor. All three cell lines have previously been used to study cannabinoid receptor signalling, including several reports of functionally selective agonist responses

(Bonhaus *et al.*, 1998; He *et al.*, 2005; Lauckner *et al.*, 2005). All three cell lines exhibited CB_1 receptor-mediated ERK activation, represented by an increase in phosphorylated ERK levels. This response has previously been observed in a number of cell types, including transfected CHO and HEK cells (Galve-Roperh *et al.*, 2002; Daigle *et al.*, 2008), and endogenously expressing U373MG human astrocytoma (Bouaboula *et al.*, 1995), Neuro 2a and murine neuroblastomal N1E-115 cells (Graham *et al.*, 2006; Bosier *et al.*, 2008), as well as in a number of cell and tissue types *in vivo* (Valjent *et al.*, 2001). These reports, combined with our observations, indicate that CB_1 receptor coupling to ERK is probably a ubiquitous signalling pathway. While the nature of the initial ERK response was generally consistent in all three cell lines i.e. a rapid, transient increase in phospho-ERK levels with a broadly similar pattern of potency and efficacy, there were some noticeable differences. First, temporally distinct $G_{i/o}$ protein-dependent and independent ERK activation were observed in the HEK cells, while the ERK responses in the CHO cells were found to be wholly $G_{i/o}$ protein-dependent. A hypertonic concentration of sucrose, which inhibits clathrin lattice formation inhibited $G_{i/o}$ protein-independent ERK activation in HEK cells – clathrin lattice formation is a necessary component of β-arrestin–mediated receptor internalisation, which in turn is an important step for β-arrestin-mediated signalling. While these results indicate a potential role for β-arrestin in this ERK response, other mechanisms could not be definitively excluded. Future experiments using siRNA, or dominant negative variants of the β-arrestin protein to inhibit its normal function will allow us to unequivocally determine the role of β-arrestin in CB_1 receptor signalling in this model. Activation of G protein and β-arrestin-dependent signalling has previously been shown for a number of GPCRs,

and has real therapeutic implications. A good example is the mu-opioid receptor, where G_i protein signalling is required for morphine antinociception, while β-arrestin-2 blockade has been shown to improve morphine-mediated analgesia and inhibit the development of analgesic tolerance (Al-Hasani & Bruchas, 2011). Such a scenario may exist with the CB_1 receptors, with G protein and β-arrestin signalling having contrasting effects on receptor-mediated effects, such as analgesia. As an example, WIN 55,212-2 is moderately biased towards the $G_{i/o}$ protein-independent signalling, meaning it may be unsuitable as a therapeutic if the aim to limit non-$G_{i/o}$ protein dependent responses, such as β-arrestin signalling.

Next, it was clear that all three cell lines exhibited CB_1 receptor-dependent inhibition of cAMP accumulation, with again broadly similar patterns of potency and efficacy. However, only the HEK cells demonstrated an increase in cAMP levels in the presence of PTX, most likely mediated by receptor activation of G_s protein. At first glance these differences in signalling between the three cell lines seems counter-intuitive, given that the series of agonists being tested and the receptor-coupled signalling pathways are the same in all three. However each cell line has a distinct pattern of protein expression, with the stoichiometry between the receptor and the signal transduction mediators dependent on the cell type. This in turn determines the ability of the receptor to couple to a certain signalling pathway in a cell line. To illustrate this point, a study by Atwood *et al*. (2011), which used microarray analysis to compare the expression of GPCRs, and associated proteins, mRNA in a number of commonly used cell lines, including HEK cells, showed significant differences in the relative expression levels of various G protein, AC, protein kinase, GRK and β-arrestin subtypes between the

cell lines. Furthermore, the differences in signalling between the three cell lines can be seen as representative of the expected cell-dependent nature of receptor signalling *in vivo*. These points highlight the importance of choosing a cell model appropriate to the target tissue type, when investigating receptor pharmacology, particularly functional selectivity.

These differences between the cell lines were also present when comparing the patterns of agonist bias, determined using the relative intrinsic activity values. Both WIN 55,212-2 and ACEA exhibited bias towards ERK activation after 5 min agonist stimulation, when compared to inhibition of cAMP accumulation. In addition, however, anandamide exhibited the same ERK bias in CHO cells only, while Δ^9-THC, methanandamide and fenofibrate exhibited bias towards ERK activation in HEK cells only. The RAi values for the Neuro 2a cells were calculated with WIN 55,212-2 as the reference agonist, as opposed to HU-210, so direct comparison with the transfected cell lines is less useful; however only HU-210 exhibited any agonist bias, again towards ERK versus cAMP, with neither anandamide nor ACEA showing any bias. Visual observation of the results for Neuro 2a indicate that WIN 55,212-2 may also exhibit some bias, this time towards cAMP signalling however this was not definitively quantified.

This thesis has provided several examples of both novel, and more established patterns of agonist bias at the CB_1 receptor, particularly towards activation of ERK, which plays a fundamental role in regulating synaptic plasticity, and away from inhibition of cAMP accumulation, which is linked to inhibition of neuronal cell function and altered gene expression. The possibility therefore exists to use

these biased compounds as the basis for new agonists with improved positive and/or negative signalling selectivities. Such compound could have great therapeutic potential by maximising activation of beneficial, and/or minimising activation of unwanted signalling pathways, providing drugs with increased therapeutic benefit and reduced side effects.

As with ERK activation, CB_1 receptor coupling to JNK and p38 MAP kinase has been reported in a number of cell types, including CHO cells (Rueda *et al.*, 2000) and in human primary coronary artery endothelial cells (Rajesh *et al.*, 2010). In addition there are many reports in which the activation of one MAP kinase, but not the other, is described, including activation of JNK in Neuro 2a and N1E-155 cells (Graham *et al.*, 2006; Bosier *et al.*, 2008) and activation of p38 in rat and mouse hippocampal slices (Derkinderen *et al.*, 2001), and human platelets (Signorello *et al.*, 2011). None of the three cell lines investigated in this thesis showed any CB_1 receptor coupling to either JNK or p38, despite the inclusion of positive controls showing these signalling pathways to be present. The most likely explanation for this is that the particular cell line subclones used in the experiments described in this thesis either lack or weakly express the cellular machinery necessary to couple the receptor to the signalling pathways. CB_1 receptor-mediated activation of JNK has been shown to involve $G_{i/o}$ protein-dependent signalling via PI3K/Ras in CHO cells (Rueda *et al.*, 2000), and Src/Rac in Neuro 2a cells (He *et al.*, 2005). The pathway by which the receptor activates p38 MAP kinase is less well understood, but has been shown to be independent of Src in rodent hippocampal neurons. As we have shown the CB_1 receptor is able to couple to $G_{i/o}$ protein in all three cell lines, it is likely downstream mediator such as those described which is limiting

effective coupling. A precedent for this already exists with the Neuro 2a cells, in which one research group clearly demonstrated CB_1 receptor-mediated JNK activation, while another unequivocally stated the absence of this response in a different subclone of the cell line. However, given more time, it would have been useful to assay JNK and p38 MAP kinase activation in these cells using immunoblotting techniques to allow for more direct comparison with the findings in the literature.

Transfected model cell lines are well suited to investigating functional selectivity, as high numbers of cells can be cultured, and the relatively high level of receptor expression allows large responses, which aid in identifying the often subtle differences in efficacy and potency between agonists at different signalling pathways. However, to ascertain whether functionally selective signalling has any physiological relevance to native systems, it is necessary to investigate it in cells which endogenously express the receptor of interest (Seifert, 2013), which in this case was the Neuro 2a cell line. While the use of more physiologically relevant cells, such as primary cell cultures would have been a more appropriate model to investigate functional selectivity, the difficultly in acquiring and culturing enough cells to perform full concentration-response experiments on numerous agonists was beyond the means of this study. Generally, the issues limiting the usefulness of native cells are the converse of those that make recombinant cell lines so advantageous – cell culture is often more restrictive, providing fewer cells for experimentation (Seifert, 2013). Also, the responses are often small compared to transfected cell lines (i.e. a small signal-to-basal window), which increases variance and allows much less scope for distinguishing between full and partial

agonism (Seifert, 2013). This was partly the case with the Neuro 2a cells, in which the phospho-ERK responses were lower than those in the CHO and HEK cells, and the maximum inhibition of cAMP accumulation was only 20 %, compared to 48 % in the CHO cells, and even greater in the HEK cells. Despite this, responses were obtained in endogenously expressing cells, and with steps to increase assay sensitivity and increased experimental numbers, future research should be able to effectively utilise native cells.

6.2. Future directions and points to consider

Many of the findings in this thesis have raised additional questions, and highlighted a number of areas of further work which would greatly contribute to our understanding of cannabinoid receptor signalling. In addition to those already mentioned, some areas where future work is warranted are outlined below.

Stimulation of HEK cells with concentrations of WIN 55,212-2 above 100 nM for 20 min produced $G_{i/o}$-dependent sub-maximal levels of ERK activation, an effect which was also indicated in the sub-basal phospho-ERK levels in the 6 hour time-course experiments in the CHO cells. One potential explanation for this is the involvement of distinct G_i and G_o protein subtypes. Future research to determine the G protein subtypes involved would help explain this novel functionally selective response.

Next, while this thesis has focused on receptor-coupled intracellular signalling pathways, investigation of a whole-cell measure of receptor activation and/or downstream physiological changes mediated by effectors such as ERK and PKA

would be useful to determining the physiological impact of functionally selective signalling. As described in Chapter 5, treatment of Neuro 2a cells with HU-210 has been shown to promote cell differentiation and neurite outgrowth (He *et al.*, 2005). Future work would aim to fully characterise concentration-responses for all the agonists tested in this thesis and then compare these results with the pattern of intracellular signalling. A series of preliminary concentration-response experiments were performed on CHO cells using the xCELLigence system (Roche Applied Science and ACEA Biosystems). This label-free whole-cell assay, detects changes in adherent cell morphology by measuring the impedance of a very weak current along the bottom of a 96-well assay plate (Scott *et* Peters. 2010). Measurement is dynamic giving both kinetic and concentration-dependent data and the consequence of GPCR activation over several hours can be easily investigated if desired. While these preliminary experiments yielded interesting results, complete data sets were not available for inclusion in this thesis.

Finally, given more time, the next step in this project would have been to investigate functional selectivity in other native systems, particularly primary cell and tissue cultures, and human native cells, where possible. Such models have yet to be widely used for research into functional selectivity at GPCRs; however some examples include the use of primary culture of rat neurons and human neutrophils (Seifert. 2013). The use of these native cells will be necessary to determining the true therapeutic relevance of bias compounds as drugs.

6.3. Conclusion

The thesis demonstrates functional selectivity at the cannabinoid type 1 receptor in a number of cell lines, expressing both native and transfected recombinant receptor. These findings contribute to our increased understand of the complexity of GPCR signalling, and potentially allow for the development of more targeted drug which are coupled to selected, beneficial signal transduction pathways.

References

Ahn KH, Mahmoud MM, Shim JY & Kendall DA (2013) Distinct Roles of beta-Arrestin 1 and beta-Arrestin 2 in ORG27569-induced Biased Signaling and Internalization of the Cannabinoid Receptor 1 (CB1). *Journal of Biological Chemistry* **288**, 9790-9800.

Al-Hasani R & Bruchas MR (2011) Molecular Mechanisms of Opioid Receptor-dependent Signaling and Behavior. *Anesthesiology* **115**, 1363-1381.

Anavi-Goffer S, Fleischer D, Hurst DP, Lynch DL, Barnett-Norris J, Shi SP, Lewis DL, Mukhopadhyay S, Howlett AC, Reggio PH & Abood ME (2007) Helix 8 Leu in the CB1 cannabinoid receptor contributes to selective signal transduction mechanisms. *Journal of Biological Chemistry* **282**, 25100-25113.

Asimaki O, Leondaritis G, Lois G, Sakellaridis N & Mangoura D (2011) Cannabinoid 1 receptor-dependent transactivation of fibroblast growth factor receptor 1 emanates from lipid rafts and amplifies extracellular signal-regulated kinase 1/2 activation in embryonic cortical neurons. *Journal of Neurochemistry* **116**, 866-873.

Asimaki O & Mangoura D (2011) Cannabinoid receptor 1 induces a biphasic ERK activation via multiprotein signaling complex formation of proximal kinases PKCε, Src, and Fyn in primary neurons. *Neurochemistry International* **58**, 135-144.

Atwood BK, Lopez J, Wager-Miller J, Mackie K & Straiker A (2011) Expression of G protein-coupled receptors and related proteins in HEK293, AtT20, BV2, and N18 cell lines as revealed by microarray analysis. *BMC genomics* **12**, 14.

Baillie GL, Horswill JG, Anavi-Goffer S, Reggio PH, Bolognini D, Abood ME, McAllister S, Strange PG, Stephens GJ, Pertwee RG & Ross RA (2013) CB1 Receptor Allosteric Modulators Display Both Agonist and Signaling Pathway Specificity. *Molecular Pharmacology* **83**, 322-338.

Baker D, Pryce G, Davies WL & Hiley CR (2006) In silico patent searching reveals a new cannabinoid receptor. *Trends in Pharmacological Sciences* **27**, 1-4.

Bartlett SE, Enquist J, Hopf FW, Lee JH, Gladher F, Kharazia V, Waldhoer M, Mailliard WS, Armstrong R, Bonci A & Whistler JL (2005) Dopamine responsiveness is regulated by targeted sorting of D2 receptors. *Proceedings of the National Academy of Sciences of the United States of America* **102**, 11521-11526.

Bauer M, Chicca A, Tamborrini M, Eisen D, Lerner R, Lutz B, Poetz O, Pluschke G & Gertsch J (2012) Identification and Quantification of a New Family of Peptide Endocannabinoids (Pepcans) Showing Negative Allosteric Modulation at CB1 Receptors. *Journal of Biological Chemistry* **287**, 36944-36967.

Begg M, Baydoun A, Parsons ME & Molleman A (2001) Signal transduction of cannabinoid CB1 receptors in a smooth muscle cell line. *Journal of Physiology-London* **531**, 95-104.

Berg KA, Maayani S, Goldfarb J, Scaramellini C, Leff P & Clarke WP (1998) Effector pathway-dependent relative efficacy at serotonin type 2A and 2C receptors: Evidence for agonist-directed trafficking of receptor stimulus. *Molecular Pharmacology* **54**, 94-104.

Bisogno T, Melck D, Bobrov MY, Gretskaya NM, Bezuglov VV, De Petrocellis L & Di Marzo V (2000) N-acyl-dopamines: novel synthetic CB1 cannabinoid-receptor ligands and inhibitors of anandamide inactivation with cannabimimetic activity in vitro and in vivo. *Biochemical Journal* **351**, 817-824.

Bonhaus DW, Chang LK, Kwan J & Martin GR (1998) Dual activation and inhibition of adenylyl cyclase by cannabinoid receptor agonists: Evidence for agonist-specific trafficking of intracellular responses. *Journal of Pharmacology and Experimental Therapeutics* **287**, 884-888.

Bosier B, Lambert DM & Hermans E (2008) Reciprocal influences of CB(1) cannabinoid receptor agonists on ERK and JNK signalling in N1E-115 cells. *Febs Letters* **582**, 3861-3867.

Bosier B, Muccioli GG, Hermans E & Lambert DM (2010) Functionally selective cannabinoid receptor signalling: Therapeutic implications and opportunities. *Biochemical Pharmacology* **80**, 1-12.

Bosier B, Muccioli GG, Mertens B, Sarre S, Michotte Y, Lambert DM & Hermans E (2012) Differential modulations of striatal tyrosine hydroxylase and

dopamine metabolism by cannabinoid agonists as evidence for functional selectivity in vivo. *Neuropharmacology* **62**, 2328-2336.

Bouaboula M, Poinotchazel C, Bourrie B, Canat X, Calandra B, Rinaldicarmona M, Lefur G & Casellas P (1995) Activation of mitogen-activated protein-kinases by stimulation of the central cannabinoid receptor CB1. *Biochemical Journal* **312**, 637-641.

Breivogel CS, Childers SR, Deadwyler SA, Hampson RE, Vogt LJ & Sim-Selley LJ (1999) Chronic Delta(9)-tetrahydrocannabinol treatment produces a time-dependent loss of cannabinoid receptors and cannabinoid receptor-activated G proteins in rat brain. *Journal of Neurochemistry* **73**, 2447-2459.

Cabral GA & Griffin-Thomas L (2009) Emerging role of the cannabinoid receptor CB2 in immune regulation: therapeutic prospects for neuroinflammation. *Expert Reviews in Molecular Medicine* **11**.

Caldwell J (1989) THE BIOCHEMICAL PHARMACOLOGY OF FENOFIBRATE. *Cardiology* **76**, 33-44.

Carlisle SJ, Marciano-Cabral F, Staab A, Ludwick C & Cabral GA (2002) Differential expression of the CB2 cannabinoid receptor by rodent macrophages and macrophage-like cells in relation to cell activation. *International Immunopharmacology* **2**, 69-82.

Carriba P, Ortiz O, Patkar K, Justinova Z, Stroik J, Themann A, Muller C, Woods AS, Hope BT, Ciruela F, Casado V, Canela EI, Lluis C, Goldberg SR, Moratalla R, Franco R & Ferre S (2007) Striatal adenosine A(2A) and Cannabinoid CB1 receptors form functional heteromeric complexes that mediate the motor effects of Cannabinoids. *Neuropsychopharmacology* **32**, 2249-2259.

Chakrabarti A, Onaivi ES & Chaudhuri G (1995a) Cloning and sequencing of a cDNA-encoding the mouse brain-type cannabinoid receptor protein. *DNA Sequence* **5**, 385-388.

Chakrabarti S, Law PY & Loh HH (1995b) NEUROBLASTOMA NEURO(2A) CELLS STABLY EXPRESSING A CLONED MU-OPIOID RECEPTOR - A SPECIFIC CELLULAR-MODEL TO STUDY ACUTE AND CHRONIC EFFECTS OF MORPHINE. *Molecular Brain Research* **30**, 269-278.

Chen HX, Kovar J, Sissons S, Cox K, Matter W, Chadwell F, Luan P, Vlahos CJ, Schutz-Geschwender A & Olive DM (2005) A cell-based immunocytochemical assay for monitoring kinase signaling pathways and drug efficacy. *Analytical Biochemistry* **338**, 136-142.

Choi IY, Ju C, Jalin A, Lee DI, Prather PL & Kim WK (2013) Activation of Cannabinoid CB2 Receptor-Mediated AMPK/CREB Pathway Reduces Cerebral Ischemic Injury. *American Journal of Pathology* **182**, 928-939.

Christopoulos A & Kenakin T (2002) G protein-coupled receptor allosterism and complexing. *Pharmacological Reviews* **54**, 323-374.

Christopoulos A & Mitchelson F (1997) Pharmacological analysis of the mode of interaction of McN-A-343 at atrial muscarinic M2 receptors. *European Journal of Pharmacology* **339**, 153-156.

Dagon Y, Avraham Y, Ilan Y, Mechoulam R & Berry EM (2007) Cannabinoids ameliorate cerebral dysfunction following liver failure via AMP-activated protein kinase. *Faseb Journal* **21**, 2431-2441.

Daigle TL, Kearn CS & Mackie K (2008) Rapid CB1 cannabinoid receptor desensitization defines the time course of ERK1/2 MAP kinase signaling. *Neuropharmacology* **54**, 36-44.

Dale CS, Pagano RDL, Rioli V, Hyslop S, Giorgi R & Ferro ES (2005) Antinociceptive action of hemopressin in experimental hyperalgesia. *Peptides* **26**, 431-436.

Dalton GD & Howlett AC (2012) Cannabinoid CB1 receptors transactivate multiple receptor tyrosine kinases and regulate serine/threonine kinases to activate ERK in neuronal cells. *British Journal of Pharmacology* **165**, 2497-2511.

Deadwyler SA, Hampson RE, Mu J, Whyte A & Childers S (1995) Cannabinoids modulate voltage-sensitive potassium A-current in hippocampal-neurons via cAMP-dependent process. *Journal of Pharmacology and Experimental Therapeutics* **273**, 734-743.

Demuth DG, Gkoumassi E, Droge MJ, Dekkers BGJ, Esselink HJ, Van Ree RM, Parsons ME, Zaagsma J, Molleman A & Nelemans SAD (2005) Arachidonic acid mediates non-capacitative calcium entry evoked by CB1-cannabinoid receptor activation in DDT1 MF-2 smooth muscle cells. *Journal of Cellular Physiology* **205**, 58-67.

Derkinderen P, Ledent C, Parmentier M & Girault JA (2001) Cannabinoids activate p38 mitogen-activated protein kinases through CB1 receptors in hippocampus. *Journal of Neurochemistry* **77**, 957-960.

Devane WA, Hanus L, Breuer A, Pertwee RG, Stevenson LA, Griffin G, Gibson D, Mandelbaum A, Etinger A & Mechoulam R (1992) Isolation and structure of a brain constituent that binds to the cannabinoid receptor. *Science* **258**, 1946-1949.

DeWire SM, Ahn S, Lefkowitz RJ & Shenoy SK (2007) beta-arrestins and cell signaling. In *Annual Review of Physiology*, pp. 483-510. Palo Alto: Annual Reviews.

Ehlert FJ (2005) Analysis of allosterism in functional assays. *Journal of Pharmacology and Experimental Therapeutics* **315**, 740-754.

Ehlert FJ (2008) On the analysis of ligand-directed signaling at G protein-coupled receptors. *Naunyn-Schmiedebergs Archives of Pharmacology* **377**, 549-577.

Ellert-Miklaszewska A, Kaminska B & Konarska L (2005) Cannabinoids down-regulate PI3K/Akt and Erk signalling pathways and activate proapoptotic function of Bad protein. *Cellular Signalling* **17**, 25-37.

Ellis J, Pediani JD, Canals M, Milasta S & Milligan G (2006) Orexin-1 receptor-cannabinoid CB1 receptor heterodimerization results in both ligand-dependent and -independent coordinated alterations of receptor localization and function. *Journal of Biological Chemistry* **281**, 38812-38824.

Felder CC, Joyce KE, Briley EM, Glass M, Mackie KP, Fahey KJ, Cullinan GJ, Hunden DC, Johnson DW, Chaney MO, Koppel GA & Brownstein M (1998) LY320135, a novel cannabinoid CB1 receptor antagonist, unmasks coupling of the CB1 receptor to stimulation of cAMP accumulation. *Journal of Pharmacology and Experimental Therapeutics* **284**, 291-297.

Felder CC, Joyce KE, Briley EM, Mansouri J, Mackie K, Blond O, Lai Y, Ma AL & Mitchell RL (1995) Comparison of the pharmacology and signal transduction of the human cannabinoid CB1 and CB2 receptors. *Molecular Pharmacology* **48**, 443-450.

Figueroa KW, Griffin MT & Ehlert FJ (2009) Selectivity of Agonists for the Active State of M-1 to M-4 Muscarinic Receptor Subtypes. *Journal of Pharmacology and Experimental Therapeutics* **328**, 331-342.

Franklin JM, Vasiljevik T, Prisinzano TE & Carrasco GA (2013) Cannabinoid agonists increase the interaction between β-Arrestin 2 and ERK1/2 and upregulate β-Arrestin 2 and 5-HT2A receptors. *Pharmacological Research* **68**, 46-58.

Fu J, Gaetani S, Oveisi F, Lo Verme J, Serrano A, de Fonseca FR, Rosengarth A, Luecke H, Di Giacomo B, Tarzia G & Piomelli D (2003) Oleylethanolamide regulates feeding and body weight through activation of the nuclear receptor PPAR-alpha. *Nature* **425**, 90-93.

Galiegue S, Mary S, Marchand J, Dussossoy D, Carriere D, Carayon P, Bouaboula M, Shire D, Lefur G & Casellas P (1995) Expression of Central and Peripheral Cannabinoid Receptors in Human Immune Tissues and Leukocyte Subpopulations. *European Journal of Biochemistry* **232**, 54-61.

Galve-Roperh I, Rueda D, Del Pulgar TG, Velasco G & Guzman M (2002) Mechanism of extracellular signal-regulated kinase activation by the CB1 cannabinoid receptor. *Molecular Pharmacology* **62**, 1385-1392.

Gantz I, Muraoka A, Yang YK, Samuelson LC, Zimmerman EM, Cook H & Yamada T (1997) Cloning and chromosomal localization of a gene (GPR18) encoding a novel seven transmembrane receptor highly expressed in spleen and testis. *Genomics* **42**, 462-466.

Georgieva T, Devanathan S, Stropova D, Park CK, Salamon Z, Tollin G, Hruby VJ, Roeske WR, Yamamura HI & Varga E (2008) Unique agonist-bound cannabinoid CB1 receptor conformations indicate agonist specificity in signaling. *European Journal of Pharmacology* **581**, 19-29.

Gerard C, Mollereau C, Vassart G & Parmentier M (1990) Nucleotide sequence of a human cannabinoid receptor cDNA. *Nucleic Acids Research* **18**, 7142-7142.

Glass M & Felder CC (1997) Concurrent stimulation of cannabinoid CB1 and dopamine D2 receptors augments cAMP accumulation in striatal neurons: Evidence for a G(s) linkage to the CB1 receptor. *Journal of Neuroscience* **17**, 5327-5333.

Glass M & Northup JK (1999) Agonist selective regulation of g proteins by cannabinoid CB1 and CB2 receptors. *Molecular Pharmacology* **56**, 1362-1369.

Goggi JL, Sardini A, Egerton A, Strange PG & Grasby PM (2007) Agonist-dependent internalization of D2 receptors: Imaging quantification by confocal microscopy. *Synapse* **61**, 231-241.

Gomes I, Dale CS, Casten K, Geigner MA, Gozzo FC, Ferro ES, Heimann AS & Devi LA (2010) Hemoglobin-derived peptides as novel type of bioactive signaling molecules. *Aaps J* **12**, 658-669.

Gomes I, Grushko JS, Golebiewska U, Hoogendoorn S, Gupta A, Heimann AS, Ferro ES, Scarlata S, Fricker LD & Devi LA (2009) Novel endogenous peptide agonists of cannabinoid receptors. *Faseb Journal* **23**, 3020-3029.

Govaerts SJ, Hermans E & Lambert DM (2004) Comparison of cannabinoid ligands affinities and efficacies in murine tissues and in transfected cells expressing human recombinant cannabinoid receptors. *European Journal of Pharmaceutical Sciences* **23**, 233-243.

Graham ES, Ball N, Scotter EL, Narayan P, Dragunow M & Glass M (2006) Induction of Krox-24 by endogenous cannabinoid type 1 receptors in Neuro2a cells is mediated by the MEK-ERK MAPK pathway and is suppressed by the phosphatidylinositol 3-kinase pathway. *Journal of Biological Chemistry* **281**, 29085-29095.

Graham FL, Smiley J, Russell WC & Nairn R (1977) Characteristics of a Human Cell Line Transformed by DNA from Human Adenovirus Type 5. *Journal of General Virology* **36**, 59-72.

Gregory KJ, Hall NE, Tobin AB, Sexton PM & Christopoulos A (2010) Identification of Orthosteric and Allosteric Site Mutations in M2 Muscarinic Acetylcholine Receptors That Contribute to Ligand-selective Signaling Bias. *Journal of Biological Chemistry* **285**, 7459-7474.

Griffin MT, Figueroa KW, Liller S & Ehlert FJ (2007) Estimation of agonist activity at G protein-coupled receptors: Analysis of M-2 muscarinic receptor signaling through G(i/o), G(s), and G(15). *Journal of Pharmacology and Experimental Therapeutics* **321**, 1193-1207.

Grimsey NL, Graham ES, Dragunow M & Glass M (2010) Cannabinoid Receptor 1 trafficking and the role of the intracellular pool: Implications for therapeutics. *Biochemical Pharmacology* **80**, 1050-1062.

Hajos N, Katona I, Naiem SS, Mackie K, Ledent C, Mody I & Freund TF (2000) Cannabinoids inhibit hippocampal GABAergic transmission and network oscillations. *European Journal of Neuroscience* **12**, 3239-3249.

Hampson RE, Evans GJO, Mu J, Zhuang SY, King VC, Childers SR & Deadwyler SA (1995) Role of cyclic-AMP-dependent protein-kinase in cannabinoid receptor modulation of potassium A-current in cultured rat hippocampal-neurons. *Life Sciences* **56**, 2081-2088.

Hanus L, Abu-Lafi S, Fride E, Breuer A, Vogel Z, Shalev DE, Kustanovich I & Mechoulam R (2001) 2-Arachidonyl glyceryl ether, an endogenous agonist of the cannabinoid CB1 receptor. *Proceedings of the National Academy of Sciences of the United States of America* **98**, 3662-3665.

He JCJ, Gomes I, Nguyen T, Jayaram G, Ram PT, Devi LA & Iyengar R (2005) The G alpha(o/)i-coupled cannabinoid receptor-mediated neurite outgrowth involves rap regulation of Src and Stat3. *Journal of Biological Chemistry* **280**, 33426-33434.

Heimann AS, Gomes L, Dale CS, Pagano RL, Gupta A, de Souza LL, Luchessi AD, Castro LM, Giorgi R, Rioli V, Ferro ES & Devi LA (2007) Hemopressin is an inverse agonist of CB1 cannabinoid receptors. *Proceedings of the National Academy of Sciences of the United States of America* **104**, 20588-20593.

Hillard CJ, Manna S, Greenberg MJ, DiCamelli R, Ross RA, Stevenson LA, Murphy V, Pertwee RG & Campbell WB (1999) Synthesis and Characterization of Potent and Selective Agonists of the Neuronal Cannabinoid Receptor (CB1). *Journal of Pharmacology and Experimental Therapeutics* **289**, 1427-1433.

Horswill JG, Bali U, Shaaban S, Keily JF, Jeevaratnam P, Babbs AJ, Reynet C & In PWK (2007) PSNCBAM-1, a novel allosteric antagonist at cannabinoid CB1 receptors with hypophagic effects in rats. *British Journal of Pharmacology* **152**, 805-814.

Howlett AC, Barth F, Bonner TI, Cabral G, Casellas P, Devane WA, Felder CC, Herkenham M, Mackie K, Martin BR, Mechoulam R & Pertwee RG (2002) International Union of Pharmacology. XXVII. Classification of cannabinoid receptors. *Pharmacological Reviews* **54**, 161-202.

Hsieh C, Brown S, Derleth C & Mackie K (1999) Internalization and recycling of the CB1 cannabinoid receptor. *Journal of Neurochemistry* **73**, 493-501.

Huang CC, Lo SW & Hsu KS (2001) Presynaptic mechanisms underlying cannabinoid inhibition of excitatory synaptic transmission in rat striatal neurons. *Journal of Physiology-London* **532**, 731-748.

Huang SM, Bisogno T, Trevisani M, Al-Hayani A, De Petrocellis L, Fezza F, Tognetto M, Petros TJ, Krey JF, Chu CJ, Miller JD, Davies SN, Geppetti P, Walker JM & Di Marzo V (2002a) An endogenous capsaicin-like substance with high potency at recombinant and native vanilloid VR1 receptors. *Proceedings of the National Academy of Sciences* **99**, 8400-8405.

Huang SM, Bisogno T, Trevisani M, Al-Hayani A, De Petrocellis L, Fezza F, Tognetto M, Petros TJ, Krey JF, Chu CJ, Miller JD, Davies SN, Geppetti P, Walker JM & Di Marzo V (2002b) An endogenous capsaicin-like substance with high potency at recombinant and native vanilloid VR1 receptors. *Proceedings of the National Academy of Sciences of the United States of America* **99**, 8400-8405.

Hudson BD, Hebert TE & Kelly MEM (2010) Ligand- and Heterodimer-Directed Signaling of the CB1 Cannabinoid Receptor. *Molecular Pharmacology* **77**, 1-9.

Ivanov A (2008) Pharmacological Inhibition of Endocytic Pathways: Is It Specific Enough to Be Useful? In *Exocytosis and Endocytosis*, pp. 15-33 [A Ivanov, editor]: Humana Press.

Izzo AA (2004) Cannabinoids and intestinal motility: welcome to CB2 receptors. *British Journal of Pharmacology* **142**, 1201-1202.

Jarrahian A, Watts VJ & Barker EL (2004) D-2 dopamine receptors modulate G alpha-subunit coupling of the CB1 cannabinoid receptor. *Journal of Pharmacology and Experimental Therapeutics* **308**, 880-886.

Jin WZ, Brown S, Roche JP, Hsieh C, Celver JP, Kovoor A, Chavkin C & Mackie K (1999) Distinct domains of the CB1 cannabinoid receptor mediate desensitization and internalization. *Journal of Neuroscience* **19**, 3773-3780.

Joost P & Methner A (2002) Phylogenetic analysis of 277 human G-protein-coupled receptors as a tool for the prediction of orphan receptor ligands. *Genome Biology* **3**.

Jordan JD, He JC, Eungdamrong NJ, Gomes I, Ali W, Nguyen T, Bivona TG, Philips MR, Devi LA & Iyengar R (2005) Cannabinoid receptor-induced neurite outgrowth is mediated by Rap1 activation through G alpha(o/i)-triggered proteasomal degradation of Rap1GAPII. *Journal of Biological Chemistry* **280**, 11413-11421.

Jung K-M, Astarita G, Thongkham D & Piomelli D (2011) Diacylglycerol Lipase-alpha and -beta Control Neurite Outgrowth in Neuro-2a Cells through Distinct Molecular Mechanisms. *Molecular Pharmacology* **80**, 60-67.

Katona I, Rancz EA, Acsady L, Ledent C, Mackie K, Hajos N & Freund TF (2001) Distribution of CB1 cannabinoid receptors in the amygdala and their role in the control of GABAergic transmission. *Journal of Neuroscience* **21**, 9506-9518.

Kearn CS, Blake-Palmer K, Daniel E, Mackie K & Glass M (2005) Concurrent stimulation of cannabinoid CB1 and dopamine D2 receptors enhances heterodimer formation: A mechanism for receptor cross-talk? *Molecular Pharmacology* **67**, 1697-1704.

Kenakin T (2001) Inverse, protean, and ligand-selective agonism: matters of receptor conformation. *Faseb Journal* **15**, 598-611.

Kenakin T (2010) G protein coupled receptors as allosteric proteins and the role of allosteric modulators. *Journal of Receptors and Signal Transduction* **30**, 313-321.

Kenakin T & Christopoulos A (2013a) OPINION Signalling bias in new drug discovery: detection, quantification and therapeutic impact. *Nature Reviews Drug Discovery* **12**, 205-216.

Kenakin T & Christopoulos A (2013b) Signalling bias in new drug discovery: detection, quantification and therapeutic impact. *Nat Rev Drug Discov* **12**, 205-216.

Kenakin T & Miller LJ (2010) Seven Transmembrane Receptors as Shapeshifting Proteins: The Impact of Allosteric Modulation and Functional Selectivity on New Drug Discovery. *Pharmacological Reviews* **62**, 265-304.

Klebe RJ & Ruddle RH (1969) NEUROBLASTOMA - CELL CULTURE ANALYSIS OF A DIFFERENTIATING STEM CELL SYSTEM. *Journal of Cell Biology* **43**, A69-&.

Knapska E & Kaczmarek L (2004) A gene for neuronal plasticity in the mammalian brain: Zif268/Egr-1/NGFI-A/Krox-24/TIS8/ZENK? *Progress in Neurobiology* **74**, 183-211.

Kobayashi Y, Arai S, Waku K & Sugiura T (2001) Activation by 2-arachidonoylglycerol, an endogenous cannabinoid receptor ligand, of p42/44 mitogen-activated protein kinase in HL-60 cells. *Journal of Biochemistry* **129**, 665-669.

Kolch W (2005) Coordinating ERK/MAPK signalling through scaffolds and inhibitors. *Nature Reviews Molecular Cell Biology* **6**, 827-837.

Kouznetsova M, Kelley B, Shen MX & Thayer SA (2002) Desensitization of cannabinoid-mediated presynaptic inhibition of neurotransmission between rat hippocampal neurons in culture. *Molecular Pharmacology* **61**, 477-485.

Lane JR, Sexton PM & Christopoulos A (2013) Bridging the gap: bitopic ligands of G-protein-coupled receptors. *Trends in Pharmacological Sciences* **34**, 59-66.

Lauckner JE, Hille B & Mackie K (2005) The cannabinoid agonist WIN55,212-2 increases intracellular calcium via CB1 receptor coupling to G(q/11) G proteins. *Proceedings of the National Academy of Sciences of the United States of America* **102**, 19144-19149.

Lefkowitz RJ & Whalen EJ (2004) β-arrestins: traffic cops of cell signaling. *Current Opinion in Cell Biology* **16**, 162-168.

Ligresti A, Villano R, Allarà M, Ujváry I & Di Marzo V (2012) Kavalactones and the endocannabinoid system: The plant-derived yangonin is a novel CB1 receptor ligand. *Pharmacological Research* **66**, 163-169.

Lin F-T, Daaka Y & Lefkowitz RJ (1998) β-Arrestins Regulate Mitogenic Signaling and Clathrin-mediated Endocytosis of the Insulin-like Growth Factor I Receptor. *Journal of Biological Chemistry* **273**, 31640-31643.

Liu J, Wang L, Harvey-White J, Huang BX, Kim HY, Luquet S, Palmiter RD, Krystal G, Rai R, Mahadevan A, Razdan RK & Kunos G (2008) Multiple pathways involved in the biosynthesis of anandamide. *Neuropharmacology* **54**, 1-7.

Louis N, Evelegh C & Graham FL (1997) Cloning and Sequencing of the Cellular–Viral Junctions from the Human Adenovirus Type 5 Transformed 293 Cell Line. *Virology* **233**, 423-429.

Lowry OH, Rosebrough NJ, Farr AL & Randall RJ (1951) PROTEIN MEASUREMENT WITH THE FOLIN PHENOL REAGENT. *Journal of Biological Chemistry* **193**, 265-275.

Lundholt BK, Scudder KM & Pagliaro L (2003) A simple technique for reducing edge effect in cell-based assays. *Journal of Biomolecular Screening* **8**, 566-570.

Luttrell LM, Daaka Y, Della Rocca GJ & Lefkowitz RJ (1997) G Protein-coupled Receptors Mediate Two Functionally Distinct Pathways of Tyrosine Phosphorylation in Rat 1a Fibroblasts: Shc PHOSPHORYLATION AND RECEPTOR ENDOCYTOSIS CORRELATE WITH ACTIVATION OF Erk KINASES. *Journal of Biological Chemistry* **272**, 31648-31656.

Mackie K (2005) Cannabinoid receptor homo- and heterodimerization. *Life Sciences* **77**, 1667-1673.

Mackie K & Hille B (1992) Cannabinoids inhibit N-type calcium channels in neuroblastoma glioma-cells. *Proceedings of the National Academy of Sciences of the United States of America* **89**, 3825-3829.

Mackie K, Lai Y, Westenbroek R & Mitchell R (1995) Cannabinoids activate an inwardly rectifying potassium conductance and inhibit Q-type calcium currents in AtT20 cells transfected with rat brain cannabinoid receptor. *Journal of Neuroscience* **15**, 6552-6561.

Maneuf YP & Brotchie JM (1997) Paradoxical action of the cannabinoid WIN 55,212-2 in stimulated and basal cyclic AMP accumulation in rat globus pallidus slices. *British Journal of Pharmacology* **120**, 1397-1398.

Martini L, Waldhoer M, Pusch M, Kharazia V, Fong J, Lee JH, Freissmuth C & Whistler JL (2007) Ligand-induced down-regulation of the cannabinoid 1 receptor is mediated by the G-protein-coupled receptor-associated sorting protein GASP1. *Faseb Journal* **21**, 802-811.

Matsuda LA, Lolait SJ, Brownstein MJ, Young AC & Bonner TI (1990) Structure of a cannabinoid receptor and functional expression of the cloned cDNA. *Nature* **346**, 561-564.

May LT, Leach K, Sexton PM & Christopoulos A (2007) Allosteric modulation of G protein-coupled receptors. In *Annual Review of Pharmacology and Toxicology*, pp. 1-51. Palo Alto: Annual Reviews.

McGuinness D, Malikzay A, Visconti R, Lin K, Bayne M, Monsma F & Lunn CA (2009) Characterizing Cannabinoid CB(2) Receptor Ligands Using DiscoveRx PathHunter (TM) beta-Arrestin Assay. *Journal of Biomolecular Screening* **14**, 49-58.

McIntosh BT, Hudson B, Yegorova S, Jollimore CAB & Kelly MEM (2007) Agonist-dependent cannabinoid receptor signalling in human trabecular meshwork cells. *British Journal of Pharmacology* **152**, 1111-1120.

Melck D, Rueda D, Galve-Roperh I, De Petrocellis L, Guzman M & Di Marzo V (1999) Involvement of the cAMP/protein kinase A pathway and of mitogen-activated protein kinase in the anti-proliferative effects of anandamide in human breast cancer cells. *Febs Letters* **463**, 235-240.

Michalik L, Auwerx J, Berger JP, Chatterjee VK, Glass CK, Gonzalez FJ, Grimaldi PA, Kadowaki T, Lazar MA, O'Rahilly S, Palmer CNA, Plutzky J, Reddy JK, Spiegelman BM, Staels B & Wahli W (2006) International Union of Pharmacology. LXI. Peroxisome proliferator-activated receptors. *Pharmacological Reviews* **58**, 726-741.

Mu J, Zhuang SY, Kirby MT, Hampson RE & Deadwyler SA (1999) Cannabinoid receptors differentially modulate potassium A and D currents in hippocampal neurons in culture. *Journal of Pharmacology and Experimental Therapeutics* **291**, 893-902.

Mukhopadhyay S & Howlett AC (2005) Chemically distinct ligands promote differential CB1 cannabinoid receptor-Gi protein interactions. *Molecular Pharmacology* **67**, 2016-2024.

Munro S, Thomas KL & Abushaar M (1993) Molecular characterization of a peripheral receptor for cannabinoids. *Nature* **365**, 61-65.

Murakami R, Murakami H, Kataoka H, Cheng XW, Takahashi R, Numaguchi Y, Murohara T & Okumura K (2010) Unmetabolized fenofibrate, but not fenofibric acid, activates AMPK and inhibits the expression of phosphoenolpyruvate carboxykinase in hepatocytes. *Life Sciences* **87**, 495-500.

Murphy WJ, Eizirik E, Johnson WE, Zhang YP, Ryder OA & O'Brien SJ (2001) Molecular phylogenetics and the origins of placental mammals. *Nature* **409**, 614-618.

Navarro G, Carriba P, Gandia J, Ciruela F, Casado V, Cortes A, Mallol J, Canela EI, Lluis C & Franco R (2008) Detection of heteromers formed by cannabinoid CB1, dopamine D2, and adenosine A2A G-protein-coupled receptors by combining bimolecular fluorescence complementation and bioluminescence energy transfer. *ScientificWorldJournal* **8**, 1088-1097.

Navarro HA, Howard JL, Pollard GT & Carroll FI (2009) Positive allosteric modulation of the human cannabinoid (CB1) receptor by RTI-371, a selective inhibitor of the dopamine transporter. *British Journal of Pharmacology* **156**, 1178-1184.

Netherland CD, Pickle TG, Bales A & Thewke DP (2010) Cannabinoid receptor type 2 (CB2) deficiency alters atherosclerotic lesion formation in hyperlipidemic Ldlr-null mice. *Atherosclerosis* **213**, 102-108.

Netzeband JG, Conroy SM, Parsons KL & Gruol DL (1999) Cannabinoids enhance NMDA-elicited Ca2+ signals in cerebellar granule neurons in culture. *Journal of Neuroscience* **19**, 8765-8777.

Niehaus JL, Liu Y, Wallis KT, Egertova M, Bhartur SG, Mukhopadhyay S, Shi S, He H, Selley DE, Howlett AC, Elphick MR & Lewis DL (2007) CB1 cannabinoid receptor activity is modulated by the cannabinoid receptor interacting protein CRIP 1a. *Molecular Pharmacology* **72**, 1557-1566.

Onaivi ES, Ishiguro H, Gong J-P, Patel S, Meozzi PA, Myers L, Perchuk A, Mora Z, Tagliaferro PA, Gardner E, Brusco A, Akinshola BE, Liu Q-R, Chirwa SS, Hope B, Lujilde J, Inada T, Iwasaki S, Macharia D, Teasenfitz L, Arinami T & Uhl GR (2008) Functional Expression of Brain Neuronal CB2 Cannabinoid Receptors Are Involved in the Effects of Drugs of Abuse and in Depression. *Annals of the New York Academy of Sciences* **1139**, 434-449.

Pagotto U, Marsicano G, Cota D, Lutz B & Pasquali R (2006) The emerging role of the endocannabinoid system in endocrine regulation and energy balance. *Endocrine Reviews* **27**, 73-100.

Pan XH, Ikeda SR & Lewis DL (1996) Rat brain cannabinoid receptor modulates N-type Ca2+ channels in a neuronal expression system. *Molecular Pharmacology* **49**, 707-714.

Pearson G, Robinson F, Gibson TB, Xu BE, Karandikar M, Berman K & Cobb MH (2001) Mitogen-activated protein (MAP) kinase pathways: Regulation and physiological functions. *Endocrine Reviews* **22**, 153-183.

Perez-Fernandez R, Fresno N, Macias-Gonzalez M, Elguero J, Decara J, Giron R, Rodriguez-Alvarez A, Martin MI, de Fonseca FR & Goya P (2011) Discovery of Potent Dual PPAR alpha Agonists/CB1 Ligands. *Acs Medicinal Chemistry Letters* **2**, 793-797.

Pertwee RG, Howlett AC, Abood ME, Alexander SPH, Di Marzo V, Elphick MR, Greasley PJ, Hansen HS, Kunos G, Mackie K, Mechoulam R & Ross RA (2010) International Union of Basic and Clinical Pharmacology. LXXIX. Cannabinoid Receptors and Their Ligands: Beyond CB1 and CB2. *Pharmacological Reviews* **62**, 588-631.

Porter AC, Sauer JM, Knierman MD, Becker GW, Berna MJ, Bao JQ, Nomikos GG, Carter P, Bymaster FP, Leese AB & Felder CC (2002) Characterization of a novel endocannabinoid, virodhamine, with antagonist activity at the CB1 receptor. *Journal of Pharmacology and Experimental Therapeutics* **301**, 1020-1024.

Price MR, Baillie GL, Thomas A, Stevenson LA, Easson M, Goodwin R, McLean A, McIntosh L, Goodwin G, Walker G, Westwood P, Marrs J, Thomson F, Cowley P, Christopoulos A, Pertwee RG & Ross RA (2005) Allosteric modulation of the cannabinoid CB1 receptor. *Molecular Pharmacology* **68**, 1484-1495.

Qi Q-R & Yang Z-M (2014) Regulation and function of signal transducer and activator of transcription 3. *World journal of biological chemistry* **5**, 231-239.

Rajagopal S, Ahn S, Rominger DH, Gowen-MacDonald W, Lam CM, DeWire SM, Violin JD & Lefkowitz RJ (2011) Quantifying Ligand Bias at Seven-Transmembrane Receptors. *Molecular Pharmacology* **80**, 367-377.

Rajesh M, Mukhopadhyay P, Haskó G, Liaudet L, Mackie K & Pacher P (2010) Cannabinoid-1 receptor activation induces reactive oxygen species-dependent and -independent mitogen-activated protein kinase activation

and cell death in human coronary artery endothelial cells. *British Journal of Pharmacology* **160**, 688-700.

Rakhshandehroo M, Knoch B, Muller M & Kersten S (2010) Peroxisome Proliferator-Activated Receptor Alpha Target Genes. *Ppar Research*.

Rioli V, Gozzo FC, Heimann AS, Linardi A, Krieger JE, Shida CS, Almeida PC, Hyslop S, Eberlin MN & Ferro ES (2003) Novel natural peptide substrates for endopeptidase 24.15, neurolysin, and angiotensin-converting enzyme. *Journal of Biological Chemistry* **278**, 8547-8555.

Rios C, Gomes I & Devi LA (2006) mu opioid and CB1 cannabinoid receptor interactions: reciprocal inhibition of receptor signaling and neuritogenesis. *British Journal of Pharmacology* **148**, 387-395.

Robbe D, Alonso G, Duchamp F, Bockaert J & Manzoni OJ (2001) Localization and mechanisms of action of cannabinoid receptors at the glutamatergic synapses of the mouse nucleus accumbens. *Journal of Neuroscience* **21**, 109-116.

Ross RA (2003) Anandamide and vanilloid TRPV1 receptors. *British Journal of Pharmacology* **140**, 790-801.

Rozenfeld R, Bushlin I, Gomes I, Tzavaras N, Gupta A, Neves S, Battini L, Gusella GL, Lachmann A, Ma'ayan A, Blitzer RD & Devi LA (2012) Receptor Heteromerization Expands the Repertoire of Cannabinoid Signaling in Rodent Neurons. *Plos One* **7**.

Rubino T, Patrini G, Parenti M, Massi P & Parolaro D (1997) Chronic treatment with a synthetic cannabinoid CP-55,940 alters G-protein expression in the rat central nervous system. *Molecular Brain Research* **44**, 191-197.

Rubino T, Vigano D, Costa B, Colleoni M & Parolaro D (2000) Loss of cannabinoid-stimulated guanosine 5 '-O-(3- S-35 thiotriphosphate) binding without receptor down-regulation in brain regions of anandamide-tolerant rats. *Journal of Neurochemistry* **75**, 2478-2484.

Rubino T, Vigano D, Premolil F, Castiglioni C, Bianchessi S, Zippel R & Parolaro D (2006) Changes in the expression of G protein-coupled receptor kinases and beta-arrestins in mouse brain during cannabinoid tolerance - A role for Ras-ERK cascade. *Molecular Neurobiology* **33**, 199-213.

Rueda D, Galve-Roperh I, Haro A & Guzmán M (2000) The CB1 Cannabinoid Receptor Is Coupled to the Activation of c-Jun N-Terminal Kinase. *Molecular Pharmacology* **58**, 814-820.

Sagar DR, Gaw AG, Okine BN, Woodhams SG, Wong A, Kendall DA & Chapman V (2009) Dynamic regulation of the endocannabinoid system: implications for analgesia. *Molecular Pain* **5**.

Sanchez C, Galve-Roperh I, Rueda D & Guzman M (1998) Involvement of sphingomyelin hydrolysis and the mitogen-activated protein kinase cascade in the Delta(9)-tetrahydrocannabinol-induced stimulation of glucose metabolism in primary astrocytes. *Molecular Pharmacology* **54**, 834-843.

Sawzdargo M, Nguyen T, Lee DK, Lynch KR, Cheng R, Heng HHQ, George SR & O'Dowd BF (1999) Identification and cloning of three novel human G protein-coupled receptor genes GPR52, Psi GPR53 and GPR55: GPR55 is extensively expressed in human brain. *Molecular Brain Research* **64**, 193-198.

Seifert R (2013) Functional selectivity of G-protein-coupled receptors: From recombinant systems to native human cells. *Biochemical Pharmacology* **86**, 853-861.

Shaul YD & Seger R (2007) The MEK/ERK cascade: From signaling specificity to diverse functions. *Biochimica Et Biophysica Acta-Molecular Cell Research* **1773**, 1213-1226.

Shaw G, Morse S, Ararat M & Graham FL (2002) Preferential transformation of human neuronal cells by human adenoviruses and the origin of HEK 293 cells. *The FASEB Journal*.

Shire D, Carillon C, Kaghad M, Calandra B, Rinaldicarmona M, Lefur G, Caput D & Ferrara P (1995) An amino-terminal variant of the central cannabinoid receptor resulting from alternative splicing. *Journal of Biological Chemistry* **270**, 3726-3731.

Shore DM, Ballie GL, Hurst DP, Navas FJ, Seltzman HH, Marcu JP, Abood ME, Ross RA & Reggio PH (2013) Allosteric Modulation of a Cannabinoid G Protein-Coupled Receptor: Binding Site Elucidation and Relationship to G Protein Signaling. *Journal of Biological Chemistry*.

Signorello MG, Giacobbe E & Leoncini G (2011) Activation by 2-Arachidonoylglycerol of Platelet p38MAPK/cPLA(2) Pathway. *Journal of Cellular Biochemistry* **112**, 2794-2802.

Sim-Selley LJ & Martin BR (2002) Effect of chronic administration of R-(+)- 2,3-dihydro-5-methyl-3- (morpholinyl)methyl pyrrolo 1,2,3-de -1,4 -benzoxazinyl -(1-naphthalenyl)methanone mesylate (WIN55,212-2) or Delta(9)-tetrahydrocannabinol on cannabinoid receptor adaptation in mice. *Journal of Pharmacology and Experimental Therapeutics* **303**, 36-44.

Sim LJ, Hampson RE, Deadwyler SA & Childers SR (1996) Effects of chronic treatment with Delta(9)-tetrahydrocannabinol on cannabinoid-stimulated S-35 GTP gamma S autoradiography in rat brain. *Journal of Neuroscience* **16**, 8057-8066.

Steffens S, Veillard NR, Arnaud C, Pelli G, Burger F, Staub C, Zimmer A, Frossard JL & Mach F (2005) Low dose oral cannabinoid therapy reduces progression of atherosclerosis in mice. *Nature* **434**, 782-786.

Stout BD, Clarke WP & Berg KA (2002) Rapid desensitization of the serotonin(2C) receptor system: Effector pathway and agonist dependence. *Journal of Pharmacology and Experimental Therapeutics* **302**, 957-962.

Sugiura T, Kodaka T, Kondo S, Tonegawa T, Nakane S, Kishimoto S, Yamashita A & Waku K (1996) 2-arachidonoylglycerol, a putative endogenous cannabinoid receptor ligand, induces rapid, transient elevation of intracellular free Ca2+ in neuroblastoma X glioma hybrid NG108-15 cells. *Biochemical and Biophysical Research Communications* **229**, 58-64.

Sugiura T, Kodaka T, Kondo S, Tonegawa T, Nakane S, Kishimoto S, Yamashita A & Waku K (1997) Inhibition by 2-arachidonoylglycerol, a novel type of possible neuromodulator, of the depolarization-induced increase in intracellular free calcium in neuroblastoma x glioma hybrid NG108-15 cells. *Biochemical and Biophysical Research Communications* **233**, 207-210.

Sun Y, Alexander SPH, Garle MJ, Gibson CL, Hewitt K, Murphy SP, Kendall DA & Bennett AJ (2007) Cannabinoid activation of PPAR alpha; a novel neuroprotective mechanism. *British Journal of Pharmacology* **152**, 734-743.

Tappe-Theodor A, Agarwal N, Katona I, Rubino T, Martini L, Swiercz J, Mackie K, Monyer H, Parolaro D, Whistler J, Kuner T & Kuner R (2007) A molecular basis of analgesic tolerance to cannabinoids. *Journal of Neuroscience* **27**, 4165-4177.

Tomiyama K & Funada M (2014) Cytotoxicity of synthetic cannabinoids on primary neuronal cells of the forebrain: the involvement of cannabinoid CB1 receptors and apoptotic cell death. *Toxicology and Applied Pharmacology* **274**, 17-23.

Tsou K, Brown S, Sanudo-Pena MC, Mackie K & Walker JM (1998) Immunohistochemical distribution of cannabinoid CB1 receptors in the rat central nervous system. *Neuroscience* **83**, 393-411.

Urban JD, Clarke WP, von Zastrow M, Nichols DE, Kobilka B, Weinstein H, Javitch JA, Roth BL, Christopoulos A, Sexton PM, Miller KJ, Spedding M & Mailman RB (2007) Functional selectivity and classical concepts of quantitative pharmacology. *Journal of Pharmacology and Experimental Therapeutics* **320**, 1-13.

Valant C, Gregory KJ, Hall NE, Scammells PJ, Lew MJ, Sexton PM & Christopoulos A (2008) A Novel Mechanism of G Protein-coupled Receptor Functional Selectivity: MUSCARINIC PARTIAL AGONIST McN-A-343 AS A BITOPIC ORTHOSTERIC/ALLOSTERIC LIGAND. *Journal of Biological Chemistry* **283**, 29312-29321.

Valant C, Lane JR, Sexton PM & Christopoulos A (2012) The Best of Both Worlds? Bitopic Orthosteric/Allosteric Ligands of G Protein-Coupled Receptors. *Annual Review of Pharmacology and Toxicology, Vol 52* **52**, 153-178.

Valjent E, Pages C, Rogard M, Besson MJ, Maldonado R & Caboche J (2001) Delta 9-tetrahydrocannabinol-induced MAPK/ERK and Elk-1 activation in vivo depends on dopaminergic transmission. *European Journal of Neuroscience* **14**, 342-352.

Vasquez C, Navarro-Polanco RA, Huerta M, Trujillo X, Andrade F, Trujillo-Hernandez B & Hernandez L (2003) Effects of cannabinoids on endogenous K+ and Ca2+ currents in HEK293 cells. *Canadian Journal of Physiology and Pharmacology* **81**, 436-442.

Vrecl M, Norregaard PK, Almholt DLC, Elster L, Pogacnik A & Heding A (2009) beta-Arrestin-Based Bret(2) Screening Assay for the "Non"-beta-Arrestin Binding CB1 Receptor. *Journal of Biomolecular Screening* **14**, 371-380.

Waelbroeck M (1994) IDENTIFICATION OF DRUGS COMPETING WITH D-TUBOCURARINE FOR AN ALLOSTERIC SITE ON CARDIAC MUSCARINIC RECEPTORS. *Molecular Pharmacology* **46**, 685-692.

Wager-Miller J, Westenbroek R & Mackie K (2002) Dimerization of G protein-coupled receptors: CB1 cannabinoid receptors as an example. *Chemistry and Physics of Lipids* **121**, 83-89.

Wang XW, Horswill JG, Whalley BJ & Stephens GJ (2011) Effects of the Allosteric Antagonist 1-(4-Chlorophenyl)-3- 3-(6-pyrrolidin-1-ylpyridin-2-yl)phenyl urea (PSNCBAM-1) on CB1 Receptor Modulation in the Cerebellum. *Molecular Pharmacology* **79**, 758-767.

Wetzker R & Bohmer F-D (2003) Transactivation joins multiple tracks to the ERK/MAPK cascade. *Nat Rev Mol Cell Biol* **4**, 651-657.

Whistler JL, Enquist J, Marley A, Fong J, Gladher F, Tsuruda P, Murray SR & von Zastro M (2002) Modulation of postendocytic sorting of G-protein coupled receptors. *Science* **297**, 615-620.

Wiley JL, Compton DR, Dai D, Lainton JAH, Phillips M, Huffman JW & Martin BR (1998) Structure-Activity Relationships of Indole- and Pyrrole-Derived Cannabinoids. *Journal of Pharmacology and Experimental Therapeutics* **285**, 995-1004.

Willson TM, Brown PJ, Sternbach DD & Henke BR (2000) The PPARs: From orphan receptors to drug discovery. *Journal of Medicinal Chemistry* **43**, 527-550.

Wright KL, Duncan M & Sharkey KA (2008) Cannabinoid CB2 receptors in the gastrointestinal tract: a regulatory system in states of inflammation. *British Journal of Pharmacology* **153**, 263-270.

Wu GS, Lu ZH & Ledeen RW (1996) GM1 ganglioside modulates prostaglandin E1 stimulated adenylyl cyclase in neuro-2A cells. *Glycoconjugate Journal* **13**, 235-239.

Yin H, Chu A, Li W, Wang B, Shelton F, Otero F, Nguyen DG, Caldwell JS & Chen YA (2009) Lipid G Protein-coupled Receptor Ligand Identification

Using β-Arrestin PathHunter™ Assay. *Journal of Biological Chemistry* **284**, 12328-12338.

Zhang L, Tetrault J, Wang W, Loh HH & Law PY (2006) Short- and long-term regulation of adenylyl cyclase activity by delta-opioid receptor are mediated by G alpha(12) in neuroblastoma N(2)A cells. *Molecular Pharmacology* **69**, 1810-1819.

Zoratti C, Kipmen-Korgun D, Osibow K, Malli R & Graier WF (2003) Anandamide initiates Ca2+ signaling via CB2 receptor linked to phospholipase C in calf pulmonary endothelial cells. *British Journal of Pharmacology* **140**, 1351-1362.

Zorina Y, Iyengar R & Bromberg KD (2010) Cannabinoid 1 Receptor and Interleukin-6 Receptor Together Induce Integration of Protein Kinase and Transcription Factor Signaling to Trigger Neurite Outgrowth. *Journal of Biological Chemistry* **285**, 1358-1370.